PTEN as a Therapeutic Target for the Promotion of Cell Survival in Cell Models of Amyotrophic Lateral Sclerosis

Cassy Ashman

Submitted for the degree of Doctor of Philosophy (PhD)

Sheffield Institute for Translational Neuroscience

University of Sheffield

January 2017

This thesis is dedicated to three people:

My Mother and Father who have taught me resilience in the face of adversity;

and Karima Steele (nee Al-Mansoori) who was too good for this world.

AKNOWLEDGEMENTS

Firstly, I would like to thank my academic supervisors, Dr Ke Ning, Prof. Dame Pamela Shaw and Dr Adrian Higginbottom for their patience, guidance, support and understanding throughout my PhD, especially during the tougher parts.

My most sincere gratitude goes to Adrian, who without his continuous practical support, knowledge, generosity, kindness, and most of all humour (yes, including the bad jokes!), I may not have been encouraged to continue. For that I will always be grateful.

I would like to thank Dr Ke Ning, who provided endless scientific expertise along with relaxed and friendly approach to life which has been a blessing.

Special thanks go to Dr Margarita Segovia Roldan who has been the most wonderful teacher, listener, and friend. Your infectious happiness and positivity made those late night tissue culture sessions to “feed our babies” a joy; as well as to Dr Martina Daly, for always providing encouraging advice and for listening.

I would also like to thank the many staff and students of SITraN past and present who have provided me with guidance, both scientific and otherwise: Dr Guillaume Hautbergue, Dr Richard Mead and Dr Laura Ferraiuolo for their always friendly scientific advice, and helping hands (or reagents!) when I needed them the most; Dr Philippa Carling for her friendship, fantastic tissue culture company, and willingness to listen to whatever I wanted to play in “the hood”; to Alex, Lisa, Dave, Crispy, Stoppy, Matt, Lady Sarah, Jenn, Natalie and Laura for their friendship, the laughs, and for always being willing to go for a drink in the Francis Newton. To the Azzouz lab, for all of the above.

Finally, I would like to thank those who have been behind the scenes. My family, Mom, Dad, Jess, Shane, for your support even when times were hard for you; P.S I’m finished now. To my amazing friends for the wine, dancing and understanding. And last but not least to Nicholas Albert. Nick thank you for putting up with my stress, my weekend trips to the lab, my long evenings at my computer, my coming back late for dinner, and still wanting to marry me. I love you and I can’t wait.

"Nature did not deem it her business to make the discovery of her laws easy for us"

ALBERT EINSTEIN

ABSTRACT

Rationale & Hypothesis:

ALS is a fatal neurodegenerative disorder for which a GGGGCC hexanucleotide repeat expansion in C9ORF72 has been identified to be the most common genetic cause. Pathologically, ALS is characterised by premature death of motor neurons. The inhibition of Phosphatase and Tensin Homologue Deleted on Chromosome Ten (PTEN) in the PI3K cell survival cascade has been found to promote cell survival, and a newly described drug Scriptaid has been found to offer neuroprotection through PTEN inhibition in this pathway. We hypothesised that inhibiting PTEN in cell models of ALS could improve cell survival.

Methodology and Objectives:

For this investigation, we aimed to generate and characterise induced pluripotent stem (iPS) cell-derived motor neurons as *in vitro* models of ALS, from C9ORF72-ALS patient and sex/age matched healthy control primary fibroblast cells. Our objectives were to determine how PTEN manipulation through inhibition with Scriptaid or knockdown with short hairpin RNA (shRNA) lentiviral particles affects cell number and survival, comparing the newly generated iPS-derived cell models to established cell models of ALS including Neuroblastoma spinal cord (NSC)-34 cells and the primary fibroblast cells the iPS cells were derived from.

Findings:

We were able to successfully differentiate iPS cells into neurons and motor neurons of intermediate maturity in both patient and control cells, with C9ORF72 patient cells maintaining hallmarks of the repeat expansion. Results revealed fibroblast cells from C9ORF72 cases exhibited significantly lower levels of basal PTEN compared to control cells, however after the conversion to iPS-derived motor neurons, no significant difference between patient or control levels of PTEN expression were identified. PTEN knockdown in iPS-derived cells was found to cause a concomitant increase in PI3K pathway activation, and revealed a significant protection of cell number for up to three weeks in patient cells compared to controls after manipulation. However, PTEN

inhibition through the use of Scriptaid had no significant effect on activating this cell survival pathway or promoting motor neuron survival in our investigations.

Conclusions and Future Avenues:

Together, these results highlight that PTEN inhibition through genetic manipulation activates the PI3K cell survival pathway to promote a positive therapeutic effect in ALS iPS-derived cell models. However, small molecule modifier of PTEN Scriptaid does not promote motor neuron cell survival or activate cell survival pathways in the cell models of ALS tested, suggesting that future experiments should use alternative methods of inhibiting PTEN directly for successful patient therapies. Comparing models, iPS cells offer a promising cell model to investigate PTEN manipulation in ALS, however further work is still needed to optimise the differentiation protocol to improve maturity and functional parameters.

PUBLICATIONS

YANG, D. J., WANG, X. L., ISMAIL, A., **ASHMAN, C. J**., VALORI, C. F., WANG, G., GAO, S., HIGGINBOTTOM, A., INCE, P. G., AZZOUZ, M., XU, J., SHAW, P. J. & NING, K. 2014b. PTEN regulates AMPA receptor-mediated cell viability in iPS-derived motor neurons. *Cell Death Dis,* 27**,** 55.

TABLE OF CONTENTS

AKNOWLEDGEMENTS ..... **iii**

ABSTRACT ..... **v**

PUBLICATIONS ..... **vii**

TABLE OF CONTENTS ..... **viii**

LIST OF FIGURES ..... **xii**

LIST OF TABLES ..... **xiv**

ABBREVIATIONS ..... **xv**

CHAPTER 1 : Introduction **1**

1.1 Amyotrophic Lateral Sclerosis (ALS) 2

1.1.1 Epidemiology and Clinical Characteristics of ALS 2

1.2 The Genetic Causes, Related Pathology, and Disease Mechanisms Underlying ALS 4

1.2.1 Superoxide Dismutase 1 (SOD1) 8

1.2.2 TAR DNA Binding Protein 43 (TDP-43) 9

1.2.3 Chromosome 9 Open Reading Frame 72 (C9ORF72) 10

1.2.4 C9ORF72 Experimental Models and Limitations 12

1.3 ALS: A Multifactorial Disease 15

1.4 PTEN as a Neuronal Target 18

1.5 PTEN and the Phosphatidylinositide 3-kinase (PI3K) Cell Survival Cascade 21

1.6 PTEN and Motor Neuron Diseases 26

1.7 PTEN and Other Neurodegenerative Diseases 28

1.7.1 PTEN and Parkinson's Disease 28

1.7.2 PTEN and Alzheimer's Disease 29

1.8 PTEN and Cancer 30

1.9 PTEN and Small Molecule Inhibition 32

1.10 The Advent of Induced Pluripotent Stem (iPS) Cells 33

1.10.1 Amyotrophic Lateral Sclerosis and iPS Cell Technology 35

1.11 Conclusion 37

1.12 Aims and Objectives 39

1.12.1 PTEN Manipulation 39

1.12.2 iPS Cell Differentiation and Characterisation 39

CHAPTER 2 : Materials and Methods **41**
2.1 Cell Culture 42
2.1.1 Neuroblastoma spinal cord (NSC)-34 Cell Culture 42
2.1.2 Primary Fibroblast Cell Culture 42
2.1.3 Human Embryonic Kidney (HEK) 293 Cell Culture 43
2.1.4 iPS Cell Maintenance and Differentiation 44
2.2 Cell Lysis 50
2.3 Protein Determination 50
2.4 Western Blotting 50
2.4.1 Sodium dodecyl sulphate polyacrylamide gel Electrophoresis (SDS-PAGE) 50
2.4.2 Immunoblotting 52
2.4.3 Image Capture and Densitometry Analysis 54
2.5 Biochemical Assays 54
2.5.1 3-(4,5-Dimethylthiazol-2-yl)-2,5-Diphenyltetrazolium bromide (MTT) assay 54
2.5.2 Lactate Dehydrogenase (LDH) Assay 55
2.5.3 CyQUANT® Cell Proliferation Assay 55
2.6 Model Characterisation and Assay Development 56
2.6.1 IPS- Derived Cell Counts- 6 to 12 Weeks Post Differentiation 56
2.6.2 Fibroblast Scriptaid Treatment for Dose response assays and Western Blot Analysis 56
2.6.3 IPS-Derived Cell Scriptaid Treatment for Dose response assays and Western Blot Analysis 57
2.6.4 iPS-Derived Cell Scriptaid Treatment for Motor Neuron Cell Counts 57
2.6.5 Immunocytochemistry 57
2.6.6 RNA Fluorescent In situ Hybridisation (RNA FISH) 60
2.6.7 Electrophysiology 61
2.7 Microscopy and Image Analysis 64
2.7.1 Confocal Microscopy 64
2.7.2 IN Cell Analyser and Workstation Analysis 64
2.7.3 Quantification of TDP-43 Localisation and Cell Counts 65
2.8 PTEN Knockdown (KD) 66
2.8.1 Establishing Commercial Lentiviral MOI Using GFP Control Lentiviral Particles in HEK and iPS Cells 66
2.8.2 PTEN Knockdown with PTEN shRNA in HEK 293 cells and iPS-Derived cells 67
2.9 Statistical Analysis and Data Presentation 68

CHAPTER 3 : Cell Culture Models of Amyotrophic Lateral Sclerosis (ALS) to Investigate PTEN Inhibition 69

3.1 Introduction 70

3.1.1 Phosphatidylinositide 3-kinase (PI3K) Pathway Modulation for PTEN Inhibition 70

3.1.2 Amyotrophic Lateral Sclerosis (ALS) Cell Model Systems 72

3.2 Aims and Objectives 74

3.3 Neuroblastoma Spinal Cord (NSC34) Cells as Models for PTEN Manipulation in ALS 75

3.3.1 Neuroblastoma Spinal Cord (NSC34) Cells Show High Sensitivity to Scriptaid Treatment 75

3.4 Fibroblast Cells as Models for PTEN Manipulation in ALS 77

3.4.1 Fibroblast Cells Show Low Sensitivity to Scriptaid Treatment 77

3.4.2 Patient Fibroblast Cells Show Low levels of PTEN but Scriptaid Treatment does not Modulate the PI3K Cell Survival Pathway. 81

3.5 Discussion 84

3.5.1 NSC-34 Cell Models And Scriptaid 84

3.5.2 Fibroblast Cell Models: Toxicity Assays 85

3.5.3 Fibroblast Cell Models: Phosphatidylinositide 3-kinase (PI3K) pathway components 86

3.6 Conclusion 89

CHAPTER 4 : Characterisation of Induced Pluripotent Stem (iPS) Cell models of ALS 90

4.1 Introduction 91

4.1.1 Modelling C9ORF72-Related ALS with Induced Pluripotent Stem Cell-Derived Models 91

4.2 Aims and Objectives 93

4.3 Induced Pluripotent Stem (iPS) Cell generation and differentiation 94

4.3.1 Characterisation of induced Pluripotent Stem (iPS) Cells 94

4.3.2 Differentiation of induced Pluripotent Stem (iPS) Cells to Motor Neurons 99

4.3.3 Differentiated induced Pluripotent Stem (iPS) cells Display Neuronal and Motor Neuronal Specific Markers 101

4.3.4 Optimisation of Choline Acetyl Transferase Immunocytochemistry (ICC) 105

4.3.5 Differentiated induced Pluripotent Stem (iPS) Cells Express Mature Motor Neuronal Marker Choline Acetyl Transferase and Quantification of iPS- Derived Motor Neuron Yield 107

4.3.6 iPS Derived-Cell Survival Post-Differentiation Protocol 109

4.3.7 Characterisation of the Electrophysiological Properties of iPS- Derived Motor Neurons 110
4.4 C9ORF72 and ALS Specific Characterisation 114
4.4.1 iPS Cells and IPS-Derived Cells express RNA FOCI and Dipeptide Repeat Proteins . 114
4.4.2 Characterisation of iPS- derived Cell TDP-43 Localisation 121
4.5 Discussion 123
4.5.1 iPS-derived cellular models for ALS 123
4.5.2 RNA Foci, Di-peptide Repeat proteins, and TDP-43 in iPS Cell Models of ALS 131
4.6 Conclusion 138

CHAPTER 5 : PTEN Modulation in iPS-Derived Cell Models 140
5.1 Introduction 141
5.1.1 PTEN inhibition and Knockdown in Neuronal Cell models 141
5.2 Aims and Objectives 142
5.3 PTEN Knockdown for a Therapeutic Effect on ALS Cell Survival 144
5.3.1 Successful PTEN Knockdown in Human Embryonic Kidney (HEK293) Cells 144
5.3.2 Successful PTEN Knockdown in iPS-Derived Cells 146
5.3.3 PTEN Knockdown Modulates iPS-Derived Cell Survival Post-Differentiation 150
5.4 iPS-Derived Cell PTEN Inhibition Through Scriptaid Treatment 152
5.4.1 iPS-Derived Cells Show Low Sensitivity to Scriptaid Treatment 152
5.4.2 Scriptaid Treatment Does Not Activate Components of the Cell Survival Pathway 156
5.4.3 Scriptaid Treatment Does Not Modulate Motor Neuron Cell Number 160
5.5 Discussion 163
5.6 Conclusion 168

CHAPTER 6 : Final Discussion 169
6.1 Lessons Learned From C9ORF72 iPS cell models of ALS 170
6.2 Molecular Hallmarks of C9ORF72 ALS in iPS-derived Cell Models 174
6.3 Cell Specific Variation of PTEN in ALS 177
6.4 Scriptaid as a PTEN Manipulator 180
6.5 Final Conclusions 182

References 185

LIST OF FIGURES

Chapter 1

Figure 1.1: PTEN structural diagram……22
Figure 1.2: Schematic representation of the PTEN- AKT-mTOR pathway and downstream effectors……25
Figure 1.3: Schematic of iPS cell generation and differentiation……35

Chapter 2

Figure 2.1: Electrophysiology of iPS derived Motor Neurons……63
Figure 2.2: Quantification of Motor Neurons using the INcell Workstation Analyser……65
Figure 2.3 Quantification of Cellular TDP-43 Staining……66

Chapter 3

Figure 3.1: The effects of Scriptaid on NSC-34 cell viability as measured by MTT assay. 76
Figure 3.2: The effects of Scriptaid on fibroblast cell viability as measured by MTT assay..... 78
Figure 3.3 Determination of LDH cytotoxicity of Scriptaid treatment on fibroblast cells. 80
Figure 3.4: The effects of Scriptaid on fibroblast cell number and proliferation as measured by CyQuant assays. 81
Figure 3.5: Scriptaid does not modulate PI3K cell survival pathway components in fibroblast cell models of ALS and controls. 83

Chapter 4

Figure 4.1: iPS cells can be generated from human patient and control fibroblast cells. 96
Figure 4.2: Characterisation of iPS cells generated from human dermal fibroblasts for markers of pluripotency..... 97
Figure 4.3: Characterisation of iPS cells generated from human dermal fibroblasts for markers of pluripotency..... 98
Figure 4.4: Schematic representation of the iPS cell differentiation protocol to generate motor neurons. 100
Figure 4.5: Neurons generated from iPS cells express neuronal specific dendritic marker MAP2 101
Figure 4.6: Neurons generated from iPS cells express markers specific to neuronal and motor neuronal lineages..... 103
Figure 4.7: Neurons generated from iPS cells express markers specific to neuronal and motor neuronal lineages..... 104
Figure 4.8: Optimisation of choline acetyl transferase immunocytochemistry 106
Figure 4.9: Neurons generated from iPS cells express markers specific to neuronal and mature motor neurons. 108
Figure 4.10: Quantification of differentiated iPS cells labelled positive for dual ChAT and Tuj1 staining at 6 weeks of differentiation. 109
Figure 4.11: Total iPS Derived cell counts. 110

Figure 4.12: Electrophysiological characterisation of iPS-derived neurons reveals no electrical activity in patients or controls. 113
Figure 4.13: iPS Cells and differentiated iPS-derived cells from C9ORF72-ALS patients contain sense RNA foci.. 116
Figure 4.14: Differentiated IPS-derived cells from C9ORF72-ALS patients contain antisense RNA foci..... 117
Figure 4.15: Comparison of sense and antisense foci number per cell.. 118
Figure 4.16: iPS cells at day 0 have cytoplasmic RNA translation proteins. 119
Figure 4.17: C9ORF72 iPS cells and differentiated iPS cells display both sense foci and GA DPR proteins. 120
Figure 4.18: TDP-43 does not co-localise with antisense foci in patient iPS-derived cells but does show reduced nuclear expression. 122

Chapter 5

Figure 5.1: Successful PTEN knockdown in HEK293 cells. 145
Figure 5.2: Successful PTEN Knockdown in iPS derived cells. 148
Figure 5.3: PTEN Knockdown in iPS-derived cells successfully reduced PTEN expression in neuronal populations. 149
Figure 5.4: PTEN KD causes a significant increase in total iPS-derived cell number at 7 to 9 weeks of differentiation. 151
Figure 5.5 The effects of Scriptaid on iPS-derived cell viability as measured by MTT assay. ... 154
Figure 5.6 Determination of LDH cytotoxicity after Scriptaid treatment on iPS-derived cells. 155
Figure 5.7: Scriptaid treatment during differentiation does not increase motor neuron cell number. 162
Figure 5.8. Scriptaid treatment to iPS derived cells does not positively impact PI3K Pathway components. 158
Figure 5.9 Scriptaid has no positive effect on pPTEN but basal pPTEN expression is significantly higher in patient cells. 159

LIST OF TABLES

Table 1.1: Important genes associated with hereditary ALS and FTD. 6
Table 2.1: Aged and sex matched primary fibroblast cells from C9ORF72 patients and controls. 43
Table 2.2: iPS cell differentiation protocol, including schedule for addition of factors and concentrations used..... 46
Table 2.3: Preparation for Lamelli buffer (10ml) 51
Table 2.4: Preparation for separating gel buffer (100ml, pH adjusted with HCL and NaOH)..... 51
Table 2.5: Preparation for separating gel for SDS-PAGE (For 2 gels of 1.5mm thickness) 51
Table 2.6: Preparation for Stacking gel buffer (100ml, pH adjusted with HCL and NaOH) 52
Table 2.7: Preparation of Stacking gel for SDS-PAGE (for 2 gels of 1.5mm thickness)..... 52
Table 2.8: Preparation of Running buffer for SDS-PAGE (700ml)..... 52
Table 2.9: Preparation of transfer buffer for SDS-PAGE (1000ml) 53
Table 2.10: Primary antibodies used for Western Blotting 53
Table 2.11: Secondary antibodies used for Western Blotting 53
Table 2.12: Primary antibodies, concentrations and incubation periods..... 58
Table 2.13: Secondary Antibodies, concentrations and incubation periods 59
Table 2.14: Volume of GFP Control Lentiviral particles ($1x10^6$ IFU), PTEN ShRNA virus ($1x10^6$ IFU), and control ShRNA Virus ($1x10^6$ IFU) calculated per coverslip at different cell densities plated. 67
Table 4.1: Raw data for membrane capacitance (Cm) (pF) and resting membrane potential (RMP) (mV) for patient and control cells iPS-derived motor neurons..... 111
Table 4.2: Average membrane capacitance (pF) for patient and control iPS-derived motor neurons 112
Table 4.3: Average Resting membrane potential (RMP) for patient and control iPS-derived motor neurons 112

ABBREVIATIONS

4-AP	4-aminopyridine
4EBP	4 E binding protein
6OHDA	6-hydroxydopamine
AAV	Adeno-associated virus
Ab	Antibody
AD	Autosomal dominant
AKT	V-akt murine thymoma viral oncogene homolog
ALS	Amyotrophic lateral sclerosis
ALS2	Alsin
ALZ	Alzheimer's disease
AMPA	2-amino-3-(3-hydroxy-5-methyl-isoxazol-4-yl) propanoic acid
ANG	Angiogenin
AR	Autosomal recessive
ASO	antisense oligonucleotide
ATXN2	Ataxin 2
Aβ	β-amyloid
BAC	Bacterial artificial chromosome
BAD	Bcl2-associated death promoter
Bcl2	B- cell lymphoma 2
BclXL	B-cell lymphoma extra large
BDNF	Brain derived neurotrophic factor
bFGF	Basic fibroblast growth factor
BpV	Bisperoxovanadium
BSA	Bovine serum albumin
C9ORF72 / C9	Chromosome 9 open reading frame 72
$CaCl_2$,	Calcium chloride
cAMP	Adenosine 3',5'-cyclic monophosphate
CD	Cowdens disease

ChAT	Choline acetyletransferase
CHCHD10	Coiled-coil-helix-coiled-coil-helix domain containing 10
CHMP2B	Chromatin modifying protein 2B
CK2	Casein kinase 2
C_m	Whole-cell capacitance
c-myc	C -v-myc avian myelocytomatosis viral oncogene
CNQX	6-cyano-7-nitroquinoxaline-2-3-dione
CNS	central nervous system
CTL	Control
DAO	D-amino acid oxidase
DENN	Differentially Expressed in Normal and Neoplasia
DMEM	Dulbecco's Modified Eagle's Medium
DMF	Dimethyl formamide
DMSO	Dimethyl sulfoxide
DNA	Deoxyribonucleic acid
dPBS	Dulbecco's phosphate-buffered saline
DPR	Dipeptide repeat
EAAT2	Excitatory amino acid transporter 2
EB	Embryoid body
EGTA	ethylene glycol-bis(β-aminoethyl ethe
ERBB4	V-erb-b2 avian erythroblastic leukemia viral oncogene homolog 4
ES	Embryonic-stem
FALS	Familial amyotrophic lateral sclerosis
FBS	Foetal bovine serum
FIG4	Polyphosphoinositide phosphatase
FTD	Frontotemporal dementia
FUS	Fused in sarcoma
GA	Glycine-Alanine
GAPDH	Glyceraldehyde-3-phosphate dehydrogenase
GDNF	Glial derived neurotrophic factor
GEF	Guanine exchange factor

GFAP	Glial fibrillary acidic protein
GFP	Green fluorescence protein
GluR	Glutamine receptor
GP	Glycine-Proline
GR	Glycine-Arginine
GSK-3β	Glycogen synthase 3β
HAT	Histone acetyltransferase
Hb9	Homeobox gene 9
HCL	Hydrochloric acid
HD	Huntington's disease
HDAC	Histone deacetylase
HEK293	Human embryonic kidney
HEPES	4-(2-hydroxyethyl)-1-piperazineethanesulfonic acid
hnRNP	Heterogeneous nuclear ribonucleoprotein
HNRNPA1	Heterogeneous nuclear ribonucleoprotein A1
IC_{50}	Half maximum inhibition
ICC	Immunocytochemistry/ immunocytochemical
IGF	Insulin-like growth factor
iPS	Induced pluripotent stem
IRS1	Insulin receptor substrate 1
JNK	Jun-N-Terminal Kinase
KCl,	Potassium chloride
KD	Knockdown
Klf4	Krüppel-like factor 4
KSR	Knockout serum replacement
LDD	Lhermitte-Duclos disease
LDH	Lactate dehydrogenase
LMC	Lateral motor column
LMN	Lower motor neuron
LOH	Loss of heterozygosity
LTP	Long term potentiation
MAP-2	Microtubule associated protein-2

MAPT	Microtubule-associated protein tau
MATR3	Matrin 3
MDM2	Mouse double minute
MEF	Mouse embryonic fibroblast
MEM NEAA	Minimum essential medium non-essential amino acid
$MgCl_2$	Magnesium Chloride
MMC	Muscle innervating medial motor column
MN	Motor neuron
MND	Motor neuron disease
mOsm	Milliosmoles
mRNA	Messenger ribonucleic acid
mTOR	Mammalian target of Rapamycin
MTT	3-(4,5-dimethylthiazol-2-yl)-2,5-diphenyltetrazolium bromide
mV	Millivolts
Na^+-ATP	Sodium Adenosine Triphosphate
Na^+-GTP	Guanosine-5'-triphosphate
NaBu	Sodium butyrate
NaCl	Sodium chloride
NADH	Nicotinamide adenine dinucleotide
NaOH	Sodium hydroxide
NEAA	Non-essential amino acids
NEDD4	Neural precursor cell expressed developmentally downregulated gene 4
NFT	Neurofibrillary tangle
NGF	Nerve growth factor
NMDA	N-Methyl-D-aspartic acid
NO	Nitric oxide
NSC34	Neuroblastoma spinal cord
Oct 3/4	Octamer-binding protein 3/4
OD	Optical density
OPTN	Optineurin
pAKT	Phosphorylated AKT (see AKT)

PBS	Phosphate buffered saline
PCR	Polymerase chain reaction
PD	Parkinson disease
PEST	Proline-glutamic acid-serine-threonine; PDZ, post synaptic density protein (PSD95)- Drosophila disc large tumour suppressor (Dlg1)- Zonula occludens-1 protein (zo-1).
pF	picofarad
PFA	Paraformaldehyde
PFN1	Profilin 1
PI3K	Phosphatidylinositide-3-kinase
PINK1	Phosphatase and tensin homolog deleted on chromosome 10-induced Kinase 1
PIP2	Phosphatidylinositol-3,4,5-triphosphate
PIP3	Phosphatidylinositol-4,5-bisphosphate
PLS	Primary lateral sclerosis
PMA	Progressive muscular atrophy
pPTEN	Phosphorylated PTEN (see PTEN)
pre-mRNA	pre-messenger ribonucleic acid
PTEN	Phosphatase and tensin homolog deleted on chromosome 10
PTEN-L	PTEN-long (see PTEN)
PUR	Purmorphamine
PVDF	Polyvinylidene difluoride
R_a	Input resistance
RA,	All-trans retinoic acid
RBP	RNA binding proteins
RCF	Relative centrifugal force
RIPA	Radioimmunoprecipitation assay
RMP	Resting membrane potential
RNA	Ribonucleic acid
RNA FISH	RNA Fluorescent In situ Hybridisation

ROS	Reactive oxygen species
R_S	Series resistance
RTK	Receptor tyrosine kinase
S6K	Serine 6 Kinase
SALS	Sporadic amyotrophic lateral sclerosis
scAAV	Self-complementary recombinant adeno-associated virus
Scram	Scrambled
SDS	Sodium dodecyl sulphate
SDS-PAGE	Sodium dodecyl sulfate polyacrylamide gel electrophoresis
SETX	Senataxin
SHH	Sonic hedgehog
shRNA	Short hairpin RNA
SIGMAR1	σ Non-opioid receptor 1
SMA	Spinal muscular atrophy
SMAΔ7	Survival motor neuron deficient
SMCR8	Smith-Magenis syndrome chromosome region 8
SMN1	Survival motor neuron 1
SNc	Substantia nigra pars compacta
SOD1	Superoxide dismutase 1
SOD1	Superoxide dismutase 1
SOX2	Sex determining region Y(SRY)-box 2
SPG11	Spatacsin
SQSTM1	Sequestosome 1
SSC	Saline sodium citrate
SSEA3/4	Stage specific embryonic antigen 3/4
SUMO	Small ubiquitin-like modifier
TARDBP	TAR DNA-binding protein
TBK1	TANK Binding Kinase 1
TBST	Tris-Buffered Saline with Tween 20
TDP-43	TAR DNA-binding protein 43
TEA	Tetraethylammonium
TEMED	Tetramethylethylenediamine

TRA-1-60/1-80	Tumour rejection antigen 1-60/ 1-80
TSA	Trichostatin A
TSC1/2	Tuberous sclerosis 1/2
TTX	Tetrodotoxin
TUBA4A	Tubulin alpha 4a
UBQLN2	Ubiquilin 2
ULK1	Unc-51-like kinase 1
UMN	Upper motor neuron
UPS	Ubiquitin protease system
UT	Untransduced
VAPB	Vesicle-associated membrane protein-associated protein B
VCP	Valosin-containing protein
VPA	Valproic acid
WT	Wild type
WT-SOD1	Wild type SOD1 (see SOD1)
αER	α oestrogen receptor

CHAPTER 1 : INTRODUCTION

1.1 Amyotrophic Lateral Sclerosis (ALS)

First described in 1869 by Jean Martin Charcot (Charcot and Joffroy, 1869), Amyotrophic Lateral Sclerosis (ALS) is a devastating and fatal neurodegenerative disorder, resulting in the loss of both upper and lower motor neurons. As a form of motor neuron disease (MND), once symptoms present, patients are given a prognosis of progressive paralysis and eventually death within 2 to 5 years, most commonly through respiratory failure (Wood-Allum and Shaw, 2010, Chio et al., 2009). Nonetheless, many features such as clinical phenotype, rate of progression, age of onset and environmental factors are thought to influence lifespan in this heterogeneous disease, with some patients living for more than 10 years past diagnosis (Kiernan et al., 2011, Chio et al., 2009).

Currently the only treatment option available is Riluzole, a benzothiazole that is believed to act by modulating glutamatergic pathways of release (Bensimon et al., 1994). However, it only extends life by up to four months, highlighting a clear need for disease modifying treatments that may ameliorate the symptoms and slow progression with a goal of extending the lifespan for those affected.

1.1.1 Epidemiology and Clinical Characteristics of ALS

Epidemiologically, in western populations the disease has an incidence in Europe of 2.08 per 100 000 and a prevalence of 5.4 per 100 000, whilst in North America, Canada and the USA have an incidence rate of 2.2 and 1.8 per 100 000 respectively (Chio et al., 2013). When you look towards Asian populations, incidence drops significantly, for instance, China has an incidence rate of 0.6 per 100 000 (Chio et al., 2013). However interestingly, Japan has a high relative incidence of 2.5 per 100 000 (Chio et al., 2013). These comparisons firstly suggest a greater tendency for ALS in Caucasian populations. Secondly, the higher incidence rates in Japan and Scandinavian countries such as Norway (2.2 per 100 000) or Sweden (3 per 100 000), also suggests an effect from isolated cultures comprised of less diverse genepools, where interracial relationships are less common due to historical, cultural or language barriers. Overall, these patterns

suggest a genetic cause, including a postulated founder effect for Caucasian populations (Saeed et al., 2009, Smith et al., 2013). However, other contributors to country specific incidence rates could include environmental exposure to pesticides, diet, and lifestyle (Ingre et al., 2015), as well as differences in average life expectancy for that country, which may be important for an age of onset disease.

ALS is also known to affect more men than women by up to 1.5 fold (Manjaly et al., 2010, Harwood et al., 2012), however of note, when hereditary cases are isolated, the incidence has been found to be similar across both sexes, suggesting sporadic cases are related to the male sex (Kiernan et al., 2011). The majority of ALS cases, 90%, are sporadic (SALS) occurring with no family history of the disorder. The remaining 10% of cases are familial (FALS), and unfortunately, as age of onset is typically in midlife at 50+ years (Harwood et al., 2012), it means many familial sufferers will have already had children before diagnosis, potentially passing on any disease causing genetic material.

Clinically, ALS can be isolated from other Motor Neuron Diseases (MND) such as the upper motor neuron (UMN) affected Primary Lateral Sclerosis (PLS) (Gordon et al., 2006); the lower motor neuron (LMN) affected Progressive Muscular Atrophy (PMA); and childhood onset form Spinal Muscular Atrophy (SMA). This is due to ALS presenting a progressive nature, both upper and lower motor neuron degeneration, and subsequent muscle wasting (Ince et al., 1998, Ferguson and Elman, 2007). However, due to the similarity of ALS symptoms across these disorders, it is important to confirm a correct diagnosis as other forms of MND can have a better prognosis. Due to the gradual onset of symptoms, it can take a year on average for the patient to present to a neurologist. Diagnosis is largely made on clinical grounds, rather than one diagnostic test, although advances in electrodiagnostics, ultrasound, and transcranial magnetic stimulation are improving this picture (Simon et al., 2015). This means that patients who have been eventually diagnosed with ALS may not obtain access to Riluzole for up to a year, further limiting the small yet positive effects of the treatment. Recent work has highlighted improvements still need to be made in the genetic testing of patients with ALS, in particular linking ALS with FTD of which only 57% of clinicians in a recent survey test for in patients, despite a clear link between the two diseases (Vajda et al., 2017). Genetic testing should be factored into more diagnostic strategies; as we understand more that ALS could be a heterogeneous collection diseases, clinical

trials are often carried out with a particular focus on a single genetic subtype of ALS (Ludolph, 2017).

In Caucasian population studies, ALS has been found to present itself with three main different phenotypes (Harwood et al., 2012) including limb-onset, which is the most common presentation of ALS; bulbar onset, characterised by slow, slurred speech and wasting of the tongue (Duffy et al., 2007); and respiratory onset, the least common presentation found in 2.7% of patients (Shoesmith et al., 2007). However, further classification can include advanced subtyping referring to the proportion of UMN or LMN degeneration to define distinct presentations; this suggests ALS is a syndrome of related diseases rather than an isolated condition (Al-Chalabi and Hardiman, 2013). Symptoms generally include: muscle weakness, fasciculations, emotional lability, behavioural changes, and weight loss. Additionally, extra neuronal involvement has been more recently associated with the disease, with up to 50% of patients also presenting other cognitive impairments such as frontotemporal dementia (FTD) (Ferguson and Elman, 2007, Ferrari et al., 2011, Lomen-Hoerth et al., 2002).

1.2 The Genetic Causes, Related Pathology, and Disease Mechanisms Underlying ALS

Ninety Percent of ALS cases occur sporadically (SALS), which leaves the remaining 10% of familial ALS cases (FALS) to characterise any causative genes, proteins and pathways involved in disease pathogenesis and progression, in expectation that any novel modifiers will translate across to the SALS population (van Blitterswijk et al., 2012). For the 10% of inherited cases of ALS, multiple genes have been identified to cause disease, and these have been classified into ALS subtypes, further highlighting how ALS in reality represents a spectrum of many related diseases (Abel et al., 2012) (Table 1). Many of the mutations commonly associated with ALS are inherited in a Mendelian fashion, and approximately 60% of inherited cases can be accounted for by mutations in two genes, Superoxide dismutase 1 (SOD1) and Chromosome 9 open reading frame 72 (C9ORF72) affecting up to 20% and up to 50% of FALS patients respectively. Nonetheless, whilst Mendelian inheritance suggests a monogenetic cause, of note,

C9ORF72 mutations show incomplete penetrance, with some carriers failing to get the disease, underlining the complexity of the genetics behind ALS. As currently 126 genes have been identified to cause or act as a modifier for ALS (ALS online database), of which for many the significance has yet to be elucidated, the focus below will be on the mutations and related pathology that have prominently impacted ALS research worldwide.

Table 1.1: Important genes associated with hereditary ALS and FTD. Genes, ALS subtype, chromosome locus, method of inheritance, their pathogenic mechanism and or functions, and reference. Abbreviations: ALS, amyotrophic lateral sclerosis; PD, Parkinson's disease; FTD, fronto-temporal dementia; AD, autosomal dominant; AR, autosomal recessive; RNA, Ribonucleic acid; DNA, Deoxyribonucleic acid, Gene (in table).

Gene	Subtype	Chromosome	Inheritance	Pathogenesis / Function	Reference
Superoxide dismutase 1 (*SOD1*)	ALS 1	21q22.11	AD / AR	Oxidative Stress	(Rosen et al., 1993)
Alsin (*ALS2*)	ALS 2	2q33.2	AR	Endosomal trafficking and Cell signalling	(Yang et al., 2001)
Unknown	ALS 3	18q21	AD	Unknown	(Hand et al., 2002)
Senataxin (*SETX*)	ALS 4	9q34.13	AD	RNA processing and transcription regulation	(Chen et al., 2004)
Spatacsin (*SPG11*)	ALS 5	15q14-q21.1	AR	DNA Damage Repair; Axonal Growth	(Orlacchio et al., 2010)
Fused in sarcoma (*FUS*)	ALS 6	16p11.2	AD / AR	RNA processing and transcription regulation	(Kwiatkowski et al., 2009, Vance et al., 2009)
Unknown	ALS 7	20p13	AD	Unknown	(Sapp et al., 2003)
Vesicle-associated membrane protein-associated protein B (*VAPB*)	ALS 8	20q13.33	AD	Endosomal trafficking and Cell signalling	(Nishimura et al., 2004)
Angiogenin (*ANG*)	ALS 9	14q11.1	AD	RNA processing and transcription regulation	(Greenway et al., 2006)
TAR DNA-binding protein (*TARDBP*)	ALS 10	1p36.22	AD	RNA processing and transcription regulation	(Sreedharan et al., 2008)
Polyphosphoinositide phosphatase (*FIG4*)	ALS 11	6q21	AD	Endosomal trafficking and Cell signalling	(Chow et al., 2009)
Optineurin (*OPTN*)	ALS 12	10p13	AD / AR	Endosomal trafficking and Cell signalling; Autophagy	(Maruyama et al., 2010)

Ataxin 2 (*ATXN2*)	ALS 13	12q23-q24.1	AD	Oxidative stress	(Elden et al., 2010)
Valosin- containing protein (VCP)	ALS 14	9p13-p12	AD	Autophagy	(Johnson et al., 2011)
Ubiquilin 2 (*UBQLN2*)	ALS 15/X	Xp11.21	X-Linked	Protein Degradation Aggregation; Autophagy	(Deng et al., 2011)
σ Non-opiod receptor 1 (*SIGMAR1*)	ALS-16/FTD	9p13.3	AD	Protein Degradation Aggregation	(Luty et al., 2010, Al-Saif et al., 2011)
Chromatin modifying protein 2B (*CHMP2B*)	ALS-17	3p12.1	AD	Endosomal trafficking and Cell signalling; Autophagy	(Parkinson et al., 2006)
Profilin 1 (*PFN1*)	ALS-18	17p13.3	AD	Cytoskeletal; Axonal Growth	(Wu et al., 2012)
v-erb-b2 avian erythroblastic leukemia viral oncogene homolog 4 (*ERBB4*)	ALS-19	2q33.3-q34	AD	Neuronal Development	(Takahashi et al., 2013)
Heterogeneous nuclear ribonucleoprotein A1 (*HNRNPA1*)	ALS-20	12q13.1	AD	RNA processing and transcription regulation	(Kim et al., 2013)
Matrin 3 (*MATR3*)	ALS-21	5q31.2	AD	RNA processing and transcription regulation	(Johnson et al., 2014)
Tubulin alpha 4a (*TUBA4A*)	ALS-22	2q35	AD	Cytoskeletal	
Chromosome 9 open reading frame 72 (*C9ORF72*)	ALS-FTD-1	9q21-q22	AD	RNA processing and transcription regulation	(Renton et al., 2011, DeJesus-Hernandez et al., 2011)
coiled-coil-helix-coiled-coil-helix domain containing 10 (*CHCHD10*)	ALS-FTD-2	22q11.23	AD	Mitochondrial	(Smith et al., 2014)
Sequestosome 1 (*SQSTM1*)	ALS-FTD-3	5q35	AD	Protein Degradation Aggregation; Autophagy	(Fecto et al., 2011)
TANK Binding Kinase 1 (*TBK1*)	ALS-FTD-4	12q14.2	AD	Autophagy	(Cirulli et al., 2015, Freischmidt et al., 2015)
Microtubule-associated protein tau (MAPT)	ALS-dementia-PD	17q21	AD	Cytoskeletal; Axonal Growth	(Hutton et al., 1998)
D-amino acid oxidase (DAO)	—	12q24	AD	Glutamate excitotoxicity	(Mitchell et al., 2010)
Never in mitosis gene a (NIMA) related kinase 1 *(NEK1)*	—	4q33	Unknown	Unknown	(Kenna et al., 2016)

1.2.1 Superoxide Dismutase 1 (SOD1)

In 1993, mutations in a gene which encodes for a 153 amino acid metalloenzyme called superoxide dismutase (SOD1) were identified as the first mutations to cause ALS (Rosen et al., 1993). These mutations were subsequently identified to contribute to around 20% of FALS cases and up to 3% of SALS. However, the mutation is not in a single location, with over 150 gene variations identified according to the ALS online database (http://alsod.iop.kcl.ac.uk/Overview/gene.aspx?gene_id=SOD1).

Endogenous SOD1 acts to prevent toxicity from oxidative stress by binding to copper and zinc ions which together can metabolize superoxide free radicals to stop them from causing cellular damage. Originally, due to finding a reduced activity of the enzyme, it was proposed that disease was caused due to loss of function of the protein (Rosen et al., 1993, Deng et al., 1993) leading to investigations into oxidative stress. However, when the gene is mutated in disease, SOD1 misfolds and aggregates are formed. It has also been suggested that these aggregates cause motor neuron cell death in a toxic gain of function mechanism which causes a disease phenotype in cells (Bruijn et al., 1998).

Interestingly, a more recent review of SOD1 activity re-visited the loss of function hypothesis, highlighting that in 48 mutations in papers reporting reduced SOD1 enzymatic activity from 1993 to 2012, an average of 58% reduction in activity is found (Saccon et al., 2013); a reduction which others have suggested could be caused by the aggregates themselves (Yoon et al., 2009). As papers present contrasting opinions as to whether or not experimentally induced increases or decreases in SOD1 does not cause (Bruijn et al., 1998) or causes (Graffmo et al., 2013) ALS like phenotypes, the endogenous function and therefore dysfunction of this protein in disease still remains to be elucidated. Recently, evidence has been gathering to suggest SOD1 aggregates act in a prion-like way, helping to propagate and spread ALS to other cells (Lee and Kim, 2015). Nevertheless, these aggregates although found in small quantities are still found in ALS patient tissue and are therefore postulated to play an important role in disease (Jonsson et al., 2004).

1.2.2 TAR DNA BINDING PROTEIN 43 (TDP-43)

SOD1 containing aggregates are the longest known pathogenic aggregates thought to be involved in both FALS and SALS (Bunton-Stasyshyn et al., 2014). However, this proteinopathy is not found in all cases of ALS and was superceeded when hyperphosphorylated TAR DNA Binding protein 43 (TDP-43) inclusions were found to be the major constituent of a more commonly found marker of ALS of ubiquitinylated protein aggregates. These TDP-43 inclusions were found in 97% of patient tissues in SALS, FALS, and FTD, and interestingly only FALS SOD1 and FUS related tissues do not display this pathology (Neumann et al., 2006, Arai et al., 2006, Mackenzie et al., 2007). This discovery was a breakthrough for characterising this common pathological marker for the disease and it was soon identified that TDP-43 underwent aberrant trafficking moving from its predominant nuclear location in healthy tissues to the cytoplasm, in a mechanism potentially causing pathogenesis (Lagier-Tourenne and Cleveland, 2009).

TDP-43 is encoded by the gene TARDBP, and is a 43 KDa Deoxyribonucleic acid (DNA) and Ribonucleic acid (RNA) binding protein (Ou et al., 1995), which in its nuclear location acts to regulate the stability and splicing of RNA transcripts. The role of TDP-43 also extends to auto-regulation, with TDP-43 found to modify its own protein levels through the self-splicing of transcripts (Polymenidou et al., 2011). Due to the aberrant cytoplasmic location of TDP-43 in ALS, it has been implicated in multiple mechanisms of motor neuron injury including: regulating cellular stress due to forming into stress granules when exposed to oxidative stress (Colombrita et al., 2009), intracellular mRNA transport (Ishiguro et al., 2016), and synaptic transmission in the processes of neuronal cells (Diaper et al., 2013). However, like many pathological aggregates found in neurodegenerative disease, identifying whether TDP-43 aggregation is a cause or a consequence of disease remains an important aim for further investigations. Nonetheless, recent work is linking TDP-43 loss of function to impaired endosomal trafficking, finding a reduced number of Rab11-associated endosomes upon TDP-43 knockdown which results in slow recycling of surface receptors important for tropic signalling (Schwenk et al., 2016). Studies like this are helping to build a picture of how this protein miss-location can cause ALS, but further work remains to be done to support such findings and link results to newer mutations such as that in C9ORF72.

1.2.3 Chromosome 9 Open Reading Frame 72 (C9ORF72)

In the 23 years since Rosen et al. first identified the gene encoding the free radical scavenger Superoxide Dismutase 1 (SOD1) as a causative agent in 20% of FALS cases, it was not until 2011 that any of the newer genes discovered were thought to affect a greater proportion of FALS sufferers than SOD1. This was when two teams simultaneously proposed a new gene, Chromosome 9 open reading frame 72 (C9ORF72) to be the most common genetic cause of ALS to date (Renton et al., 2011, DeJesus-Hernandez et al., 2011). The mutation affects up to 50% of FALS cases (van Blitterswijk et al., 2012, Cooper-Knock et al., 2015c), around 7% of apparently sporadic patients (Renton et al., 2011, Sabatelli et al., 2012, van Blitterswijk et al., 2012) and is linked to FTD (Orr, 2011, van Blitterswijk et al., 2012), as well as other neurodegenerative disorders (Cooper-Knock et al., 2015c) implying the importance of investigations into C9ORF72 due to the widespread nature of the mutation. Fascinatingly, the expansion mutation has also been found in healthy individuals suggesting incomplete penetrance and a possible multifactorial pathogenesis (Harms et al., 2013).

The mutation in C9ORF72 is a GGGGCC hexanucleotide repeat expansion in intron 1 of the C9ORF72 gene. In healthy individuals, less than 30 repeats are found, however in disease, between 30 and over 1000 repeats are reported to contribute towards both ALS and FTD (Renton et al., 2011, Rutherford et al., 2012, van der Zee et al., 2013). Although a threshold for disease has been reported in mouse models (Jiang et al., 2016), and there have been correlations found between dysregulated splicing and repeat length (Cooper-Knock et al., 2015a), researchers are only just beginning to gather evidence suggesting that expansion repeat length correlates with factors such as onset, progression, severity or anticipation (Dafinca et al., 2016).

The function of the protein product of C9ORF72 has yet to be revealed, but as the gene is highly conserved, with mice and rats showing respectively 98.75% and 97.1% amino acid similarity to the human form, it is thought to have an important biological function. There are three isoforms of C9ORF72 called variants 1-3. Variant 2 encodes a 222 amino acid protein also known as the short form, whilst variants 1 and 3 encode a 481 amino acid protein known as the long form(DeJesus-Hernandez et al., 2011). Both

variants are thought to be highly transcribed in neuronal cells (Suzuki et al., 2013). Although commercially available C9ORF72 antibodies may lack the desired specificity to accurately delineate the subcellular location of C9ORF72, and it is possible the protein is present at a low abundance in cells, attempts have been made in identifying its distribution. C9ORF72 has been found to be located in both the nucleus and cytoplasm of cells, with different isoforms potentially carrying different functions due to their location, for example isoform 1 has been found to accumulate at the synapses of cells (Atkinson et al., 2015). Its location has also been described as dynamic, moving between the nucleus and the cytoplasm during development (Ferguson et al., 2016). Others have found the short form can translocate from the nuclear membrane to the plasma membrane in disease, suggesting roles in nucleocytoplasmic transport (Xiao et al., 2015). Mouse studies have pointed to expression in embryonic and early postnatal neurons, including expression in multiple areas of the brain such as the cortex, hippocampus, olfactory bulb, along with high expression in the spinal cord grey matter and dorsal root ganglia (Koppers et al., 2015, Suzuki et al., 2013, Jiang et al., 2016, Ferguson et al., 2016). This reported high expression in neural tissue suggests a specific importance to these cells which could explain why neurons are so affected by its malfunction. As the mutation is an intronic expansion rather than a coding mutation, misregulated expression or dysregulated RNA splicing could cause this malfunction.

The C9ORF72 protein has not been fully structurally characterised, albeit publications have identified a sequence homology to Differentially Expressed in Normal and Neoplasia (DENN) proteins which suggest a Guanine Exchange Factor (GEF) function for Rab GTPases in regulating intramembrane traffic (Levine et al., 2013, Zhang et al., 2012a). Indeed C9ORF72 has been found to co-localise with several Rab proteins in neuronal and motor neuronal cells (Farg et al., 2014) which supports this hypothesis, although this result remains to be clarified with more specific antibody preparations. Of note, a recent paper has added further evidence to this theory, proposing C9ORF72 interacts with Rab1a as part of a regulatory pathway for the initiation of autophagy (Webster et al., 2016). The study found that C9ORF72 when ablated from HeLa cells or primary motor neurons, prevented autophagy initiation. They later found that C9ORF72 interacts with Unc-51-like kinase 1 (ULK1) as part of the autophagy initiation complex, and also bound to Rab1. They proposed that the role of C9ORF72 was to act

as a Rab1 effector, recruiting Rab1 to ULK1, which regulates the trafficking of ULK1 in the early stages of autophagy (Webster et al., 2016); this was in contrast to a Rab GEF role proposed by previous studies (Farg et al., 2014).

The mechanism for C9ORF72 related pathogenesis in ALS has naturally been the objective of a number of different investigators work and has led to several schools of thought. These include haploinsufficiency, where having only one functional copy of the allele for the gene results in a reduction in the amount of protein product, in a proposed loss of function mechanism (Gijselinck et al., 2012). To add to this, a toxic gain of function mechanism has been suggested, where transcription of the repeat in both directions results in aberrant extended repeat-containing RNA transcripts. These transcripts then form into RNA foci and affect protein translation by sequestering RNA binding proteins from their roles elsewhere, thus causing a cascade of problems such as alternative splicing or modifications in gene expression (Harms et al., 2013). Finally, it has been shown that the GGGGCC repeat is translated into hydrophobic dipeptide repeat (DPR) proteins that may aggregate intracellularly (Mori et al., 2013b). The mechanism for this has been hypothesised to be due to repeat associated non-ATG translation initiation; translation not from a start codon but due to hairpin formation of the repeat-containing RNA (Pearson, 2011, Zu et al., 2011, Kovanda et al., 2015).

Neuropathologically, C9ORF72 cases have been associated with TDP-43 skein-like and neuronal cytoplasmic inclusions, as well as p62 inclusions, Bunina bodies, and ubiquitylated inclusions (Cooper-Knock et al., 2012). However, a portfolio of evidence has now included new molecular pathology such as RNA foci and di-peptide repeat proteins as additional hallmarks of the C9ORF72 repeat expansion. Nevertheless, although, this pathology is suggestive of a toxic gain of function mechanism of pathogenesis (Gendron et al., 2013, Cooper-Knock et al., 2015b, Mori et al., 2013a), studies have yet to find a correlation between DPR protein aggregates and disease (Davidson et al., 2016).

1.2.4 C9ORF72 Experimental Models and Limitations

Due to the significance of C9ORF72 mutations in ALS with the repeat affecting up to 50% of familial cases, as well as a high prevalence in SALS populations (7-10%), there is a high research need for robust cell models containing the pathogenic expansion.

However, a caveat to the excitement C9ORF72 has created in the field of ALS research is the fact that the CG rich mutation has previously slowed down the generation of cell and animal models containing the repeat expansion. This is due to technical difficulties in repeat primed PCR methods to demarcate expansions of more than 30 repeats, as screening is hampered by the secondary structure formed by the repeat expansion which leads to instability in the receiving vector (Renton et al., 2011). The extreme length of the expansions has also proved technically challenging for the generation of transgenic mice due to presenting germline somatic instability and bacterial artificial chromosome (BAC) instability. Therefore only recently, conditional knockout and overexpression animal models of C9ORF72 have surfaced with different outcomes.

Significantly to the field, the effect of C9ORF72 ablation in mice appeared at first not to cause a degenerative motor neuron phenotype, nor present any motor defects akin to that seen in SOD1 mouse models. Koppers et al. were one of the first groups to discover that conditional knockout C9ORF72 mice did not display degeneration of motor neurons, poor motor function, nor changes in survival. However they did find a significantly lower body weight in models which is akin to the human patient phenotype who also experience weight loss in disease. Of interest, later studies, show that homozygous knockout C9ORF72-mice, display unique symptoms of enlarged spleens and lymph nodes, a reduced life expectancy and, in contrast to the previously published results, mild motor deficits (Jiang et al., 2016). However, Jiang and colleagues also found comparative results in increased weight loss, suggesting some overlap with models generated. In more recent results, in contrast to their own previous reports, Koppers et al. have found that ablation of C9ORF72 does cause reduced survival, and also reported splenomegaly and increased lymph node size (Sudria-Lopez et al., 2016). However, mice still did not show any motor neuron defects, with the reported reduced survival hypothesised to be due to immune deficiencies in mice (Sudria-Lopez et al., 2016). Together, the lack of neurodegeneration in these mice models supports the theory that loss of C9ORF72 does not result in neurodegeneration, suggesting haploinsufficiency may not be the cause of disease in ALS.

When the C9ORF72 BAC transgenic mice were generated to express the repeat expansion at different lengths, at first no obvious signs of neurodegeneration or motor

neuron dysfunction were found (Peters et al., 2015, O'Rourke et al., 2015). These studies also failed to find any TDP-43-related pathology commonly found in C9-ALS patients; however, they did find the presence of molecular pathology related with C9-ALS in the form of RNA foci and DPR protein aggregates which were thought to increase in prevalence with age and showed the BAC constructs were being expressed. More recent work using similar transgenic lines also found no motor neuron loss, no reduced performance in motor functional tests or TDP-43 pathology (Jiang et al., 2016). However, they did find evidence of cognitive impairment in high repeat containing models and interestingly an age and repeat length associated increase in both foci and DPR products (Jiang et al., 2016). This could suggest that the foci and DPR products may not be a cause for the neurodegenerative phenotype, but are a consequence of the mutation or even a protective response which is activated to a higher extent with factors such as age, disease severity, and repeat length. Of recent note, a new study has generated a C9 BAC transgenic mouse expressing the expanded repeat, which in contrast to previous studies found abnormalities in gait, reduced survival, a progressive phenotype, degeneration of spinal motor neurons, and RNA-related and TDP-43 pathology which collectively Lui et al. describe as a motor neuron disease phenotype (Liu et al., 2016). With C9 mouse models failing to recapitulate disease phenotypes across multiple groups this could reflect the different animal genetic backgrounds and laboratory conditions tested, including differences in level of expression, size and timing of expression. However, it also could mean that presence of the mutation alone does not cause disease; an important finding as similar sequence homology from mouse to human C9ORF72 suggests a translatable phenotype for humans. If this is true, potentially a second hit, for example with environmental factors or cellular stressors, is required for pathogenesis in C9-ALS. Nevertheless, without a solid consensus on the effect C9ORF72 mutation to the motor neurons and phenotype of the mice models generated, results still suggests multiple mechanisms including the possibility of both loss and gain of function contributing to pathogenesis.

1.3 ALS: A MULTIFACTORIAL DISEASE

Key players in ALS are reactive oxygen species (ROS); free radicals that upon accumulation in neuronal cells, cause aberrant cytotoxic (Shaw et al., 1995) and genetic oxidative damage (Chang et al., 2008b). Accumulation is thought to occur partly from the malfunction of free radical scavengers such as SOD1, generating rather than removing ROS (Wiedau-Pazos et al., 1996). The evidence for this has been found in ALS patient post-mortem examinations which have increased and thus pathogenic levels of oxidation (Shaw et al., 1995), as well as studies which have found increased levels of ROS such as hydrogen peroxide in familial forms of the disease compared to sporadic and control cases (Said Ahmed et al., 2000).

Neuronal support cells, such as astrocytes have also been implicated in the progression of ALS, for instance, deleting mutant SOD1 in astrocytes has been found to slow the progression of disease (Yamanaka et al., 2008). Interestingly, the presence of conditioned media from mutated SOD1 astrocytes can cause motor neuron cell death (Rojas et al., 2014), suggesting the astrocytes release a substance that is toxic to motor neurons and indicating that the astrocytes may initiate disease in other cells. Suggested components of toxicity released by astrocytes include increased release of the precursor of nerve growth factor which can cause an aberrant increase in p75 receptors and signalling from them in motor neurons, while a reduction in lactate release is thought to also trigger motor neuron death due to a lack of nutritional support (Ferraiuolo et al., 2011). To add to this, media from mutant SOD1 astrocytes has been found to cause increased persistent sodium channel currents in motor neurons, resulting in toxic hyper-excitability of the cells and a highlighting another potential mechanism of disease (Fritz et al., 2013). Recent studies have suggested that this hyper-excitability may be the start of a cascade that results in increased calcium uptake, mitochondrial dysfunction, and therefore increased release of ROS which trigger c-abl cell death cascades in motor neurons (Rojas et al., 2015), again pointing towards astrocytes as the cells which initiate or at least contribute towards motor neuron cell death.

Mitochondrial dysfunction is another major contributor to pathogenesis in ALS, with neuronal mitochondria from ALS SOD1 G93A murine models exhibiting dysfunctional

calcium uptake (Damiano et al., 2006). This coupled with increased glutamatergic signalling from enhanced 2-amino-3-(3-hydroxy-5-methyl-isoxazol-4-yl) propanoic acid (AMPA) and N-Methyl-D-aspartic acid (NMDA) receptor expression or activity (van Zundert et al., 2012, Williams et al., 1997) and reduced removal of glutamate from the synaptic cleft by excitatory amino acid transporter 2 (EAAT2), can increase levels of intracellular calcium and thus is likely to create a pathophysiological feedback loop between motor neuron excitotoxicity, failed mitochondrial calcium buffering and ROS production by mitochondria (Grosskreutz et al., 2010). This has formed the basis of the excitotoxicity neurodegeneration hypothesis, where excessive glutamatergic synaptic activity leads to calcium overload, increased membrane excitability and motor neuron cell death (Cleveland and Rothstein, 2001). To add to this, protein aggregates in mutant SOD1 ALS cases have been found to cluster in the intermembrane space of mitochondria, promoting further mitochondrial dysfunction (Wong et al., 1995). As the mitochondria's main role is in the production of energy, upon their failure, the reduction in energy stores could lead to an escalating cycle of motor neuron injury. An example includes reduced axonal transport, which in motor neurons is vital due to their long processes requiring a higher than normal energy demand. Indeed, defects in axonal transport have been identified in mutant SOD1 mice (Bilsland et al., 2010, De Vos et al., 2007) and may be an early event in degeneration (Williamson and Cleveland, 1999).

Other forms of cellular transport are also implicated in ALS, including nucleocytoplasmic transport and nuclear export. Ran- mediated nucleocytoplasmic transport uses Ran GTPases modulated by RanGEF in the nucleus and RanGAP in the cytoplasm to mediate the trafficking of cargo from the nucleus and the cytoplasm in the cell (Stewart, 2014). It has been suggested that the hexanucleotide repeat expansion in C9ORF72 may contribute to defects in nucleocytoplasmic transport and lead to cellular stress and disease propagating mechanisms. Due to hairpin formation of the transcribed repeat, the secondary structure is thought to cause the binding of proteins including nucleolin which is found in the nucleolus of cells (Haeusler et al., 2014). This interaction was specific to patient cells and was found to cause nucleolar stress, as identified by a dispersed nucleolus (Haeusler et al., 2014). Later work by the same group, this time in Drosophila melanogaster animal models, identified impaired

nuclear import due to expression of the expansion, and were able to rescue this defect using antisense oligonucleotide (ASO) therapy targeted to the complex secondary structures formed by the repeat (Zhang et al., 2015a). Further studies in flies corroborating this have found failed RNA nuclear export and morphological defects in the nuclear envelope (Freibaum et al., 2015), while screens in both Drosophila melanogaster and Saccharomyces cerevisiae have found Ran-mediated nucleocytoplasmic transport and nuclear pore components to be associated with DPR protein mediated cellular toxicity (Jovicic et al., 2015, Boeynaems et al., 2016).

Intracellular transport, trafficking and the regulation and degradation of cellular components have also been connected to ALS pathogenesis. Autophagy, in particular macro-autophagy, is the catabolic degradation of intracellular components through formation of a double membrane-bound vesicle encapsulating components for lysosomal-bound degradation. Autophagy defects have been previously linked to Parkinson's disease and Alzheimer's disease (Harris and Rubinsztein, 2012), but recently the process has been postulated to play an important role in C9ORF72-related ALS. Proteomic analysis to identify C9ORF72 binding partners have discovered a complex forming between C9ORF72 and WDR41 a 52 KDa protein whose function is unknown, as well as between C9ORF72 and Smith-Magenis syndrome chromosome region 8 (SMCR8), a 105 kDa protein containing a DENN domain which has previously been known to interact with autophagy initiator proteins (Sellier et al., 2016). Of note, Sellier and colleagues also found the complex interacts with Rab proteins including Rab 8 and Rab39b, a finding which supports the previous notion that C9ORF72 acts as a GEF (Farg et al., 2014). This theory is also supported by the identity of other Rab8 interactors which include Optineurin (OPTN) and TANK binding kinase 1 (TBK1); proteins which are mutated in ALS subtype 12 and ALS-FTD type 4 respectively (Table 1). Further to this theory, when C9ORF72 is knocked down via short hairpin RNA (shRNA), it prevents the initiation of autophagy, supporting mouse model evidence that C9ORF72 ablation can cause lysosomal accumulation (O'Rourke et al., 2016). More recent work also links the initiation of autophagy in C9ORF72 ALS. A study by Webster et al. found C9ORF72 interacts with Rab1, and suggested in contrast to Farg et al. that C9ORF72 does not act as GEF for Rab proteins but instead acts as an effector, helping to bring together components for the initiation of autophagy (Webster et al., 2016).

In the childhood form of MND, Spinal Muscular Atrophy, the SMA determining gene, survival motor neuron 1 (SMN1) (Lefebvre et al., 1995), has roles in building small nuclear ribonucleoproteins and splicing pre-messenger ribonucleic acid (pre-mRNA). As mutations to SMN1 were found to be causal to disease pathogenesis (Burghes and Beattie, 2009), this has led to predictions for a role of RNA processing, transcriptional regulation, and RNA binding in MND pathology due to the similarity of cells affected. Of note, the nuclear protein TDP-43 prominently associated with ALS has been found to bind to and possibly modulate many RNAs implicated in neurodegenerative disorders and examples include Fused in Sarcoma (FUS), Tau, Ataxin as well as binding to itself (Sephton et al., 2011). To add to this, the ever increasing knowledge of C9ORF72 pathology has found that the aberrant RNA may also sequester RNA binding proteins (RBPs) which could propagate disease in ALS by causing dysregulation of RNA metabolism and splicing. Heterogeneous nuclear ribonucleoproteins (hnRNPs), amongst other RBPs, have been shown in a number of studies to bind to C9ORF72 and include hnRNPs A1, A2/B2, A3, F, H, K and U, ADARBP2 and PURα as probable candidates (Donnelly et al., 2013b, Sareen et al., 2013, Haeusler et al., 2014, Cooper-Knock et al., 2015b, Cooper-Knock et al., 2014). Whilst these studies may not fully reveal the normal function of the C9ORF72 protein, they indeed reveal factors and pathways which are aberrant and potentially underpin disease pathogenesis in ALS.

1.4 PTEN AS A NEURONAL TARGET

Over recent years, a building portfolio of work on phosphatase and tensin homologue deleted on chromosome 10 (PTEN) has shifted the focus of research on this established tumour suppressor, from cancer (Myers et al., 1997, Steck et al., 1997) to neurodegenerative disorders. The reason for this lies in the proposed neuroprotective features of PTEN inhibition. PTEN inhibition has been found to not only increase neuronal cell survival and reduce apoptosis, but also to improve axon growth and branching in neuronal cell and animal models (Ning et al., 2004, Shi et al., 2011a, Zhang et al., 2012b).

PTEN is strongly expressed in central nervous system (CNS) neuronal cells, mirroring the expression of interactor phosphatidylinositide 3-kinase (PI3K) (Lachyankar et al.,

2000). The highest expression is found in mature neurons, whereas low levels of PTEN are found in immature astrocytes, an expression which is lost in maturity (Lachyankar et al., 2000). In neuronal development, PTEN controls neuronal differentiation (Lachyankar et al., 2000) and axonal growth (Kwon et al., 2006), and is essential to development, with mice showing embryonic lethality when PTEN is mutated in tissues (Suzuki et al., 1998).

PTEN is located in both the cytoplasm and nucleus of neuronal cells (Lachyankar et al., 2000, Ning et al., 2010) and there is evidence to suggest that the subcellular localisation of neuronal PTEN reflects varying mechanistic actions. Cytoplasmic PTEN modulates apoptosis (Li et al., 2009) and when PTEN is located in specific cytoplasmic sub-compartments, it can initiate additional roles such as associating with mitochondrial membranes and the endoplasmic reticulum for control of calcium signalling and release that can cause apoptosis (Bononi et al., 2013, Zhu et al., 2006). Nuclear PTEN is postulated to work independently from cytoplasmic roles, thought to control G1 cell cycle arrest (Chang et al., 2008a, Liu et al., 2005) and may even confer neuroprotection as opposed to the cell survival suppression in the cytoplasm (Goh et al., 2014). As nuclear pools of phosphatidylinositol 3, 4, 5 triphosphate (PIP3) have been found to be resistant to PTEN (Lindsay et al., 2006), this discovery along with the finding that nuclear PTEN is unable to modulate v-akt murine thymoma viral oncogene homolog (AKT) phosphorylation and activation (Liu et al., 2005) suggests distinct mechanistic roles for the compartmentalised protein. Notably, studies have identified that PTEN can accumulate in the nuclei of post-mitotic neurons after injury, suggestive of an activated neuroprotective mechanism (Howitt et al., 2012, Zhang et al., 2013).

Significant recent work has also identified a novel 75KDa species of post-translationally modified PTEN, of which small ubiquitin-like modifier (SUMOylation) promoted the nuclear localization of PTEN (Bassi et al., 2013). The same study found loss of nuclear PTEN increased sensitivity of the cells to DNA damage, again implying that nuclear PTEN expression confers a protective phenotype (Bassi et al., 2013). In simultaneously published findings, an alternative translation codon was identified, which encodes an additional 173 amino acid domain at the beginning of the N terminus to create an alternative 75KDa longer version of PTEN termed PTEN-L (Hopkins et al., 2013). This longer form of PTEN was also found to inhibit the AKT pathway through the

phosphatase domain, but most remarkably it can be secreted from cells to interact with additional receptors and can be used as an external agent to reduce basal AKT phosphorylation (Hopkins et al., 2013). It was recently found that PTEN-L also has distinct roles in membrane binding compared to wild type PTEN, suggesting unique intracellular targets which may be of significance to cell survival (Masson et al., 2016). These fascinating findings also suggest that it may be possible to use a cell penetrating form of PTEN as a therapeutic; if found to be amenable to modulation to phosphatase inactive forms the therapeutic potential of PTEN could be extended even further.

Indicators that this pathway is an important target in neuronal cell death were first learned from studies which found an increase in the inactive phosphorylated form of PTEN after middle cerebral artery occlusion (Omori et al., 2002). Additionally, when the downstream effectors of PTEN: PI3K, AKT and pAKT, were seen to have increased expression after nerve crush injury (Ito et al., 1996) and up-regulation in rat post-ischemic cerebral cortex (Cai et al., 2009), this coupled with promoted motor neuron survival (Namikawa et al., 2000), suggested an endogenous activation of the AKT cell survival pathway in the face of injury. This work implied that neurons attempt to promote their own survival after acute injury, prompting the question as to whether this occurs in chronic neurodegenerative disease.

Whilst increased neuronal cell survival is a vital parameter in identifying a promising therapeutic strategy, it is also important to discover if surviving neurons are both functional and confer an ability to regenerate after injury and in disease. Park and colleagues in 2008 (Park et al., 2008), used adeno-associated (AAV) viruses expressing Cre floxed mice for PTEN mediated deletion, to show after retinal ganglion cell injury, along with increased survival, an increased and robust axon regeneration beyond the sites of insult, therefore identifying that PTEN deletion enables axons to overcome the hostile environment in and around the lesion. PTEN deletion in other neuronal cell types such as adult corticospinal neurons, retinal ganglion cells, and SMN-deficient motor neurons, was also found to increase the ability of neurons to grow and form synaptic like structures (Liu et al., 2010, Huang et al., 2017). The next logical steps were to identify if these axons reach their intended targets and secondly, to perform electrophysiology experiments to examine how functional the regenerated axons become. These steps were undertaken in subsequent work where PTEN knockdown

was found to increase branching, neurite outgrowth, myelinated axon regrowth, axon number and more importantly accelerated compound muscle action potentials, indicative of neuronal cell functionality (Danilov and Steward, 2015, Singh et al., 2014). Li et al. in 2015 explored a similar hypothesis and found that AAV depletion of both PTEN and suppressor of cytokine signalling 3 (SOC3) genes in mice promoted long-distance axonal regeneration after nerve crush injuries, evoked excitatory post synaptic currents through glutamatergic synaptic transmission, and promoted return of locomotive function, highlighting a possible cocktail of cellular targets which may underpin the beneficial effects of PTEN deletion (Jin et al., 2015). Finally, despite zebrafish models, unlike mammalian models conferring an ability to recover from CNS injury, upon inhibition of one of the two zebrafish homolog genes for PTEN, PTENa, zebrafish were found to also show improved regeneration of axons and locomotor recovery after spinal cord injury (Liu et al., 2014). This result further supported the use of PTEN inhibition to promote neuronal cell survival and cell growth.

1.5 PTEN AND THE PHOSPHATIDYLINOSITIDE 3-KINASE (PI3K) CELL SURVIVAL CASCADE

The PTEN gene is found on chromosome 10q23.3 and encodes a 55 KDa protein which was first identified in 1997 (Steck et al., 1997, Datta et al., 1999). It consists of a C-terminal domain with roles in regulation, stability, protein to protein interactions via the PEST sequence, as well as a PDZ binding motif for binding to the plasma membrane (Lee et al., 1999) and acting as a scaffold for other proteins to regulate contact polarity dependent cell signalling pathways. For example, PTEN binds to PTPN13 a protein tyrosine phosphatase, via the PDZ binding motif to mediate some of its tumour suppressor activities (Sotelo et al., 2015). The N-terminal domain has roles as a dual specificity protein and lipid phosphatase (figure 1.1) (Lazar and Saltiel, 2006). The pathways of cell survival mediated by v-akt murine thymoma viral oncogene homolog (AKT) are regulated by the lipid phosphatase activities of PTEN, whilst the protein phosphatase activities of PTEN dephosphorylate tyrosine, serine, and threonine

residues (Myers et al., 1997), and are postulated to play a role in neuroprotection (Ning et al., 2004).

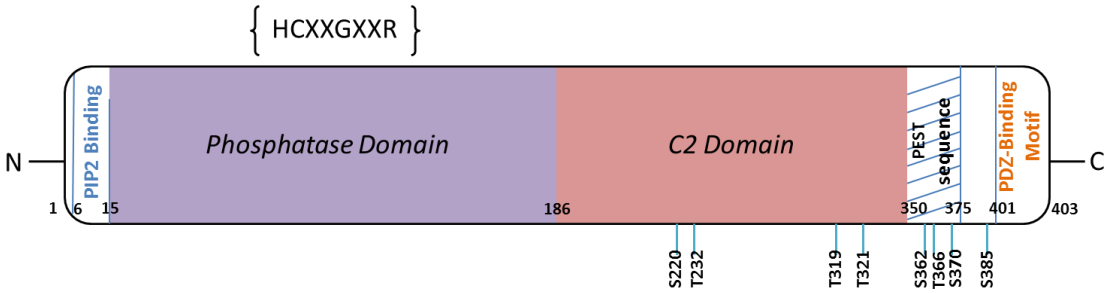

Figure 1.1: PTEN structural diagram
PTEN is a 403 amino acid long protein comprising a PIP2 binding sequence from residues 6 to 15, an N-terminal HCXXGXXR containing sequence for phosphatase activity from residues 15 to 186 (purple), a C2 domain from residues 186 to 351 (pink), and a C terminal region from residues 352 to 403 containing the PEST sequence (blue stripes) (350 to 375) and PDZ binding motifs (401 to 403) for regulation, stability, protein to protein interactions and binding to the plasma membrane. The blue stalks highlight serine and threonine phosphorylation points. Abbreviations: PIP2, phosphatidylinositol 4,5 bisphosphate, PEST, proline-glutamic acid-serine-threonine; PDZ, post synaptic density protein (PSD95)- Drosophila disc large tumour suppressor (Dlg1)- Zonula occludens-1 protein (zo-1).

PTEN is proposed to be a good target for neuronal survival due to the role of PTEN in the PI3K cell survival pathway. PTEN is a dual phosphoinositide 3 phosphatase, which means it has the ability to dephosphorylate residues on phosphatidylinositol 3, 4, 5 triphosphate (PIP3) to form phosphatidylinositol 4, 5 bisphosphate (PIP2), reducing the total levels of PIP3 *in vivo* (Maehama and Dixon, 1998). This is important as PIP3 binds to AKT which causes its relocation to the cell membrane (Datta et al., 1999), where it is activated through phosphorylation. AKT in its phosphorylated and active form can promote cell survival due to inhibiting components of cellular apoptosis pathways including, Bcl2/BclxL- associated death protein (BAD) (Datta et al., 1999) (figure 1.2). Additional downstream components of the PI3K pathway are also of

importance to neuronal cells, and include mammalian target of rapamycin (mTOR) known to be involved in the phosphorylation of Serine 6 Kinase (S6K) which in turn phosphorylates the ribosomal protein Serine 6 (S6) which can promote axon elongation from protein synthesis (figure 1.2). The key driver of this pathway is phosphatidylinositide 3 kinase (PI3K), which acts opposite to PTEN by phosphorylating and converting PIP2 to PIP3 thus promoting cell survival through AKT activation. However, important interactors in this pathway also include glycogen synthase 3β (GSK3β) which acts in a negative feedback loop with PTEN**.** Whilst GSK3β can inactivate PTEN, PTEN can also inactivate GSK3β through AKT mediated phosphorylation of GSK3β serine residues, thereafter modulating glycogen synthesis (Frame and Cohen, 2001).

With PTEN regulation in mind, rather than turning on a constitutively active cell survival pathway, the focus of research has been on controlling the action of PTEN through the inhibition of its dephosphorylating activities, in order to promote cell survival through altered inhibition of the pathway. However, other benefits may also be realised. Apart from associations with the cell membrane in the PI3K pathway, PTEN is also known to bind to and interact with extrasynaptic N-Methyl-D-aspartic acid (NMDA) receptors. Studies have shown that when PTEN levels are experimentally decreased, a reduction in NMDA receptor activity, levels of expression and a promotion of cell survival have been identified (Ning et al., 2004). Secondary activities of PTEN such as interactions with NMDA receptors could be utilised to promote additional therapeutic effects, especially as increased NMDA receptor calcium induced excitotoxicity is an important part of the pathogenesis of neurodegenerative disorders (van Zundert et al., 2012).

PTEN is regulated through many different mechanisms and cellular interactors which are of significance to neurodegenerative disorders. Neural precursor cell-expressed developmentally down regulated gene 4 (NEDD4), is involved in controlling PTEN for nuclear transport and degradation through the ubiquitin proteasome system (UPS) (Trotman et al., 2007, Christie et al., 2012, Wang et al., 2007) and it was recently identified that this system could also be used to secrete PTEN through exosomes (Putz et al., 2015). Post-translational modification of PTEN, specifically involving nitric oxide (NO) signalling and nitrosylation, are also important in regulating PTEN (Numajiri et al.,

2011). Increased levels of s- nitrosylated PTEN levels have been found in Alzheimer's disease (AD), Parkinson's disease (PD), and stroke patient brains, and this nitrosylation can be mediated by endogenously produced NO (Kwak et al., 2010). Alongside this, it has been found that the role of nitrosylation could be to mark PTEN for degradation via NEDD4, as a reduction in NEDD4 also stopped a nitrosylation-mediated reduction in PTEN (Kwak et al., 2010). Studies have suggested that the relationship between PTEN and NEDD4 might be more complex than previously thought as PTEN may also negatively regulate NEDD4 and promote axon outgrowth via activated protein translation machinery (Hsia et al., 2014). Gene expression of PTEN has been found to occur through trans-activation by p53 (Stambolic et al., 2001), with which it can physically associate via the C2 domain (Freeman et al., 2003). However, studies have found that PTEN can self-regulate its own expression by increasing the expression and stabilisation of p53, independent of its lipid and protein phosphatase activities (Tang and Eng, 2006). This evidence is important as it proposes that PTEN holds greater autoregulation of its activities, operating as both a negative and a positive regulator and potentially offering a level of protection via feedback loops that promote cell survival along the PI3K pathway, as well as being able to manipulate its own transcription.

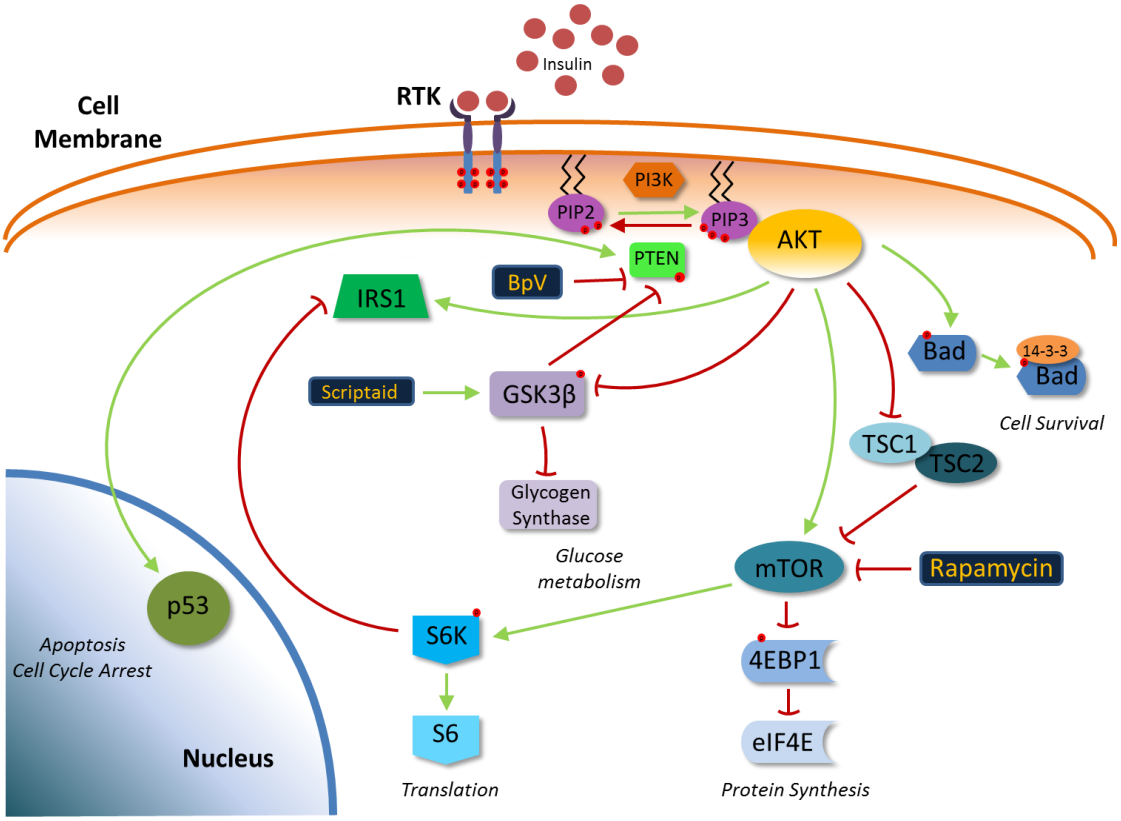

Figure 1.2: Schematic representation of the PTEN- AKT-mTOR pathway and downstream effectors. RTKs allow the binding of ligands activating PI3K. PTEN acts to dephosphorylate PIP3 to PIP2 whilst PI3K phosphorylates PIP2 to PIP3. PIP3 binds to and causes the translocation of AKT to the cell membrane where it phosphorylates and subsequently promotes the sequestration of cell death component BAD and blocks GSK-3β glycogen synthase inhibition. mTOR is also activated by AKT so mTOR can now phosphorylate S6K which in turn phosphorylates the ribosomal protein Serine 6 and 4EBP promoting cell growth and translation. TSC2 a GTPase activating protein involved in a complex with TSC1, a scaffolding protein, normally inhibits mTOR via Rheb, however when it is phosphorylated by AKT, TSC1 is inactivated so mTOR is then activated. A negative feedback loop from S6K separates IRS1 from its normal binding to PI3K. Rapamycin inhibits mTOR
Abbreviations: RTK, Receptor tyrosine kinase; PIP2, phosphatidylinositol 4,5 bisphosphate; PIP3, phosphatidylinositol 3,4,5 triphosphate; PI3K, phosphatidylinositide 3-kinase; BAD, Bcl2/BclxL-associated death protein; GSK-3β, glycogen synthase kinase 3 β; mTOR, mammalian target of rapamycin; S6K, Serine 6 Kinase ; 4EBP1, Eukaryotic Initiation factor 4E binding protein; eIF4E, Eukaryotic Initiation factor 4E; IRS1, Insulin receptor substrate 1; TSC1/2, tuberous sclerosis 1/2; MDM2, mouse double minute 2

1.6 PTEN AND MOTOR NEURON DISEASES

In ALS the characteristic dying back of neuronal processes and the premature death of motor neurons is a prominent aspect of the phenotype (Pun et al., 2006, Fischer et al., 2004). However, as multiple mechanisms of disease and conflicting hypotheses for pathogenesis are currently being deliberated, identifying one target can be difficult, particularly if there are still questions as to whether or not the abnormalities are causal or consequential of disease. This perhaps explains why promoting the survival of the cells that are affected in ALS, the motor neurons, is an attractive therapeutic objective and research direction.

Aberrant oxidative and glutamatergic stress are prominent features of ALS, and interestingly research has found links between oxidative stress and the cell survival pathways it negatively affects. A study by Chang et al. identified that under increased oxidative stress there is a prevention of PTEN nuclear export by a p53 dependent mechanism, which might be to not only activate p53 mediated cell cycle arrest, but also to act as a dual mechanism to prevent the accumulation of cytoplasmic PTEN, thought to have a pro-apoptotic effect (Chang et al., 2008a). Gary and Mattson illustrated that overexpression of wild type PTEN in neuronal cells increased the levels of apoptosis, as well as glutamate-induced apoptosis. When PTEN was knocked down, the heterozygous mice showed increased survival of neurons in excitotoxic conditions (Gary and Mattson, 2002) in an important link to not only MND but other neurodegenerative disorders where glutamate induced excitotoxicity can be a key driver to degeneration.

As PTEN depletion seemed to be an appropriate tool to promote phosphorylation of AKT and thus pathways of survival and growth, multiple attempts experimentally to modulate the behaviour of PTEN have been conducted in motor neuron disease research. As expected, PTEN depletion in models of MND were shown to increase the phosphorylation of AKT and of the components downstream in the pathway including BAD, S6 and mammalian target of Rapamycin (mTOR), coupled with a decrease in apoptosis (Kirby et al., 2011, Ning et al., 2010, Ning et al., 2004, Shi et al., 2011a). Moreover, work conducted on two different cell models of MND- SMN deficient mice (Ning et al., 2010) and murine G93A SOD1 motor neurons (Kirby et al., 2011)-

demonstrated higher neuronal survival rates. PTEN silencing via systematic delivery of self-complementary recombinant adeno-associated virus (scAAV9) vectors resulted in an increase in the life span of SMN deficient (SMAΔ7) mice, implying PTEN knockdown could be a good therapeutic target for SMA, a childhood form of motor neuron disease (Little et al., 2015), however as a monogenetic form of MND the focus of research currently lies in gene therapy of the mutated gene to treat the cause of SMA. Interestingly, a significant reduction of active pAKT level has been found in ALS patient motor neurons (Dewil et al., 2007) as well as a failure to up-regulate S6K involved in axon growth (Wagey et al., 1998), pointing to a potential malfunction of this pathway in disease. In contrast, gene expression profiling studies in 2011 found 34 genes involved in apoptosis were differentially expressed in human SOD1 motor neurons compared to controls, with a decrease in PTEN expression and an increase in expression of pro-survival components such as AKT and PI3K (Kirby et al., 2011). In this study, the motor neurons were laser capture micro-dissected from human post-mortem material therefore were inevitably those that had persisted through the disease process. It is possible that an activated endogenous neuroprotective mechanism occurs in surviving motor neurons whilst those that die have a reduction in the activity of this cell survival pathway. Indeed, recent studies on ALS patient induced pluripotent stem (iPS) cells have identified an increased cell death response as well as a 50% and 75% reduction in anti-apoptotic components downstream of the PI3K pathway of Bcl2 and Bcl XL respectively (Dafinca et al., 2016). Furthermore, in 2017 innovative new studies developing inducible cell models of C9ORF72-ALS, found that partial PTEN knockdown was protective against toxicity previously identified in the cell models (Stopford et al., 2017). However of note, the same study also identified a single nucleotide polymorphism (SNP) in PTEN, a missense change that results in loss of PTEN function, which associated with protection against ALS. These studies are indicative that upstream targeting via PTEN inhibition or reduction in function could promote a return to normal cell death regulation in disease, whilst also confirming this target for treatment could offer protection against cell death in ALS specifically.

A recent study has implicated a prominent nucleolar protein, nucleolin, in ALS pathogenesis. In cases of C9ORF72-realted ALS, (Renton et al., 2011, DeJesus-Hernandez et al., 2011), nucleolar stress has been revealed in patient iPS-derived

motor neurons compared to control cells, with nucleolin appearing more dispersed in the disease-related cells (Haeusler et al., 2014). Another recent study discovered that PTEN when localised to the nucleolus, co-localises with nucleolin and contributes towards nucleolar homeostasis (Li et al., 2014). In the same study, when nucleolar PTEN was knocked down, they noticed an increased number of nucleoli and a change in nucleolar morphology, in keeping with the work of Haeusler and colleagues. Interestingly, this relates to a study performed in 2003 by Borgatti et al. (Borgatti et al., 2003) where they found that upon stimulation, AKT translocates to the nucleus with pAKT found to co-immunoprecipitate with nucleolin. These studies suggest a potential link between PTEN and AKT nuclear localisation in a possible mechanism to activate ribosome biogenesis and intrinsic cell survival pathways simultaneously. With nucleoli morphological changes identified in both ALS and in PTEN manipulation studies, PTEN may also be a potential therapeutic target to rescue the nucleolar defects recently reported in ALS.

1.7 PTEN and Other Neurodegenerative Diseases

1.7.1 PTEN and Parkinson's Disease

Parkinson's disease (PD) is a neurodegenerative disorder caused by the progressive degeneration of dopaminergic neurons in the substantia nigra pars compacta (SNc) of the midbrain. Dopaminergic neurons project to the striatum which is important in coordinating movement. PD is characterised by aberrant motor symptoms comprising resting tremor, bradykinesia, and rigidity. PTEN has regulatory roles on PTEN induced kinase 1 (PINK1) a 581 amino acid protein expressed throughout the brain which has been postulated to control mitochondrial oxidative phosphorylation and stress. Mutations in PINK1 contribute towards autosomal recessive early onset PD (Valente et al., 2004, Glasl et al., 2012). Cytosolic PINK1, much like cytosolic PTEN, is important in dopaminergic neuronal survival (Haque et al., 2008). However, PINK1, in contrast to PTEN, is thought to endogenously promote neuronal survival via mechanisms controlling oxidative stress (Petit et al., 2005). Evidence to support this has been found in PINK1 overexpression models, which not only enhance neuronal survival, but also

reduce the formation of ROS, in a thapsigargin induced model of oxidative stress (Li and Hu, 2015).

Distinct from PINK1, PTEN has also been implicated in PD directly. Conditional inactivation of PTEN using a Cre-LoxP system driven by a dopamine transporter to acquire specific deletion of PTEN in dopaminergic neurons, caused an increase in the number of neurons located in the SNc (Diaz-Ruiz et al., 2009). Moreover, specific deletion of PTEN in this way is neuroprotective against 6-hydroxydopamine (6OHDA) induced models of PD, with recorded survival rates of 51% (Domanskyi et al., 2011) and 89% (Diaz-Ruiz et al., 2009) of SNc tyrosine hydroxylase (TH) positive neurons. Other mouse models of PD have found PTEN-deficient dopamine neurons display enhanced survival and neurite outgrowth when transplanted into the depleted striatum of parkinsonian mice (Zhang et al., 2012b), whilst genetic mouse models show that the loss of PTEN rescues locomotor defects (Domanskyi et al., 2011). In another link to oxidative stress, knockdown of PTEN reduced the levels of ROS in hippocampal cell models of PD and cerebral ischemia (Zhu et al., 2007), again verifying that targeted PTEN manipulation may ameliorate many other types of neuronal degeneration where oxidative stress is implicated (Xu et al., 2014). When constitutively active, AKT has also been found to offer neuroprotection against 6OHDA PD models through increased survival and reduced axonal loss (Ries et al., 2006), which supports the concept that manipulating the PI3K pathway is a valid neuroprotective strategy.

1.7.2 PTEN and Alzheimer's Disease

Alzheimer's disease (ALZ) is the most common neurodegenerative disorder affecting over half a million people in the UK alone. Most commonly, ALZ presents symptoms of memory loss and progressive cognitive dysfunction, whilst neuropathological tissues contain neurofibrillary tangles (NFTs) comprising hyper-phosphorylated tau, as well as insoluble β-amyloid (Aβ) plaques. In similar findings to other neurodegenerative investigations, PTEN immunoreactivity was found to be increased in organo-typic slice cultures in synthetic Aβ peptide models of ALZ, coupled with a decrease in active phosphorylated AKT, and as expected, an increase in cell death (Nassif et al., 2007). However, the relationship of PTEN in ALZ may be more complex. The pathology of

PTEN distribution in ALZ neurons shows a decrease in total protein levels of PTEN as well as increases in phosphorylated AKT, mTOR at the AKT target site Ser2448 (Chiang and Abraham, 2005), and 4EBP1, which correlate with disease progression (Griffin et al., 2005, Rickle et al., 2006, Li et al., 2005, Tramutola et al., 2015). Recently, increased phosphorylation of PI3K has also been found in ALZ and mild cognitive impairment but not in preclinical ALZ or controls (Tramutola et al., 2015). This response could indicate an up-regulation of the PI3K pathway in ALZ, which may be a reflection of an effort to rescue damaged neurons with increased protein synthesis and activated cell survival pathways. Nevertheless, recent studies have shown promising results by inhibiting PTEN in mouse models of ALZ, finding that inhibition rescued synaptic function and ameliorated defects in long term potentiation (LTP) in hippocampal neurons highlighting the cross-degenerative potential of targeting this pathway in neuronal cells (Knafo et al., 2016).

1.8 PTEN AND CANCER

With PTEN holding such a prominent role in cell survival pathways it is not surprising that before connections with neurodegeneration were established, PTEN was implicated in cancer. As a tumour suppressor gene, PTEN was discovered to be mutated in some forms of cancer including glioblastoma, breast, prostate, and kidney cancers (Myers et al., 1997, Steck et al., 1997). PTEN has also been linked to: Cowden disease (CD), a syndrome that presents multiple benign hamartomas and predisposes to breast and thyroid cancers; the associated Lhermitte-Duclos Disease (LDD) which causes seizures due to increased cerebellar glial cell growth; and juvenile polyposis coli (Liaw et al., 1997).

Genetically, the connection to cancer is thought to involve a loss of heterozygosity (LOH) of the PTEN tumour suppressor gene on chromosome 10q23.3 (Sano et al., 1999, Bostrom et al., 1998). At a cellular level, the important role of PTEN in preventing downstream activation of cell survival and growth pathways was demonstrated in experiments where wild type PTEN introduced into PTEN deficient glioma cells suppressed their growth, a suppression that was abolished with an inactive form of PTEN (Furnari et al., 1997). Additionally, constitutively active AKT and

increased phosphorylation of AKT and S6 have been found in various models of PTEN deficiency (Groszer et al., 2001, Suzuki et al., 1998, Backman et al., 2001, Stambolic et al., 2000).

Glioblastoma multiforme is the most common and most malignant glioma with a high connection to LOH of PTEN (Liu et al., 1997, Myers et al., 1997)**.** Recent studies have found that specific Glioblastoma multiforme-associated mutations in PTEN prevent PTEN localisation to the cell membrane and nucleus in a lipid phosphatase dependent mechanism, which reduces the stability of PTEN generating enzymatically inactive proteins which can no longer regulate AKT signalling(Yang et al., 2017). PTEN has been found to localise endogenously in neural tissues in the nuclei, cytoplasm as well as in the processes of various neurons, yet interestingly is absent from neurotrophic support cells such as astrocytes (Cai et al., 2009, Lachyankar et al., 2000)**.** This may explain why in some studies no PTEN mutations have been identified in astrocytomas (Duerr et al., 1998) and infers that in cases of glioblastoma genesis, the natural low expression of PTEN may be a pathogenic cause. With less endogenous protein levels at the outset any further reduction via haploinsufficiency or LOH could be detrimental. Importantly, the associated LOH of PTEN in cancer is more common later rather than earlier in tumour development (Myers et al., 1997). Further to this, recent work has also found that loss of PTEN was more common in brain metastasise in comparison to primary tumours, and is a loss which is micro-environment specific, meaning it can be restored on exposure to a different environment (Zhang et al., 2015b). Of note, the study also found that astrocytes may release exosomes containing PTEN targeting microRNAs which act on other cells to promote metastases.

In work selectively deleting PTEN in mature glial and neuronal cells of the cerebellum, no tumour formation was observed (Marino et al., 2002). One reason for this could be due to the post-mitotic non-proliferative nature of cerebellar neurons, which like motor neurons may be more resistant to neoplasia and thus more responsive to PTEN depletion. However, it could also be related to the above mentioned lack of PTEN involvement in tumorigenesis (Xiao et al., 2005). Therefore, if PTEN inhibition was used therapeutically for regenerative purposes, a transient inhibition would perhaps be beneficial to avoid potential late tumour involvement, besides the importance of specifically targeting neuronal cells of interest.

1.9 PTEN AND SMALL MOLECULE INHIBITION

Whilst many of the PTEN depletion models mentioned above involving methods such as viral vector mediated knockdown make excellent models experimentally, and the technicalities of gene therapy are constantly being perfected to allow administration of therapeutic agents past the blood brain barrier via the AAV9 serotype (Valori et al., 2010, Dayton et al., 2012, Foust et al., 2009), unfortunately, results are effective primarily in new born mice and applications of gene therapy research clinically are hindered by slow movement through to clinical trials. Therefore, other options for PTEN downregulation such as the use of PTEN inhibitors as therapeutics are compelling, and perhaps quicker alternatives. As small molecule inhibition provides a titratable and reversible response, in comparison to irreversible permanent gene therapy knockdown which may result in off-target effects, it presents an attractive solution for manipulation of a tumour suppressor protein which has in the past been a concern.

In 2004, Bisperoxovanadium (BpV) compounds were found to be new non-toxic PTEN inhibitors (Schmid et al., 2004) and when used *in vivo* in adult rats after spinal cord injury, an increased number of motor neurons was recorded at the injury site 6 weeks later compared to saline treated controls (Walker et al., 2012). Notably, Walker et al. found that administration of BpV improved coordinated limb movement compared to controls (Walker et al., 2012) and further evidence includes: BpV treatment reducing neuronal cell death post-ischemia and oxygen glucose deprivation (Shi et al., 2011a, Zhao et al., 2013, Zhao et al., 2016); increasing the regenerative ability of injured peripheral sensory neurons *in vivo* (Christie et al., 2010); and during *in vitro* human embryonic stem cell derived neuronal progenitor cell studies, a dose dependent increase in neurite outgrowth after BpV treatment was discovered (Wyatt et al., 2014). In recent studies, Walker and colleagues have further validated the use of BpV compounds for PTEN inhibition, where they have also included oligodendrocytes and Schwann cells in the neuroprotective and increased functional effects of BpV administration in models of spinal cord injury (Walker and Xu, 2014, Walker et al., 2015). In addition, the positive effects of PTEN inhibition have been found to work in other neuronal functions specifically in injured neurons, including the ability to rescue

a previously identified reduction in hippocampal long-term potentiation (LTP) and memory, caused by anaesthetic use (Wang et al., 2015b). In an interesting connection with pathological glutamate dependent excitotoxicity, BpV when administered to Sprague-Dawley rats in a model of subarachnoid haemorrhage, decreased Glutamate receptor 1 (GluR1) AMPA receptor subunit expression (Chen et al., 2015). Comparably, our work also found PTEN knockdown can reduce AMPA receptor GluR1, GluR2 and GluR3 subunit expression and decrease AMPA induced whole cell currents in iPS derived MNs (Yang et al., 2014a). Therefore, PTEN small molecule inhibition modulates multiple aspects of PTEN machinery, meaning it may be possible to ameliorate simultaneous neurodegenerative mechanisms of action through this target.

1.10 The Advent of Induced Pluripotent Stem (iPS) Cells

In 2006, Kazutoshi Takahashi and Shinya Yamanaka published findings which greatly advanced the field of genetic engineering, due to their discovery of four defined factors which induce pluripotency in differentiated somatic cells (Takahashi and Yamanaka, 2006). By demonstrating the ability to reprogram somatic cells into an embryonic–like stem cell state, their finding proved so innovative that Shinya Yamanaka shared the Nobel Prize in Physiology or Medicine with Sir John B Gurdon in 2012, for the discovery that mature cells can be made to become pluripotent, (https://www.nobelprize.org/nobel_prizes/medicine/laureates/2012/).

To induce pluripotency in somatic cells, at first the group isolated 24 genes thought to confer the maintenance of pluripotency in early embryos and embryonic-stem (ES) cells. After a process of careful elimination, 4 were revealed as sufficient to reprogram mouse embryonic and adult fibroblast cells to a progenitor-like state when retrovirally transduced into the cells (Takahashi and Yamanaka, 2006). The factors were octamer-binding protein 3/4 (Oct 3/4); krüppel-like factor 4 (Klf4); c -v-myc avian myelocytomatosis viral oncogene homolog (c-myc); and sex determining region Y(SRY)-box 2 (SOX2). After a battery of confirmatory tests, comparing their similarity to ES cells by identifying the transduced cells ability to differentiate into any cell type of the body, as well as their ability to continuously self-renew, the cells were coined induced pluripotent stem (iPS) cells (figure 1.3).

When iPS cells were inevitably later generated from human dermal fibroblasts (Takahashi et al., 2007), these new cell models brought with them the anticipation of producing “designer cells” for use in human regenerative medicine, due to the ability of iPS cells to be converted into any cell type of interest. One example would be *in vivo* re-integration of motor neurons to replace those lost in ALS, as by generating cells from the patient’s own tissues, any difficulties surrounding transplanted cell rejection can in theory be mitigated (Liu and Zhang, 2010). Important for this, later work by Thompsons group also identified Nanog and Lin28 could replace c-myc and Klf4, as when combined with Oct3/4 and Sox2 they were also sufficient to reprogram human somatic cells to pluripotency (Yu et al., 2007). Therefore, this work revealed new methods which may circumvent difficulties around potential viral integration into the host genome with the use of transcription factors such as c-myc.

1.10.1 Amyotrophic Lateral Sclerosis and iPS Cell Technology

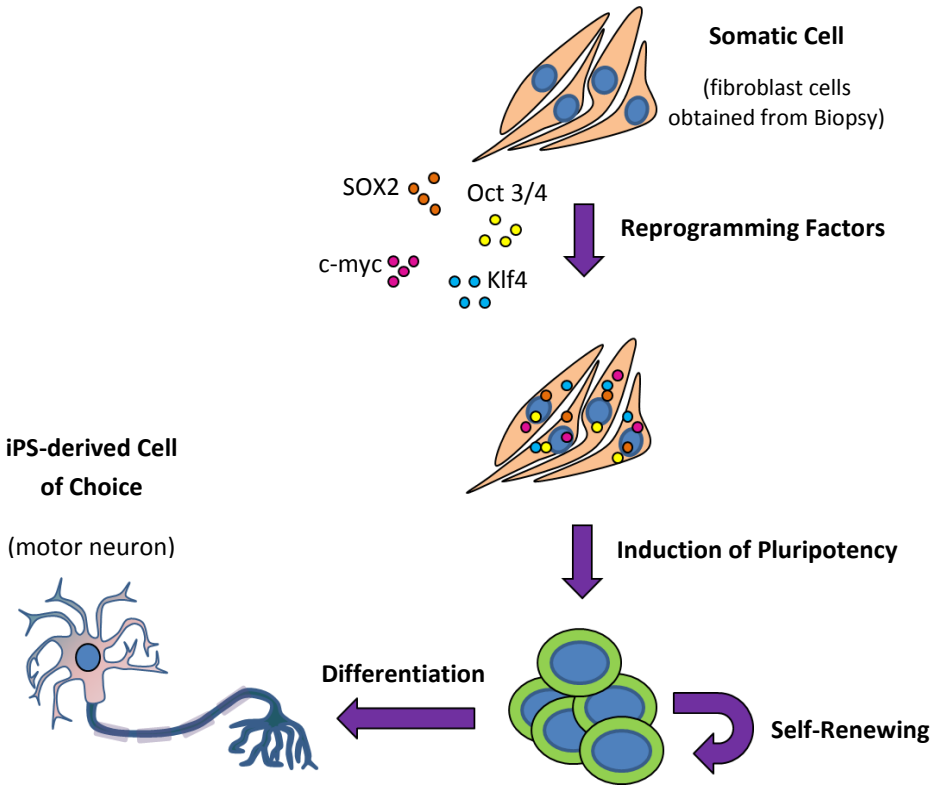

Figure 1.3: Schematic of iPS cell generation and differentiation. Somatic cells from patients with ALS or controls without ALS are removed and exposed to four reprogramming or Yamanaka factors (SOX2, Oct 3/4, c-myc, and Klf4) via retroviral transduction. Factors induce pluripotency in somatic cells to generate induced pluripotent stem cells with ability to self-renew and differentiate into any cell type of the body. iPS cells are directly differentiated into the cell of choice for investigation, in this instance the motor neuron. Abbreviations: octamer-binding protein 3/4 (Oct 3/4); krüppel-like factor 4 (Klf4); c -v-myc avian myelocytomatosis viral oncogene homolog (c-myc); and sex determining region Y(SRY)-box 2 (SOX2); induced pluripotent stem (iPS)

Several aspects of ALS make it an ideal candidate for *in vitro* iPS cell modelling. Firstly, unlike other cells from the human body, motor neurons cannot be obtained from living donors and post-mortem material may not accurately represent disease pathogenesis or progression, as these are the cells that have endured the disease and therefore only represent the final stages of ALS. In addition, the degeneration and loss of motor

neurons as a fundamental characteristic of ALS highlights an obvious need for the production of human cellular models to mimic the cells which degenerate. Therefore, iPS-derived cell models of motor neurons could provide an ongoing supply of motor neuron-like cells for investigation. Secondly, alternative methods to model ALS each hold inherent limitations. For example, embryonic stem (ES) cell models of both human and non-human origin have been used in the past with some success in ALS research (Di Giorgio et al., 2007). However, it is difficult to produce ES cells which are disease and patient specific (Takahashi et al., 2007); a particularly pertinent point for a disease which manifests in later life, as the ES cells would have to be obtained before disease onset from foetal tissue. Alongside this iPS derived-cell models are able to provide a tangible model of a disease with an unknown genetic background, for example sporadic forms of the disease. Finally, there is no need to overcome the inherent technical challenges of manipulating a large repeat expansion with iPS-derived cell models, important in the light of recent genetic mutations discovered in C9ORF72 (DeJesus-Hernandez et al., 2011) . Even now, although animal models of C9ORF72 are available, unlike SOD1 animal models of the past (Gurney et al., 1994, Bruijn et al., 1997), they have been found to present weaker phenotypes and do not fully recapitulate disease, possibly due to poor representation of repeat length (Koppers et al., 2015, Peters et al., 2015). Of note, mouse models with stronger phenotypes of ALS, such as that of the SOD1 mutant mouse, have failed to generate any drugs that ameliorate disease more than the currently prescribed Riluzole (Benatar, 2007). Whilst these studies may reflect the poor ability of mouse models of all genotypes to accurately recapitulate the human disease of ALS, as the expansion mutation is found to be naturally stably expressed in fibroblasts and iPS cells, it makes them a relevant model for investigating this form of ALS.

Dimos et al. were the first group to make use of the newly discovered technology for ALS by reprograming human fibroblast cells from an 82 year old female with a familial SOD 1-realted form of the disease (Dimos et al., 2008). Whilst it is likely that the mechanisms underpinning disease occur years before symptoms present, this study confirmed that mature motor neuron-like cells as evidenced by marker expression, can be developed as models for the disease. Additional studies have generated motor neurons for other forms of motor neuron disease, including spinal muscular atrophy

(SMA) a childhood form of the disease (Ebert et al., 2009). In contrast to the previous study, fibroblast cells from a child were converted to iPS cells which were shown to effectively reprogram, differentiate into motor neurons and glia, and mimic traits of SMA including showing reduced SMN transcripts, an indicator of disease (Ebert et al., 2009). Furthermore, in an extension of the work by Dimos and colleagues, studies have been able to measure neuronal cell electrical activity, generating mature electrically active cells capable of displaying action potentials on depolarising stimulation (Karumbayaram et al., 2009, Sareen et al., 2013, Wainger et al., 2014, Devlin et al., 2015).

Together, this evidence suggests human iPS-derived cell models of ALS are an excellent resource to model the human disease of ALS. They provide an opportunity to examine how motor neuron-like cells react to disease modifying treatments, which due to their similarity to their human counterparts, could provide a more accurate representation of the endogenous response in patients and lead to translatable clinical findings.

1.11 Conclusion

As PTEN has a central role in cell survival pathways, it is important to exert caution in relation to using PTEN manipulators as therapeutic agents. Although the balance can be tipped in favour of either cell death and neurodegeneration or cell survival and tumorigenesis in certain disease states, this does not mean that the PTEN signalling pathway cannot be targeted for disease modifying treatments, as long as specific and carefully controlled neuronal targets were established beforehand. For example when PTEN knockdown is employed, to avoid systemic deletion and limit targeting to the disease affected cells, only specific viral or promoter selection could be used.

Interestingly, collective studies point to the idea that PTEN manipulation will need to vary across neurodegenerative targets, in particular reference to the results found in ALZ research discussed above. In addition creative new techniques for PTEN manipulation will need to be further investigated, especially as new methods have been recognised from molecules that interact with PTEN endogenously such as NEDD4. Overall, these studies identify possible endogenous mechanisms to mediate

neuroprotection in neurodegenerative diseases, underscore the importance of PTEN in multiple cases of neuronal cell survival and qualifies PTEN manipulation as an important therapeutic target for many forms of neurodegeneration.

In ALS, the specific degeneration of motor neurons is a consistent and causative feature of disease, which subsequently removes their important function from the human body. Whilst many interesting studies have identified new potential causes for ALS, identifying new genes of interest, including that of C9ORF72, we are still in the process of identifying why these mutations cause ALS and why the more prevalent sporadic ALS population is also affected. Whilst these studies are imperative to understanding the disease as a whole, by identifying techniques to target the survival of the cells which die in ALS, it may help provide translatable and quicker therapies which may supersede the poor alternatives currently available for patients.

The advances in genetic engineering, cellular and molecular biology now mean we work in an era with exciting and potentially life changing methodologies. Induced pluripotent stem cell technology is one of these. These new models of disease could potentially act as better models of ALS than those currently available for several reasons. The patient iPS cell-derived motor neurons would contain pathogenic genetic changes inherently as they would be generated from somatic cells containing the mutation, which would also mean they would be human in origin. Additionally, as motor neuron- like cells they would be a near example of the cells affected in ALS including characteristics such as being post-mitotic and non-dividing: an advantage compared to some of the current models used for ALS research, for example Neuroblastoma spinal cord (NSC)-34 cells which do not have these features. Therefore, by employing the use of a cellular model which not only counteracts caveats found in other cell models for ALS research, but provides new opportunities to discover therapies for ALS in a self-renewing capacity, together in combination with previously established cell models, we may be able to make steps towards ameliorating the devastating disease of ALS.

1.12 Aims and Objectives

1.12.1 PTEN Manipulation

The primary aims of this project are to identify if PTEN manipulation via inhibition of its activity or reduction of the total protein levels positively impacts the survival pathways and thus cellular survival of cell models of Amyotrophic Lateral Sclerosis (ALS). We will first work up methodologies in simpler and established cell lines and models of ALS including NSC-34 cells and primary fibroblast cells, whilst optimising iPS differentiation protocols. We will study the role of PTEN modulation using small molecule activators and knockdown, with a goal of comparing the effects of PTEN manipulation across all the models investigated. We will note how the changes in PTEN status affects components of the AKT cell survival cascade, as well as monitor the effect on cell survival through cell number in patient and control cells. We will also note any changes in the differentiation and maturation of iPS cells to motor neurons after PTEN manipulation through motor neuron cell counts, to identify whether or not the genetic background of mutated C9ORF72 makes a difference to the positive effects previously seen in PTEN manipulation studies in ALS and neurodegenerative research.

1.12.2 iPS Cell Differentiation and Characterisation

We aim to generate induced pluripotent stem (iPS) cell- derived motor neurons, by using three age and sex matched patient and control fibroblast cells with a genetic background from the newly discovered C9ORF72 hexanucleotide repeat expansion, proposed to be implicated prominently in ALS pathogenesis (Renton et al., 2011). The originating iPS cells will be converted from patient and control fibroblast cells, via transfection with retroviral vectors encoding 4 Yamanaka Factors, and will be subsequently directed into the fate of motor neurons. The cells will be monitored and tracked in their progression to a neuronal and motor neuronal identities by techniques such as immunocytochemical (ICC) staining of generated cells with known markers of differentiation. Once generated, by examining the cell survival through the number of

these iPS derived cells, we can determine if any differences occur between basal control and C9ORF72- ALS iPS derived cells, which will highlight any patient specific vulnerabilities of the model. For a final authentication of the motor neurons generated, electrophysiological studies will be performed to identify the ability of motor neurons to generate action potentials and convey electrical characteristics associated with a mature motor neuron. In a further step, characterisation will also include examining the maintenance of the expansion in the cell models post-differentiation via identification of ALS-specific molecular pathologies. This will be observed through the presence of newly established hallmarks of the hexanucleotide repeat expansion, including RNA foci and the presence of dipeptide repeat proteins, which will be identified through RNA FISH and ICC techniques respectively. Their identification if any, will also act to further validate or negate proposed hypotheses of C9ORF72-related causes of pathogenesis in ALS.

This thesis aims to study the potential role of modulating PTEN in the PI3K pathway in motor neuron models of ALS, using both genetic engineering and small molecule approaches. This is with the hope of validating the pathway and finding a potential therapeutic agent that could translate to a human clinical trial.

CHAPTER 2 : MATERIALS AND METHODS

2.1 Cell Culture

2.1.1 Neuroblastoma spinal cord (NSC)-34 Cell Culture

Neuroblastoma Spinal cord (NSC-4) cells were cultured on 10cm^2 Nunclon^{TM} Surface plates (Nunc) in Dulbecco's Modified Eagle's Medium (DMEM) (Sigma) with 10% Fetal Calf Serum (Biosera) and additional 1% L- glutamine (Lonza). The NSC-34 cells that were stably transfected with pIRESneo (Clontech, Saint-Germain France) using Lipofectamine 2000 (Invitrogen) with empty vector (pIRES cells), pIRESneo containing wild type human SOD1 (WT SOD1 cells), or pIRESneo containing mutant human SOD1 G93A (G93A cells). For the WT SOD1, pIRES and G93A cells, G418 Sulphate (250µg/ml) (Geneticin) was used to select for the vector. Cells were split no more than 1 in 5, and harvested by washing the cells gently from the plates. Due to the high metabolic activity of the cells, a full media change was required every 2 to 3 days. Cell stocks were defrosted into 10cm^2 dishes by adding warm media to the frozen vial and plating immediately to 10ml of media without G418. When they had reached a confluence of 30- 40% density, G418 was then added. All cells were kept at 37˚C in humidified incubators with 5% carbon dioxide.

2.1.2 Primary Fibroblast Cell Culture

Primary Human Fibroblasts cells were cultured from skin biopsies produced in SITraN by Anne Gregory and the technical team from three C9ORF72 positive ALS patients (C9ORF72) and three aged and sex matched controls (Control) (Table 1). All samples were collected after correct ethical permission was granted (REC 12/YH/0330 NRES Committee Yorkshire & the Humber-Sheffield). Cells were cultured in 75cm^2 Nunclon^{TM} treated flasks blue filter cap (Nunc) or 10cm^2 plates in Dulbecco's Modified Eagle's Medium (DMEM) (Gibco) with 10% Foetal Bovine Serum (FBS) (Biosera), 1% Penicillin Streptomycin (Lonza), 1% Minimum Essential Medium Non-Essential Amino Acid (Gibco) and 1% GlutaMAX^{TM}(Gibco) (full media). Cells were kept at 37˚C in humidified incubators with 5% carbon dioxide.

Cells were harvested by removing media from the flasks and washing twice with Phosphate Buffered Saline (PBS) to remove any remaining media. For each flask or plate, 5ml or 4ml respectively of 1X Trypsin (Lonza) was added and vessels were incubated at 37˚C for 2 minutes or until the cells had detached from the base of the flask. Subsequently 10ml of Full media from the cells was added to quench the trypsin. Cells were then spun down at 400g relative centrifugal force (RCF) for 4 minutes and re-suspended in 12ml of media for splitting between flasks or plates.

Table 2.1: Aged and sex matched primary fibroblast cells from C9ORF72 patients and controls.

Pair	C9ORF72		CONTROL	
	Code	Sex / Year of birth	Code	Sex / Year of birth
1	FIBMND 3009	Female / 1952	CON 159	Female / 1949
2	FIBPAT 206	Female / 1945	CON 195	Female / 1944
3	FIBMND 3026	Male / 1962	CON 170	Male / 1948

2.1.3 Human Embryonic Kidney (HEK) 293 Cell Culture

Human embryonic kidney (HEK) 293 cells were cultured in 10cm^2 Nunclon^{TM} surface plates (Nunc) with 10% FBS and 1% Penicillin Streptomycin (Lonza). Cells were grown until 80% confluence on which they were split no more than 1 in 5 via gently washing the cells from the plate, without the use of enzymes. Cells were kept at 37˚C in humidified incubators with 5% carbon dioxide.

Cells were harvested by removing media from the flasks and gently washing the cells from the base of the plate. Cells were then spun down at 400 RCF for 4 minutes and re-suspended in 12ml of media for splitting between plates.

2.1.4 iPS Cell Maintenance and Differentiation

The iPS cells were grown on a monolayer. The monolayer was prepared by first coating a T25 cm^2 Nunclon™ flask (Nunc) with 0.1% gelatin (Sigma) and then adding a layer of mouse embryonic fibroblast (MEF) cells. The MEF cells were previously treated with 10µg/ml mitomycin-C (American Type Culture Collection), an antineoplastic antibiotic that inhibits DNA synthesis to prevent the division of fibroblasts yet allowing the cells to survive and produce key proteins such as LIF (Leukemia inducing factor) which support the renewal of stem cells.

The iPS cells were first cultured in "iPSC media" containing DMEM/F12 (Gibco), 20% knockout serum replacement (KSR, Gibco), 1% non-essential amino acids (NEAA, Gibco), 1% GlutaMAX (Gibco), 0.1 mM β-mercaptoethanol (Sigma), 4ng/ml basic fibroblast growth factor (bFGF, Invitrogen), 1% penicillin streptomycin (Lonza) and were incubated at 37°C, 5% CO2. The media was changed every 24 hours until colonies had formed.

In order to generate motor neurons, iPS colonies were passaged using 1mg/ml collagenase type IV (Gibco), triturated into smaller cell clumps and plated onto T25 cm^2 flasks with a layer of MEF cells at 80 % confluence, or onto 4, 10mm coverslips (VWR International) in CELLSTAR® 35x10mm culture dishes with 4 inner rings (Grenier Bio-one). For each media change throughout differentiation, the cells in T25 flasks were kept in 4ml of media, whilst the cells plated onto coverslips were kept in 2ml of media.

For days 1 and 2 of differentiation, the colonies were cultured in iPSC media, containing 10 µM Y27632 Rho-associated kinase inhibitor to enhance single cell survival, 0.2 µM LDN193189 for neuralization and 20 ng/ml bFGF (Invitrogen) to enhance growth. On day 3, cells were maintained in a "neural induction media" comprised of "iPS media" without β-mercaptoethanol, but with added 2µg/ml heparin (Sigma), and 1% N2 supplement (Gibco). On day 5, 1µM all-trans retinoic acid (RA, Sigma) along with 0.4 µg/ml ascorbic acid (Sigma), and 10ng/ml brain derived neurotrophic factor (BDNF, Sigma) was added to modulate and enhance the differentiation and maturation of neurons. On day 7 hedgehog signalling was initiated

by application of 200 ng/ml sonic hedgehog (SHH, R&D Systems) and 1µM purmorphamine (PUR, Selleckchem) until day 29 when the media was changed to "neurobasal media" (Invitrogen) containing 1% NEAA, 1% GlutaMAX, 1% penicillin streptomycin, 2% horse serum, 2% B27 supplement (Gibco), with 1µM RA, 10ng/ml insulin-like growth factor (IGF, Gibco), 10ng/ml glial derived neurotrophic factor (GDNF, Gibco), 10ng/ml ciliary neurotrophic factor (CNTF, Sigma), 1µM adenosine 3',5'-cyclic monophosphate (cAMP, Sigma). At day 30, cells were dissociated with 1X trypsin (Lonza) and plated onto poly-DL-ornithine hydrobromide (Sigma) and natural mouse laminin (Invitrogen) coated culture dishes or 10mm coverslips (VWR International). Cells were plated on coverslips at densities of 5000, 10 000, 20 000 or 40 000 cells per coverslip; 20 000 cells per 12 well; and 100 000 to 200 000 cells per 6 well. At day 30, cells were cultured in the same media as above with addition of 200 ng /ml ascorbic acid (Sigma). Cells were cultured up to 12 weeks, maintained at 37˚C in humidified incubators with 5% carbon dioxide.

Table 2.2: iPS cell differentiation protocol, including schedule for addition of factors and concentrations used.

Day of Differentiation	Media	Factor	Concentration	Supplier	Additional Information
1-2	iPS Media	Y27632 Rho-associated kinase inhibitor	10 µM	LTK Laboratories (#Y1000)	Enhances single cell survival (Watanabe et al., 2007)
		LDN193189	0.2 µM	Biovision (#1995-5,25)	Inhibits BMP type I receptors which co-ordinate endoderm and mesoderm developmental patterning to promote differentiation of neural progenitor cells from human pluripotent stem (Boergermann et al., 2010)
		basic Fibroblast Growth Factor (bFGF)	20 ng/ml	Gibco (#PHG0264)	Growth enhancement and mitogenic agent, important for SHH expression (Kitchens et al., 1994)
3- 4	Neural Induction Media	n/a	n/a	n/a	n/a
5- 6	Neural Induction Media	All trans-Retinoic acid	1 µM	Sigma (#R2625)	Induces caudal neurons and promotes differentiation of neurons through the modification of neuronal cell surface receptors (Scheibe and Wagner, 1992)

		Ascorbic acid	0.4 µg/ml	Sigma (#A1300000)	Enhances differentiation (Takahashi et al., 2003)
		Brain-Derived Neurotropic factor (BDNF)	10ng/ml	Sigma (#B3795)	Neurotrophic, enhances survival and differentiation of neurons (Jones et al., 1994)
7-16	Neural Induction Media	All trans-Retinoic acid	1 µM	See above	See above
		Brain Derived Neurotropic factor (BDNF)	10 ng/ml	See above	See above
		Sonic Hedgehog (SHH)	200 ng/ml	BioLegend (#597204)	Ventralisation through morphogen patterning midline structure of the spinal cord and brain (Carpenter et al., 1998)
		Purmorphamine (PUR)	1 µM	Selleckchem (#S3042)	Activates Hedgehog pathways by binding and activating smoothened (Sinha and Chen, 2006)
17-29	Neurobasal Media	All trans-Retinoic acid	1 µM	See above	See above
		Adenosine 3', 5'- cyclic monophosphate (cAMP)	1 µM	Sigma (#A9501)	Determinant of neuronal differentiation. Important second

				messenger for neurotransmitter induced receptor stimulation (Stachowiak et al., 2003)
	Insulin-like Growth Factor 1 (IGF-1)	10 ng/ml	Gibco (#PHG0071)	Family members of insulin-like growth factors structurally homologous to proinsulin
	Glial-Derived Neurotrophic Factor (GDNF)	10 ng/ml	Gibco (#PHC7045)	Promotes the survival and differentiation of dopaminergic neurons in culture, and prevents the apoptosis of motor neurons (Lin et al., 1993)
	Ciliary Neurotrophic Factor (CNTF)	10ng/ml	Gibco (#PHC7015)	Neurotropic factor supporting survival of neurons and regulates their differentiation and maturation (Vergara and Ramirez, 2004)

30-42+	Neurobasal Media	All trans-Retinoic acid	1 µM	See above	
		Adenosine 3', 5'- cyclic monophosphate (cAMP)	1 µM	See above	
		Insulin-like Growth Factor 1 (IGF-1)	10 ng/ml	See above	
		Glial-Derived Neurotrophic Factor (GDNF)	10 ng/ml	See above	
		Ciliary Neurotrophic Factor (CNTF)	10ng/ml	See above	
		Ascorbic acid	0.2ug/ml	See above	
		2-mercaptoethanol	0.1mM	Gibco (#21985-023)	A potent reducing agent used to prevent toxic levels of oxygen radicals in media

2.2 Cell Lysis

For pelleting cells to store at -80°C for future lysis, cell pellets were re-suspended in 1ml sterile PBS, and cells were transferred to a 1.5ml tube for centrifugation at 400g RCF for 4mins. Next, the PBS was completely removed to produce a dry pellet which was stored at -80°C. All cells were lysed via membrane, nuclear, and cytoplasmic fractionation using 50µl of lysis buffer per pellet of 1 000 000 cells, containing: Radio immunoprecipitation assay **(**RIPA) buffer, complete Mini, EDTA free Protease Inhibitor cocktail (Roche) and PhosSTOP, phosphatase inhibitor cocktail (Roch) and kept on ice for 20 minutes. Next cells were centrifuged at 10,800g RCF for 10 minutes at 4˚C, and the supernatants were collected for protein determination using a Bradford assay.

2.3 Protein Determination

In the Bradford assay for protein determination, 2µl of 1, 0.5, 0.25, 0.125, 0.0625 and 0.03125 mg/ml Bovine Serum Albumin (BSA) (Sigma) was added to 50µl of Coomassie Protein Assay Reagent (Thermo Scientific) to produce a standard curve. Next 2µl of cell lysate, diluted in PBS to 1 in 10 and 1 in 20, was added to 50µl of Coomassie Protein Assay Reagent. Wells were carefully mixed with a multichannel pipette and any bubbles were popped with a needle. Absorbance was read at 595nm using a PHERAstar FS plate reader (BMG labtech) and values were calculated from raw data using Microsoft Excel.

2.4 Western Blotting

2.4.1 Sodium dodecyl sulphate polyacrylamide gel Electrophoresis (SDS-PAGE)

For western blot analysis, cell lysate protein extracts, previously measured for protein concentrations were added to Lamelli sample buffer (4x) and made up to volume with ddH_2O (table 2). The samples were vortexed and heated at 95°C for 5 minutes in order

to reduce and denature the proteins, and the samples were finally spun in a microfuge to ensure the whole volume of the sample was collected.

Table 2.3: Preparation for Lamelli buffer (10ml)

Lamelli Sample Buffer (4X)	
Glycerol	4ml
10% SDS	2ml
Bromophenol blue	0.25mg
Stacking Gel Buffer (table)	2.5ml
B-mercaptoethanol	0.5ml
dH2O	to 10ml

40µg/µl of denatured protein cell lysates were resolved by 10% sodium dodecyl sulphate polyacrylamide gel electrophoresis (SDS-PAGE) (table 3 and 4) used with a 5% stacking gel (table 5 and 6). Gels were run at a constant voltage in running buffer (table 7) at 50V for 30 minutes or until through the stacking gel, and then 120V until the dye front reached the base of the gel.

Table 2.4: Preparation for separating gel buffer (100ml, pH adjusted with HCL and NaOH)

Separating Gel Buffer pH 8.8	
Tris Base	18.17g
10% SDS	4ml
dH2O	to 100ml

Table 2.5: Preparation for separating gel for SDS-PAGE (For 2 gels of 1.5mm thickness)

	10% Separating Gel (ml)
H_2O	9.3ml
30% Acrylamide	7.2ml
Separating Gel Buffer	5.7ml
10% APS	0.336µl
Tetramethylethylenediamine (TEMED)	0.15µl

Table 2.6: Preparation for Stacking gel buffer (100ml, pH adjusted with HCL and NaOH)

Stacking Gel Buffer pH 6.8	
Tris Base	6.06g
10% SDS	4ml
dH_2O	To 100ml

Table 2.7: Preparation of Stacking gel for SDS-PAGE (for 2 gels of 1.5mm thickness)

	5% Stacking Gel (ml)
H_2O	2
30% Acrylamide	0.6
Stacking Gel Buffer	0.888
10% APS	0.056
TEMED	0.10

Table 2.8: Preparation of Running buffer for SDS-PAGE (700ml)

Running Buffer	
Tris-Glycine (5X)	200ml
H2O	490ml
10% SDS	10ml

2.4.2 IMMUNOBLOTTING

Proteins were transferred to a methanol rinsed polyvinylidene difluoride (PVDF) membrane (Millipore) according to the manufacturer's instructions under constant current 250mA for 1 hour 30 minutes, or 40mA overnight on ice in transfer buffer (table 8). To check that the transfer was successful and to confirm equal loading, membranes were probed with Ponceau dye for 30 seconds. Next, to remove the Ponceau, membranes were washed with Tris-Buffered Saline with Tween 20 (TBST) for 10 minutes. Subsequently, membranes were blocked to prevent non-specific binding

of primary antibodies in 5% BSA-TBST (Sigma) rolling for 1 hour at room temperature or overnight rolling at 4˚C. Membranes were incubated overnight with primary antibodies (table 9) made in 5% BSA-TBST. Next, membranes were washed 3 times for 15 minutes in TBST at room temperature and then probed with the appropriate secondary antibodies made in TBST for 1 hour rolling at room temperature (table 10).

Table 2.9: Preparation of transfer buffer for SDS-PAGE (1000ml)

Transfer Buffer	
Tris-Glycine (5x)	200ml
Methanol	150ml
dH_2O	650ml

Table 2.10: Primary antibodies used for Western Blotting

Antibody	**Molecular Weight (kDa)**	**Species**	**Concentration**	**Supplier**
Phospho-AKT(Ser473) (D9E) XP	60	Rabbit Monoclonal	1:500	Cell Signaling Technology
AKT(pan) (C67E7)	60	Rabbit monoclonal	1:500	Cell Signaling Technology
PTEN (26H9)	54	Mouse monoclonal	1:1000	Cell Signaling Technology
pPTEN (s380)	54	Rabbit polyclonal	1:1000	Cell Signaling Technology
GAPDH	37	Rabbit monoclonal	1:10 000	Cell Signaling Technology

Table 2.11: Secondary antibodies used for Western Blotting

Antibody	**Species**	**Concentration**	**Supplier**
Goat anti-rabbit HRP	Rabbit polyclonal	1:5000	Dako
Goat anti-mouse HRP	Mouse polyclonal	1:5000	Dako

2.4.3 Image Capture and Densitometry Analysis

Protein bands were visualized with a chemiluminescence detection system (Biological industries) and a G-BOX imaging system with GeneSnap software (Syngene). Blots were captured using Intelli Chemi which detects the signal from the membrane to generate a sub-saturated image.

To determine the relative levels of protein for each immunoblot, densitometry analysis on GeneTools (Syngene) software was used. Manual band quantification was used with automatic background correction, to measure percentage raw volume and quantity for each band. Protein levels were determined as a fraction to loading control Glyceraldehyde 3-phosphate dehydrogenase (GAPDH). Where more than one membrane was required, each membrane contained both a basal and vehicle control, which was used as a baseline to normalise to, to ensure consistency.

2.5 Biochemical Assays

2.5.1 3-(4,5-Dimethylthiazol-2-yl)-2,5-Diphenyltetrazolium bromide (MTT) assay

To measure cell viability, NSC-34, primary human fibroblasts, and iPS derived cells were plated in a Cellstar® 96 well culture plates (Greiner bio-one), in 100µl of the correct full media for the cell type and left for 3 days to attach. Cell viability was assessed by adding 0.1 volumes of 5mg/ml thiozolyl blue tetrazolium bromide (Sigma) in PBS to each well and the plate was incubated for 1 hour (NSC-34 cells) or 6 hours (primary human fibroblasts, iPS- derived motor neurons) so the insoluble purple formazan product could be formed in viable cells. Next, the formazan product was dissolved in 20% sodium dodecyl sulphate (Sigma) in 50% dimethyl formamide (Sigma), pH 4.7 (SDS/DMF) and mixed at room temperature on an orbital shaker for 1 to 2 hours. Once the crystals had fully dissolved, the solution was mixed with a multichannel pipette and bubbles popped before absorbance was read at 595nm using a PHERAstar FS plate reader (BMG labtech).

2.5.2 Lactate Dehydrogenase (LDH) Assay

A Thermo Scientific Pierce LDH Cytotoxicity Assay Kit (Thermo-fisher) was used to measure cell cytotoxicity via LDH release into the media. Firstly, primary human fibroblasts, and iPS derived cells were plated in 96 well culture plates, in 100µl of the correct full media for the cell type and left for 3 days to attach. Duplicate wells were plated for each of the 6 control and patient cell samples and extra wells were plated also in duplicate for spontaneous and maximum LDH controls. Cytotoxicity was measured via collection of the media from all conditions, samples and time points, as well as from spontaneous and maximum LDH controls for quantification of cellular cytotoxicity following protocol in the Thermo Scientific Pierce LDH Cytotoxicity Assay Kit. Absorbance was read at 490nm and 680nm using a PHERAstar FS plate reader (BMG labtech).

2.5.3 CyQUANT® Cell Proliferation Assay

A CyQUANT® Cell Proliferation Assay Kit (Invitrogen, #C7026) was used to measure cell number and proliferation. Primary human fibroblasts, were plated in triplicate in 96 well culture plates in 100µl of full media and left for 3 days to attach. The plates were then washed once with sterile PBS to remove any remaining media containing phenol red to avoid interference with the reading, and plates were then frozen at -80°C. When ready to perform the cell count the cells were thawed and instructions were followed according to the CyQUANT® Cell Proliferation Assay Kit following the protocol for the cell proliferation assay including a serial dilution of cells to quantify cell number. Fluorescence was read at 480/520nm for CyQUANT® GR dye bound to nucleic acids.

2.6 Model Characterisation and Assay Development

2.6.1 IPS- Derived Cell Counts- 6 to 12 Weeks Post Differentiation

For basal iPS-derived cell counts differentiated iPS cells were first plated at 6 weeks of differentiation. For PTEN knockdown assays, cells were first plated at 5 weeks of differentiation, to allow for the additional period of lentiviral vector treatment at 6 weeks of differentiation. For both cell counting assays, cells were plated at a density of 1000 cells per 10mm coverslip, with 4 coverslips plated for each sample, patient or control, and if applicable condition, untransduced, green fluorescence protein (GFP), Scrambled or PTEN knockdown.

Manual cell counts were performed by counting the 4 separate coverslips for each sample and condition. Three random fields of view per coverslip at a 10x objective were used in each cell count covering 80% of the total coverslip. Cells counts were taken each week from week 7 up to 12 weeks of differentiation and the same coverslips were tracked counted at each cell count.

2.6.2 Fibroblast Scriptaid Treatment for Dose response assays and Western Blot Analysis

For the treatment of primary human fibroblast cells with Scriptaid (Calbiochem), 750 000 cells were plated onto 10cm^2 plates (western blotting) or 1000 cells per well were plated into 96 well plates (dose response assays) and left to attach for 48 hours. Prior to treatment the media was replaced with 10ml of serum free media (minimum media) for a serum starvation for 2 hours in order to reduce growth factor receptor activation. This was subsequently replaced with 10ml minimum media containing 0.3% DMSO (vehicle), or 3µM, 10µM or 30µM of Scriptaid with a final DMSO concentration of 0.3%. Control plates were also set up for non-treated control with cells growing in full media (basal). Cells were incubated for 24 hours at 37˚C and finally harvested for western blot analysis as previously described in sections 2.2, 2.3 and 2.4, or assayed for dose response as previously described in section 2.5.

2.6.3 IPS-Derived Cell Scriptaid Treatment for Dose response assays and Western Blot Analysis

For the treatment of differentiated iPS cells with Scriptaid, firstly 100 000 cells were plated onto 6 well plates (western blotting) or 2000 cells per well were plated into 96 well plates (dose response assays) and left to attach and left to attach for 3 days. The iPS cells were then grown in serum free media containing 0.3% DMSO (vehicle), or 3µM, 10µM or 30µM of Scriptaid with a final DMSO concentration of 0.3%. Control plates were also set up for non-treated control with cells growing in full media (basal). Cells were incubated for 24 hours at 37˚C and finally harvested for western blot analysis as previously described in sections 2.2, 2.3 and 2.4 or assayed for dose response as previously described in section 2.5.

2.6.4 iPS-Derived Cell Scriptaid Treatment for Motor Neuron Cell Counts

For the treatment of iPS cells during the differentiation process, iPS cells were plated on coverslips in their undifferentiated state. They were incubated with one of the following: 3µM Scriptaid for treated conditions, 0.3% DMSO for vehicle control conditions, or full media only for basal control conditions. The incubation period occurred either for 24 hours at day 0, or week 2, 4, or 6 of differentiation in a single application of the drug, or each week at weekly intervals from day 0. At the end for the differentiation protocol at 6 weeks, the cells were fixed as described above and dual stained for choline-O-acetyltransferase (ChAT) and neuron-specific class III β-tubulin (Tuj1) as described in the protocol for immunocytochemistry.

2.6.5 Immunocytochemistry

For immunocytochemistry undifferentiated iPS cells and those differentiated for 2, 4, 6, 9 and 12 weeks were stained. The media was removed from the cells and they were washed once in 1ml Dulbecco's phosphate-buffered saline (dPBS) (Gibco) to remove

cell debris. Cells were then fixed in sterile filtered 4% paraformaldehyde (PFA, Sigma) in PBS for 15 minutes at room temperature. Permeabilization and blocking was achieved by exposing cells to a buffer of 0.25% Triton-PBS with 10% goat serum (Gibco). Cells were incubated overnight (unless otherwise stated) at 4°C with the primary antibody (table 11). The primary antibody was then removed completely and cells were washed 3 times for 5 minutes in 1ml PBS. The appropriate fluorescent secondary antibody was then applied for 2 hours in the dark at room temperature (table 12). Next the secondary antibody was removed and the cells were incubated with Hoechst 1µg/ml (Cell Signalling Technologies) for 5 minutes at room temperature in the dark, and the cells were finally washed 4 times for 10 minutes in 1 ml PBS. Coverslips were mounted onto glass twin frost 0.8-1mm microscope slides (Fisher brand) using 10µl fluorescent mounting medium (Dako) and left to dry completely, in the dark, before sealing with clear nail varnish. Slides were stored at 4°C in dark, until visualisation using an IN CELL Analyser 2000 (GE Healthcare).

Table 2.12: Primary antibodies, concentrations and incubation periods.

Primary Antibody	Host/Isotype	Concentration	Incubation	Supplier
TuJ-1 (neuron-specific class III β-tubulin)	Mouse Monoclonal IgG2A	1:100	Overnight, 4°C	Neuromics (#MO15013)
Anti-Beta III Tubulin	Chicken Polyclonal IgY	1:100	Overnight, 4°C	Chemicon International (#AB9354)
Anti-SSEA4 (stage-specific embryonic antigen 4)	Mouse Monoclonal IgG3	1:50	Overnight, 4°C	Invitrogen (#41-4000)
MAP-2 (microtubule associated protein)	Mouse Monoclonal IgG1	1:50	Overnight, 4°C	Neuromics (#MO30000)

ChAT (choline-O-acetyltransferase)	Mouse Monoclonal IgG, Kappa	1:50	3 Days, 4°C	Neuromics (#MO20019)
Anti-TRA-1-60	Mouse Monoclonal IgM	1:50	Overnight, 4°C	Invitrogen (#41-1000)
c-Myc	Rabbit Affinity purified (EQKLISEEDL)	1:100	Overnight, 4°C	Neuromics (#RA25085)
HB9/pan MNR2	Mouse Monoclonal IgG1,Kappa Light chain	1:50	Overnight, 4°C	Developmental Studies Hybridoma Bank (DSHB) (81.5C10)
Islet 1/2 (H-120)	Rabbit polyclonal	1:50	Overnight, 4°C	Santa Cruz Biotechnology (# sc-30200)
Anti-GA	Mouse (clone 5F2)		Overnight, 4°C	Gifted by Dieter Edbauer
TDP-43	Rabbit polyclonal	1:200	Overnight, 4°C	Proteintech (#10782-2-AP)
PTEN (Y184)	Rabbit monoclonal	1:50	Overnight, 4°C	Abcam (#ab32199)

Table 2.13: Secondary Antibodies, concentrations and incubation periods

Secondary Antibody	Isotype	Concentration	Incubation	Supplier
Rabbit Anti-Mouse FITC	Polyclonal IgG	1:200	2 hours, room temperature	Dako (#F0232)
Rabbit Anti-Mouse TRITC	Polyclonal IgG	1:200	2 hours, room temperature	Dako (#R0270)
Swine Anti Rabbit TRITC	Polyclonal IgG	1:200	2 hours, room temperature	Dako (#R0150)
Swine Anti-Rabbit	Polyclonal	1:200	2 hours, room	Dako (#F0205)

FITC	IgG		temperature	
Alexa Fluor 488 Goat Anti Chicken	IgG (H+L)	1:500	2 hours, room temperature	Invitrogen (#A11039)
Alexa Fluor 488 Donkey Anti-Rabbit	IgG (H+L)	1:1000	2 hours, room temperature	Invitrogen (#A21206)
Alexa Fluor 555 Donkey Anti-Mouse	IgG (H+L)	1:1000	2 hours, room temperature	Invitrogen (#A51570)

2.6.6 RNA Fluorescent In situ Hybridisation (RNA FISH)

All solutions were made in DEPC treated ddH20. Coverslips fixed with 4% PFA (as described above) placed in a 24 well plate were incubated at 66°C for 1 hour in hybridisation buffer containing, 100mg/ml dextran sulphate, 2X saline sodium citrate buffer pH5 with citric acid (SSC), 50mM sodium phosphate pH 7, 50% formamide. A 5' TYE-563-labelled LNA (16-mer fluorescent)-incorporated DNA probe was used against the sense RNA hexanucleotide repeat (Exiqon Inc, batch #607323) or antisense RNA hexanucleotide repeat (Exiqon Inc, batch #610331). Both sense and anti-sense probes were heated for 75 seconds to 80°C then placed immediately on ice to denature the probe. Next, coverslips were incubated with 100µl of hybridisation buffer containing 400ng/ml probe overnight at 66°C. The coverslips were then washed with 500µl of a high-stringency wash solution of 2X SSC/0.1% Tween 20 for 5- 10mins at room temperature. This was then removed and the coverslips were then washed three times in a second wash solution of 0.1X SSC for 10 minutes at 65°C. If cells were to be exposed with a primary antibody in addition to RNA FISH, a UV crosslinking step was added to ensure the probe was not washed away in subsequent washing procedures. Coverslips kept in 0.1X SSC wash were placed in a tray with ice and exposed to 0.3J/cm^2 energy per area in a TL-2000 ultraviolet translinker (Ultra-Violet Products). Coverslips were next incubated either with primary antibodies for immunocytochemistry as described above, and incubated with Hoechst 1µg/ml (Cell Signalling Technologies) for 5 minutes at room temperature in the dark, or only incubated with Hoechst stain if the probe was to be visualised alone. The cells were

finally washed 4 times for 10 minutes in 1 ml PBS. Coverslips were mounted onto the glass slides (Fisher brand microscope slides twin frost 0.8-1mm) using 10µl mounting medium (Dako) and left to dry completely before sealing with clear nail varnish. Slides were stored at 4°C in dark, until images were obtained using a SP5 confocal microscope (Leica).

2.6.7 Electrophysiology

Differentiated iPS cells plated onto coverslips at a density of 30 000 cells per coverslip were measured for recordings at 6, 7, 8, 9 and 10 weeks post-differentiation. Coverslips were placed into a bath on an upright microscope (Olympus) containing the extracellular solution at pH7.4 composing of 150 mM NaCl, 5.4 mM KCl, 2 mM $MgCl_2$, 2 mM $CaCl_2$, 10 mM HEPES, 10 mM Glucose osmolarity,~305 mOsm/Kg. The internal solution of the pipette was composed of 140mM K^+-gluconate, 10 mM KCl, 1 mM $MgCl_2$, 0.2mM EGTA, 9 mM NaCl, 10 mM HEPES, 0.3 mM Na^+-GTP, and 3 mM Na^+-ATP adjusted to 298 mOsm/Kg at pH7.4. For both solutions glucose, EGTA, Na^+-GTP, and Na^+-ATP were added fresh on each day of the experiment. All recordings were performed at room temperature and all reagents for solutions were purchased from Sigma.

Electrodes for patch clamping were pulled on a Sutter P-97 horizontal puller (Sutter Instrument Company) from borosilicate glass capillaries (World Precision Instruments) to produce a tip resistance of 3-5.5MΩ.

To identify the motor neurons present, cells were visualised using the microscope x40 objective, and those with a triangular cell body and processes to indicate a motor neuronal morphology were selected (figure 2.3). In order to not disturb the cell, each recording is from a single cell and a minimum of 4 cells were used per condition. Recordings from cells were amplified using Multiclamp 700B patch-clamp amplifier (Molecular Devices) in current-clamp mode to measure depolarized evoked action potential firing in the cells using a 10 step protocol for a duration of 500 miliseconds, injecting current from -40pA , every 20pA. As well as this a voltage-clamp mode was

used to measure currents. To ensure a good seal during patch clamp, cells were monitored for the shape of the pulse (figure 2.3). Recordings were acquired at ≥10 kHz using a Digidata 1440A analogue-to-digital board and pClamp10 software (Axon Instruments).

Whole-cell capacitance (C_m), input resistance (R_a), series resistance (R_S) and resting membrane potential (RMP) values were measured during the recording using pClamp10 software. Only cells with an R_s<20MΩ, a RMP more hyperpolarized than −40 mV and R_a>500 MΩ were included in data analysis. Electrophysiological data were analysed using Clampfit10 software (Axon Instruments).

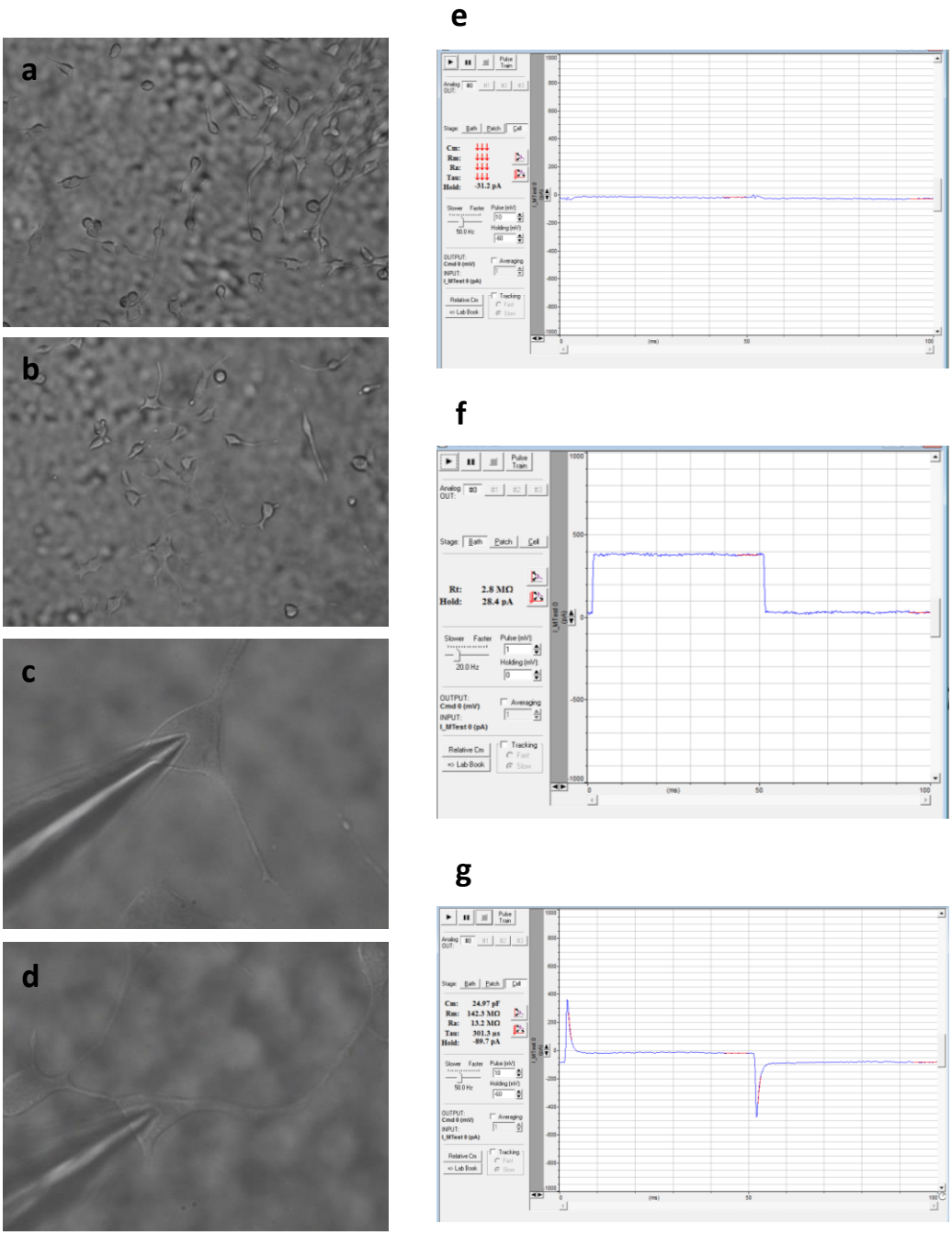

Figure 2.1: Electrophysiology of iPS-derived Motor Neurons. **a-b)** Images of iPS cells plated for electrophysiology. **c-d)** Images of iPS cells selected for recording based on morphology including a triangular cell body and processes. **e)** Image of a flat line pulse which corresponds with the current detected between the pipette and the external solution. **f)** Membrane seal or cell attached configuration producing a square pulse which corresponds with the membrane blocking the pipette tip, at this point the membrane is inside the pipette. **g)** Whole cell configuration where the pipette connects with the whole cell after the membrane seal has been broken.

2.7 Microscopy and Image Analysis

2.7.1 Confocal Microscopy

Visualization of sense and anti-sense foci was performing using the Leica SP5 confocal microscope using an x63/1.4 oil immersion objective lens. Images were taken at high resolution taking a Z-stack comprised of images at a 0.13µm thickness throughout the whole nuclear volume of each cell analysed. More than 30 iPS-derived cells from each sample were imaged and counted for RNA foci.

2.7.2 IN Cell Analyser and Workstation Analysis

Images of iPS-derived cells from immunocytochemistry experiments was performed on the IN CELL Analyser 2000 (GE Healthcare) automated microscope, taking images on coverslips with all channels set to 2D deconvolution. A minimum of 5 random fields of view were imaged for each coverslip and images were taken using the large camera air objectives of 10x (Nikon, 0.45 NA), 20x (Nikon, 0.75 NA) or 60x (Nikon 0.70 NA).

For analysis of images taken with the INCELL automated microscope, the IN Cell workstation analyser was used to quantify total cell numbers, and the number of motor neurons in the population as assessed by dual staining for ChAT and Tuj1. A threshold was set for the intensity of the staining for all channels used, and motor neuron counts were obtained by cells that showed co-localised expression of ChaT, Tuj1 and with an associated DAPI nucleus kernel (figure 2.1).

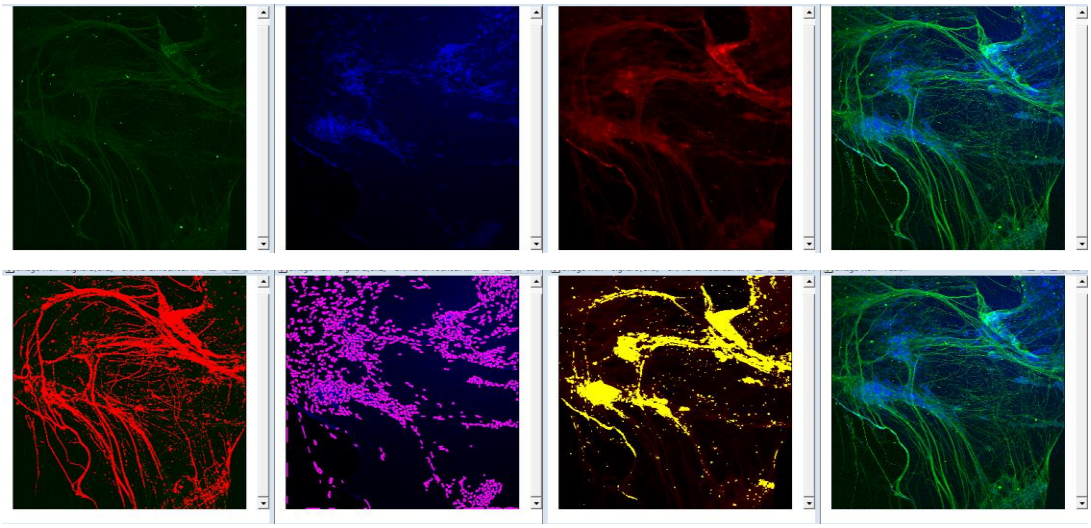

Figure 2.2: Quantification of Motor Neurons using the INcell Workstation Analyser. Top row highlights Cells labelled green for Tuj1, blue for DAPI or red for ChAT were quantified for intensity of fluorescence set for each respective channel. Bottom row indicates cells selected for counts in each channel that meet the threshold intensity staining for each respective channel.

2.7.3 Quantification of TDP-43 Localisation and Cell Counts

For the quantification of the localisation of TDP-43 staining in all cell populations, cells were manually traced on ImageJ for the whole cell including the nucleus, cytoplasm and processes, and a separate trace was made for the nucleus mask, generated using DAPI. The total area of the whole cell as well as the minimum, maximum and mean intensity of TDP-43 staining was recorded (figure2.2). The total area of the nucleus including the minimum, maximum and mean intensity of TDP-43 staining was also recorded. The intensity of each cell TDP-43 staining for the whole cell and the nucleus was calculated, normalising for total cell area. The results generated an intensity of TDP-43 staining for the whole cell and an intensity of TDP-43 staining for the nucleus, which was used to determine TDP-43 mislocalisation. A minimum of 50 cells per cell line were quantified.

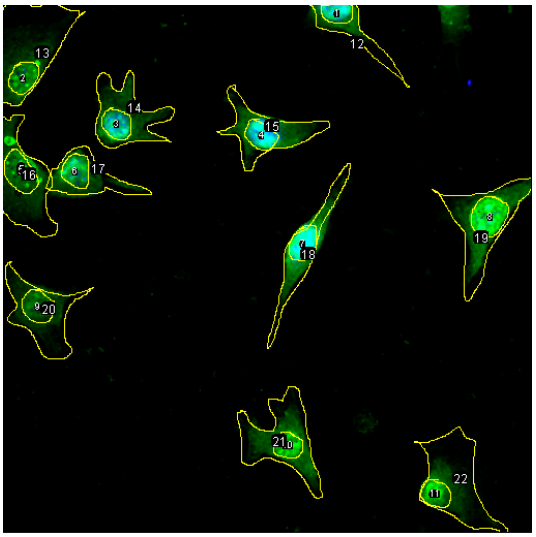

Figure 2.3 Quantification of Cellular TDP-43 Staining. Whole cell and nuclei traces were made for each cell within a mixed population including glial cells (shown here), and the intensity of TDP43 (green) in each respective area was quantified.

2.8 PTEN Knockdown (KD)

2.8.1 Establishing Commercial Lentiviral MOI Using GFP Control Lentiviral Particles in HEK and iPS Cells

Using GFP control lentiviral particles (Santa Cruz Biotechnology) of the same titre ($1x10^6$ Infectious Units) of the viral particles for PTEN knockdown (KD) (Santa Cruz Biotechnology) and Scrambled controls (Santa Cruz Biotechnology), the appropriate multiplicity of infection (MOI) was established for HEK cells and iPS-derived cells. HEK cells were plated into 96 well plates at 1000 cells per well in triplicate wells and iPS-derived cells were plated in duplicate onto 10mm coverslips previously coated with poly-DL-ornithine and laminin at a density of 2000 cells per coverslip, placed in CELLSTAR® 35x10mm culture dishes with 4 inner rings. After 24 hours (HEK) or 72 hours (iPS-derived cell) of culture *in vitro* post-plating, the appropriate volume of virus (table 14) was added to each well or coverslip for the cell number plated and MOI investigated (1, 2, 5) made up to a final volume of 100µl (HEK) or 50µl (iPS) with appropriate media for the cell type used. For the iPS-derived cells, after 4-6 hours the

dishes containing coverslips were topped up with 2ml fresh media, which was replaced every 24 hours for the following 7 days. Untransduced controls were treated with 100µl of media without viral particles to maintain the same conditions for all cells analysed. The volume of virus was calculated using the following formula:

$$\text{MOI} = \frac{\text{Volume of virus x Titre}}{\text{Number of cells}}.$$

After 3-5 days (HEK) or 7 days (iPS) in culture, determination of transduction efficiency was assessed by cells, counting total transfections of GFP staining in transduced cells against total cell numbers.

Table 2.14: Volume of GFP Control Lentiviral particles (1x10^6 IFU), PTEN ShRNA virus (1x10^6 IFU), and control ShRNA Virus (1x10^6 IFU) calculated per coverslip at different cell densities plated.

Cell Number	MOI (volume required to achieve)				
	1	**2**	**5**	**10**	**30**
1000	1µl	2µl	5µl	10µl	30µl
2000	2µl	4µl	10µl	20µl	60µl
3000	3µl	6µl	15µl	30µl	90 µl
4000	4 µl	8µl	20µl	40µl	120µl
5000	5µl	10µl	25µl	50µl	150µl
10 000	10µl	20µl	50µl	100µl	300µl

2.8.2 PTEN KNOCKDOWN WITH PTEN SHRNA IN HEK 293 CELLS AND IPS-DERIVED CELLS

Cells were cultured in the previously described media for the cell type investigated and were plated at 10 000 cells (HEK 293 cells) or 20 000 cells (iPS-derived cells) per well in 12 well plates. After 24 hours (HEK 293 cells) or 72 hours (iPS-derived cells), for each condition 4 wells were transduced at an MOI of 5 previously established with GFP transduction. The virus was made up in media to a final volume of 500µl per well, with either the lentiviral particles for PTEN ShRNA: sc-29459 (Transduced) 1 x10^6 IFU

(infectious units of virus), control ShRNA: sc-108080 (Scrambled) 1 x10^6 IFU. The untransduced controls were given a media change without virus to maintain the same conditions for the cells. Three days (HEK 293 cells) or seven days (iPS-derived cells) later, cells were harvested from the plates and a Bradford assay was performed for protein determination as described above. Identification of PTEN knockdown was performed via western blot analysis probing for total PTEN, pPTEN, pAKT, AKT(pan) and GAPDH (table 10) using previously described protocols.

2.9 Statistical Analysis and Data Presentation

Unless otherwise stated in the figure, all experiments were performed in triplicate in three independent experiments. All statistical analysis was performed using GraphPad Prism version 6 software (GraphPad Software). Data represent the mean of the three patient, or three control cell lines ± standard error of the mean, and were analysed with either students T test, or Two-way ANOVA as stated in the corresponding figure legend. Where drug treatment groups were used, each treatment group was normalised to vehicle control and results were expressed as a percentage of the control group mean.

CHAPTER 3 : CELL CULTURE MODELS OF AMYOTROPHIC LATERAL SCLEROSIS (ALS) TO INVESTIGATE PTEN INHIBITION

3.1 Introduction

3.1.1 Phosphatidylinositide 3-kinase (PI3K) Pathway Modulation for PTEN Inhibition

The phosphatidylinositide 3-kinase (PI3K) pathway is a well described cell cascade important in survival and growth (Chalhoub and Baker, 2009). The pathway itself is controlled by a positive regulator and a negative regulator, PI3K and phosphatase and tensin homologue deleted on chromosome 10 (PTEN) respectively, of which PTEN has been proposed to be an important target for research in neurodegeneration (Ismail et al., 2012). PTEN is a tumour suppressor gene which in its unphosphorylated and active form, acts as a phosphoinositide 3 phosphatase, dephosphorylating phosphatidylinositol 3, 4, 5 triphosphate (PIP3) to phosphatidylinositol 4, 5 bisphosphate (PIP2) *in vivo* (Maehama and Dixon, 1998). The consequential reduction in the levels of PIP3 also reduces cell survival, as the role of PIP3 is to bind to and cause the translocation of v-akt murine thymoma viral oncogene homolog (AKT) towards the cell membrane (Datta et al., 1999). At the cell membrane, AKT is able to phosphorylate and subsequently promote the sequestration of cell death components such as BCL2/BCLXL- associated death protein (BAD) and GSK-3β (glycogen synthase kinase 3 β), preventing them from implementing apoptotic cascades towards cell death and thus promoting cell survival (Datta et al., 1999). It is thought that by acting upstream of this pathway, preventing the action of PTEN or increasing phosphorylation of PTEN, to shift PTEN to its inactive form, it is possible to promote cell survival due to increased AKT phosphorylation by PIP3.

Methods to block the action of PTEN for a desired pro-survival effect have taken two main forms in previous research, which are PTEN knockdown, to reduce PTEN protein expression (Yang et al., 2014a), and inhibition of PTEN with direct small molecule inhibitors. However more recently, work with histone deacetylase (HDAC) inhibitors which act to counteract endogenous transcriptional repression, have built a portfolio of evidence towards utilising these non-direct modulators of the PI3K pathway to provide a protective effect in neural cells.

In eukaryotic cells, DNA is organised into a compacted structure called chromatin, which is made up of nucleosomes consisting of DNA linked to histone proteins. The histones, connected to DNA can be post-translationally modified via the addition or removal of acetyl groups to lysine residues. This acetylation and deacetylation is controlled by histone acetyltransferases (HATs) or histone deacetylases (HDACs) respectively, and is important in conferring an open or closed structure of chromatin. Acetylation allows the chromatin structure to become more open and relaxed, to allow access for transcriptional machinery to activate transcription. On the other hand, deacetylation promotes a more closed structure causing transcriptional repression.

Evidence for using HDAC inhibitors for neuroprotection is varied. Studies have found increased survival after oxidative stress when cortical neurons were exposed to HDAC inhibitors (Kozikowski et al., 2007). In investigations examining the re-growth of neurons after injury, HDAC inhibition has been found to be neuroprotective against oxidative stress and also been found to promote the growth of neuronal projections (Rivieccio et al., 2009). Of note to the field, in 2012 a HDAC inhibitor called Scriptaid was found to decrease motor deficits, promote motor function consistently for 4 weeks after injury, as well as increase neuronal survival when delivered after traumatic brain injury in an *in vivo* mouse model of controlled cortical impact (Wang et al., 2012a)**.** What was particularly interesting about this work, was that Scriptaid was also shown to reduce the levels of active PTEN available by increasing the phosphorylation of PTEN, alongside increasing phosphorylated AKT, in what was thought to be the mechanism behind the pro-survival effect (Wang et al., 2012a). These PTEN inhibitory effects as well as an increase in motor function, declined in the presence of an AKT inhibitor, providing evidence for AKT pathway involvement. Although the researchers were unable to investigate a direct mechanism of action for how Scriptaid modulated these pathway components, it suggested the changes found were more likely to arise from an indirect response of PTEN and thus AKT to the drug (Wang et al., 2012a). Later work by the same group in microglia and oligodendrocyte cells, proposed GSK3β as a component which mediated the phosphorylation and inactivation of PTEN, by reducing the total levels of active PTEN available (Wang et al., 2015a), and maintaining an indirect mechanism of the action of Scriptaid on this pathway, describing Scriptaid as a PTEN modulator.

Scriptaid is a cell permeable pan-HDAC inhibitor and a member of the hydroxamic acid group of HDAC inhibitors which also includes trichostatin A (TSA) (Hahnen et al., 2008). Hydroxamic acid HDAC inhibitors work by binding to zinc ions present on the HDAC active site (Finnin et al., 1999). Scriptaid is reported to have one of the lowest toxicities for inhibitors in this group, for example when histone deacetylases purified from rat liver were analysed, inhibition at highly potent doses, -log 6.73 ± 0.02 (0.19µM) were found when tested for half maximum inhibition (IC_{50}) of total HDAC activity (Hahnen et al., 2008). To add to this, although inhibition of individual HDAC activities vary, for HDACs 1, 2, 3 and 6, proposed to be important for neurodegenerative research (Sancho-Pelluz et al., 2010, Hahnen et al., 2008, Simoes-Pires et al., 2013), the $IC_{50's}$ for each of these HDACs were found to be less than 10nM (Shi et al., 2011b). Further studies have found that Scriptaid at 6µM concentrations resulted in a more than 100 fold increase in histone acetylation in cultured PANC-1 cells, a human pancreatic carcinoma cell line, and reported limited effects on survival (80% survival) on MDAMB-468 cells, a human mammary carcinoma cell line (Su et al., 2000). Collectively, as these studies highlighted a potential therapeutic effect via PTEN modulation, low levels of toxicity in the cells tested, coupled with a review of the literature which revealed limited previous investigations of Scriptaid in neurodegenerative disease research, it prompted us to consider it an interesting and novel method for modulating PTEN in the ALS cell model systems we had readily available and were developing.

3.1.2 Amyotrophic Lateral Sclerosis (ALS) Cell Model Systems

Neuroblastoma spinal cord 34 (NSC-34) cells are a mouse neuronal hybrid immortal cell line created by Neil Cashman's group in 1992. These cells hold selected desirable characteristics of primary mouse motor neurons and are found to be motor neuron-like due to: their expression of mature cholinergic neuronal enzyme Choline Acetyl transferase (ChAT); the ability of differentiated cells to generate action potentials; their expression of motor neuronal cytoskeletal proteins; as well as displaying acetyl choline receptors (Cashman et al., 1992). However, unlike post-mitotic primary motor neurons which require longer and more complex methods to obtain and develop successfully in culture, NSC-34 cells grow rapidly taking around 5-10 days in culture. To

add to this, NSC-34 cells can be transfected with human SOD1 mutations, for example G93A, to create a model which not only mimics motor neurons but is also a model of ALS. These cell lines were used along with NSC-34 cells transfected with wild type human SOD1 (WT SOD1) and empty vector (pIRES cells) controls, to establish if PTEN manipulation promotes survival in these models of ALS.

As an additional model to investigate the effects of PTEN manipulation on cellular models of ALS, primary patient fibroblast cells were used. As previously discussed, the ability to differentiate iPS cells to motor neurons as models for ALS has been recently established in several bodies of work (Dimos et al., 2008, Donnelly et al., 2013a, Haeusler et al., 2014). An important aim for this project detailed in later chapters 4 and 5, was to develop a neurological model from the newly discovered C9ORF72 genotype, of iPS-derived motor neurons, which were to be used as a further model for PTEN manipulation. The iPS cells used later in this thesis are originally derived from the same three pairs of age and sex matched patient and control fibroblast cells used in this chapter, the details of which can been found outlined in chapter 2. This is particularly important as any effects seen from PTEN manipulation in fibroblast cells may give insights into the response later seen in iPS-derived motor neurons. In addition, any forthcoming work yields directly comparable results, as by comparing the effect of PTEN manipulation both before and after the iPS cell to motor neuron transition, it could reveal interesting changes in the response of components in the PI3K pathway, which may be indicative of motor neuron and fibroblast specific effects.

3.2 Aims and Objectives

The aims of the work described in this chapter are to identify if Scriptaid treatment can modulate the components of the PI3K cell survival pathway to promote survival in NSC-34 cell models of ALS, as well as primary C9ORF72-ALS patient fibroblast cells and their matched controls. As BpV had been extensively used in previous studies, Scriptaid was chosen as a novel PTEN modulator for investigation in ALS. Firstly, a series of biochemical assays will determine from a range of doses which can be safely used to treat both cell model systems recruited without seeing negative effects. Cellular viability will be measured using 3-(4,5-Dimethylthiazol-2-yl)-2,5-Diphenyltetrazolium bromide (MTT) assays to determine how the drug affects cell survival. Additionally, we will use cellular cytotoxicity assays to determine the levels LDH release after Scriptaid treatment, whilst CyQuant assays will identify how Scriptaid affects cell number and proliferation. Finally, we will then identify if Scriptaid modulates the PI3K cell survival pathway components, in stressed conditions in comparison to basal and untreated controls. Western blot analysis, will document changes in the levels of PTEN and AKT, but more importantly the phosphorylation of AKT at serine 473 which indicates activation of the cell survival pathway which we are ultimately aiming to turn on. On completion, this work will tell us how Scriptaid modulates PI3K pathway components, which could result in positive changes in cell survival in cell models of ALS to our knowledge previously un-investigated with this drug.

3.3 Neuroblastoma Spinal Cord (NSC34) Cells as Models for PTEN Manipulation in ALS

3.3.1 Neuroblastoma Spinal Cord (NSC34) Cells Show High Sensitivity to Scriptaid Treatment

Scriptaid is reported to have an IC_{50} of less than 5nM for HDACs 1, 2, and 6, and less than 9nM for HDAC 3 (Shi et al., 2011b). For total HDAC inhibition, an IC_{50} of 0.19µM has been identified (Hahnen et al., 2008). However, studies on PANC-1 cells identified 6µM as an optimal concentration to use for HDAC inhibition with limited toxicity (Su et al., 2000), whilst 0.1, 1, and 10µM concentrations were used in synaptogenesis studies on rat hippocampal neuron and fibroblast co-cultures, where 1µM and 10µM were found to actively increase total synapsin intensity by 1.5 fold (Shi et al., 2011b). Although some have reported nM activity, we decided to choose concentrations, derived from active concentrations of Scriptaid cited in previously published literature on neuronal populations (Shi et al., 2011b). Neuroblastoma Spinal Cord (NSC-34) cells were therefore treated with Scriptaid for 24 hours to assess the viability of the cells when exposed to the drug at 1µM and 10µM concentrations.

Firstly a 3-(4, 5-Dimethylthiazol-2-yl)-2,5-Diphenyltetrazolium bromide (MTT) assay was performed to measure the cellular viability via metabolic activity from the reduction of a yellow tetrazolium salt dye. In viable cells NADH reduces the dye which increases with increased Nicotinamide adenine dinucleotide (NADH) activity in the cells. The result of the reaction is a purple formazan product which once quantified by spectrophotometry, acts as a measure for cellular changes in viability. By doing this, we would be able to establish the dose at which we can use Scriptaid without it exerting toxic negative effects on cellular viability.

The results in NSC-34 cell models showed a significant decrease in the viability of the cells at both concentrations tested, across all three NSC-34 cell models including WT SOD1 and pIRES controls (figure 3.1). There were no significant differences between the three different NSC-34 cell lines tested within treatment conditions, and no significant disease specific effects were found, suggesting all cell models reacted negatively to the drug. The greatest effects were found at the highest concentration tested on piRES controls, with the lowest effects found in G93A mutant SOD1 models

at 10 µM whose viability still dropped below vehicle control, but not to significant levels (figure 3.1). Because two concentrations with a difference of 10 fold were tested, but the level of toxicity found was similar, it suggests the NSC-34 cell response to Scriptaid is that of greatly reduced viability. Lower concentrations at 0.01µM and 0.1µM were also tested with limited replicates (n=2), however they also showed greatly reduced viability, with an average of 39% and 44% viability across all three cell lines (data not shown), therefore were not investigated further because of this.

Consequently, as significantly reduced cell survival was found after exposure to the drug at concentrations in the region of previously published results, NSC-34 cell models of ALS were found to be too sensitive to Scriptaid. As a result, further investigations to identify levels of AKT activation via stress assays and western blot analysis were not performed in these cell models as it was considered that a better, less sensitive cell model of ALS should be used for subsequent experiments.

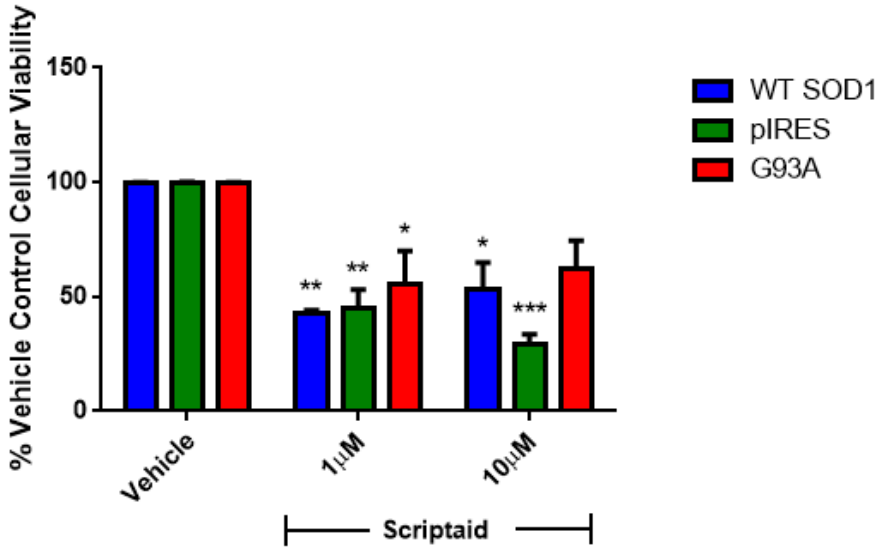

FIGURE 3.1: The effects of Scriptaid on NSC-34 cell viability as measured by MTT assay. Results revealed significant declines in cellular viability at both 1µM and 10µM concentrations of the drug in both controls WT SOD1 and pIRES NSC-34 cells, as well as in ALS mutant SOD1 (G93A) NSC-34 cells. (Data presented as percentage of vehicle control, mean of n=3 independent experiments. ±SEM *p=<0.05, **p=<0.005 ***p=<0.0005, analysed with two-way ANOVA)

3.4 Fibroblast Cells as Models for PTEN Manipulation in ALS

At the time this project began, the field of ALS research had an exciting new discovery; a mutation in a new gene designated Chromosome 9 Open Reading Frame 72 (C9ORF72) which was found to be the most common genetic cause of ALS to date (DeJesus-Hernandez et al., 2011, Renton et al., 2011). As described in chapter 1 the mutation was found to be a hexanucleotide repeat expansion of GGGGCC in intron 1 of the gene C9ORF72. Consequently, as at the time no cell models existed for the C9ORF72 mutation in ALS, and primary fibroblast cells derived from patients with C9ORF72- related ALS were readily available, it was felt adding this fibroblast cell model with this feature would have provided valuable insights into PTEN manipulation on a previously unexplored mutational background, especially if a therapy became available which may have positive effects for both sporadic and familial forms due to the shared cell survival pathway.

Fibroblasts from patients by skin biopsy were produced in house by Anne Gregory and the technical team in SITraN. Although fibroblasts are slow growing, requiring 14-21 days in culture to develop, compared to NSC-34 cells which take 5-10 days, and are cells which are not affected in ALS, they have been found to show aberrant disease-related features. These include reduced mitochondrial respiration (Allen et al., 2014), as well as expression of pathology related to the disease found in motor neurons, including RNA foci, hallmarks of the C9ORF72 mutation (Lagier-Tourenne et al., 2013), and reduced nuclear TDP43 protein (Sabatelli et al., 2015). Of note, the NSC-34 cell models previously used in this chapter were a SOD1 model of ALS, which is not only a rarer ALS-causing mutation, but research using this mutation has failed to produce any effective therapeutic interventions for ALS since its discovery (Gong et al., 2000, Boillee et al., 2006, Miller et al., 2006). Therefore, using fibroblast cells without these characteristics but with a relevant genotype of interest made them an excellent additional cell model to study.

3.4.1 Fibroblast Cells Show Low Sensitivity to Scriptaid Treatment

Fibroblast cells were first measured for levels of viability via an MTT assay after exposure to Scriptaid for 24 hours, at 3µM, 10µM, 30µM and 50µM concentrations to examine if the drug had any effects on cell survival.

Results across all three pairs of fibroblast cells tested revealed a steady decline in viability with increasing concentration (figure 3.2). Between vehicle treated conditions and 3µM, as well as between vehicle and 10µM doses, no significant changes in cell viability were noted, suggesting using 3µM or 10µM concentrations on cells would not be detrimental for the cellular viability in both patients and controls. However, at higher concentrations beyond 10µM detrimental effects on viability were found, with both patients and controls showing a significant decline in cellular viability at 30µM and 50µM doses, compared to vehicle and 10 µM conditions, suggesting toxic effects on fibroblast cell viability.

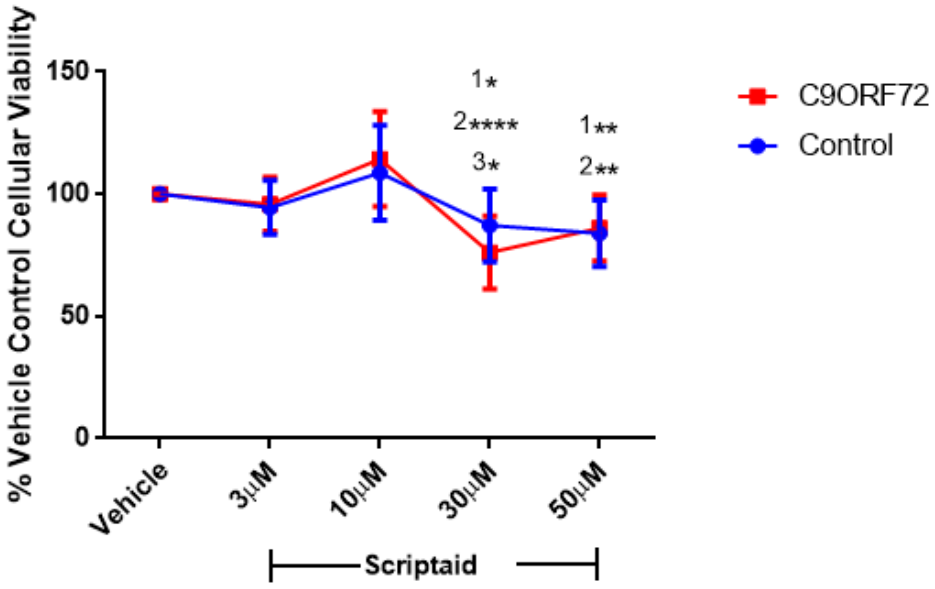

FIGURE 3.2: The effects of Scriptaid on fibroblast cell viability as measured by MTT assay. Three matching pairs of primary fibroblast cells revealed no significant changes in cellular viability between vehicle and 3µM or vehicle and 10µM doses. Both controls (1) and patients (2) exhibited significant declines in cell viability between 10µM doses and concentrations labelled above However, C9ORF72 ALS patients revealed a significant reduction in viability between vehicle and 30µM doses (3). (Data presented as percentage of vehicle control, mean of *n*=9 independent experiments. ±SEM, 1= significant difference between control Scriptaid dose labelled and control Scriptaid at 10µM, 2= significant difference between C9ORF72 Scriptaid dose labelled and C9ORF72 Scriptaid at 10µM, 3= significant difference between C9ORF72 Scriptaid dose labelled and C9ORF72 vehicle. *p=<0.05, **p=<0.005, ****p=<0.0001. Analysed with two-way ANOVA, Bonferroni's correction)

Whilst the MTT assay is a widely used test for cellular viability and toxicity, the test is not without its limitations. Although the MTT readout is a classed as a measure of cellular viability, the cells ability to reduce the dye also represents the rate of mitochondrial metabolism in the cell, which is in turn representative of the rate of NADH production from glycolysis, therefore MTT assays could be classed as mitochondrial test (Berridge et al., 2005, Riss TL, 2013). Instances where this would affect readouts include for example, fibroblast cells in a confluent monolayer which may have different metabolic rates compared to those that are not, as well as cell line to cell line differences in metabolic rates possibly having an effect on the readout.

As a cell measurement that relates to mitochondrial activity is used to describe viability, it is possible that treatment with Scriptaid may inhibit mitochondrial activity without causing cell death. Therefore, in addition to the MTT assay, we also performed other biochemical assays for confirmation, including the lactate dehydrogenase (LDH) assay for cellular cytotoxicity. The LDH assay requires the use of the media, for a cumulative measure of LDH release from damaged cells which can be quantified in a colorimetric assay. As the monolayer of cells were not required, the experimental design allowed for multiplexing options, meaning that the MTT data and LDH data could be obtained from the same cells treated on the same day, under the same conditions, increasing the reliability of comparisons between them.

Results revealed no significant change in LDH cytotoxicity at any concentration tested, suggesting the reductions in viability seen at higher doses in the previously performed MTT assay were not due to increased cell death, but due to an inhibited growth rate (figure 3.3). Results also revealed no significant difference in patient cells compared to controls with the shape of the response, suggesting both cell lines reacted similarly to Scriptaid (figure 3.3). Consequently, as no significant changes in cytotoxicity were found at any concentration tested compared to vehicle control, the data indicates that Scriptaid is non-toxic to fibroblast cells.

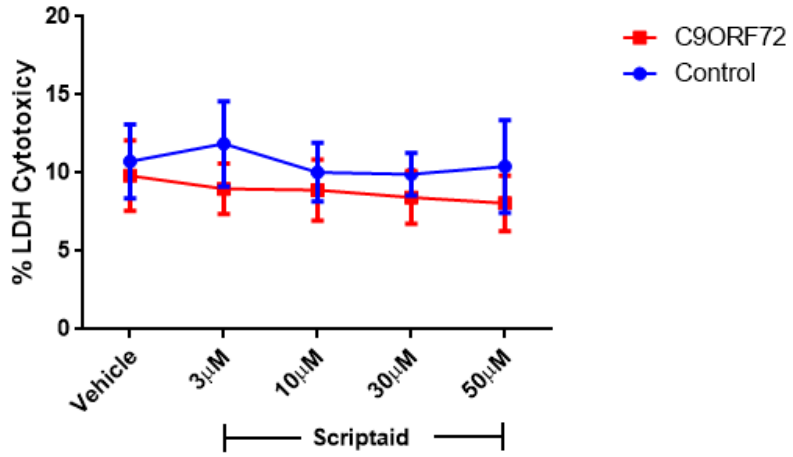

FIGURE 3.3 Determination of LDH cytotoxicity of Scriptaid treatment on fibroblast cells. Fibroblast cells revealed no significant changes in cytotoxicity between vehicle and drug treated conditions or between patient and controls at all treatment conditions. (Data presented as percentage of LDH cytotoxicity, mean of *n*=9 independent experiments. ±SEM. Analysed with two-way ANOVA, Bonferroni's correction)

The MTT and LDH assays revealed limited toxicity of the fibroblast cells to Scriptaid, however to identify if cell number was affected, a final biochemical assay to measure cell number and proliferation, a CyQuant® assay, was performed. CyQuant® assays are a measure for fluorescence rather than absorbance, therefore the use of this additional test offsets any concerns with regards to the sensitivity of biochemical assays using absorbance measures such as MTT and LDH assays, which are generally regarded as less sensitive than fluorescence methods (Riss TL, 2013).

CyQuant® assays were performed on all three fibroblast pairs after treatment with Scriptaid for 24 hours at 3µM, 10µM, 30µM and 50µM concentrations. Results across all three cell pairs showed a trend towards a decline in cell number in both patients and controls with increasing concentration (figure 3.4). However no significant changes in cell number were identified, further suggesting the reduced cellular viability seen in MTT assays above was not due to cell death, but due to inhibited growth rate. Additionally, no significant difference was found in cell number between patients and controls under any condition highlighting that patient fibroblast growth was not

affected by disease. Overall, the CyQuant® assay results suggest Scriptaid had little to no effect on cellular proliferation, which coupled with the toxicity data obtained from MTT and LDH assays above, also implies minimal cell death on application of the drug.

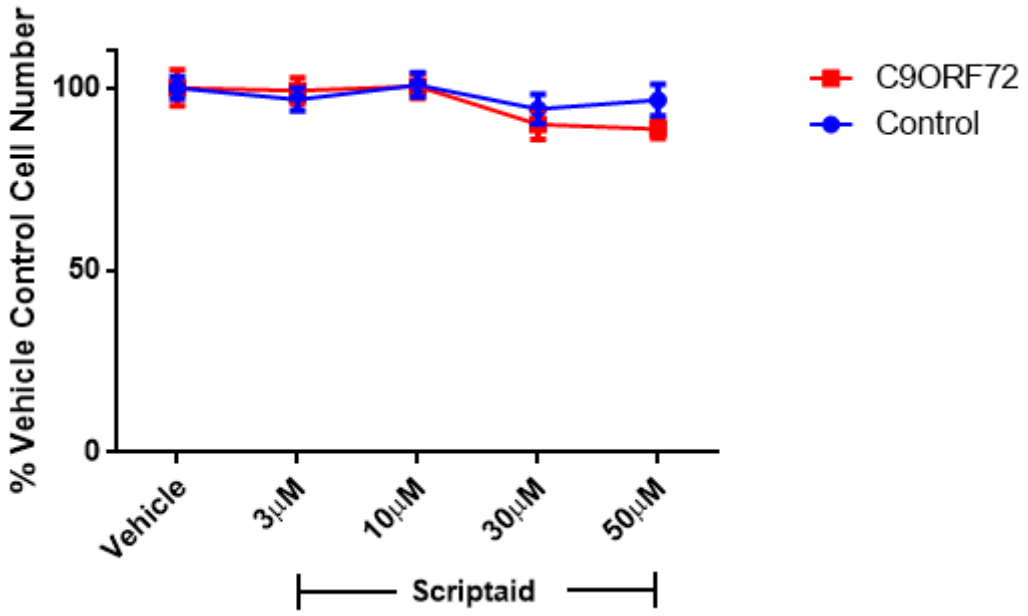

FIGURE 3.4: The effects of Scriptaid on fibroblast cell number and proliferation as measured by CyQuant assays. Fibroblast cells revealed no significant changes in cell number between vehicle and drug treated conditions or between patient and control grouped data across all treatment conditions. (Data presented as percentage of vehicle control, mean of *n*=9 independent experiments. ±SEM. Analysed with two-way ANOVA, Bonferroni's correction)

3.4.2 PATIENT FIBROBLAST CELLS SHOW LOW LEVELS OF PTEN BUT SCRIPTAID TREATMENT DOES NOT MODULATE THE PI3K CELL SURVIVAL PATHWAY.

The previous biochemical assays showed fibroblast cells tolerated treatment with Scriptaid well, therefore it was next decided to look at how the PI3K cell survival pathway responded to Scriptaid treatment in patient and control samples. As the fibroblast cells are not affected in ALS, to emulate stressed conditions, a stress assay was conducted on the cells where serum withdrawal acted as the stressor (Simm et al.,

1997, Arrington and Schnellmann, 2008). Patients and controls were observed for differences in activation of PI3K pathway components in both basal and stressed conditions, and comparisons were made between them. The same three pairs of fibroblast cells used in the above experiments were treated with Scriptaid at 3µM, 10µM, and 30µM concentrations for 24 hours and subsequently collected, lysed and measured for protein expression levels via western blotting. The PI3K pathway components probed for included phosphorylated AKT(Ser473) (pAKT), total AKT(pan) (AKT), total PTEN (PTEN) and GAPDH (loading control) which were chosen on a basis that they would point to activation or inactivation of the PI3K cell survival pathway.

The western blot is a representative image of one pair of the 3 pairs of fibroblasts, whereas the graphs are the summation of the all 3 pairs. Western blotting revealed that in basal conditions patients exhibited significantly lower levels of PTEN and pAKT compared to controls (figure 3.5 b, c), suggesting that in patient fibroblasts cells these pathway proteins are present in lower quantities, possibly indicative of a disease-related trait. Interestingly, when stressed conditions were applied with serum withdrawal, controls showed a significant decline in total PTEN, pAKT, and total AKT(pan) in all stressed conditions, whilst patients show no significant changes in total PTEN or pAKT(figure 3.5). This indicates a potential resistance to serum withdrawal-induced stress in patient cells.

Upon treatment of the cells with Scriptaid, little to no effect on total PTEN or pAKT protein expression was found in both patients and controls, when compared to vehicle control (figure 3.5 b, c). A trend towards increased protein levels of pAKT (figure 3.5 c) and the ratio of pAKT to total AKT (figure 3.5 e) was found with increasing dose, however these effects were not significantly above vehicle control. These results suggest that Scriptaid does not have a measurable effect as on the PI3K cell survival pathway measured by Western blot analysis.

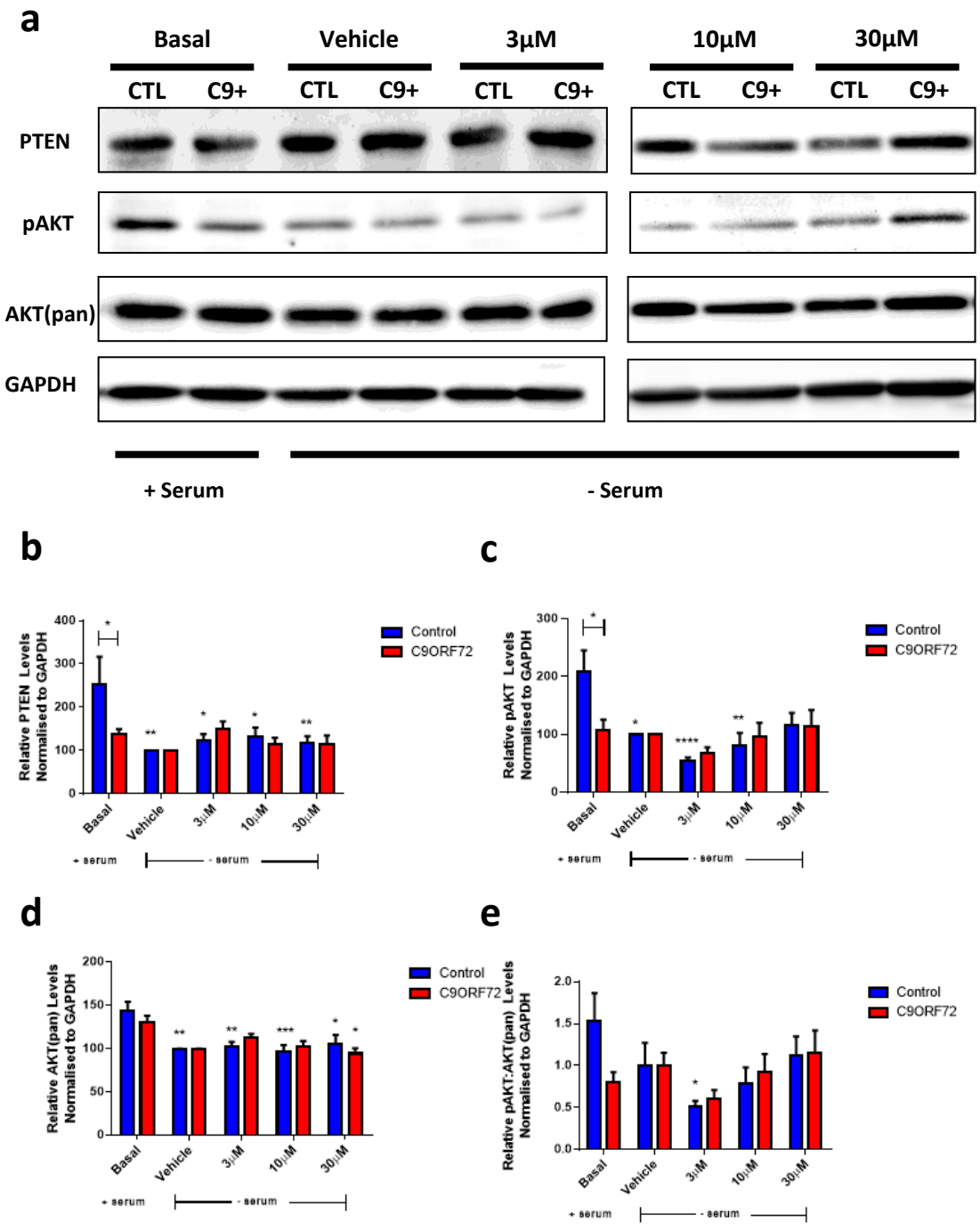

FIGURE 3.5: Scriptaid does not modulate PI3K cell survival pathway components in fibroblast cell models of ALS and controls. a) Western blots probing for PTEN, pAKT, AKT(pan), and loading control GAPDH in primary C9ORF72 patient fibroblasts and age and sex matched controls revealed a significant downregulation of **b)** PTEN and **c)** pAKT) in control cell serum starved conditions compared to basal conditions, and significantly lower levels of PTEN and pAKT in patient cells compared to controls in basal conditions. **d)** A significant reduction in total AKT levels were found in control but not patient cells and **e)** the ratio of pAKT:AKT revealed a significant reduction of pAKT at 3µM doses in control cells compared to basal controls, Representative western blot shown. (Data are mean of *n*=9 independent experiments and normalised to GAPDH loading control. Where more than one membrane was required, each membrane contained both a basal and vehicle control for comparison- see chapter 2 section 2.4.3. ±SEM *p=<0.05, **p=<0.005 ***p=<0.0005, ****p=<0.0001 analysed with two-way ANOVA)

3.5 Discussion

3.5.1 NSC-34 Cell Models And Scriptaid

Evidence has suggested that apoptotic motor neurons have low levels of histone acetylation (Rouaux et al., 2003), indicating the use of a HDAC inhibitors to release transcriptional repression may be an alternative strategy to enhance survival of cells in ALS. Previous studies have found that HDAC inhibitors, in similar NSC-34 mutant SOD1 expression models to those used in this study, protected against oxidative stress (Rouaux et al., 2007). The study used three HDAC inhibitors, valproic acid (VPA), sodium butyrate (NaBu) and trichostatin A (TSA) which all rescued NSC-34 cells from oxidative stress induced cell death (Rouaux et al., 2007). Other models of motor neuron disease including Spinal Muscular Atrophy (SMA) have also seen successes in HDAC inhibition studies (Sumner et al., 2003, Kernochan et al., 2005). In SMA, a mutation in the gene SMN1 causes a reduction in SMN protein product. While this is partially compensated by SMN2, SMN2 produces an unstable truncated protein due to exon 7 exclusion during transcription (Sumner et al., 2003). It has been found that HDAC inhibitors, including VPA, increase protein levels of SMN by activating the SMN2 promotor in NSC-34 cells (Sumner et al., 2003, Kernochan et al., 2005). These studies, along with work showing Scriptaid can successfully manipulate the PI3K cell survival pathway to increase neuronal cell survival (Wang et al., 2012a, Wang et al., 2015a), added to a body of evidence that suggested PTEN manipulation through the use of HDAC inhibitor Scriptaid could be a valid therapeutic strategy in ALS. However, in the above work when NSC-34 G93A models of ALS, along with WT-SOD1 and pIRES controls were treated with Scriptaid with an aim to modulate PTEN and therefore downstream components of the pathway, MTT assays revealed a significant reduction in cellular viability compared to vehicle controls at even the lowest concentrations of the drug tested of 1µM (figure 3.1) and 0.01µM (data not shown). These findings suggest a high sensitivity of the cells to Scriptaid which may discount the use of this drug on this cell model. Nevertheless, a caveat to the use of MTT assays lies in the limitations of the test itself, as they are a measure mitochondrial metabolism, which means the readout portrayed may not be fully reflective of cellular viability if the drug

used causes affects outside of mitochondrial activity. Further assays complementary to MTT would clarify any results obtained.

It has been suggested that the use of differentiated NSC-34 cells which display action potentials and processes more akin to primary motor neurons (Durham et al., 1993) may be better models for neurotoxicity testing than undifferentiated cells. Work by Maier et al. in 2013 found undifferentiated NSC-34 cells were more vulnerable to cytotoxic agents including glutamate cytotoxicity than those differentiated by retinoic acid application. They found differentiated cells had a lower proliferation rate, and increased protein expression of well-known neuronal markers Choline acetyltransferase (ChAT) and microtubule associated protein 2 (MAP2). They also found differentiated cells had increased BCL-2 mRNA, a downstream component in the PTEN-AKT cell cascade, which they thought helped confer a higher resistance to apoptosis (Maier et al., 2013). It is important to note that cell model sensitivity may not reflect the *in vivo* situation and the results seen may highlight the un-differentiated cells vulnerability when looked at in isolation. Therefore, before overlooking the use of NSC-34 cell models with Scriptaid, future work could try differentiated NSC-34 cell models of ALS as an alternative approach.

In previous studies, NSC-34 cells with experimentally reduced PTEN protein expression via PTEN knockdown (KD) have shown functional changes in the expression of key downstream proteins in this pathway, including increased phosphorylation of AKT and pro-survival pathway activation (Kirby et al., 2011). The same study identified that PTEN KD increased survival after oxidative stress to NSC-34 cells transfected with mutant G93A SOD1, an increase from 47% to 68% (Kirby et al., 2011). This work highlights the positive benefits to activation of this pro-survival pathway via PTEN manipulation in these cells, therefore other methods of PTEN manipulation, for instance the use of direct inhibitors of PTEN, such as BpV compounds (Walker and Xu, 2014) may be an additional option to consider for future work with these cell lines.

3.5.2 Fibroblast Cell Models: Toxicity Assays

When biochemical assays were performed to ascertain levels of toxicity for the use of Scriptaid treatment on fibroblast cells, MTT assays first revealed a steady decline in

cellular viability with dose and suggested that concentrations of 30µM and 50µM were too high to use on the cells, resulting in unfavourable declines in viability. These results fit with previous reports of the drug which have reported a similar reduction in survival rates at concentrations above 10µM (Su et al., 2000). On the other hand, concentrations of 3µM and 10µM did not negatively affect cellular viability. Although the assays did not reveal any significant improvement in cell survival or growth with addition of the drug, these cells were currently not under stressed conditions, therefore treatment with Scriptaid may not improve cell survival at this stage.

LDH assays revealed no significant toxicity at all doses tested (figure 3.3) and as the higher concentrations of 30µM and 50µM did not show any increased cytotoxicity, we can say the declines in cellular viability witnessed in the MTT assay at these doses were not indicative of cell death. This result, coupled with the MTT and CyQuant assays, suggests in fibroblast cells Scriptaid treatment is non-toxic, particularly at doses 10µM and below.

In conclusion, the fibroblast cells displayed a lower sensitivity to Scriptaid at concentrations of 10µM and 3µM, in comparison to NSC-34 cells used in previous experiments which showed significant declines in cellular viability at these doses (figure 3.1). Fibroblast cells in this instance are better cellular models of ALS for the continued investigation into the effects of Scriptaid on cell survival pathways compared to the NSC-34 cell models.

3.5.3 Fibroblast Cell Models: Phosphatidylinositide 3-kinase (PI3K) pathway components

From our experiments, western blots revealed patients had significantly lower levels of total PTEN expression compared to controls under basal conditions (figure 3.5 b). This interestingly links with gene expression profiling studies performed in 2011, which found 34 genes involved in apoptosis were differentially expressed in human samples of motor neurons from SOD1-ALS patients compared to controls, and included a decrease in PTEN expression (Kirby et al., 2011). Here, the patient cells used also exhibited reduced PTEN in basal conditions, highlighting a common pathway is altered in two genetic subtypes of ALS, suggesting disease could cause or create an aberrant

reduction in this protein. One possible explanation for this could be that patient cells with ALS attempt to reduce total PTEN levels in an effort to promote cell survival via reduced inhibition of the PI3K pathway. However, whether these findings are a cause or consequence of disease and how it affects downstream components in the pathway remain to be elucidated. Further studies to examine the effect of reduced PTEN in other genetic subtypes and sporadic ALS cell models, as well as examine the effect on other cascade components including BAD and S6 kinase, would confirm the extent of PI3K pathway activation in ALS.

Next, examining the effect of reduced total PTEN protein in basal patient cells on AKT phosphorylation, we found no change in relative pAKT protein as a result (figure 3.5 c). The reason for a lack of increased AKT phosphorylation with reduced total PTEN could lie in dynamic changes the phosphorylation status of PTEN. As described above we observed changes in total PTEN which includes both phosphorylated and un-phosphorylated forms. Phosphorylated PTEN is the inactive form of the protein, therefore if the ratio of pPTEN to total PTEN is in favour of the active form, higher levels of pathway inhibition could prevent the activation of AKT and thus inhibition of the cell survival pathway. Although attempts to re-probe the western blot membranes used above for pPTEN were made by stripping the membrane of previously labelled proteins, unfortunately blots failed to provide a conclusive band at the appropriate weight, most likely due to the dynamics of phosphorylated PTEN protein being too low to detect under the conditions tested. It has previously been reported that the phosphorylation and regulation of PTEN is a complex and multifactorial mechanism. PTEN phosphorylation can be controlled by multiple entities (Torres and Pulido, 2001, Miller et al., 2002) and the subcellular localisation of PTEN, in particular membrane binding has also been found to modulate its regulation and roles (Ross and Gericke, 2009, Li et al., 2009, Chang et al., 2008a, Goh et al., 2014, Rahdar et al., 2009). Additionally, PTEN has also been suggested to regulate its own phosphorylation status (Tang and Eng, 2006). It was not within the scope of the project, or a primary aim to optimise the conditions for visualizing the dynamics of phosphorylated PTEN in fibroblasts, or examine the relationship between the intracellular localisation of PTEN and its phosphorylation status, particularly as the drug did not show any effect. Nonetheless, investigations to optimise assay conditions to identify PTEN

phosphorylation levels and the subcellular localisation of PTEN would be a next step for further investigations in these cell models.

The literature proposed that Scriptaid could modulate PTEN and components of the PI3K cell survival pathway with positive effects in neuronal cell models. However, unfortunately the drug had no effect on total PTEN protein levels compared to vehicle control, and importantly no significant effect on AKT activation. A reduction in pAKT protein was found in control cells compared to basal conditions, and a trend towards higher levels of pAKT protein was found with increasing dose. However, no significant changes were found in pAKT compared to vehicle control at any concentration tested, suggesting that the drug had no positive effect on this pathway and the reduced activation of AKT in control cells was due to a serum starvation effect. As discussed above, pPTEN expression levels here may reveal more interesting findings, as studies have identified changes in pPTEN but not total PTEN with Scriptaid, where the drug was found to increase the phosphorylated form but not total PTEN protein (Wang et al., 2015a). It is highly possible that the total PTEN protein measured above is masking subtle changes in phosphorylated PTEN, and therefore the ratio of phosphorylated to total PTEN available. However, even if this was revealed there are still no positive effects on pAKT to indicate pathway activation suggesting that Scriptaid does not modulate the PI3K pathway to generate increased AKT phosphorylation and thus increase cell survival.

When the cells were exposed to additional stressors via serum withdrawal, control cells saw a significant reduction in PI3K pathway components, causing a reduction in PTEN protein expression in all stress treated conditions. This finding agrees with our observation of patient cells showing lower total PTEN protein in disease, as it indicates the cells could also be under stressed conditions. However, as Scriptaid treatment had no effect on the total PTEN protein expression as it did not reduce total PTEN further to give greater cell survival activation, it suggests the stressed conditions had a maximal effect on this measure. Of note, studies in lung cancer cells found TSA a HDAC inhibitor belonging to the same family as Scriptaid, helped to restore PTEN protein levels to endogenous levels, in artificially reduced PTEN lung cancer cell lines (Noro et al., 2007), but had no effect on cell lines with higher levels of PTEN, implying total PTEN protein levels may not be altered by HDAC inhibition unless already aberrantly

reduced in the cell. In this work, whilst we do see significantly lower levels of PTEN in patients compared to controls and a reduction in PTEN in controls with serum starvation, Scriptaid unlike other HDAC inhibitors did not modulate patient protein levels of PTEN after application. The primary fibroblast cells used in this study are otherwise healthy cells, with ALS patient fibroblasts not exhibiting deterioration despite holding a genetic background of ALS. Therefore, although Scriptaid treatment has no significance to fibroblast cell PI3K pathway activation, or an effect on total PTEN, it is possible Scriptaid may still have a positive survival effect in other cell models with a genetic background for ALS which are known to deteriorate in the disease.

3.6 Conclusion

In conclusion, the NSC-34 cell models were identified to be too vulnerable to the toxicity of Scriptaid to be viable cell models to continue investigating its effects on the PI3K pathway in disease. When primary human fibroblasts were used, although they revealed minimal toxicity to the drug, they also gave minimal PI3K pathway modulation and failed to increase AKT phosphorylation levels to indicate increased activation of the pathway. Whilst this suggests that PTEN has yet known activities, this result could also be due to fibroblast cells not being susceptible to the disease effects of ALS, where the motor neurons are the primary cells affected. Subsequent chapters will therefore continue to focus on developing a model that more accurately reflects ALS, to examine if PTEN modulation can significantly promote the survival of cells in disease.

CHAPTER 4 : CHARACTERISATION OF INDUCED PLURIPOTENT STEM (iPS) CELL MODELS OF ALS

4.1 Introduction

4.1.1 Modelling C9ORF72-Related ALS with Induced Pluripotent Stem Cell-Derived Models

After the discovery of GGGGCC hexanucleotide repeat expansion in the non-coding region of the gene C9ORF72 was found to be the most common mutation for the pathogenesis of ALS, as discussed above it soon became apparent that the long GC rich expanded repeat proved technically challenging for many aspects of molecular cloning and targeting (Donnelly et al., 2013a). Nevertheless, it is not surprising that only two years after the discovery, these difficulties were circumvented when the first studies developing iPS cells from patient somatic cells with C9ORF72-related ALS were published.

An initial important observation from the iPS-derived cells produced, related to the stability of the repeat expansion after the processes of somatic cell reprogramming and cell model generation. Studies found that the transition from somatic cell to iPS cell did not delete the expansion; however of note, repeat instability has been reported. This included both increases and decreases in expansion length found in iPS cells and differentiated counterparts. (Almeida et al., 2013, Sareen et al., 2013, Donnelly et al., 2013a). The reasons behind these changes in repeat length most likely stem from clonal variation and selection of fibroblasts of differing repeat sizes (Almeida et al., 2013, Sareen et al., 2013, Donnelly et al., 2013a). However, somatic heterogeneity within a single cell type and variability in repeat size in different regions of patient brains has also been reported (Beck et al., 2013), suggesting that the discrepancies in repeat length may simply reflect these endogenous traits. This heterogeneity also creates difficulties in identifying correlations between the expansion size and disease-related features such as onset, severity and progression.

A second observation was that the differentiation of iPS cells to generate post-mitotic neurons was not affected by the presence of the repeat expansion (Almeida et al., 2013, Sareen et al., 2013). However interestingly, although mature and electrically active motor neurons have been generated, contrasting findings in their electrical

properties have been reported. Mammalian neurons are known to have a resting membrane potential at around -60mV and have the ability to generate multiple trains of both voltage induced and spontaneous action potentials (Baranyi et al., 1993). In comparison iPS-derived motor neurons do not quite recapitulate the *in vivo* adult cell state with a tendency towards immature motor neuron electrophysiological properties such as low spontaneous action potential generation and a lack of repetitive firing (Sances et al., 2016). ALS motor neurons from iPS cells have been found to exhibit hyper-excitability, with faster firing rates due to increased sodium currents and reduced potassium currents (Wainger et al., 2014, Kanai et al., 2006, Devlin et al., 2015). In contrast, slower firing rates and reduced synaptic activity have also been reported (Sareen et al., 2013, Devlin et al., 2015); possibly a compensatory feature of prolonged iPS cell-derived motor neuron tissue culture and differentiation.

So far studies with C9ORF72 have primarily focussed on how the pathogenic mutation causes disease, gathering interesting evidence for or against different mechanisms of action including: haploinsufficiency (Harms et al., 2013), RNA toxic gain of function (DeJesus-Hernandez et al., 2011), and non-ATG (RAN) translation resulting in toxic products of di-peptide repeat proteins (DRPs) (Mori et al., 2013b). Subsequently, differentiated iPS cell- derived neurons have been found to contain RNA foci (Almeida et al., 2013, Sareen et al., 2013, Donnelly et al., 2013a), hallmarks of the hexanucleotide repeat expansion (DeJesus-Hernandez et al., 2011) which are proposed to be indicative of the importance of RNA toxicity in C9ORF72 pathogenesis. In addition, RNA binding proteins have been found to be associated with foci in some (Sareen et al., 2013, Donnelly et al., 2013a) but not all (Almeida et al., 2013) investigations, adding to the theory that these foci aberrantly sequester RNA binding proteins from their normal binding partners.

Here, we wanted to develop iPS cell derived neuronal and motor neuronal cell models to investigate ALS. Therefore, this chapter focuses upon the important first stage of characterisation and investigation of these newer cell models of disease, including comparison between patients and controls, and evaluation against previously established iPS cell models from other groups.

4.2 Aims and Objectives

The aims of the work described in this chapter were to optimise and characterise induced pluripotent stem cells, derived from three C9ORF72- related ALS patients and their healthy matched controls, and their differentiated counterparts, with the aim to successfully differentiate the cells into motor neurons to be studied as a cell model of C9ORF72-related ALS. The iPS cells were generated by our collaborating group at Tongji University School of Medicine, Shanghai, China, by retroviral transduction of four Yamanaka factors: Oct4, c-myc, Sox-2 and Klf4. They were then characterised for pluripotency by labelling the reprogrammed cells for expression of markers associated with pluripotency. Next cells were differentiated comparing protocols previously established in the literature to optimise the differentiation of cells into a motor neuron-like fate. The cells generated were then characterised for markers that indicate progression into a neuronal and motor neuronal identity. Following this, the cells were quantified for total motor neuron yield obtained as percentage of cells in the mixed population that expressed dual Tuj1 (neuronal) and ChAT (mature motor neuronal) marker expression.

Whilst immunocytochemical staining for markers of pluripotency can be a good indicator of the cells terminal identify after differentiation, representation of markers alone does not indicate if the neuron is functional. For this reason our next aim was to perform electrophysiological experiments to confirm the firing properties of the cell, measuring for action potential generation after a depolarising stimulus, as a measure to characterise motor neuron maturity. This was achieved through whole cell patch clamping techniques.

Finally, to show our methods for the generation of iPS cells and the differentiation of iPS cells to motor neurons did not remove the C9ORF72 expansion from ALS patients, we also aimed to characterise the cells for C9ORF72-ALS specific hallmarks. We assessed the iPS cells and differentiated iPS cells for the presence of sense and antisense RNA foci, and then whether these lead to detectable dipeptide repeat proteins and changes in TDP-43 localisation; markers commonly associated with ALS

cell models. Moieties were quantified for number, and subcellular localisation in comparison to previously established findings.

4.3 Induced Pluripotent Stem (iPS) Cell generation and differentiation

4.3.1 Characterisation of induced Pluripotent Stem (iPS) Cells

The iPS cells were generated in our collaborating lab by Yang and colleagues at Tongji University School of Medicine, Shanghai, China, from three primary human dermal fibroblasts from patients with C9ORF72-related ALS, along with their healthy matched controls (figure 4.1 a). To verify the identity of the fibroblasts immunocytochemical (ICC) staining confirmed the presence of TE-7 (figure 4.1 b), an anti-fibroblast antibody frequently used in the literature (Haynes et al., 1984). Fibroblasts were subsequently transduced with retroviruses expressing Oct4, c-myc, Sox-2 and Klf4, or GFP as a control to re-programme the somatic cells to pluripotency using previously described protocols (Takahashi and Yamanaka, 2006, Takahashi et al., 2007, Yang et al., 2014b) (figure 4.1 c).

To validate that the fibroblast cells had been successfully reprogrammed, iPS cells were examined for their morphological and biochemical similarities with human embryonic stem cells. The cells had lost their fibroblast-like appearance to form large colonies of tightly packed cells with defined edges, with cells displaying a large nucleus to cytoplasm ratio, a morphology associated with human embryonic stem cells (figure 4.1 d, figure 4.2, figure 4.3). Colonies also showed a uniform density, confirming no spontaneous differentiation (figure 4.1d), however alkaline phosphatase staining, a marker of embryonic stem cell pluripotency (O'Connor et al., 2008), confirmed that the cells were pluripotent and undifferentiated (figure 4.1 e, f).

Using markers of pluripotency, it was found both human embryonic stem cells (figure 4.1 g) and the iPS cells generated (figure 4.1 h) expressed Oct4 and Sox2, transcription factors which induce pluripotency, as well as cell surface antigens SSEA-3, SSEA-4, TRA-1-60, and TRA-1-81. Alongside this, the iPS cell lines also displayed a normal human

karyotype with no abnormalities observed (figure 4.1 i). Finally, to confirm the cells ability to form cell types from all three germ layers, iPS cells were transplanted into the hind limb of severe combined immune deficiency mice which resulted in the formation of teratomas containing tissue of ectodermal (figure 4.1 j), mesodermal (figure 4.1 k, l) and endodermal (figure 4.1 m) origin.

The collaboration of, the collection and generation of IPS cells in China and work conducted in Sheffield was all done with prior ethical permission in place. Human fibroblasts have have (STH14653 REC: 07/Q2305/9) NRES Committee Yorkshire & the Humber approval. After arrival in Sheffield, cells were cultured in iPS media containing basic fibroblast growth factor (bFGF) on a feeder layer of mitomycin C treated mouse embryonic fibroblasts (MEFs), and additional confirmatory tests were performed to conform that the cells remained undifferentiated. To replicate the conditions the iPS cells were kept under in China, we re-confirmed expression of pluripotency markers TRA-1-60 and SSEA-4 by dual staining with an additional marker of pluripotency and one of the transcription factors used to reprogram the fibroblasts, c-myc (figure 4.2 and 4.3). Therefore we confirmed in our hands that the findings reported to us from China were correct before commencing work. Together, as cells remained morphologically and biochemically similar to human ES cells, these findings demonstrate the fibroblast cells had been successfully re-programmed to a pluripotent state.

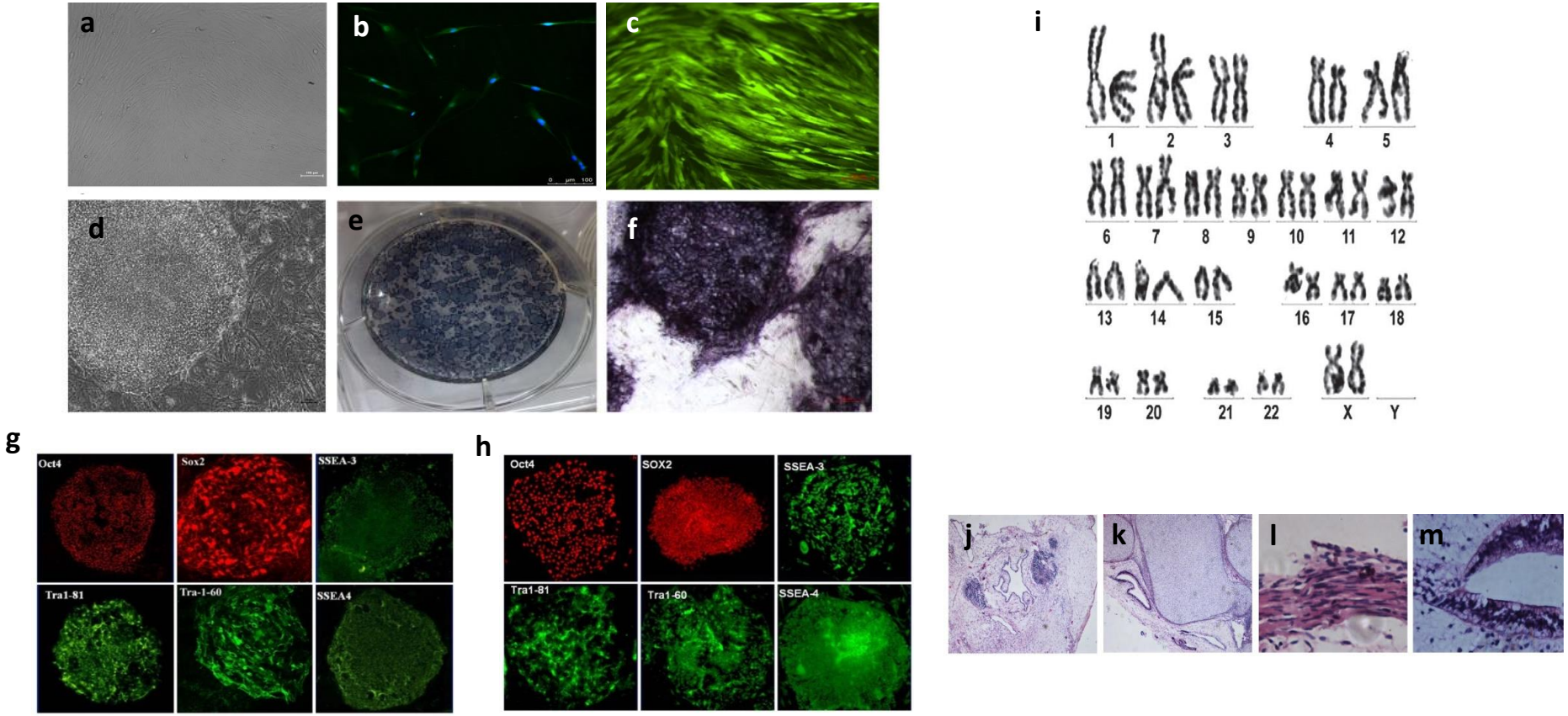

Figure 4.1: iPS cells can be generated from human patient and control fibroblast cells. **a)** Human dermal fibroblast cells stained for **b)** TE-7 to confirm fibroblast identify, **c)** fibroblasts transfected with GFP retroviruses, **d)** Flat multicellular iPS cell colony with cells containing a high nucleus to cytoplasm ratio, **e)** and **f)** iPS Colonies demonstrate expression of alkaline phosphatase. Comparison of **g)** human embryonic stem (ES) cells to **h)** control human iPS cells reveals expression of the same markers for nuclear pluripotency (Sox-2, Oct4) and embryonic cell surface markers (SSEA-3, SSEA-4, TRA-1-60, TRA-1-81). **i)** IPS cells generated display a normal human karyotype. Injection of iPS cells into NOD/SCID mice causes teratoma formation made of **j)** neural ectodermal tissue; **k)** cartilage mesodermal tissue; **l)** muscle mesodermal tissue **m)** and primitive gut endodermal tissue (Abbreviations: Oct 3/4, octamer-binding protein 3/4; SOX2, sex determining region Y (SRY) -box 2; SSEA3/4, stage specific embryonic antigen 3/4; TRA-1-60/1-80, tumour rejection antigen 1-60/ 1-80 Scale bar=) (Work conducted by Yang et. al Tongji University School of Medicine, Shanghai, China)

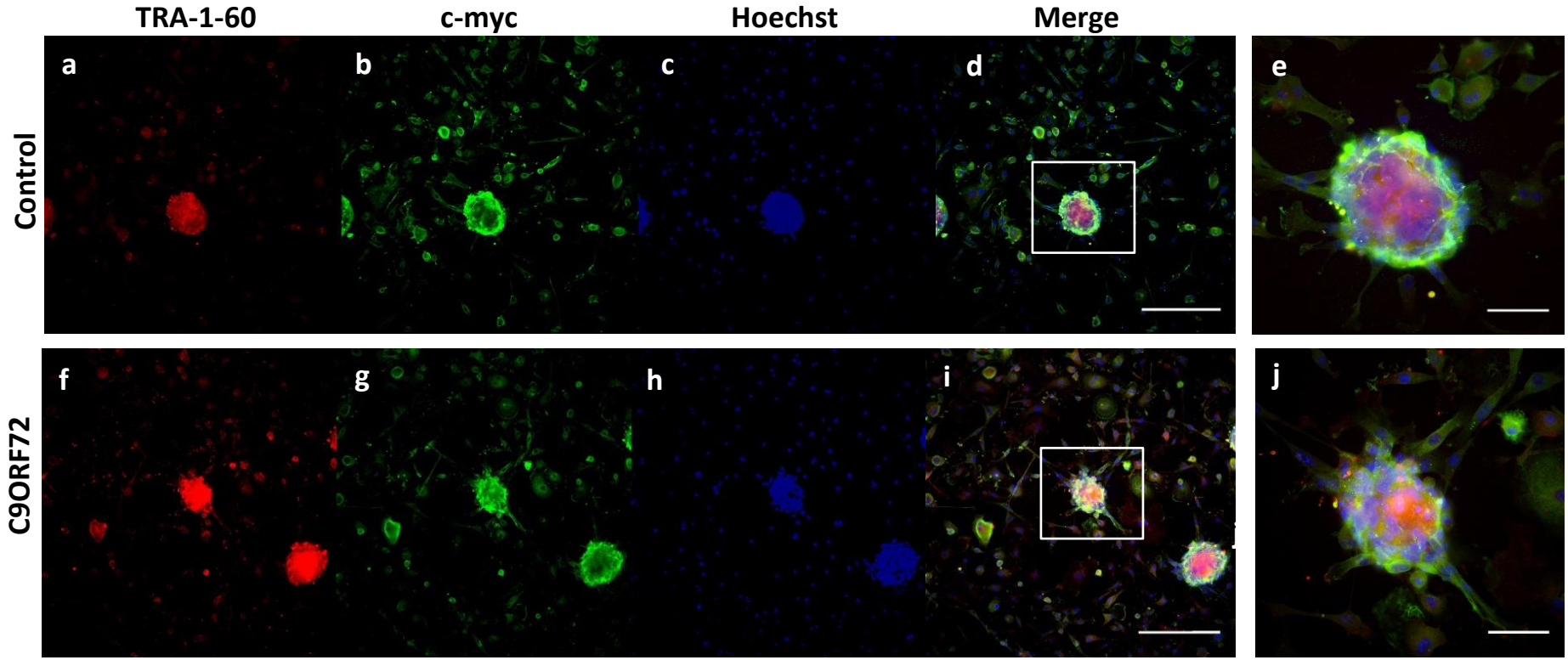

Figure 4.2: Characterisation of iPS cells generated from human dermal fibroblasts for markers of pluripotency. Control and patient iPS cells revealed positive dual expression for **a)** and **f)** TRA-1-60; **b)** and **g)** c-myc when stained via immunocytochemistry. **c)** and **h)** Hoechst labels nuclei blue. **d)** and **i)** merge. **e)** and **J)** zoom of insert (Abbreviations: TRA-1-60, tumour rejection antigen 1-60; c-myc, cellular-avian myelocytomatosis. Scale bar=200µM d) and i); Scale bar= 50µM e) and j))

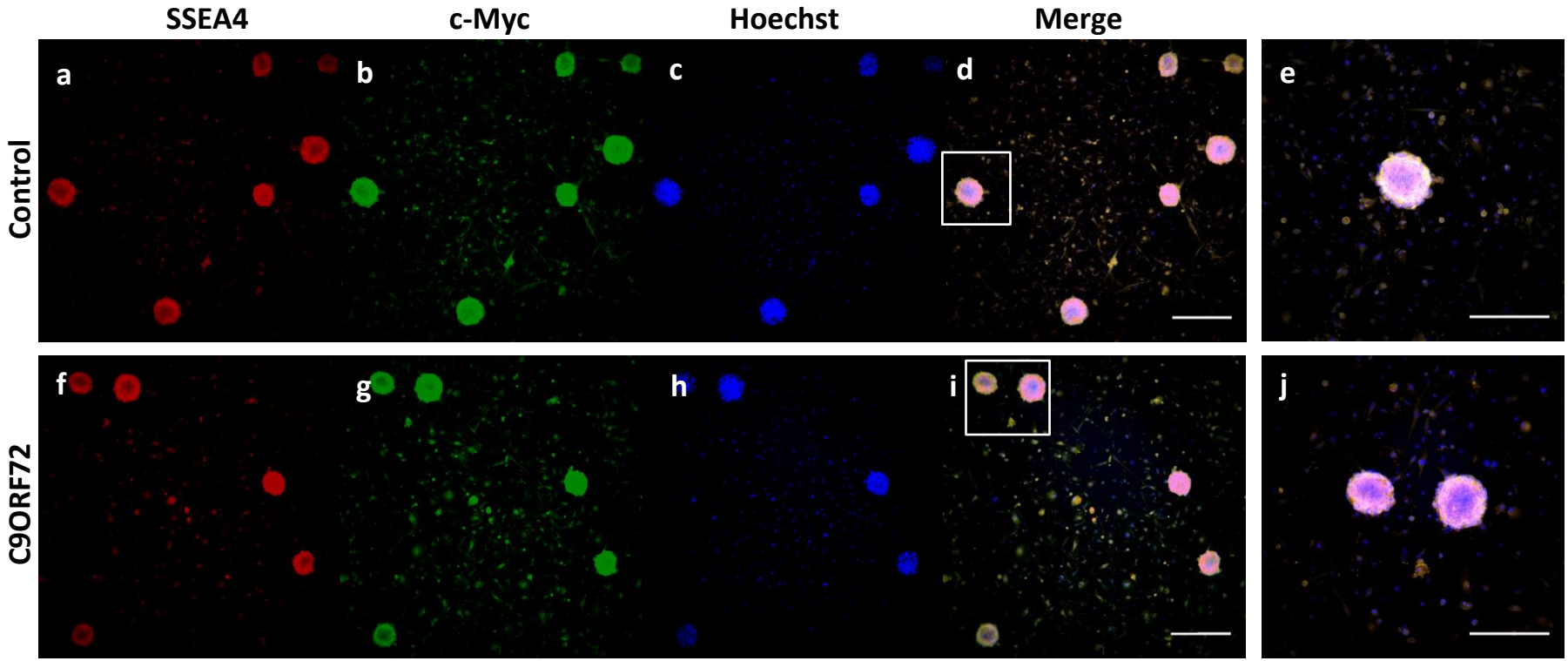

Figure 4.3: Characterisation of iPS cells generated from human dermal fibroblasts for markers of pluripotency. Control and patient iPS cells revealed positive dual expression for **a)** and **f)** SSEA-4; **b)** and **g)** c-myc when stained via immunocytochemistry. **c)** and **h)** Hoechst labels nuclei blue. **d)** and **i)** merge. **e)** and **J)** zoom of insert (Abbreviations: SSEA-4, stage specific embryonic antigen 4; c-myc, cellular-avian myelocytomatosis. Scale bar=300µM d) and i); Scale bar= 200µM e) and j)

4.3.2 Differentiation of induced Pluripotent Stem (iPS) Cells to Motor Neurons

To differentiate iPS cells into cells of a neural lineage, and more specifically into motor neurons, attached colonies were first grown in an iPS media containing bFGF, as well as Rho kinase inhibitor Y27632 and LDN193189 which were added to enhance single cell survival and induce a default neural identity via SMAD inhibition respectively (Chambers et al., 2009). This promoted the formation of embryoid bodies (EBs) as well as the beginning of neuralisation. The neuralisation process continued from days 3 to 16, in which cells were cultured in a neural induction media comprising mainly of DMEM:F12 and knock-out serum (partially purified bovine serum albumin) which prevents spontaneous differentiation and reduces astrocyte formation promoted by the addition of FBS (Li et al., 2015). Over the course of neural induction, retinoic acid was added from day 5 onwards to promote caudalisation. This was followed by sonic hedgehog (SHH), as well as smoothened agonist purmorphamine (PUR) which together act to promote sonic hedgehog activation and thus ventralisation of the developing cells (Ericson et al., 1996, Jessell and Sanes, 2000). During this period of neural induction, brain derived neurotrophic factor (BDNF) was also added for neurotrophic support (Jones et al., 1994). From day 17 to the end of differentiation and beyond, day 42+ (6 weeks), cells were maintained in neurobasal media supplemented with three additional neurotrophic factors: insulin-like growth factor 1 (IGF-1), glial derived neurotrophic factor (GDNF), and ciliary neurotrophic factor (CNTF), used to promote the maturation of motor neurons. This protocol was followed as it recapitulates the process of embryonic motor neuron development *in vitro* of blastocyst pluripotency, gastrulation, neuralisation, caudalisation, ventralisation, and maturation (figure 4.4).

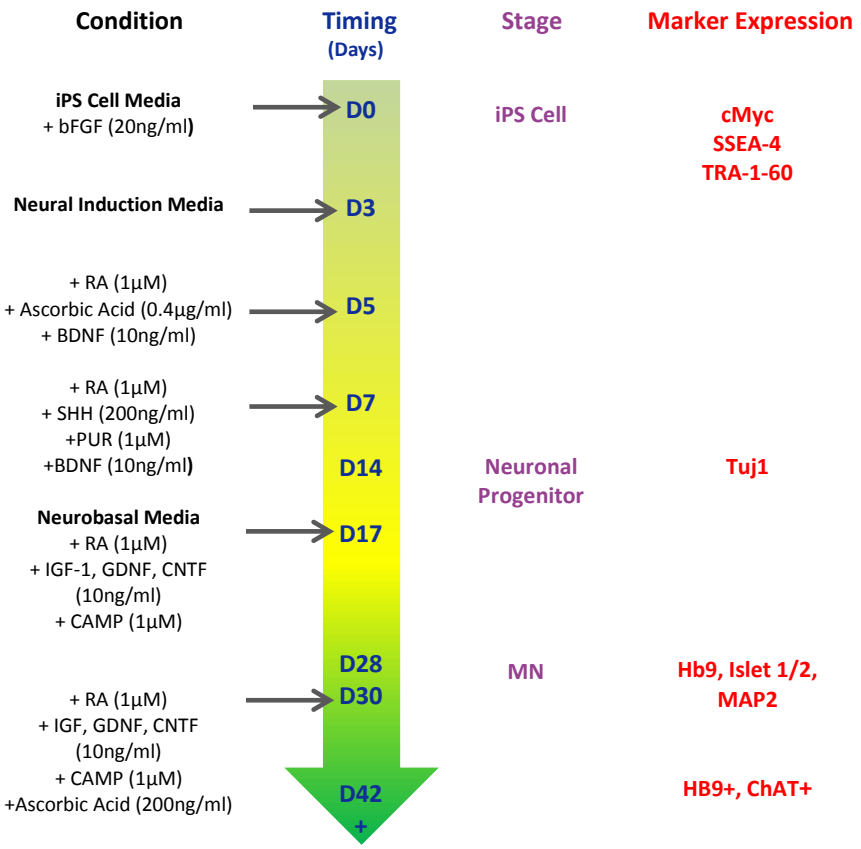

Figure 4.4: Schematic representation of the iPS cell differentiation protocol to generate motor neurons. iPS colonies from day 0 undergo neural induction by addition of various factors isolated from embryonic motor neuronal development. By day 14 neuronal progenitors are formed expressing TuJ1 and by day 28 cells express specific MN markers Hb9, islet 1/2 as well as neuronal marker MAP2. At the end of the differentiation protocol and beyond, cells express mature motor neuronal marker ChAT as well as continued Hb9 expression. (Abbreviations: iPS, induced pluripotent stem; bFGF, basic fibroblast growth factor; RA, retinoic acid; BDNF, brain derived neurotrophic factor; SHH, sonic hedgehog; PUR, purmorphamine; IGF, insulin-like growth factor 1; GDNF, glial derived neurotrophic factor; CNTF, ciliary neurotrophic factor; CAMP, Adenosine 3', 5'- cyclic monophosphate; MN, motor neuron; c-myc, cellular-avian myelocytomatosis; SSEA-4, stage specific embryonic antigen 4; TRA-1-60, tumour rejection antigen 1-60; Tuj1, β III tubulin;; Hb9, homeobox gene 9; MAP2, microtubule associated protein 2; ChAT, choline acetyl transferase)

4.3.3 Differentiated induced Pluripotent Stem (iPS) cells Display Neuronal and Motor Neuronal Specific Markers

First, to confirm that the differentiation of iPS cells was directed towards a neuronal fate, cells were analysed longitudinally throughout differentiation. Cells were fixed and stained for neuronal marker microtubule associated protein 2 (MAP2) which is localised to neuronal dendritic processes. Immunocytochemical (ICC) staining revealed positive expression of MAP2 in cells from 4 weeks onwards, with extensive processes and branches emerging from multiple cells (figure 4.5). This suggests that a subset of cells had gained a neural identity from our differentiation protocol.

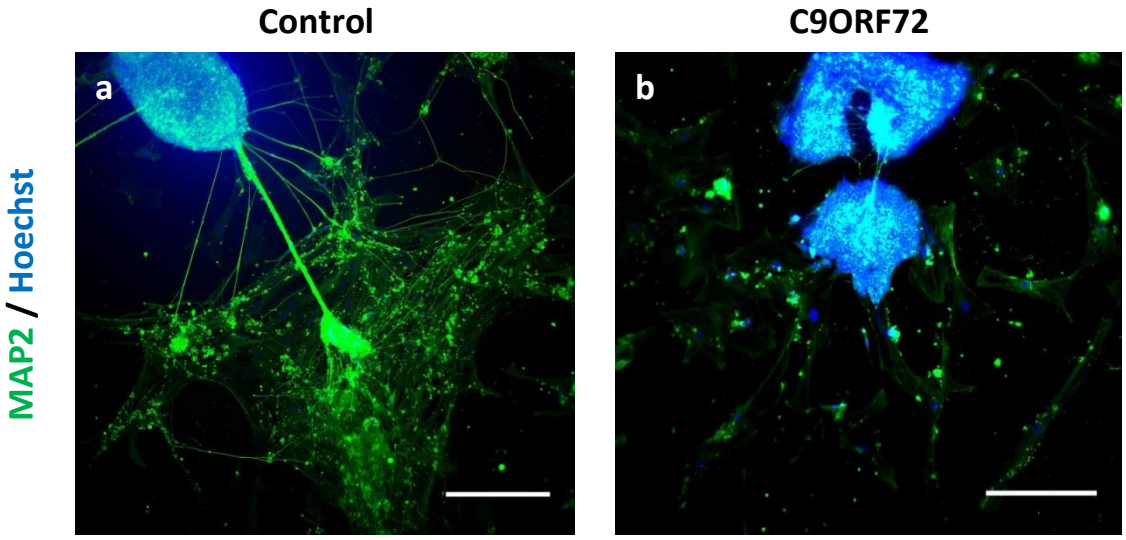

Figure 4.5: Neurons generated from iPS cells express neuronal specific dendritic marker MAP2 in both **a)** control and **b)** patient cells from 4 weeks of differentiation. (Abbreviations: MAP2, microtubule associated protein 2. Scale bar = 300µM)

Next, to verify if the differentiated cells generated with this protocol were progressing towards a spinal lower motor neuronal identity, cells were immunostained for LIM homeodomain markers specific for motor neurons including islet 1/2, a transcription factor involved in regulating the differentiation of motor neurons in the neural tube, and Homeobox gene 9 (Hb9) another motor neuron specific transcription factor important in specifying motor neuron fate (Arber et al., 1999). In an additional level of validation, cells were dual stained with a neuronal specific class of β III Tubulin (Tuj1), which stains the processes of neuronal cells.

Results revealed positive dual expression of islet1/2 and Tuj1, labelling both patients and controls from 4 weeks of differentiation (figure 4.6). Additionally, cells revealed positive dual staining for Hb9 and Tuj1 (figure 4.7) in both patients and control cells, with staining found from 4 weeks onwards. Hb9 and islet 1/2 staining were mainly nuclear and co-localised with Hoechst nuclear stain, however some processes towards the nuclear periphery also stained, which is in line with previous reports of immunostaining with these markers (Dimos et al., 2008, Karumbayaram et al., 2009). Interestingly, larger processes could be found in cells which were tightly packed together (figure 4.4, figure 4.6), with long and extensive outgrowth from EBs which had not broken up during the process of differentiation. These groups of cells (figure 4.6) were not disease specific and could be found in both patient and control conditions, along with areas of dispersed single cell populations (figure 4.5). Remaining EBs during differentiation is an observation which matches previously established reports in iPS cell to motor neuron differentiation studies (Dimos et al., 2008).

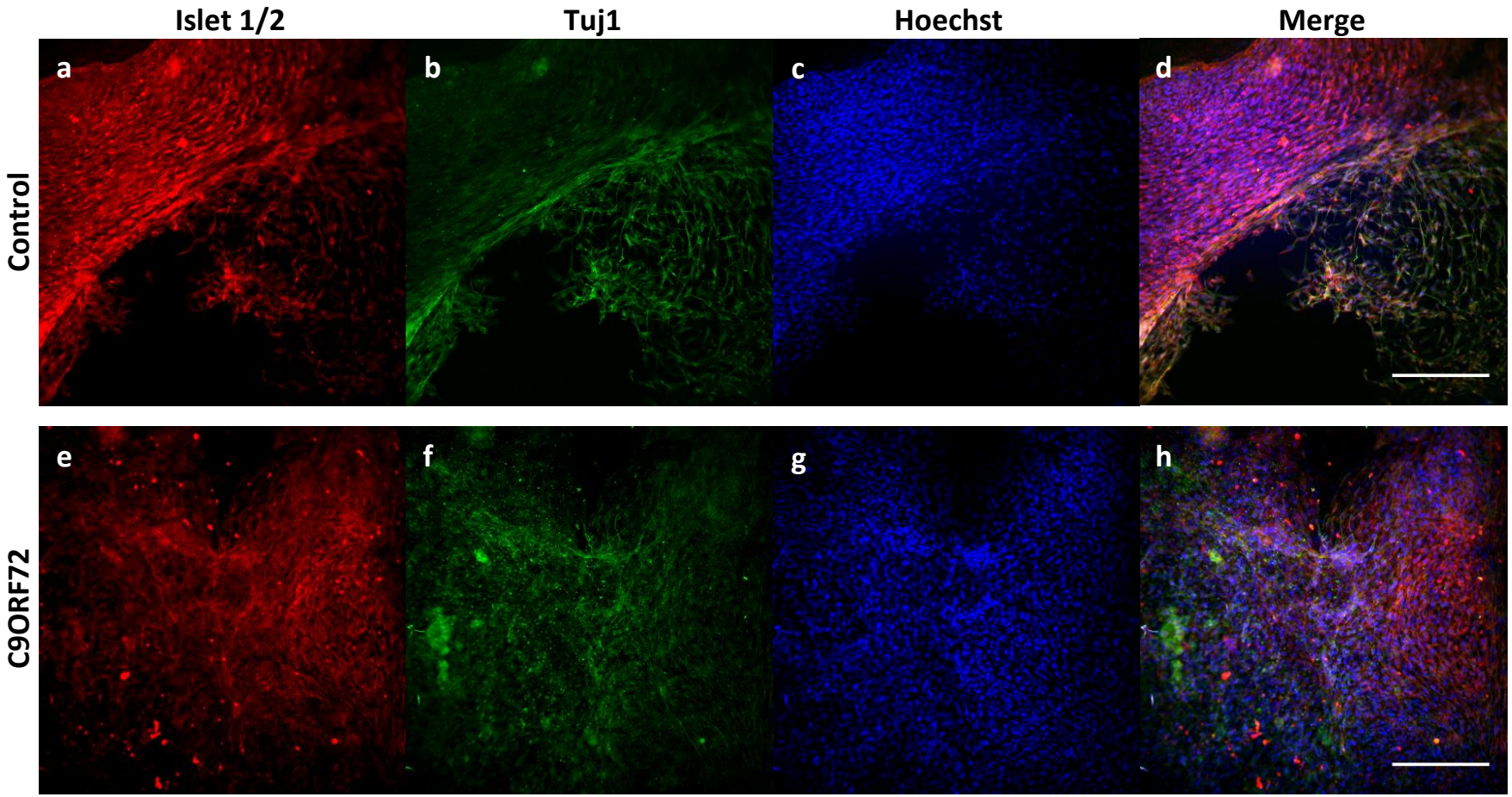

Figure 4.6: Neurons generated from iPS cells express markers specific to neuronal and motor neuronal lineages. a-d) control and **e-h)** patient iPS-derived cells express dual positive staining for islet 1/2 a transcription factor that regulates motor neuron differentiation in the neural tube, along with Tuj1, a neuronal specific class of β III tubulin and a pan neuronal marker, found in axons and cell bodies from 4 weeks of differentiation (Abbreviations: Tuj1, β III tubulin. Scale bar = 300μM)

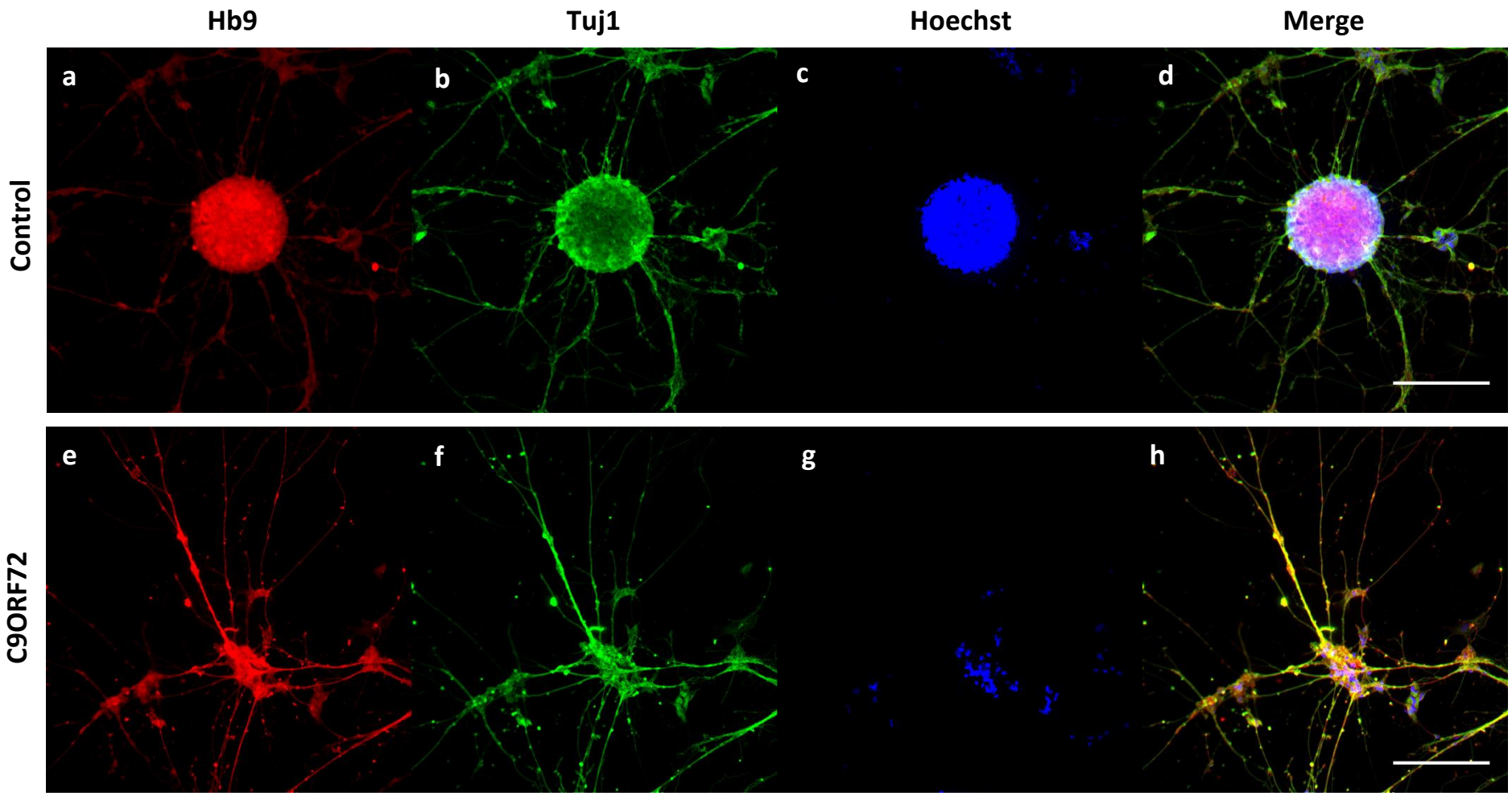

Figure 4.7: Neurons generated from iPS cells express markers specific to neuronal and motor neuronal lineages. a-d) control and **e-h)** patient iPS-derived cells express dual positive staining for Hb9 a motor neuron specific transcription factor found in cellular nuclei and processes, along with Tuj1, a neuronal specific class of β III tubulin expressed in neuronal processes and cell bodies from 4 weeks of differentiation (Abbreviations: Hb9, homeobox gene 9; Tuj1, β III tubulin. Scale bar = 300μM)

4.3.4 Optimisation of Choline Acetyl Transferase Immunocytochemistry (ICC)

While Hb9 has been described as a specific motor neuronal marker (Arber et al., 1999), the presence of Hb9 positive expression in some glutamatergic ventral spinal interneurons (Wilson et al., 2005) and the reduced expression of both Hb9 and islet 1/2 with maturity (Thaler et al., 2004) highlights problems in using these markers alone for mature motor neuron immunocytochemistry. Therefore, to identify mature motor neurons amongst a mixed population of cells, along with MAP2 and Tuj1 neuronal staining, and complementary to islet 1/2 and Hb9 motor neuronal specific staining, it was important to also confirm the expression of mature motor neuronal marker choline acetyltransferase (ChAT).

Previous studies performed in our department have identified that ChAT antibody staining requires a long incubation period to achieve optimal staining of motor neuron cell bodies and processes. This encouraged us to optimise a time course as early experiments suggested no motor neurons were present in our samples.
Our first efforts to label differentiated cells with ChAT for an incubation period of 24 hours did not produce any visible staining, in line with previous observations from departmental colleagues, which lead us to optimise the protocol for immunocytochemistry (ICC) for this antibody, incubating the cells at 6 weeks of differentiation, for 48 and 72 hours. To control for the possibility that the cells were not mature enough to express ChAT at 6 weeks of differentiation; we also incubated cells differentiated up to 9 weeks for 72 hours. In addition, as a positive control we also incubated primary mouse motor neurons for 72 hours with ChAT to ensure the antibody used was functional. After a 72 hours incubation period, results confirmed that the staining observed was specific and motor neurons were detectable from 6 weeks of differentiation onwards (figure 4.8).

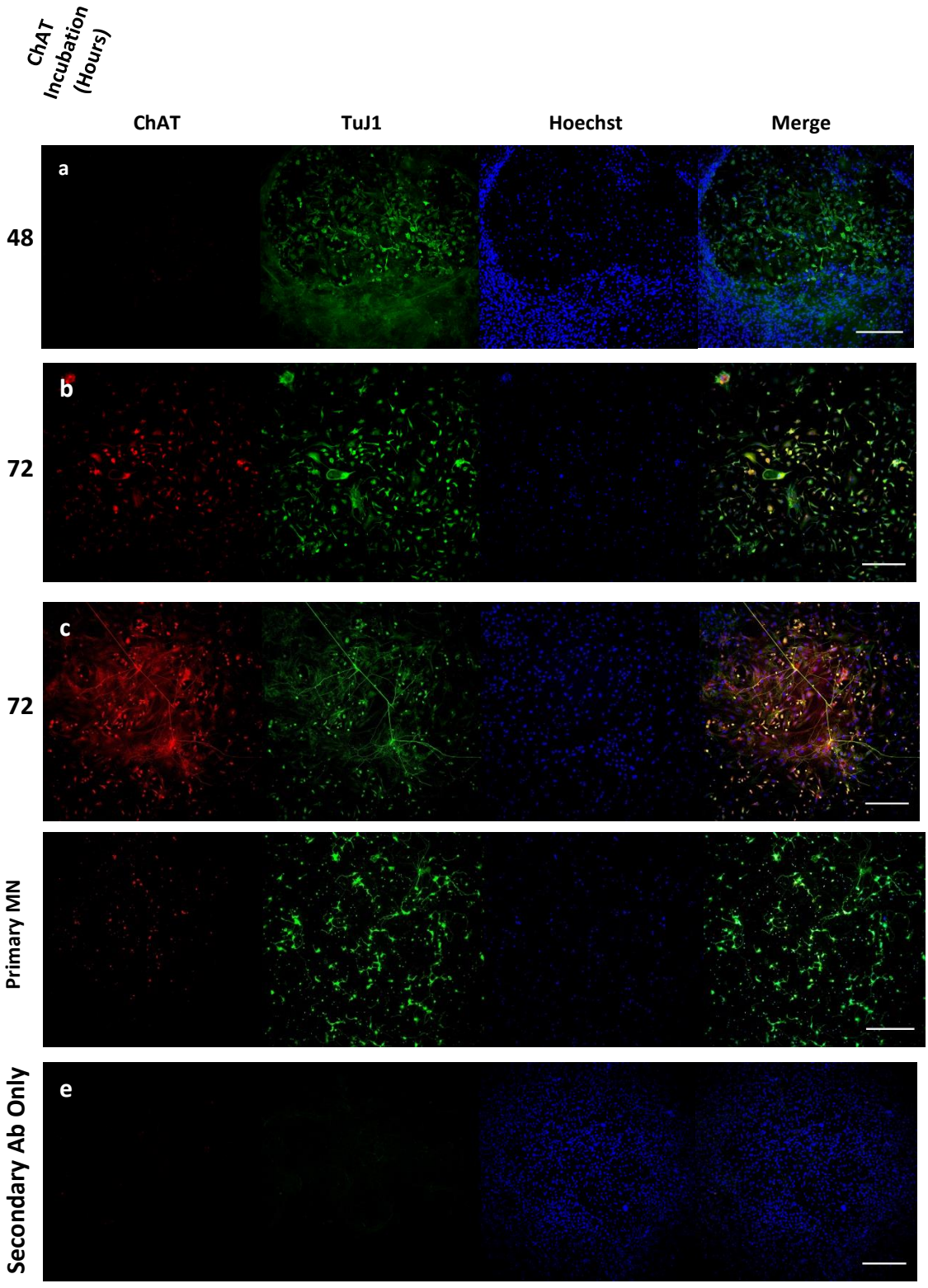

Figure 4.8: Optimisation of choline acetyl transferase immunocytochemistry a) 48 hour incubation period of ChAT antibodies did not label mature motor neurons at 6 weeks of differentiation. However after a 72 hour incubation time, cells at **b)** 6 weeks and **c)** 9 weeks of differentiation, a subset of cells labelled positively for mature motor neuronal marker ChAT, in staining comparable to **d**) primary mouse motor neurons positive controls. Incubation of differentiated iPS cells at 6 weeks with **e)** secondary antibodies only revealed low level background staining. (Abbreviations: Ab, antibody; ChAT, choline acetyl transferase; Tuj1, β III tubulin; MN, motor neuron, . Scale bar = 300μM)

4.3.5 Differentiated induced Pluripotent Stem (iPS) Cells Express Mature Motor Neuronal Marker Choline Acetyl Transferase and Quantification of iPS- Derived Motor Neuron Yield

After the successful optimisation of the ICC protocol for ChAT expression in differentiated iPS cells, to establish that the differentiation protocol produces mature motor neurons, we next dual stained patient and control iPS cells at 6 weeks of differentiation for ChAT and Tuj1 in all 6 cell lines.

Results revealed a positive correlation of both markers in a subset of differentiated cells that morphologically represented MNs, with triangular cell bodies emitting processes including axons and dendrites. The MNs expressed ChAT, co-localising with the nuclei of positive populations, with some processes also staining positively for the marker (figure 4.9 d, h). Tuj1 expression as expected, was found to be highest in the processes of cells with some fainter expression visualised in cell bodies (figure 4.9 b f). Taken together, these results indicated that our differentiation protocol was able to generate mature motor neuronal cells as exemplified by recognised motor neuron marker expression.

Next, to confirm the percentage of mature motor neurons generated amongst a mixed population of cells, we quantified the number of cells labelled positive for dual expression of ChAT and Tuj1. At 6 weeks of differentiation at the end of the protocol, we found controls had an average of 38.3% (±SD 8.3)cells labelled with dual ChAT and Tuj1 in a mixed population of cells, whilst patients had 24.9% (±SD 7.8) motor neurons with total cell number established by Hoechst stained nuclei (figure 4.10). However, despite the trend towards patients exhibiting less motor neurons than controls, there was no significant difference in total motor neurons produced between patients and control cells which suggested the presence of the disease causing mutation in patient iPS cells does not negatively affect the generation of motor neuron cell models from C9ORF72-iPS cells.

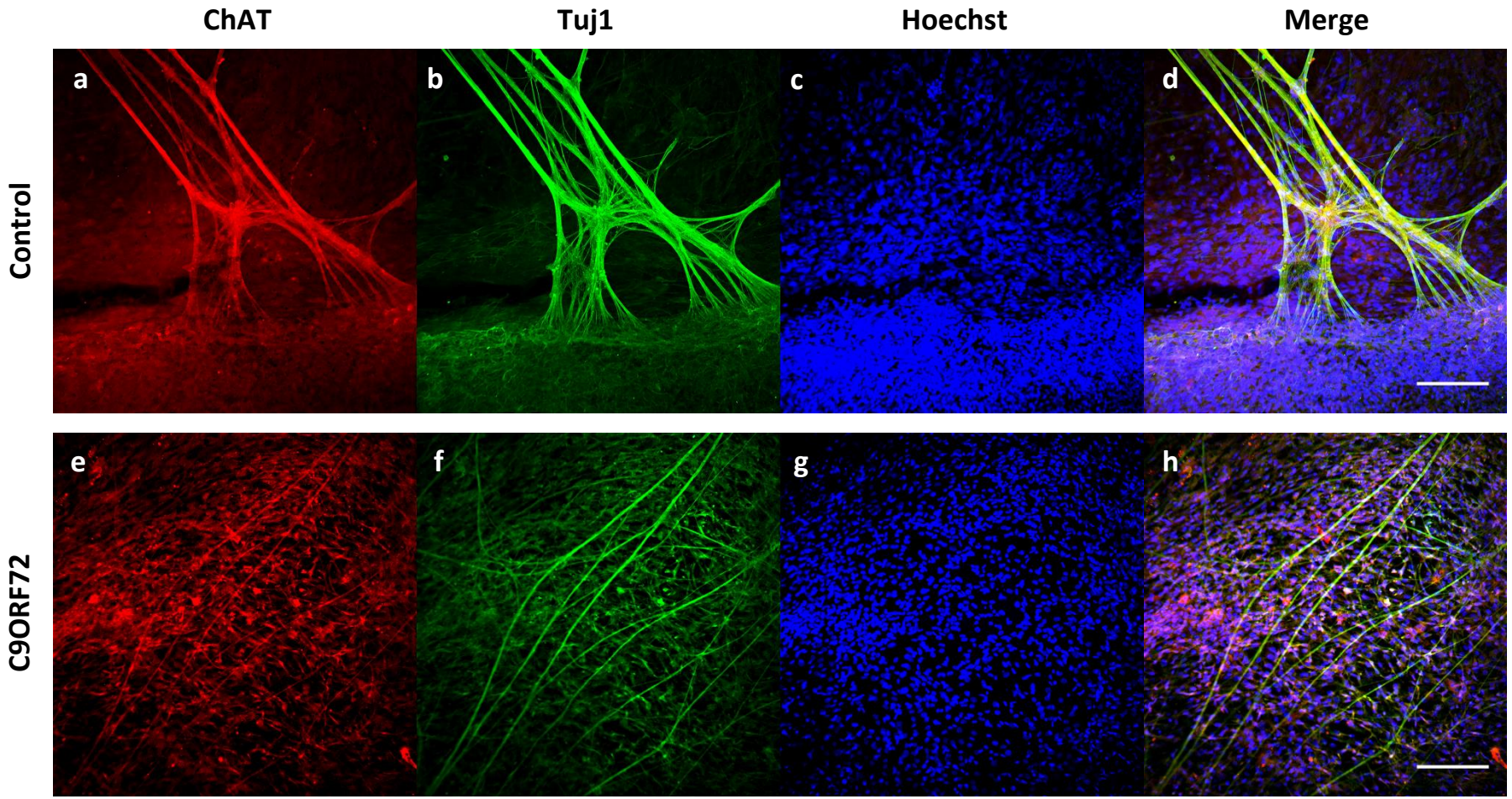

Figure 4.9: **Neurons generated from iPS cells express markers specific to neuronal and mature motor neurons. a-d)** control and **e-h)** patient iPS-derived cells express dual positive staining for ChAT expressed in mature motor neuron cell bodies and processes, along with Tuj1, a neuronal specific class of β III tubulin and a pan neuronal marker found in axons and cell bodies, from 6 weeks + of differentiation (Abbreviations: ChAT, choline acetyl transferase; Tuj1, β III tubulin. Scale bar = 300μM)

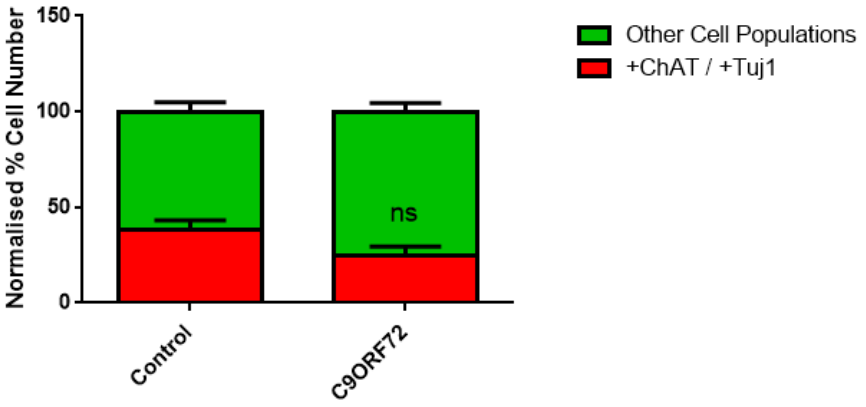

Figure 4.10: Quantification of differentiated iPS cells labelled positive for dual ChAT and Tuj1 staining at 6 weeks of differentiation. Results revealed control motor neurons showed 38.3% of the total cell population staining positively for both markers. Patient C9ORF72 differentiated iPS cells showed an average of 24.9% of cells staining for both markers. There was no significant difference between patients and controls in the number of motor neurons generated. (Data presented as percentage of total cell number at 6 weeks, mean of n=3 independent experiments. ±SEM, analysed with two-way ANOVA)

4.3.6 iPS Derived-Cell Survival Post-Differentiation Protocol

As we did not observe any significant difference in the yield of motor neurons produced between patients and controls, we next postulated if over time, as the cells matured we would see a difference in survival, as exemplified by changes in the total cell number of patient cells compared to controls. We performed total cell counts each week for up to 6 weeks after the initial 6 week differentiation protocol was complete, bringing the total time of cell tissue culture to 12 weeks *in vitro*. Over three independent experiments, results revealed a continuous and significant weekly reduction in total cell number between 7 and 12 weeks in both patients and controls, with the steepest reduction found between 7 and 8 weeks of differentiation (figure 4.11). Primary motor neuron cultures exhibit a decline with cultures optimally maintained for up to 2 weeks after plating, therefore comparatively, these results also suggest a 2 week optimal maintenance period after complete differentiation. Interestingly no difference was found between patient and control cell cultures in the number of iPS-derived cells over time, suggesting C9ORF72 related ALS had no effect of the maturation and survival of the cells post differentiation, otherwise exhibiting similar cell survival phenotypes.

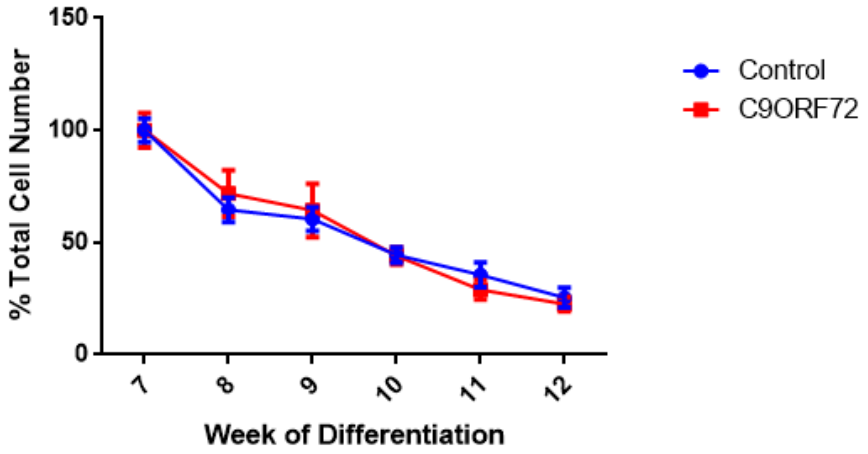

Figure 4.11: Total iPS Derived cell counts. iPS-Derived cells post differentiation revealed a significant decline in total cell numbers from week 7 to 12, with total cell numbers significantly and steadily declining each week in both patients and controls. There was no significant difference in the number of cells between patients and controls at any week post-differentiation (Data presented as percentage of total cell number at 7 weeks, mean of n=3 independent experiments. ±SEM, cell number comparisons between each week analysed with two-way ANOVA, cell number between patients and controls analysed with paired t-test)

4.3.7 Characterisation of the Electrophysiological Properties of iPS- Derived Motor Neurons

To confirm the electrophysiological characteristics of the iPS-derived motor neurons generated, we performed whole cell patch clamp procedures on individual iPS-derived neurons which were identified by their morphology including triangular cell bodies emitting processes (Figure 4.12 a). We obtained recordings from multiple cells across 6 cell lines, from three rounds of differentiation, and from 6-9 weeks of differentiation, to identify if we could record normal depolarization induced action potentials in our cells. To first measure the cells ability to fire depolarized evoked action potentials, cells were recorded in current-clamp mode under a depolarising stimulus of a 10 step protocol for a duration of 500 milliseconds, injecting current from -40pA, every 20pA. Unfortunately, we were unable to identify any motor neurons which were electrically excitable for both patient and control cells at 6 to 9 weeks differentiation, the majority

of cells displaying no firing or single firing action potentials (figure 4.12b). As no repetitive or adaptive action potentials were recorded, the lack of action potentials suggests an immature motor neuronal phenotype.

In order to ascertain the electrical properties of the neurons, we checked the resting membrane potential (RMP), membrane capacitance, and series resistance for each recording across all 6 cell lines. All the recordings considered for analysis were taken with less than -50pA of leak current and less than 20MΩ of series resistance. Although patients exhibited a trend towards a lower membrane capacitance (average 17.79pF control and 13.58pF patients), and a lower resting membrane potential (average of -11.22mV control and -14mV patients), results revealed no significant difference between patients or controls in either of these two parameters (tables 1- 3 figure, 4.12c and d). Whilst the similarities suggest that any differences found will not be due to changes in the health of the cell or membrane baseline capacitance between patient and control cell lines, the RMP is too low to consider the neurons as a mature, as we expect to have values around -40 to -60 mV for a mature neuronal cell.

Table 4.1: Raw data for membrane capacitance (Cm) (pF) and resting membrane potential (RMP) (mV) for patient and control cells iPS-derived motor neurons

Control		Patient	
Cm (pF)	**RMP (mV)**	**Cm (pF)**	**RMP(mV)**
13.33	-10	12.67	-20
28.62	-10	10.3	-10
10.32	-12	6.61	-20
14.11	-5	22.51	-22
22.51	-12	11.13	-6
11.55	-8	20.67	-8
18.13	-20	11.2	-12
28.85	-12	-	-
10.69	-12	-	-

Table 4.2: Average membrane capacitance (pF) for patient and control iPS-derived motor neurons

	Control	Patient
Average Cm (pF)	17.79	13.58429
SD	6.885968	5.369852
N	9	7

Table 4.3: Average Resting membrane potential (RMP) for patient and control iPS-derived motor neurons

	Control	Patient
Average RMP (mV)	-11.2222	-14
SD	3.823256	6.047432
N	9	7

Alongside measuring the excitability of neuronal cells generated from our differentiation protocol, we also performed voltage clamp experiments to measure the transmembrane ion currents required to maintain voltage in our cells. By identifying general inward and outward currents we may identify why we were unable to see any action potentials in our recordings. Results revealed minimal inward currents with no significant differences between patients and controls (figure 4.12 g) which when normalised to individual cellular capacitance, a reading directly proportional to cell surface area and an indicator of the size of the cell, again revealed no significant patient differences (figure 4.12 i). This suggests that both patients and controls have little to no inward current activity. With regards to outward currents, cells revealed higher amplitudes of currents compared to inward currents (figure 4.12h), and when normalised to membrane capacitance, results showed a trend towards separation of patient and control outward current density under higher voltage conditions (figure 4.12 j). This finding suggests that the outward currents are more developed than inward currents in our cell models.

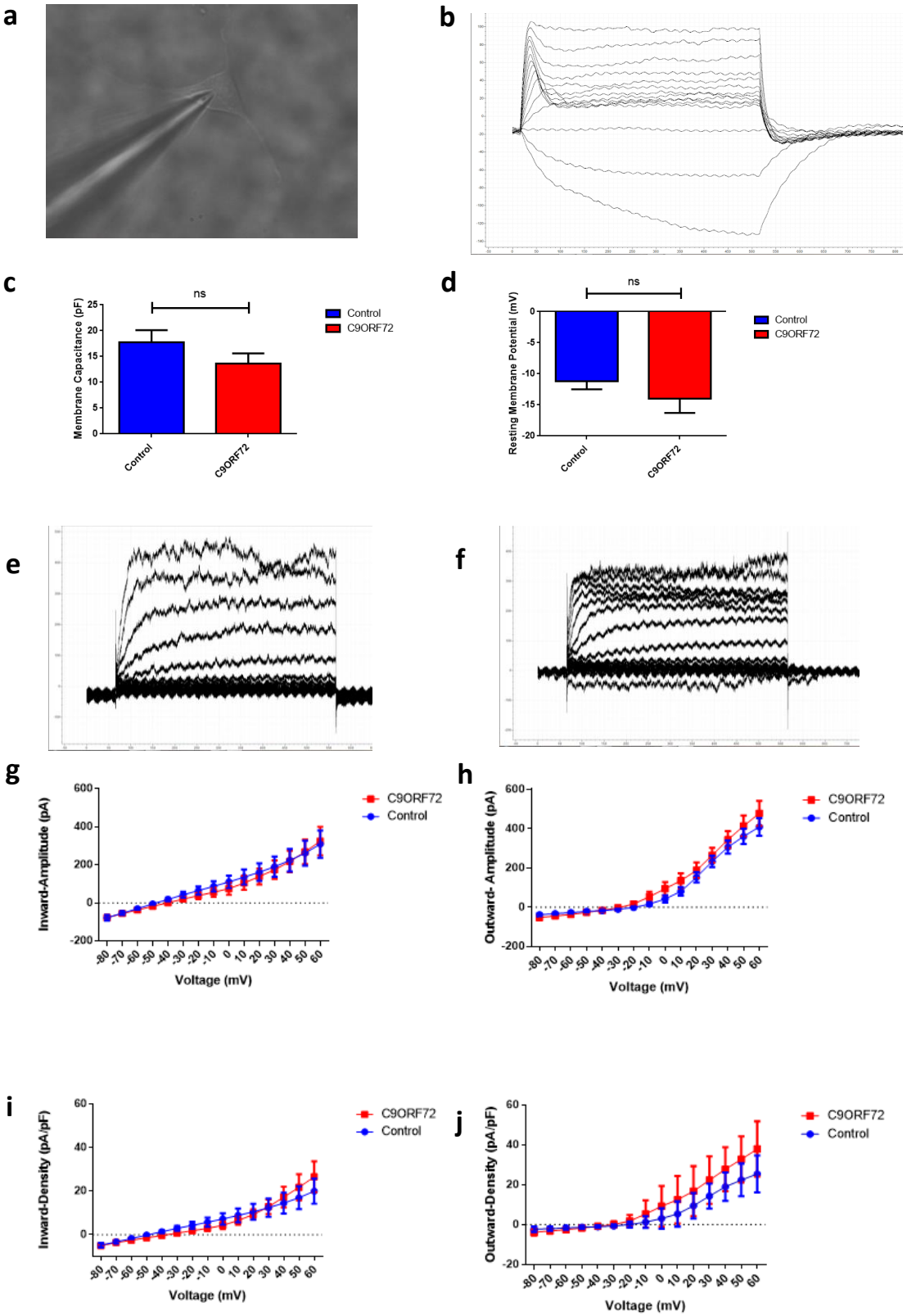

Figure 4.12: Electrophysiological characterisation of iPS-derived neurons reveals no electrical activity in patients or controls. a) iPS-derived cells were selected based on MN-like morphology**. b)** Sample current-clamp recordings from a patient ALS-derived neuron differentiated for 9 weeks. **c)** Average membrane capacitance and **d)** Resting membrane potential in patient and control iPS derived cells revealed no significant differences. **e)** control and **f)** patient sample voltage-clamp recordings from iPS-derived neurons. **g)** voltage-clamp to measure general inward currents and **h)** outward currents for both patient and controls. **i)** Inward current amplitude and **j)** outward current amplitude normalised to cell capacitance in patient and control iPS-derived neurons. (Depolarization protocol from -80mV to +60 mV; controls n=9, patients n=7; data are mean ±SEM, analysed with paired t-test)

4.4 C9ORF72 AND ALS SPECIFIC CHARACTERISATION

4.4.1 iPS CELLS AND IPS-DERIVED CELLS EXPRESS RNA FOCI AND DIPEPTIDE REPEAT PROTEINS

The discovery of an expansion mutation in C9ORF72 classified this subtype of ALS as nucleotide repeat expansion disorders. As previously reported, pathogenic expansions in diseases such as myotonic dystrophy caused the formation of aberrant nuclear accumulations called RNA foci (Taneja et al., 1995), it prompted the question: are these pathognomonic aggregates present in C9ORF72-related ALS models? Therefore, for the next step in the characterisation of iPS-derived cells, it was important to establish the presence of RNA foci, which are hallmarks of the hexanucleotide repeat expansion in cells (DeJesus-Hernandez et al., 2011) and proposed indicators of disease pathogenesis, whilst also checking its presence as an indicator of stability of the expansion in the model.

Induced pluripotent stem (iPS) cell culture can hold inherent technical and practical limitations which can impede the generation of enough material of motor neurons for southern blot detection of the repeat expansion in differentiated cells. Probing for RNA foci can be achieved through single cell investigation which is achievable with smaller quantities of material through RNA fluorescence in situ hybridisation (RNA FISH). In addition difficulties obtaining an optimal antibody for C9ORF72 protein detection meant confirmation of the presence of RNA foci would act to validate this molecular pathology in patient cells compared to controls in the absence of western blotting or immunocytochemistry for the protein. Whilst RNA FISH would identify whether or not an expansion was made and its presence suggests stability during the time investigated, it does not tell us about the size of the expansion. Nevertheless, many studies have successfully used RNA FISH as one methodology to confirm the presence of the expansion in similar cell models of ALS (Almeida et al., 2013, Donnelly et al., 2013a, Sareen et al., 2013).

First, differentiated iPS cells at 6 weeks were fixed and probed using a TYE-563-labelled LNA (16-mer fluorescent)-incorporated DNA probe against the sense RNA

hexanucleotide repeat or antisense RNA hexanucleotide repeat. Both sense and antisense foci were detected in patient iPS cells but not controls, with sense foci found in 31.89% of cells, and antisense foci found in 21.64% of cells (figure 4.13 and 4.14). In good support that the FISH staining was specific and confirming the RNA composition of the aggregates, staining was only observed in C9 patients and in the absence of RNase A (figure 4.13 h and 4.14 d). Of note, cells exposed to the sense RNA probe at day 0 also exhibited foci present in patient but not control cell colonies (figure 4.13 a, c), suggesting that the foci do not develop over the differentiation protocol.

Out of the cells with foci present, the majority of both sense and antisense foci observed were cytoplasmic in location, with occasional nuclear or peri-nuclear foci identified (figure 4.13 g, figure 4.14 c yellow arrows). However where nuclear located foci were identified, they contained a single aggregate, compared to cytoplasmic foci which tended to be present in larger numbers. Not all cells contained RNA foci, independently screened assays found 31.89% of total cells contained sense RNA foci, and 21.64% of total cells contained antisense RNA foci (figure 4.13 i, 4.14 e). The number of foci found per cell showed a similar distribution for both sense and antisense species, with 1 being the most common number of foci per cell (figure 4.15).

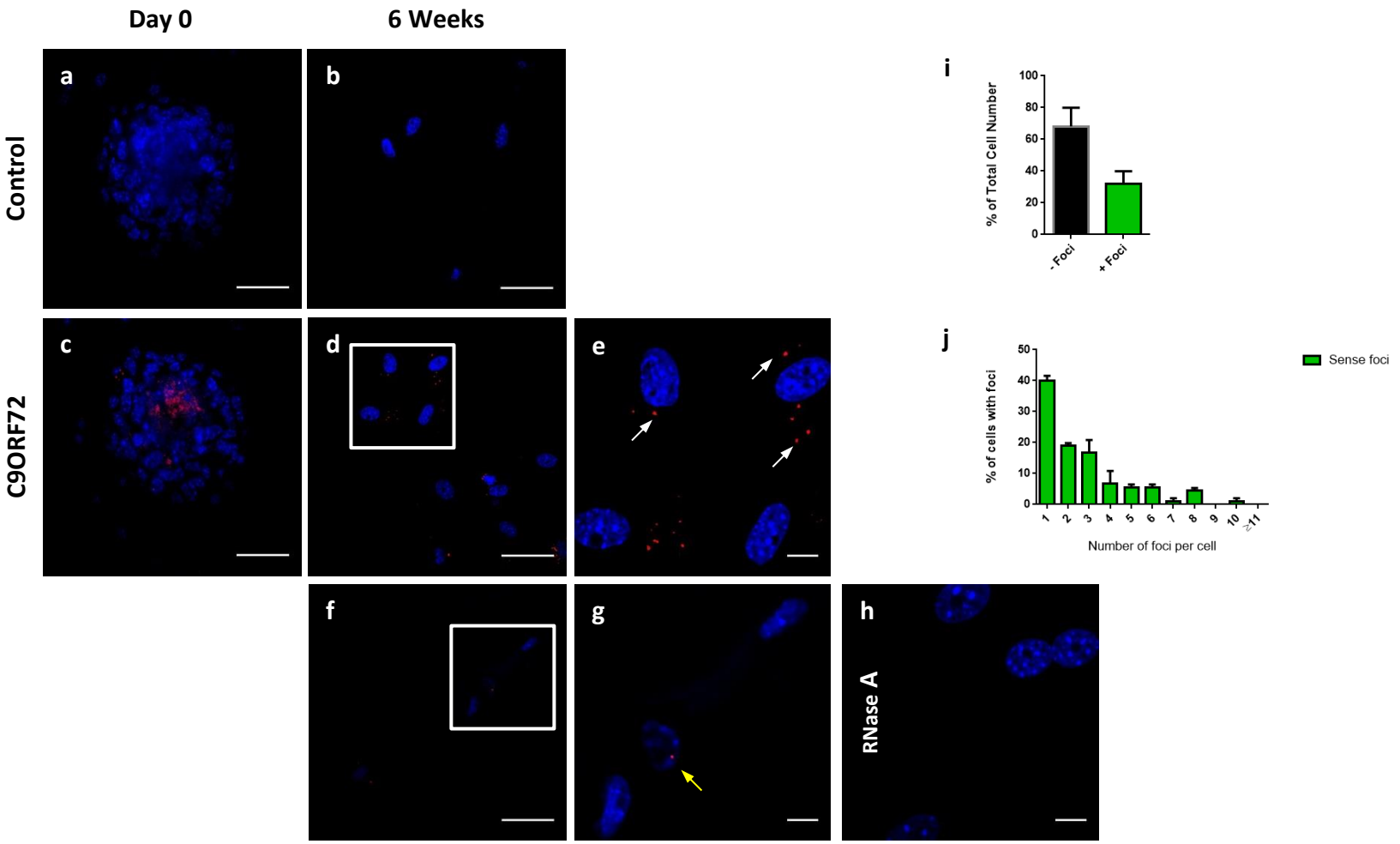

Figure 4.13: iPS Cells and differentiated iPS-derived cells from C9ORF72-ALS patients contain sense RNA foci. Fluorescence *in situ* hybridisation (FISH) using a sense probe to GGGGCC revealed the presence to RNA foci in iPS cells at day 0 **c)** and 6 weeks of differentiation **(d-g)** in patients **(c-g),** but not controls **(a-b).** Foci were mainly found in the cytoplasm of cells **e)** white arrows, but also could less frequently be found in the nuclei of cells **g)** yellow arrow. **h)** Treatment with RNase A removed foci confirming the foci were made of RNA. **i)** Around 30% of patient cells had sense foci. **J)** Histogram showing the number of foci found per patient cell. Hoechst labels nuclei blue (e) and g) inserts from d) and f) respectively. Scale bar= 50µM a),b) c), d) and f); Scale bar = 10µM e), g), h) Error bars ± SEM).

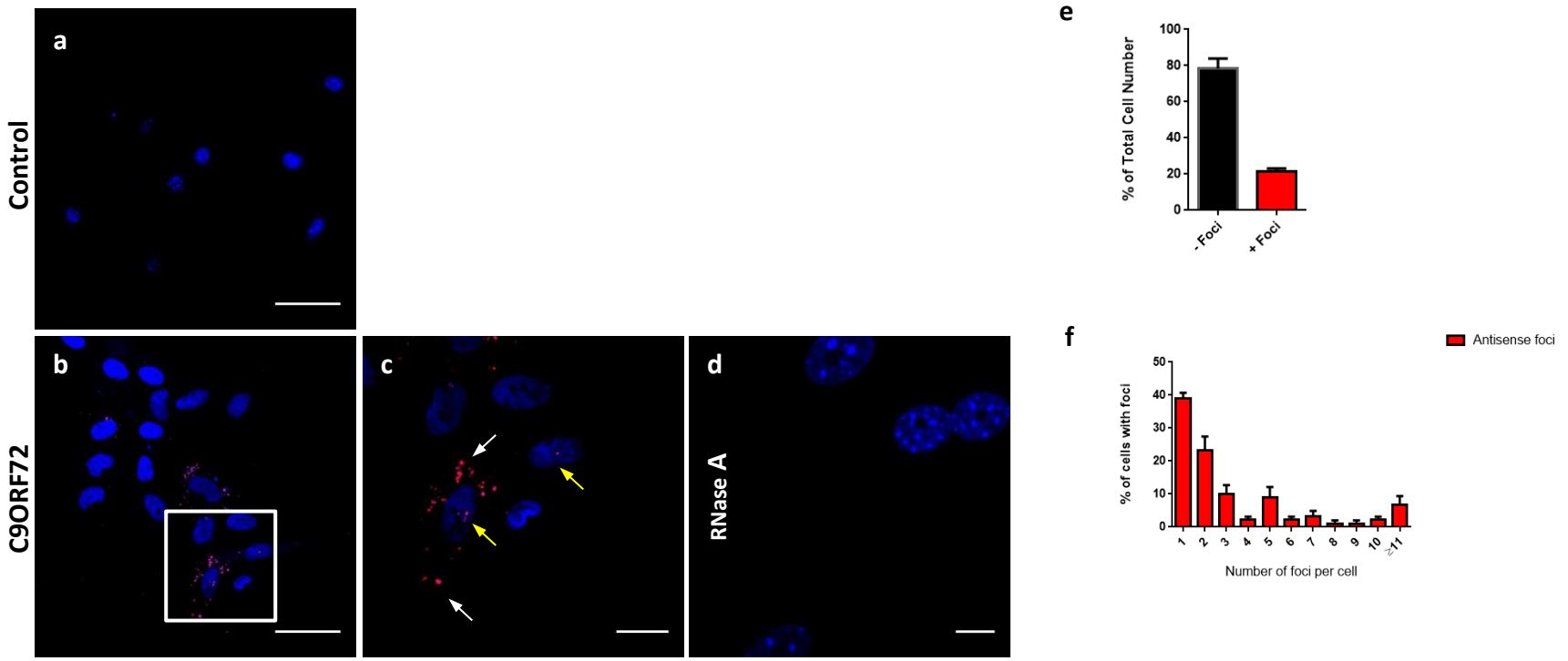

Figure 4.14: Differentiated IPS-derived cells from C9ORF72-ALS patients contain antisense RNA foci. Fluorescence *in situ* hybridisation (FISH) using an antisense probe to GGGGCC revealed the presence to RNA foci in iPS cells at 6 weeks of differentiation in patients **(b-c)** but not controls **a).** Foci were mainly found in the cytoplasm of cells **c)** white arrows, but also could less frequently be found in the nuclei of cells **c)** yellow arrow. **d)** Treatment with RNase A removes foci confirming the foci were made of RNA. **e)** Around 20% of patient cells had sense foci. **f)** Histogram showing the number of foci found per patient cell. Hoechst labels nuclei blue (c) insert from b). Scale bar= 50µM a), b), c); Scale bar = 20µM c); Scale bar =10µM d) Error bars ± SEM).

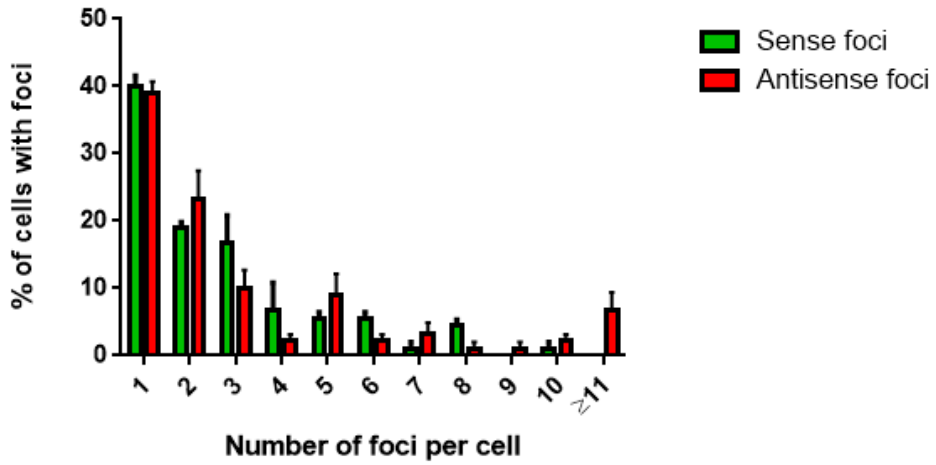

Figure 4.15: Comparison of sense and antisense foci number per cell. Histogram reveals antisense foci are more likely to be prevalent in higher numbers per patient cell compared to sense foci. (Data presented as percentage of total patient cells with foci, mean of n=3 independent experiments, Error bars ± SEM).

The heterogeneity of non-coding repeat expansion disorders has led to a number of hypotheses about the way in which the repeat may lead to disease in C9ORF72-ALS. One possibility is that hairpin secondary structures formed by the repeat mRNA can cause non-ATG-initiated (RAN) translation, a phenomenon which has been found in other repeat expansion disorders to form protein aggregates which are potentially pathogenic (Zu et al., 2011). A study by Zu and colleagues found that even after mutation of the ATG initiation codon, transcripts were still generated in all three reading frames and produced three protein products polyGln, polyAla and polySer. Mori et al. hypothesised this would occur in C9ORF72- repeat expansion disorders, and found translation of GGGGCC could result in five protein products with sense and antisense translation called di-peptide repeat (DPR) proteins.

Given that the RNA foci were predominantly found in the cytoplasm and erroneous export of intronic RNA is required to produce DPR proteins we thought it was likely that this model would express DPR proteins. Therefore, using antibodies against DPR proteins for one of the DPR proteins polyGly-Ala (GA) we probed our cells via ICC. In the same methodology for RNA foci visualisation, we scanned the entirety of the cells using z-stacks on a confocal microscope to gain images from multiple planes. We found

patient iPS cells at day 0 contained cytoplasmic GA DPR proteins which were not found in control iPS cell colonies (figure 4.16). Although attempts were made, unfortunately we were unable to convincingly visualise other DPRs including PA GP and PR in our cells.

These results prompted us to examine if GA DRP's presence correlated or co-localised with RNA foci in patient cells, therefore we next examined the presence of sense RNA foci using FISH coupled with ICC for anti-GA DPR proteins. Results revealed iPS cells at day 0 and differentiated iPS-derived cells at 6 weeks could be found with both RNA foci and GA DPR proteins (figure 4.17). Images identified that both aggregate types were predominantly cytoplasmic in line with previous observations. The two species were found as single entities in individual cells, but also RNA foci and GA DPR proteins could be found together in the same cell (figure 4.17). Although on occasions the two species could be found co-localised it was rare (figure 4.17). Similar to previously found results, foci were present from the beginning to the end of differentiation, and were heterogeneous in size.

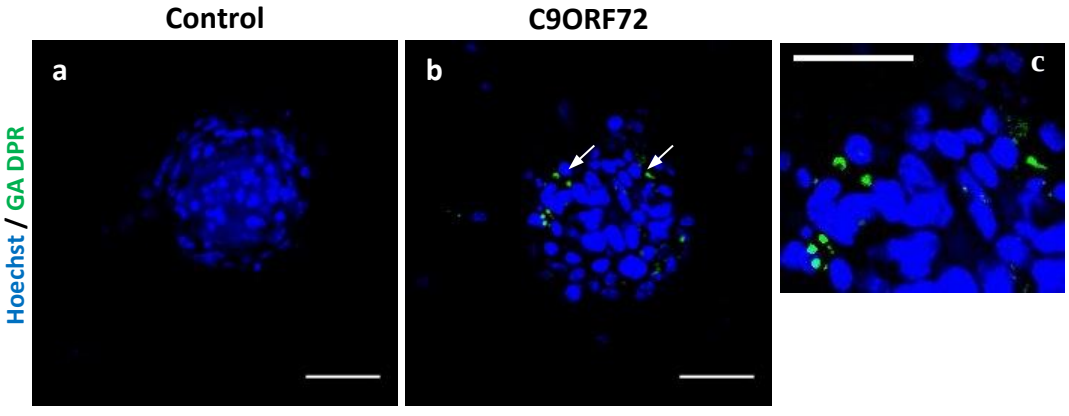

Figure 4.16: iPS cells at day 0 have cytoplasmic RNA translation proteins.
Immunocytochemistry of IPS cells at day 0 reprogrammed from **b)** patient fibroblasts have cytoplasmic GA di-peptide repeat proteins (white arrows) which are not found in **a)** controls. **c)** Insert of **b)**. Hoechst labels nuclei blue (a and b Scale bar=50µM; c Scale bar =10 µM)

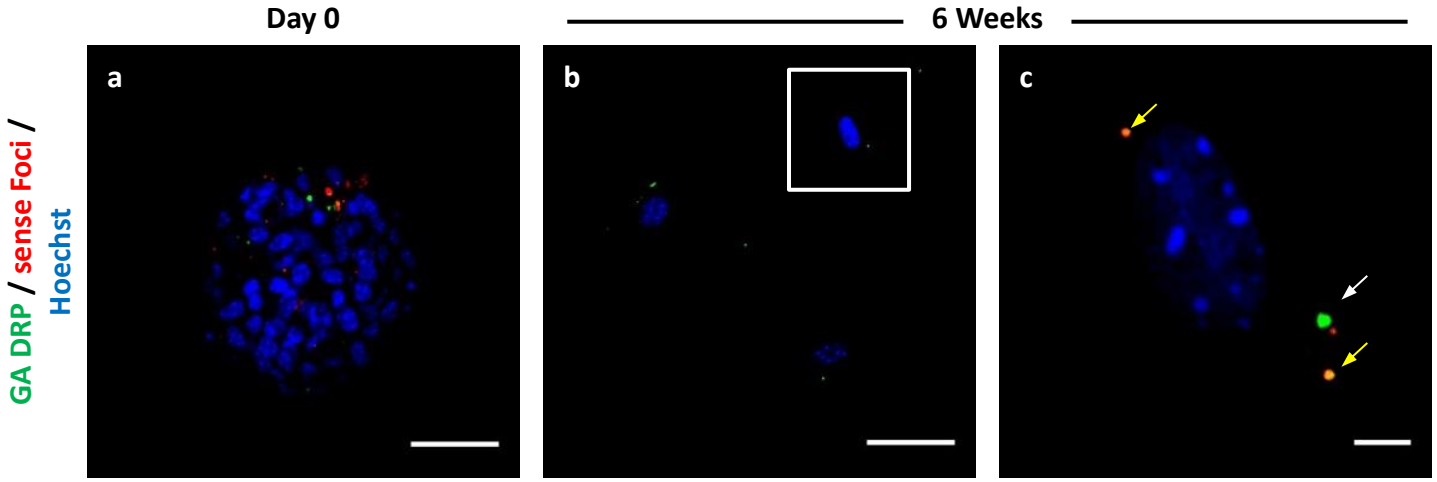

Figure 4.17: C9ORF72 iPS cells and differentiated iPS cells display both sense foci and GA DPR proteins. a) iPS cells reprogrammed from patient fibroblasts display sense RNA foci and GA DPR proteins. **b)** and **c)** differentiated iPS cells at 6 weeks show cytoplasmic RNA foci and DPR proteins which co-localise (yellow arrow) and exist as separate aggregates (white arrow). (Hoechst labels nuclei blue c) insert from b). Scale bar= 50µM a), b); Scale bar= 5 µM c))

4.4.2 Characterisation of iPS- derived Cell TDP-43 Localisation

The sequestration of RNA binding proteins and splicing factors in non-coding repeat expansion disorders has been proposed as a possible mechanism of disease pathogenesis for ALS (Todd and Paulson, 2010). Tar DNA binding protein 43 (TDP-43) is an important DNA and RNA binding protein of which mutations are known to contribute towards the pathogenesis of ALS. Re-localisation of TDP-43 from its predominantly nuclear location to the cytoplasm, as well as aggregate formation is a well described cellular pathology of ALS and FTD cases (Lagier-Tourenne and Cleveland, 2009). For this reason we chose to investigate the cellular localisation and potential redistribution of TDP-43 in conjunction with antisense foci. Whilst not found in fibroblast cells, antisense foci have been previously identified to correlate with TDP-43 distribution in the motor neurons of C9-ALS patients (Cooper-Knock et al., 2015b).

As previously identified, we found antisense foci in patient but not control cells with the foci predominantly in the cytoplasm of the cells (figure 4.18 b-e). In addition we found that patient cells showed diffuse patterns of TDP-43 staining, expressing a greater proportion of TDP-43 in the cytoplasm, with 42.5% (±SD 2) of patient cells expressing cytoplasmic TDP-43 staining compared to 21.3% (± SD 10) of controls, although this difference did not reach significance (figure 4.18 a-f). We found no observed correlation between cells expressing antisense foci and cytoplasmic TDP-43, with some cells showing cytoplasmic TDP-43 and no foci (figure 4.18 a-f).

As the redistribution of TDP-43 did not reveal a strong nuclear depletion phenotype, we decided to quantify the intensity of TDP-43 nuclear staining to determine the extent of nuclear TDP-43 loss, as well as total cell staining between patients and controls to determine total TDP-43 levels. Of note, patient cells exhibited significantly lower levels of nuclear TDP-43 compared to controls, as well as significantly lower total levels of TDP-43 in cells (figure 4.18 g).

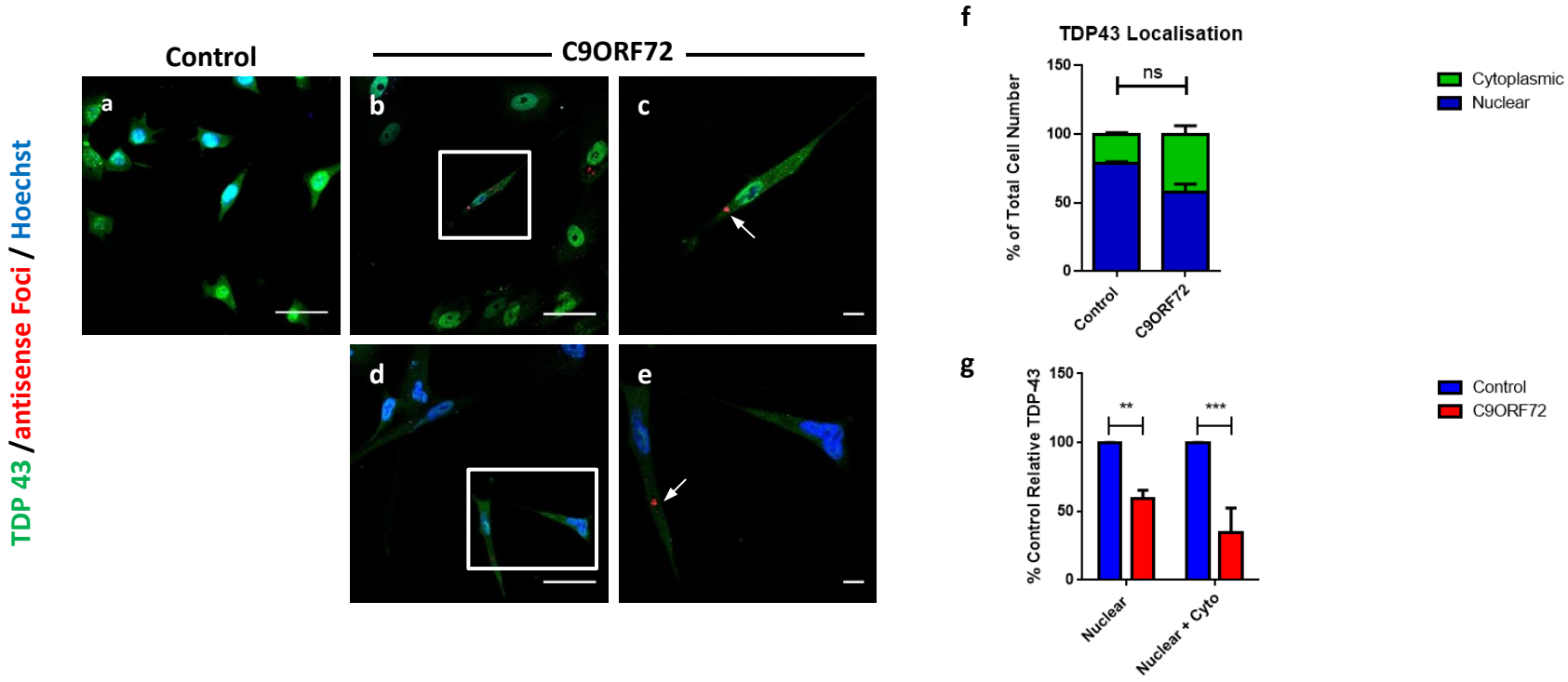

Figure 4.18: TDP-43 does not co-localise with antisense foci in patient iPS-derived cells but does show reduced nuclear expression. a) control differentiated iPS cells with predominantly nuclear expression compared to **b-e)** patient cells with reduced nuclear expression and a more diffuse pattern. Antisense foci were detected in patient cells but not controls, however, there was no co-localisation of TDP-43 aggregates with the foci **c)** and **e). f)** Quantification of the number of cells with predominantly nuclear or cytoplasmic TDP-43 revealed no significant differences between patients and controls. **g)** Quantification of the intensity of nuclear TDP-43 compared to total TDP-43 in the cell revealed a significantly lower level of nuclear and total TDP-43 intensity in patients compared to controls. Hoechst labels nuclei blue (c) insert from b). Scale bar= 50µM a), b), d); Scale bar = 5µM c) and e) Data presented as percentage of total cell number f), and as percentage of control g), mean of n=3 independent experiments, ±SEM, **p=<0.005 ***p=<0.0005 analysed with two-way ANOVA, Bonferroni's correction).

4.5 Discussion

4.5.1 iPS-derived cellular models for ALS

Generating motor neurons from human induced pluripotent stem cells is fast becoming a desirable method for the production of new cell models of C9ORF72-ALS. However, with the techniques having only just seen their 10th birthday, many variations remain not only in the yield of desirable cells produced, but also in the differentiation protocol used between groups around the world. Until these variations diminish, it continues to be an imperative step to describe the desired population of cells generated, by ensuring cellular descriptive markers are present, and expected functionality is maintained.

Upon initial inspection of the cells, it was apparent we were observing a culture of multiple cell types, with Hoechst staining revealing several sizes of nuclei indicative of a mixed population. Whilst we could identify by morphology neuronal and motor neuronal populations displaying features such as long and branching neurites, and of note to motor neurons, triangular cell bodies, we also saw cells with large diffuse cytoplasm and a stellate like appearance which may be associated with a more astrocytic-like glial population. Whilst we did attempt to stain and quantify glial populations for Glial fibrillary acidic protein (GFAP) and S-100β, ICC experiment unfortunately failed to label populations of cells convincingly, and we were unable to optimise this procedure under the time constraints of this project. Future work to optimise the use of such antibodies would help to confirm the prevalence of glial and support cells derived from our differentiation techniques. This quantification step could be important, as recent work has identified that oligodendrocytes, in addition to astrocytes, could contribute to toxicity in motor neurons through impaired lactate signalling, which is ALS subtype specific (Ferraiuolo et al., 2016). ALS treatment may require a multiple targeted approach, as studies have recently shown that targeting both neurons and astrocytes through separate mechanisms can yield significant positive effects on survival and motor function (Frakes et al., 2017), therefore future work to characterise cell populations other than motor neurons will be important for

future studies and trials using iPS-derived cell models. Despite specific labelling in our studies, based on morphology, intermediary bipolar astrocytic populations with long projections were found present, which have been previously identified as radial glial rather than astrocytes, and may be related to the maturity of these cellular populations (Li et al., 2015). One particular observation made in reference to neuronal populations, was that cells found remaining in EBs or present in densely packed populations were more likely to be of neuronal identity, projecting longer and more processes therefore communicating with more neighbouring cells of both neuronal and astrocytic morphology (figure 4.5, 4.7). One reason for this may be that the neuronal cells are providing increased trophic support in large numbers, which may aid their growth and development as well as their connections to other cells. Indeed studies have found that plating larger cell numbers resulted in improved cell survival of iPS-derived neurons (Beaudet et al., 2015).

Consistent with the literature, as these observations highlighted we were producing a mixed population, it was importantly for us to identify and quantify the neuronal and motor neuronal cells. In our population, we were able to first see cells labelled with markers of neuronal lineage from 2 and 4 weeks of differentiation for Tuj1 and MAP2 respectively. A historical paper, written in 1954 by Nieuwkoop and Nigtevecht, was first to outline the hypothesis that the prosencenphalon or forebrain, developed by a default process called activation for the anterior tissues, whilst a subsequent transformation process occurred for posterior tissues such as the rhombencephalon or hindbrain, and spinal cord (Nieuwkoop and Nigtevecht, 1954). More recent work has proposed molecules such as retinoic acid and FGF signalling to be potential contributors to this developmental pathway (Stern, 2001). As Tuj1 expression was found in cells as early as 2 weeks into the differentiation protocol (figure 4.4), it suggested the default neural lineage hypothesis may indeed be correct. Our cells then later showing expression of motor neuronal markers (figure 4.4, 4.6, 4.7), is consistent with the notion that spinal cord development is the next step in the differentiation process, and exerts confidence in our protocol for neuronal and motor neuronal lineage differentiation.

Markers accepted in the literature for lower motor neuron (LMN) characterisation are Hb9 and islet 1/2, which along with Tuj1, were found to be expressed in our differentiated cells (figure 4.6, 4.7), confirming their neuronal and motor neuronal identity. However caution must be noted as Hb9 expression, whilst thought to be a specific marker for MNs is also found in interneuron cell populations (Wilson et al., 2005), and can be absent from some populations of LMNs (Thaler et al., 2004). In turn, islet 1/2 expression and Hb9 expression can diminish as motor neurons mature. Therefore a battery of markers were used and it is the combination of all the markers expressed, plus the use of a mature motor neuronal marker such as ChAT that helped us to confirm that the cells are of LMN descent.

Choline acetyl transferase (ChAT) is a cholinergic neuronal marker which can be used to label mature LMNs, however staining proved to be difficult in our cellular populations which at first was thought to be due to a lack of mature motor neuronal development (figure 4.8). Yet, after optimisation of the staining protocol, labelling motor neuronal populations at 6 weeks and beyond (figure 4.8 b, c) indicated that our protocol for differentiation was able to generate populations of mature motor neuronal cells. Interestingly, it is also possible to further define MN types generated such as rostral or caudal by identifying Hox gene expression patterns which modulate the differentiation of different motor neuron subtypes in development (Lippmann et al., 2015, Philippidou and Dasen, 2013). One example would be to define LMNs into lateral motor column (LMC) and axial muscle innervating medial motor column (MMC) subtypes, by analysing gene expression profile markers, such as retinoic acid dehydrogenase for LMC-LMNs (Sockanathan and Jessell, 1998). These steps are going to become increasingly important in the use of differentiated MNs from iPS cells for the analysis of ALS subtypes such as bulbar or lower limb onset, and are possible future extensions to the immunocytochemical characterisation performed here.

An important point to make with motor neuron differentiation protocols is that different groups use varying protocols to achieve MN cultures, a point which was reviewed in a recent publication, with protocols found to produce yields of motor neurons ranging from 20% to 95% (Sances et al., 2016). We have obtained a mixed population of cells as identified by morphology, however we have generated a

subpopulation of motor neurons as characterised by marker staining to be 38.3% in controls and 24.9% in patients, and is a yield comparable to recent studies and characterisation techniques (Lopez-Gonzalez et al., 2016). Despite the trend towards reduced MN cell numbers in patient samples, this difference was not significant, which is in line with previous reports of differentiation of iPS cells to motor neurons (Devlin et al., 2015, Donnelly et al., 2013a). Interestingly, an overall figure of 31.62% of motor neurons across both patients and controls was found which is akin to the yield of 30% of motor neurons obtained by Amoroso and colleagues who used a very similar protocol to ours. They utilised the same factors for similar time periods, and also started differentiation with EB formation and neural induction, followed by motor neuron generation and neural maturation (Amoroso et al., 2013).

At the time of MN differentiation, the studies which obtained higher yields of MNs, up to 95% had not yet been published (Du et al., 2015), and as the optimisation and assay development for a new protocol for MN would take a considerable amount of time and resource, within the scope of this project it was decided to use previously established protocols for MN generation (Yang et al., 2014b). However, future studies could adopt a different approach in aim to increase MN cell yield from differentiation. Recent studies have found that changing the concentration of retinoic acid and purmorphamine throughout differentiation, for instance from 0.1µM to 0.5µM (RA) and 0.5µM to 0.1µM (PUR), coupled with use of CHIR99021 to activate Wnt signalling, can increase LMN yield to 95% (Du et al., 2015). Manipulation of RA throughout differentiation may also help to deliver motor neurons of more specific LMN populations (Maury et al., 2015, Lippmann et al., 2015) therefore may be a strategy that works to improve our differentiation in two ways. Additionally, future work to establish the percentage of glial cells for instance astrocytes, and other neuronal subtypes such as interneurons would be interesting to reveal the make-up of the total population. Such studies would also point towards mechanisms by which we can refine our differentiation protocol to increase the yield of MNs produced, which may enable us to successfully purify mixed populations to achieve close to 100% MN's.

When we observed total cell counts for 6 weeks after the differentiation protocol was complete, cells saw a steady decline in survival over time, and interestingly no

difference was seen between patients and controls in rates of survival (figure 4.11). This result matches previously reported studies on iPS derived motor neuron cell death, which have also found no difference between C9ORF72 patients and control cell survival (Sareen et al., 2013, Devlin et al., 2015, Donnelly et al., 2013a). However, more recent work has found, upon closer biochemical analysis, increased cleaved caspase-3 is found in patient cells indicative of aberrant apoptotic activation (Dafinca et al., 2016). Employing caspase-3 cleaveage assays in further work on our cells may reveal similar sub-levels of degeneration not thus found from our cell counts, and could be key to identifying a cell death phenotype in our models. In other studies, SMA-iPS derived cell models and non-disease controls produce a comparable percentage yield of MNs at the end of the differentiation protocol. However, beyond this, longitudinal observations note a greater reduction in SMA-iPS derived patient cell numbers compared to controls, in what the authors describe as a possible degenerative phenotype of the model (Ebert et al., 2009). An explanation for a lack of a degenerative phenotype could stem from the fact the iPS cells are embryonic in nature, and as ALS is a disease found with increased prevalence with age, the iPS-derived motor neurons produced may not yet express the lifetime of stress and triggers required for the onset of disease. The finding that SMA iPS cell models do show degeneration post-differentiation may support this, as SMA is usually a childhood disease. One lab have thought of an inventive solution to the problem, by over-expressing progerin, a truncated Lamin A protein found in premature aging disease Hutchinson-Gilford progeria syndrome (HGPS), in iPS- derived cells (Miller et al., 2013). The study not only confirmed that age-related markers are not re-developed over culture in iPS-derived cells, but also found that overexpression of progerin resulted in an increased degenerative phenotype. As the work was performed in neuronal cell models of Parkinson's disease, it provided potential new mechanisms to improve iPS cell derived models for late-onset diseases. In addition, newer techniques to directly re-programme human somatic cells to neurons could be used in future experiments as complementary models to those investigated here (Mertens et al., 2015). This is because the direct conversion to motor neurons does not cause the complete removal of epigenetic features developed in the life of the somatic cell; features which may be important in conferring an aged phenotype in the differentiated cells of interest.

Interestingly, the results in SOD1 iPS-derived models see different results to C9ORF72 iPS-derived cell models, with patient cells in one study found to display a more aggressive cell death phenotype with increased apoptosis compared to controls (Kiskinis et al., 2014). As SOD1 ALS onset is in adults, why do we see a cell death phenotype in the iPS-derived MNs of SOD1 models but not C9ORF72? As mouse models of C9ORF72 have also failed to produce a strong degenerative phenotype that models ALS as well as SOD1 mouse models have done previously, it highlights distinct phenotypes and pathways to disease which may not be so easily comparable. A reason for this could be that C9ORF72 ALS is more likely to lead to pathogenesis though exposure to lifetime cellular stressors compared to SOD1-related ALS, which may explain why some people have been found to contain the C9ORF72 mutation without developing ALS. It is possible, a "second hit" of additional cellular stressors such as increased oxidative stress may help C9ORF72 cell models mirror the human phenotype more accurately. Alternatively, it has been suggested that multiple events are required for ALS to occur, with a paper by Al-Chalabi et al. has suggested from population modelling studies that 6 steps are required which if identified could reveal a pathway towards disease (Al-Chalabi et al., 2014). Additionally, work to elucidate the differences between these two models of ALS- iPS derived cell models, for instance via direct comparison of MNs cell yield, cell survival, and manipulation of survival pathways, could reveal if the differences found in survival between these models are due to fundamental and thus important differences in ALS pathogenesis, or are artefactual through differences in iPS cell model differentiation and cell culture between laboratories.

Mature primary motor neurons repetitively fire action potentials in response to a depolarizing stimulus, so in a measure of the iPS-derived motor neuron maturity, whole cell patch clamp electrophysiological recordings were taken on individual iPS derived motor neurons to measure depolarization evoked action potential firing. Although it is expected to see action potentials in the time frame of 6 to 9 weeks of differentiation, some studies note recordings of action potentials as young as 4 weeks into differentiation where cells are found to express increased spontaneous firing and hyperexcitability (Wainger et al., 2014). Alternatively, others have found that at later

time points (9 weeks and beyond) iPS derived neurons show normal spontaneous and depolarisation induced action potentials (43 cells out of 60) (Sareen et al., 2013). This prompted us to identify if we could record normal depolarization induced action potentials in our differentiated motor neurons. The results obtained show that unfortunately were unable to record repetitive firing action potentials evoked by a depolarising stimulus in the majority of cells, with only a few cells displaying single action potentials (2 out of 100), in waveforms which displayed wide spikes (figure 4.12b). The lack of action potential generation and the shape of those that were generated suggest an immature phenotype of the cells (Sances et al., 2016, Johnson et al., 2007, Cashman et al., 1992). Of note, it has been previously described that cell lines can display varying action potential firing rates across different rounds of differentiation (Wainger et al., 2014), therefore it may also be appropriate to measure multiple further rounds of differentiation at these time scales for confirmation.

Membrane capacitance is a measure of a cells ability to hold charge for a particular voltage across the membrane, and is a commonly used measure in electrophysiology. The membrane capacitance is proportional to the size of the cell; a large cell will have a larger membrane which holds more channels, therefore would display a higher capacitance, which is why we used this parameter to normalize the values of the currents in voltage-clamp mode. While, iPS derived motor neuron models do display a lower capacitance than *in vivo* animal models (Gogliotti et al., 2012), the capacitance measured in our cells for both patients and controls was particularly low (figure 4.12c) especially in comparison to previous reports of capacitance in similar cell models (Wainger et al., 2014). This suggests cells with low levels of excitability, of a smaller size with less complex cytoarchitecture and arborisations, less membrane surface area, and therefore fewer channels. Despite the low measured cellular capacitance, the capacitance measured in controls (17.70pF) was similar to those recorded in immature hES-derived neurons recorded by other groups at 4 weeks of differentiation (17.0pF) (Johnson et al., 2007). As they found an increase in capacitance with extended tissue culture, they suggested capacitance can act as a measure of maturity developing in cells which supports prolonged tissue culture times for our cell models prior to recording. As motor neurons are large cells, the low capacitance recorded again

suggests an immature phenotype representative of smaller underdeveloped cells in our culture.

A spinal motor neuron holds a hyperpolarized resting membrane potential to aid action potential generation and electrical signal transmission in the cell, therefore by measuring this parameter in iPS-derived motor neurons it acts as an additional form of characterisation. Of note, similar discrepancies were found in the resting membrane potential which were measured to be higher in our cultures compared to previous reports (figure 4.12d) (Wainger et al., 2014, Sareen et al., 2013). Although a depolarised resting membrane potential is common in iPS cells (Sances et al., 2016), the higher resting membrane potential as observed in our cell models may point to an increase in sodium channel inactivation which will act as a preventative measure for the generation of action potentials (Wainger et al., 2014). Other motor neuron like cell models such as NSC-34 cells show a similar relationship between the ability to fire and resting membrane potential; NSC-34 cells with a resting membrane potential above -20mV are unable to fire action potentials (Cashman et al., 1992). Again, this aberrant measure found in our cells reflects an immature neuron that requires further development in culture, with previous studies showing over several weeks significant hyperpolarisation of cell membranes with time in culture (Johnson et al., 2007).

To confirm whether or not collective outward or collective inward-bound currents were responsible for the lack of action potentials, voltage-clamp recordings were made on both patient and control cells. Results revealed larger out-bound currents than in-bound currents (figure 4.12 g-j). When there is no depolarising current entering the cell this could be due to a lack of mature and developed sodium channels, potentially offering another explanation for the lack of firing in these cells. Further studies to block specific ion channels in iPS-derived motor neurons would help to answer this question. Another explanation for this difference could be that the outward channels are trying to compensate for an already high resting membrane potential (table 4.1) to reduce the RMP to a more mature hyperpolarized level (Johnson et al., 2007, Wainger et al., 2014).

Of note, two caveats of the electrophysiological recordings obtained above are: firstly, we have been selecting cells based on morphology, rather than by labelling for motor neuron markers, which means in some instances we may be recording from neurons which are not motor neuronal due to the mixed population of cells present. Whilst previously published work has also been known to use trapezoidal cell bodies and emitting processes as selection criteria (Sareen et al., 2013), recently, we have made successful attempts to generate our own lentiviral particles that transfect Hb9 expressing motor neurons only. Due to the time limitations of this project we were unable to utilise this technique to visualise motor neurons for electrophysiological recording. However, future attempts will use this marker to pinpoint and isolate motor neuronal cells in our cultures. Secondly, our voltage-clamp recordings are currently examining general outbound and general in-bound currents without the use of ion-channel blockers to isolate specific currents. This more general measure has previously been performed in similar iPS cell models of ALS (Dafinca et al., 2016), and although we can say that the inbound currents are largely composed of sodium, and the outbound currents of potassium, future work to employ the use of channel blockers would isolate and define currents further. Tetrodotoxin (TTX) to block sodium channel inbound currents, 4-aminopyridine (4-AP) would eliminate fast inactivating potassium currents, Tetraethylammonium (TEA) could be employed to diminish further sustained potassium outbound currents, and 6-cyano-7-nitroquinoxaline-2-3-dione (CNQX) could be used to block AMPA-receptor mediated currents important for synaptic activity. In order to see pure or larger inward currents (Sodium and calcium currents), future work will use potassium blockers to block outward potassium current. The inward currents of calcium or sodium can be further isolated by adding calcium or sodium channel blockers.

4.5.2 RNA Foci, Di-peptide Repeat proteins, and TDP-43 in iPS Cell Models of ALS

The presence of RNA foci has long been reported for non-coding expanded nucleotide repeat disorders such as myotonic dystrophy (Taneja et al., 1995). It has been shown that the expanded repeat is transcribed in both the sense and antisense direction to

form pre-mRNA with complex secondary structures. These structures due to their size and complexity can aberrantly alter transport, translation and RNA binding protein interactions, whilst also aggregating with themselves and RNA binding proteins to form the foci structures visualised in disease (Todd and Paulson, 2010). To add to this, due to the RNA foci sequestering RNA binding proteins, it prevents them from undergoing their roles elsewhere in the cell thus adding to the problem.

As C9ORF72-ALS cases contain a non-coding repeat expansion, it was important to identify whether or not RNA foci were present, to confirm presence of the mutation and show the expansion had survived iPS generation and differentiation. Southern blotting was not performed on the iPS cells or originating fibroblasts. However, of note lymphoblastoid cells from patient sample 3009 were found to have two expansions present, one of 50 repeats and another of more than 2000 repeats (Cooper-Knock et al., 2013). Due to an unavailability of lymphoblastoid cell lines for the remaining two patients, these have not been sized, however repeat-primed PCR from blood DNA samples has identified these patients have more than 30 repeats. Results identified that both sense and antisense foci were found in differentiated patient iPS cells but not controls (figure 4.13, 4.14) correlating with previous reports which have found similar structures in C9ORF72-ALS cases and suggesting that the C9ORF72 repeat expansion was still present in patient cells (Almeida et al., 2013, Mizielinska et al., 2013, Lagier-Tourenne et al., 2013, Donnelly et al., 2013a, Cooper-Knock et al., 2015b).

To show that the expansion was retained in undifferentiated cells, iPS cells at day 0 were examined for sense foci. Interestingly, sense foci were found at day 0 in iPS cells as well as post-differentiation at 6 weeks, suggesting the foci found post-differentiation were not generated during the motor neuron directed protocol. Coupled with previous studies finding RNA foci in fibroblasts from patients with C9ORF72 ALS (Lagier-Tourenne et al., 2013), this result suggests that the reprogramming of fibroblast to iPS cells and the subsequent iPS cell differentiation, does not remove hallmarks of the disease, validating the use of differentiated iPS cells as models of C9ORF72-ALS due to their ability to recapitulate disease associated pathology (Cooper-Knock et al., 2015b). Further validation of whether or not foci remain throughout cell model development could be gained from future work

screening the originating fibroblasts used to differentiate these iPS cells for both sense and antisense RNA foci.

We found 31.89% of cells contained sense foci, and 21.64% of cells contained antisense foci. Out of those found, for both sense and antisense the majority of cells contained 1-3 foci per cell, fitting with previous reports of the number of foci found in C9ORF72 cell models (figure 4.15) (Lagier-Tourenne et al., 2013, Sareen et al., 2013, Mizielinska et al., 2013). Differences in the number of cells with foci as well as the number of foci per cell were found between sense and antisense foci. More cells were found with sense foci (31.89%) compared to antisense foci (21.64%), yet cells with 11 or more foci per cell were only observed in antisense conditions (figure 4.13, 4.14, 4.15). This relates to previously reported findings that antisense foci are found in cells less frequently in the total cell population but when they are observed, a higher number of species were found per cell (Mizielinska et al., 2013, Lagier-Tourenne et al., 2013). As tissue culture conditions were consistent, it highlights a potential difference in the rate of foci formation or degradation for sense or antisense foci, or possible differences in their nuclear export mechanisms, particularly as we made an observed finding of larger antisense foci then sense. Additionally, at the time these experiments were conducted, the techniques to visualise both sense and antisense foci together in cells were still in the process of optimisation. If the foci already counted are not coincident then around 50% of cells in the total population are expressing foci. Identifying coincident expression of both sense and antisense foci in future work would reveal total foci expression at any time as well as any relationships between the two.

The foci found were predominantly cytoplasmic which is in contrast to previously identified RNA foci studies in ALS (Almeida et al., 2013, Mizielinska et al., 2013, Sareen et al., 2013, Lagier-Tourenne et al., 2013). However, the presence of cytoplasmic foci is not unusual (Cooper-Knock et al., 2015b), and has been reported to be more commonly found in iPS-derived cells (Donnelly et al., 2013a). One explanation for increased cytoplasmic foci could be related to the cellular population studied. As differentiated iPS cells from a mixed population were analysed, presumably a subset of the cells were post-mitotic (of neuronal identity) and others mitotic (glial supporting

cells), therefore it is possible that foci in mitotic cells which were once in the nucleus may have been pushed out into the cytoplasm at the end of mitosis and so were excluded when the nuclei reform; a possibility which has been suggested in foci observations in mitotically active fibroblasts (Lagier-Tourenne et al., 2013). Foci have been found in iPS-derived neuronal cells, glial cells and non-neuronal cells (Lagier-Tourenne et al., 2013), and cytoplasmic foci in motor neurons have also been previously reported (Cooper-Knock et al., 2015b). Foci expression in a variety of cells may mean their presence is context specific; as motor neurons develop to maturity gene expression changes will manipulate what proteins are expressed and if they are more vulnerable to the presence of foci species. To clarify which cells are more likely to contain nuclear or cytoplasmic foci of both species, future work to co-label sub-populations of iPS-derived cells with glial and neuronal markers would identify this and perhaps highlight cell specific patterns.

Due to the G- rich content of the repeat expansion, it has been suggested that complex secondary structures could be formed from long sense strands of RNA sticking together in parallel and anti-parallel fashions. One of these structures termed G-quadruplexes is commonly formed from G-rich sequences and is a sense specific occurrence frequently found in 5' un-translated regions, intron 1, and 3' un-translated regions of RNA (Huppert et al., 2008, Eddy and Maizels, 2008). This is of particular relevance to the 5'-intron-1 situated C9ORF72 mutation. Indeed, C9ORF72 repeat sense RNA transcripts have been found to fold into G-quadruplex stable secondary structures (Fratta et al., 2012, Kovanda et al., 2015), with implications for RNA binding protein sequestration and foci formation. Interestingly, 3' G-quadruplex RNA structures have been found to be vital for neurite localisation for a subset of neural mRNAs (Subramanian et al., 2011). Whilst it remains to be identified if 5' G-quadruplexes contribute to mRNA localisation, with predominantly cytoplasmic RNA foci identified in our studies, it could be possible that if mRNA G-quadruplexes are formed in the iPS-derived neurons, they too could be acting as localisation signals, attracting RNA foci elsewhere in the cell and explaining why we have generated a high proportion of cytoplasmic RNA aggregates.

The presence of cytoplasmic sense and antisense foci suggests nuclear export of the RNA sequences, particularly as mRNA export adaptors have been found to co-localise with the RNA entities (Cooper-Knock et al., 2015b). However, an important point to note is that if mRNA is found in the cytoplasm of the cells, it also means foci would have access to the translation machinery in this location. If the RNA is formed of complex secondary structures, for instance hairpin loops and G-quadruplexes, this could trigger non-ATG initiated (RAN) translation (Zu et al., 2011, Pearson, 2011). Expanded polyglutamine repeats formed by multiple CAG trinucleotides are found in disorders such Huntington's disease, spinal spinocerebellar ataxia and myotonic dystrophy (Pearson, 2011). Transcription of the repeat containing DNA can be bi-direction, both sense and antisense, resulting in the formation of two potentially toxic mRNAs for translation which when translated through typical AUG translation or RAN translation can result in the formation of additional protein products (Pearson, 2011, Zu et al., 2011). These in addition to the toxic RNA aggregates are thought to be pathogenic. If the expansion in C9ORF72 related ALS was translated into protein through this mechanism, it too would create additional intracellular aggregates of di-peptide repeat proteins it generates from sense and antisense bi-directional translation (Mori et al., 2013b, Mori et al., 2013a).

Out of the DPR protein antibodies tested, GA DPR proteins associated with sense translation of RNA, were found in both iPS cells at day 0 as well as in differentiated cells (figure 4.13, figure 4.14). This matches previous reports where this pathology has also been found in C9ORF72-related ALS (Mori et al., 2013b, Ash et al., 2013, Almeida et al., 2013). We were unable to identify other DPR proteins in our cells however this could be because some studies have reported GA to be the most commonly found DPR protein in cells due to being the most aggregation prone (Zhang et al., 2014). However, it is important to note if the GA antibody has the strongest affinity this statement could be artefactual. The distinct aggregation of the GA protein is also of interest, particularly as studies have identified aggregated DPR proteins to be more toxic than diffuse staining (Wen et al., 2014), a pattern which could be indicative of disease progression. Interestingly, papers reveal different levels of toxicity with DPR proteins with some stating PR to be the most toxic (Wen et al., 2014) while other state GA as more toxic (Zhang et al., 2014). Wen et al. predict in their results that PR is so

toxic it kills motor neurons cells faster than other DPR proteins, thus the reason we may not be able to see other DPR proteins could be due to the premature death of the cells containing them before visualisation was possible. Future work utilising techniques such as dot blot analysis for DPR proteins (Dafinca et al., 2016) while a less quantitative technique, could offer an alternative method of detection to ICC where the limits of detection for these species are relatively low.

We also observed sense RNA foci co-localised with GA DPR proteins (figure 4.17). Although co-localisation of the two entities suggests a possible interaction, additional studies will need to be undertaken to identify if similar to antisense reports they are mutually exclusive (Gendron et al., 2013), as well as to identify what percentage of foci are co-localising and whether or not there a relationship between them. The DPR proteins may cause pathogenesis by aberrantly sticking to foci and other proteins in the cell, disrupting RNA processing and transport. Certainly synthetic DPR products have previously been identified to bind to both nucleoli of cells and RNA binding protein hnRNPA2 causing cell death (Kwon et al., 2014), whilst poly-GA has been found to specifically bind with and sequester Unc119, a transport factor important for neuronal axonal functionality and vital for neuronal cell branching (May et al., 2014). In very recent work, GA has been found to co-aggregate with p62, Rad23b and Mlf2 in mouse and patients, however similarly to our work the presence of GA aggregates did not correlate with neuronal loss or cell death suggesting their contribution to disease may be prior to disease onset or part of the asymptomatic portion of ALS (Schludi et al., 2017). Indeed, additional recent work has found similarly GP DPR proteins are present in significant levels in asymptomatic C9- ALS carriers compared to non-diseased controls, but did not correlate with disease onset and damage to axons suggesting again this could be a marker for “pre-ALS”(Lehmer et al., 2017). An interesting additional step for our work would be to establish if antisense foci co-localise with antisense DPR proteins, anti-PA or anti PR, especially as antisense foci have been found in some studies to be more abundant in cells (Lagier-Tourenne et al., 2013, Mizielinska et al., 2013) implying antisense DPR proteins could also be more abundant.

TDP-43 mutations are known to cause familial and some sporadic cases of ALS, with re-distribution of the DNA/ RNA binding protein from the nucleus to the cytoplasm and the generation of inclusions in the neurons of ALS patients becoming a common pathological marker (Lagier-Tourenne and Cleveland, 2009). Miss-localised TDP-43 has also been recently identified to be present in circulating monocytes of ALS patients, suggesting this proteinopathy could be used to aid diagnosis (De Marco et al., 2017). For this reason, we were interested in characterising our differentiated iPS cells for TDP-43 distribution, coupled with screening for our more abundant RNA aggregate, antisense RNA foci (figure 4.18). As previously identified, patient cells were found to have antisense RNA foci while controls did not. Patient cells were also found to have a trend towards increased cytoplasmic TDP-43 staining compared to controls, with a diffuse granular pattern observed, which was found in cells bearing RNA foci (figure 4.18 c, e). Although no significant changes in the number of cells expressing miss-localised TDP-43 were found, the diffuse granular pattern of TDP-43 yet the presence of RNA foci prompted us to quantify the intensity of TDP-43 staining in both the cell as a whole and the nucleus. Results revealed that C9 patient cells expressed not only significantly lower total levels of TDP-43 in the nucleus, but also significantly lower total staining for the protein (figure 4.18 g). Interestingly studies have reported mixed results in TDP-43 localisation in patient cells (Lagier-Tourenne and Cleveland, 2009, Mizielinska et al., 2013, Bilican et al., 2012, Almeida et al., 2013, Zhang et al., 2015a) which may be related to the extent of disease pathology and possibly progression. The less apparent nuclear loss and more diffuse cytoplasmic staining found in our patient cells may point to an intermediary stage in TDP-43 aggregate formation; particularly as we did not observe many TDP-43 inclusions in our cells indicative of a more severe TDP-43 proteinopathy. Work looking at FUS miss-localisation has similarly found intermediate phenotypes in mice models, including incomplete nuclear clearance of FUS, which the authors suggest could represent an early stage of ALS (Scekic-Zahirovic et al., 2017). Similar to previous studies (Lagier-Tourenne et al., 2013), we too did not identify co-localisation of RNA foci with TDP-43 aggregates, potentially because of the low levels of TDP-43 inclusions observed. Again, there have been mixed reports documenting the relationship with foci and TDP-43, with some studies reporting no relationship between TDP-43 and RNA foci (Mizielinska et al., 2013, Lagier-Tourenne et al., 2013), while others find an association between the two (Cooper-Knock et al.,

2015b). However, it has not been ruled out that RNA foci and TDP-43 proteinopathy may be two independent hallmarks of ALS pathology. In addition, a final note of caution must be included as we know we are looking at iPS cells differentiated from a clonal population. Therefore, whilst there may be significant changes in TDP-43 intensity, it is possible that we are showing a decrease in TDP-43 intensity due to clonal variation rather than a potentially pathogenic redistribution. However, to mitigate this possibility, we have always represented our data as three patients versus three controls.

So far, findings in our work identify iPS cells and iPS-derived cells which contain some of the features of C9ORF72-ALS reported in previous studies. However, from the work performed above we cannot confirm if these are indicative of toxic gain of function mechanisms alone, or rule out that our model does not also have C9ORF72 haploinsufficiency mechanisms towards disease. Nevertheless, it remains to be identified if these markers of disease are a cause or a consequence of ALS. Questions arise as to why the foci, if prominent in pathogenesis, do not cause disease earlier in life, and why when present in unaffected cells of the body such as fibroblasts they do not contribute to that cells death. Longitudinal studies to examine if pathogenic markers like foci and DPR proteins occur before disease onset may shed light on this. Positively, work using antisense oligonucleotides reducing the levels of sense RNA foci have been found to rescue toxic effects found in iPS-derived cell models of C9ORF72-ALS (Sareen et al., 2013, Donnelly et al., 2013a) which suggests they may contribute to disease. To add to this, further work needs to be done to identify the effect of removing the more abundant species of antisense foci, as well as work to identify how the foci cause these toxic effects, which may explain why removing them is a valid therapeutic strategy.

4.6 Conclusion

Overall, the work described in this chapter highlights the development of a promising cell model of C9ORF72- ALS. We have been able to successfully reprogram fibroblasts cells to pluripotency and have generated stocks of iPS cells for 6 cell lines. In addition,

we have demonstrated the ability of these cells to be differentiated into neuronal and motor neuronal linages, expressing common markers widely associated with these fates. Although there is work left to be done with regards to improving their electrical maturity, whilst this is a limitation of the model that needs improving to better model the disease, these steps are possible with changes to the environment in which the cells are currently cultured. As the models generated express molecular pathological hallmarks of the C9ORF72 mutation, via the expression of RNA foci and DPR protein products, this confirms their ability to recapitulate several newly discovered features of the disease. Next, we will be able to take these cell models forward to identify if modulation of PTEN has a positive effect on the PI3 cell survival pathway, which may translate into increased cell survival and therefore the development of disease modifying therapeutics agents aimed at this target.

CHAPTER 5 : PTEN MODULATION IN iPS-DERIVED CELL MODELS

5.1 INTRODUCTION

5.1.1 PTEN INHIBITION AND KNOCKDOWN IN NEURONAL CELL MODELS

Inhibiting the action of PTEN has been long established to provide a therapeutic benefit to neuronal cell models of neuronal injury and neurodegenerative disease. Due to this, research groups have employed different approaches to achieving this aim, including the use of small molecules to inhibit PTEN, as well as PTEN knockdown (KD) via short hairpin RNA (shRNA).

Taking a look of some of the successes in PTEN KD studies, PTEN depletion has been found to rescue the growth of motor neuronal processes in SMA models of motor neuron disease (Ning et al., 2010); significantly improve the regeneration of adult spinal neuronal axons after injury (Liu et al., 2010); and activate intrinsic regenerative outgrowth of peripheral adult sensory neurons (Christie et al., 2010). Comparatively, Bisperoxovanadium (BpV) compounds previously believed to be specific PTEN inhibitors have shown that inhibition can prevent the degeneration of neurons after injury (Walker and Xu, 2014, Walker et al., 2015, Chen et al., 2015, Mao et al., 2013). The differences between these two methods are important to their relative effects on the cellular activities of PTEN and thus generate distinctive outcomes. Knockdown via shRNAs can affect longer term gene expression as well as cause off-target effects, whilst inhibition with titratable modulating compounds may provide a method to more specifically target the catalytic roles of PTEN in the PI3K pathway. Although both are valid methods, recently work has identified caveats in using BpV compounds to inhibit PTEN as they were found to inhibit other phosphatases (Spinelli et al., 2015). This lack of specificity calls into question potential safety concerns in relation to their further use in human clinical trials.

The limitations of both methods have led researchers to identify new compounds and techniques that target PTEN in the PI3K cascade, and Scriptaid is an example of an established compound that has been re-purposed for this pathway. Scriptaid as discussed in Chapter 3 of this thesis, was identified by Wang et al. in 2012 to promote cell survival and protect against traumatic brain injury via the PI3k pathway (Wang et al., 2012b). The HDAC inhibitor was found to increase the phosphorylation of both

PTEN and AKT, a finding which was verified again in later work (Wang et al., 2015a). This positive effect was found in multiple cell types including neuronal cells and glia, in a mechanism postulated to act through cellular interactors of PTEN including GSK3-β, and provided an indirect route for activating this pathway for neuro-protection. As a cell permeable pan-HDAC inhibitor, Scriptaid has been found to inhibit HDAC activity at highly potent doses with half maximum inhibition (IC_{50}) of total HDAC activity, -log 6.73 ± 0.02 (0.19µM) identified (Hahnen et al., 2008). For individual HDAC activity Scriptaid inhibits HDACs 1, 2, 3 and 6 with $IC_{50's}$ of less than 10nM (Shi et al., 2011b). Furthermore, studies in cultured PANC-1 cells and MDAMB-468 cells have found that Scriptaid presents a low toxicity, with 6µM doses resulting in a significant increase in histone acetylation, yet maintaining 80% cell survival (Su et al., 2000).

Having previously tested Scriptaid in two cell models of ALS (see Chapter 3), whilst the first ALS model of SOD1 NSC-34 cells proved to be too sensitive to treatment with the drug, the second model of patient and control fibroblast cells was not. Even though subsequent findings showed no significant effect of the drug on cell survival, we found that basal C9ORF72 patient fibroblast cells expressed significantly lower levels of total PTEN protein compared to their controls. This result prompted us to try Scriptaid in a cell model which more accurately represented the motor neuron cells affected in ALS as well as the previously tested neuronal cell models in other Scriptaid treatment studies (Wang et al., 2015a).

5.2 Aims and Objectives

Using the generated and characterised iPS-derived cell models of ALS and controls described in Chapter 4, our aims were to identify if manipulation of PTEN via inhibition or reduction of PTEN protein expression in the PI3K pathway positively benefited survival pathways in these cells.

Using shRNA techniques we identified the effect of PTEN knockdown (KD) upon iPS-derived cells. To confirm whether or not PTEN KD was successful and to validate the functionality of the lentiviral particles used, we first performed PTEN KD, followed by protein level determination of total PTEN protein and downstream components in the

PI3K pathway, through western blotting in two cell models including HEK293 cells as a work-up model given the complexity of iPS-derived cells, followed by iPS-derived cells. Next, we aimed to further validate the success of PTEN knockdown in neuronal cell populations specifically, immunocytochemistry was used to visualize PTEN reduction in neuronal cells dual stained for a neuronal specific marker TuJ1 as well as PTEN. As our previous findings had identified a steady decline in total cell numbers between 7 and 12 weeks of differentiation, we wanted to identify if PTEN knockdown performed at the end of the differentiation protocol, reversed this decline by causing a positive increase in total cell numbers.

Finally, with the objective to find a quick and translatable form of PTEN manipulation, we used Scriptaid, a PTEN modulator identified to activate the PI3K pathway resulting in a positive neuroprotective effect. We first established whether the iPS-derived cells were vulnerable to application of the drug, by performing MTT and LDH assays for cellular viability and cytotoxicity effects respectively. These experiments would also serve to identify the maximum dose and optimal incubation period for the use of Scriptaid on iPS-derived cells. We then applied Scriptaid during the 6 week differentiation protocol and subsequently quantified the effect that treatment had on both patient and control motor neuron cell numbers generated at the end of the differentiation protocol.

5.3 PTEN Knockdown for a Therapeutic Effect on ALS Cell Survival

Firstly, to validate the PI3K pathway as a therapeutic target in the cells generated, we decided to perform PTEN knockdown through the use of shRNA lentiviral particles which would confirm activation of key components in this cell survival pathway. As well as this, by monitoring cell numbers after PTEN knockdown, we also were able to identify whether reducing total PTEN protein and activating the PI3K cell survival pathway resulted in a beneficial increase in iPS-derived cell number in C9ORF72 ALS patients and controls.

5.3.1 Successful PTEN Knockdown in Human Embryonic Kidney (HEK293) Cells

To validate the viral and control constructs specificity, we used human embryonic kidney (HEK293) cells as a preliminary and less time-intensive cell model compared to iPS-derived cell models. Using GFP lentiviral particles of the same viral titre as PTEN lentiviral particles, we established that an MOI of 5 was sufficient to transduce the cells (data not shown). We then exposed HEK293 cells to lentiviral particles for PTEN knockdown and performed western blotting, probing for PTEN, pAKT and AKT to determine their protein expression levels. Results revealed an MOI of 5 was sufficient to reduce total PTEN protein to a relative level of 5.24, from a relative level of 100 for untransduced (UT) controls (figure 5.1 a, b). Knockdown also caused a concomitant increase in relative pAKT levels from 100 (UT) and 106 (Scram), to 281 (PTEN KD) without modulating total AKT protein levels (figure 5.1 a, c, d). These findings confirmed that the virus was able to activate pAKT through PTEN knockdown, and therefore could be used in following experiments on iPS-derived cell models for the same effect.

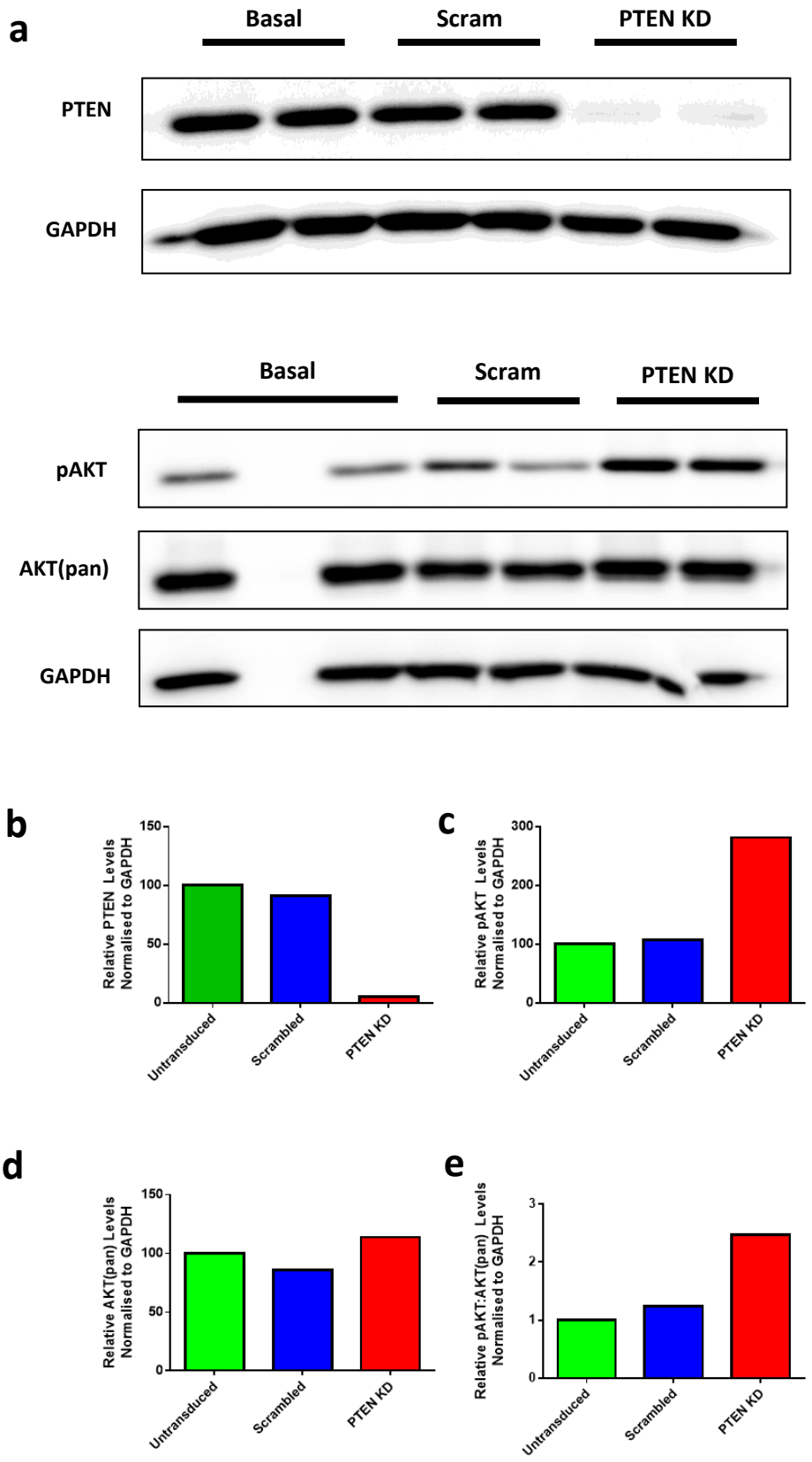

FIGURE 5.1: Successful PTEN knockdown in HEK293 cells. a) Knockdown of PTEN after exposure to lentiviral particles for PTEN reduction caused a **b)** reduction in total PTEN protein and a **c)** concomitant increase in pAKT in the PI3k cell survival pathway. **d)** total AKT(pan) was not affected and **e)** The ratio of pAKT to total AKT(pan) revealed concomitant increases after PTEN knockdown compared to controls. MOI =5, n=1. Abbreviations: GAPDH, Glyceraldehyde 3-phosphate dehydrogenase; KD, Knockdown; PTEN, phosphatase and tensin homologue deleted on chromosome 10)

5.3.2 Successful PTEN Knockdown in iPS-Derived Cells

Next, to confirm that PTEN can be reduced successfully in iPS-derived cell populations, patient and control iPS-derived cells at 6 weeks of differentiation were exposed to lentiviral particles for PTEN knockdown, and the results were compared to untransduced and scrambled lentiviral particle controls. Western blotting for components in the PI3K pathway revealed a significant reduction in both pPTEN and total PTEN protein levels after exposure to the virus for 7 days (figure 5.2 a, b, d). Although this resulted in a concomitant increase in pAKT unfortunately this increase did not reach significance when analysed by unpaired t-test comparing to scrambled control (figure 5.2 c). Total levels of AKT remained similar across all conditions, and results for the amount of pAKT available in the total population although not significant showed a trend for an increase in ratio of pAKT to total AKT after PTEN KD, confirming knockdown of PTEN is responsible for increases in the active form of the protein which could contribute towards promotion of cell survival (figure 5.2 g).

As PTEN knockdown was performed in a mixed population of differentiated iPS-derived cells, we wanted to identify if neuronal populations were specifically affected by PTEN knockdown, particularly as pAKT increases did not reach to significant levels which could suggest some populations of cells were not targeted. Obtaining a pure population of iPS-derived motor neurons can be technically challenging (Sances et al., 2016) particularly when faced with low yields of MN's, therefore we decided to use immunocytochemistry techniques to dual label cells for total PTEN expression alongside the neuronal specific marker Tuj1.

Results demonstrated that neuronal populations were targeted by the viral mediated knockdown of PTEN, because iPS-derived cells after exposure to lentiviral particles for PTEN knockdown were found to express lower levels of PTEN staining compared to controls (figure 5.3). Both large populations of closely packed cells and single cell populations exhibited a reduced expression of PTEN in its endogenous cell body location after PTEN knockdown. This result was found in both neuronal cells and non-neuronal cell populations, highlighting that knockdown was achieved across different

cell types, however some populations of clumped cells may not have been as effectively transduced with the virus as single cell populations (figure 5.3 e, f).

Together these results confirm the successful knockdown of PTEN in iPS-derived cells including neuronal populations, validating the use of this technique for the next stage of experimentation; to identify if downregulation of PTEN results in a positive change to iPS-derived cell number in ALS.

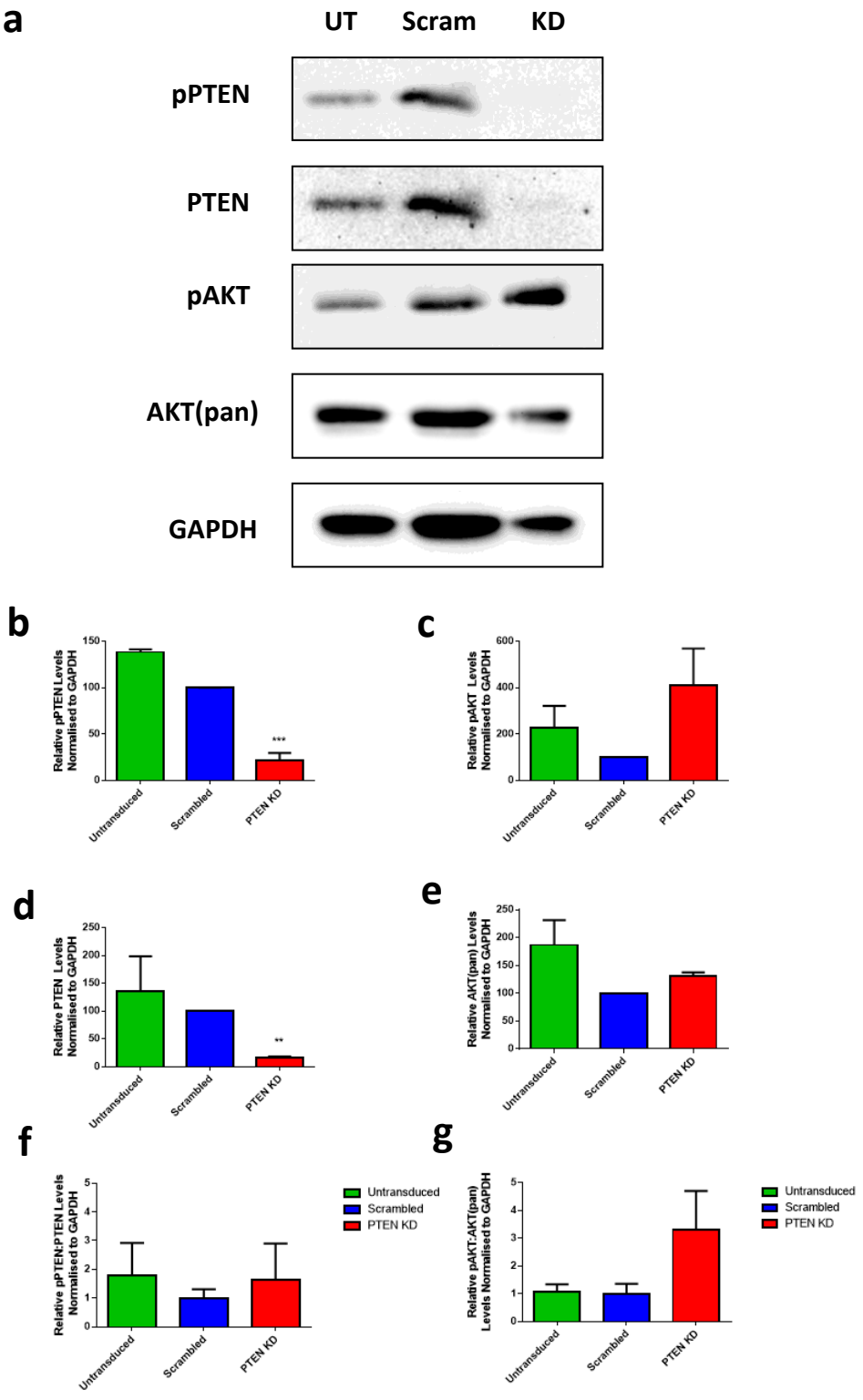

Figure 5.2: Successful PTEN Knockdown in iPS derived cells. a) Western blots reveal a significant reduction in **b)** pPTEN and **d)** total PTEN, compared to scrambled control. A non-significant increase in **c)** pAKT was found after PTEN KD. No significant changes in **e)** total AKT **f)** pPTEN:PTEN and a non-significant increase in **g)** pAKT:AKT(pan) were observed. MOI =5, n=3. Representative western blot shown. (Data are mean of *n*=3 independent experiments of pooled cells and normalised to GAPDH loading control. ±SEM, **p=<0.005, ***p=<0.0005 analysed with unpaired t-test)

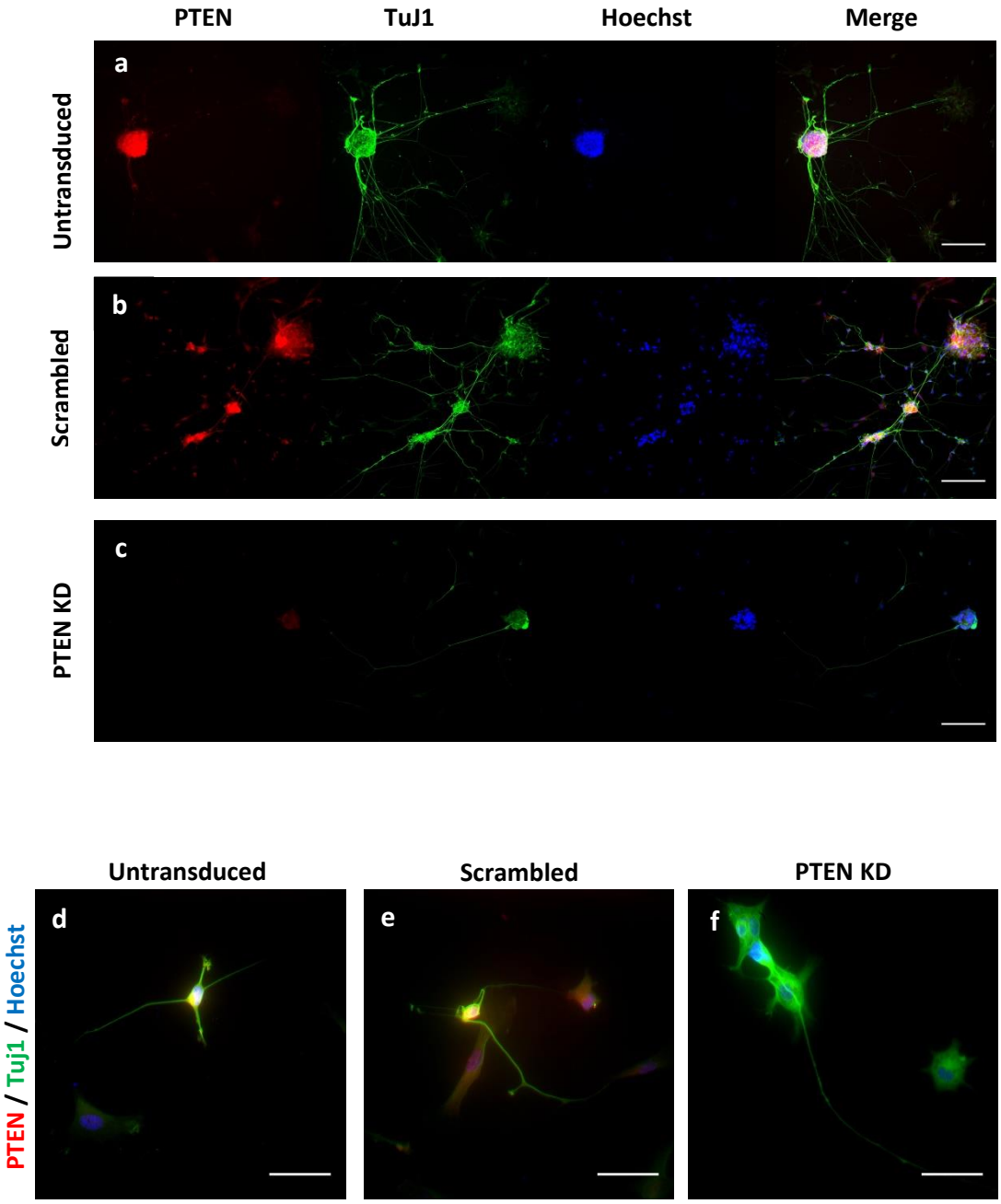

Figure 5.3: PTEN Knockdown in iPS-derived cells successfully reduced PTEN expression in neuronal populations. IPS-derived cells showed expression of PTEN in primarily in the cell body of cell in **a)** an **d)** untransduced and **b)** and **e)** Scrambled conditions. **c)** and **f)** Cells exposed to lentiviral particles showed a reduced expression of PTEN in the cell body, compared to control conditions. Representative image shown of pooled cells (Abbreviations: PTEN, phosphatase and tensin homologue deleted on chromosome 10; Tuj1, β III tubulin. Scale bar = 300µM a) to c); Scale bar= 50µM d) to f))

5.3.3 PTEN Knockdown Modulates iPS-Derived Cell Survival Post-Differentiation

Having confirmed successful PTEN knockdown was achieved in iPS-derived cells to produce an associated increase in AKT activation; we next performed PTEN KD on iPS-derived cells at 6 weeks of differentiation and monitored total iPS-derived cell counts in real time up to 12 weeks of differentiation. The results would identify if PTEN manipulation via knockdown had an effect on total iPS-derived cell number. Although PTEN depletion in other stem cell models has been previously reported not to affect the differentiation of the cells into all three germ linages (Duan et al., 2015), we decided to perform the inhibition at the end of the differentiation protocol to avoid any negative effects due to the reported important role of PTEN in preventing stem cell neoplastic transformation (Duan et al., 2015).

Both patient and control cells in all conditions showed a steady decline in cell numbers from 7 to 12 weeks of differentiation, matching previously identified results for basal total iPS-derived cell counts (chapter 4, figure 4.11). However, PTEN knockdown was found to induce a significant increase in C9ORF72 patient cell numbers compared to PTEN knockdown performed in control cells at 7 to 9 weeks of differentiation, as well significant increases compared to C9ORF72 scrambled and untransduced controls at the same week of differentiation (figure 5.4). These results suggest that whilst the total population of iPS-derived cells does decline with increasing culture length, total cell numbers specifically in patient populations can be protected for up to 3 weeks post-PTEN manipulation, highlighting PTEN manipulation could have a positive effect on cell survival.

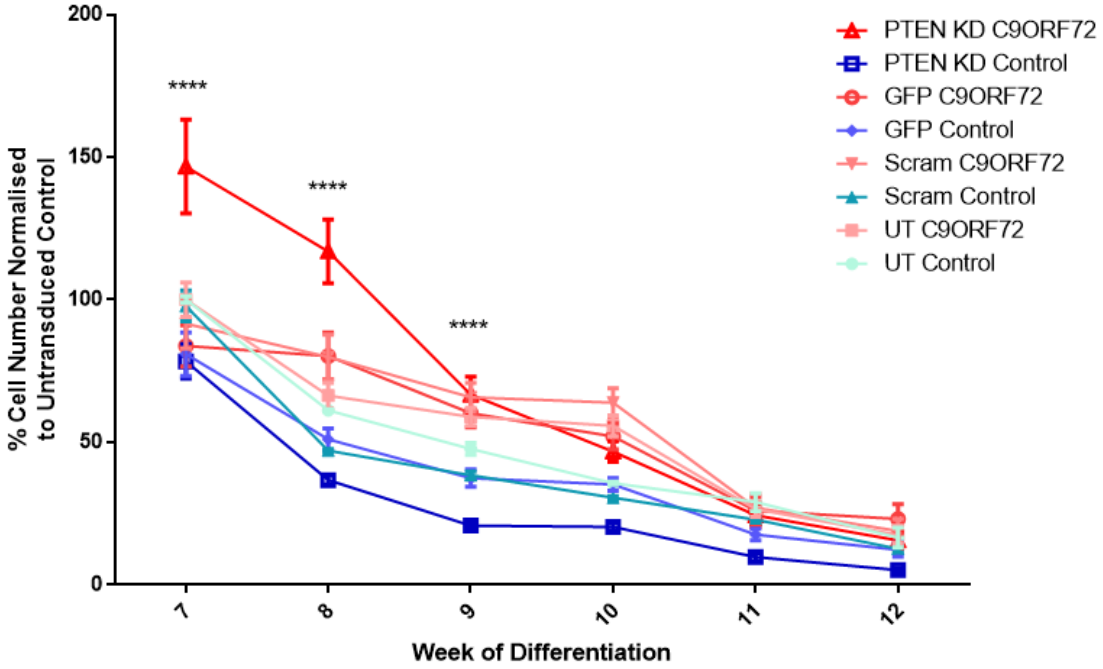

Figure 5.4: PTEN KD causes a significant increase in total iPS-derived cell number at 7 to 9 weeks of differentiation. iPS derived cells reveal a steady decline in total cell numbers from 7 to 12 weeks of differentiation, in both patients and controls. PTEN knockdown caused a significant increase in total iPS-derived cell number in patient cells at 7, 8 and 9 weeks of differentiation compared to PTEN knockdown in control cells. (Data presented as percentage of total cell number of matched untransduced control, mean of n=3 independent experiments from pooled cells. ±SEM,**** p=<0.0001 analysed with two-way ANOVA, Bonferroni's correction)

5.4 iPS-Derived Cell PTEN Inhibition Through Scriptaid Treatment

After confirming that the reduction of PTEN expression results in a measurable increase in AKT phosphorylation and increased cell number in iPS derived cell populations, we decided to investigate the use of a therapeutic molecule with more realistic potential for clinical translation than a knockdown approach, which at the time of investigation still held difficulties in translating gene therapies to patients. Scriptaid, as mentioned above, was proposed as a likely therapeutic agent for research due to its therapeutic and neuroprotective effect for damaged neuronal cells (Wang et al., 2012a).

5.4.1 iPS-Derived Cells Show Low Sensitivity to Scriptaid Treatment

Previously identified, NSC-34 cell models of ALS treated with Scriptaid were found to show an increased vulnerability to treatment with the drug (Chapter 3, figure 3.1), therefore we wanted to verify if the known active concentrations (Su et al., 2000, Wang et al., 2015a) were compatible with differentiated iPS cell models. The experiments would also act to optimise the appropriate concentration and incubation length to treat the cells with, as we exposed cells to a range of concentrations over two time periods. For this, MTT assays were performed after treatment to measure the cellular viability when the cells were exposed to 3µM, 10µM and 30µM concentrations for 24 hours and 48 hour, time points derived from previous use of Scriptaid in the literature (Wang et al., 2012a). Results at both 24 and 48 hour incubation periods revealed no significant declines in cellular viability at all three concentrations tested compared to vehicle control, which suggests that Scriptaid does not have a toxic effect on the viability of the total iPS-derived cell population (figure 5.5).

In a second assay, iPS derived cells were examined for changes in cellular cytotoxicity via quantification of LDH released into the media. This test would counteract any caveats of solely using MTT assays (see Chapter 3) and would also highlight any additional effects that may be of importance to the survival biochemistry of the cells.

In the same multiplexing methodology employed in the fibroblast cell assays (see chapter 3), the MTT assay utilised the cells that were attached to the bottom on the multiwall plate, allowing the remaining media to be used for LDH reads to obtain directly comparable results. Assays examining LDH release on exposure to Scriptaid showed at both 24 and 48 hour incubation periods a trend towards increased LDH cytotoxicity with increasing concentration compared to vehicle control, however no significant effects on cellular cytotoxicity were identified therefore there is no measureable toxicity (figure 5.6). These results suggest, similarly to the MTT findings, that the cells exhibit a low level of cytotoxicity to Scriptaid.

Overall, iPS-derived cells did not display a significant toxic response to treatment with Scriptaid prompting continued investigation into the activities of this drug on the cells, selecting 3µM for 24 hours as the desired dose and length of incubation.

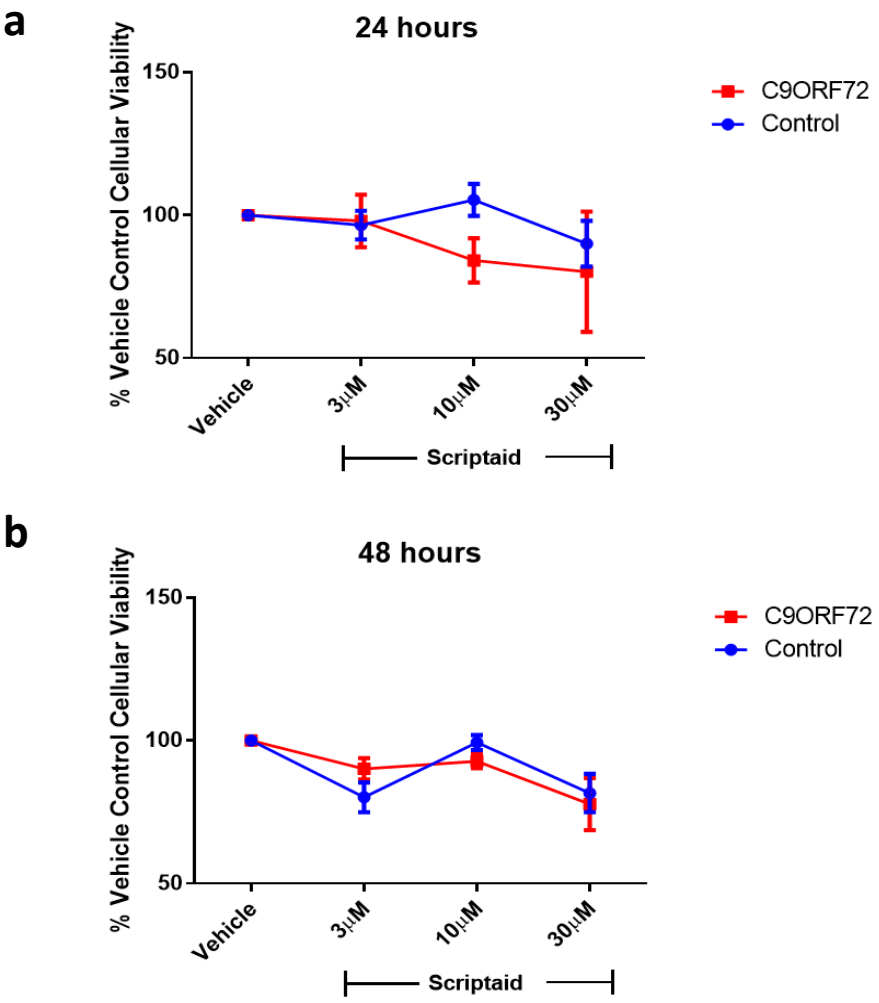

Figure 5.5 The effects of Scriptaid on iPS-derived cell viability as measured by MTT assay. Pooled cells from 3 matching C9ORF72 and control iPS-derived cells revealed no significant changes in cellular viability between vehicle and any treated condition at both **a)** 24 and **b)** 48 hour incubation periods. **a)** At 24 hours both patients and controls exhibited a trend towards reduced cellular viability with increasing Scriptaid concentration, with patients more affected by this trend compared to controls. **b)** At 48 hours incubation periods, both patients and controls showed a steeper decline in viability at 3uM doses compared to 24 hour incubation periods. (Data presented as percentage of vehicle control, mean of *n*=3 independent experiments on pooled cells. ±SEM. Analysed with two-way ANOVA, Bonferroni's correction.)

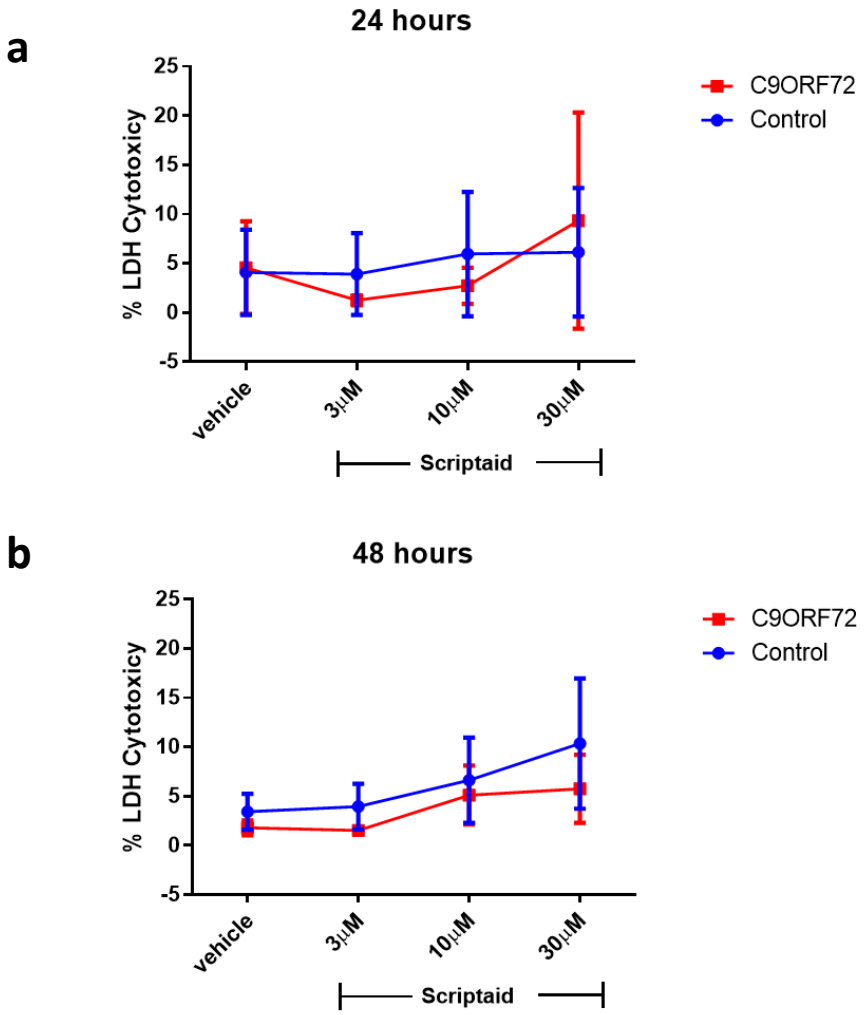

Figure 5.6 Determination of LDH cytotoxicity after Scriptaid treatment on iPS-derived cells. **a)** At 24 hour incubation periods and **b)** 48 hour incubation periods there was a trend towards increased cellular cytotoxicity witnessed in both patients and controls with increasing concentration, but no significant effects were identified. (Data presented as percentage of LDH cytotoxicity, mean of *n*=3 independent experiments on pooled cells. ±SEM, Analysed with two-way ANOVA, Bonferroni's correction)

5.4.2 Scriptaid Treatment Does Not Activate Components of the Cell Survival Pathway

In light of the KD result we wanted to look for pAKT activation at the three doses originally tested to show whether or not Scriptaid had engaged the pathway in iPS-derived cells. Therefore, we performed western blots on iPS-derived cells at the end of the differentiation protocol that had been treated with Scriptaid for 24 hours at 3µM, 10µM and 30µM concentrations, and probed for total PTEN, total AKT and pAKT. The patient iPS-derived cells had not shown a reduced cell number compared to controls in our studies (chapter 4 figure 4.1), therefore similar to the assay performed on fibroblast cells (chapter 3), we decided to induce a stressed condition through serum withdrawal from the cells (Simm et al., 1997, Arrington and Schnellmann, 2008).

Results identified that Scriptaid did not elicit a significant positive change to total PTEN levels, nor a significant positive increase in pAKT expression or total pAKT available (figure 5.7), suggesting that the drug did not activate the cell survival pathway as intended. As Scriptaid treatment did not reveal a significant positive effect on total motor neuron cell number, this could be due to an insignificant effect of Scriptaid on PI3K pathway components. The only noted effects were a reduction in pAKT found upon serum withdrawal in control cells compared to basal conditions, a result also found in fibroblast cells (figure 5.7c). Interestingly, dissimilar to fibroblast cells which found patents exhibited significantly lower levels of total PTEN (chapter 3 figure 3.5), iPS-derived cell populations showed that levels of PTEN between patient and control cells were similar. This indicates that the transition from fibroblast to differentiated iPS cell could have caused an increase in total PTEN expression in patient cells to sit more closely to that of controls, highlighting a fundamental difference in PTEN control in different cell types, which may aberrantly affect the survival of the cells in disease (figure 5.7 b).

As Scriptaid was recently identified to cause changes to PTEN by increasing the levels of the phosphorylated inactive form of the protein (Wang et al., 2015a), we also decided to identify to what degree pPTEN was affected by the drug compared to basal levels, by performing the same experiment as above but this time probing for pPTEN in addition to total PTEN. We found that Scriptaid caused a significant reduction in pPTEN

in cells compared to vehicle control and caused no effect on the total amount of pPTEN available (figure 5.8) suggesting Scriptaid does not have a positive effect on PTEN via inhibition. Of note, these experiments did identify in basal cells a higher level of pPTEN expression in patient cells (figure 5.8b), highlighting an increased inhibition in disease. However, when we look at the total PTEN available, although there is a trend towards higher pPTEN levels, there is no significant difference in basal conditions between patients and controls, implying the positive effects of PTEN inactivation may not be realised into cell survival benefits for the cells; a result which is validated by reduced AKT phosphorylation also found in patient cells in basal conditions (figure 5.7c).

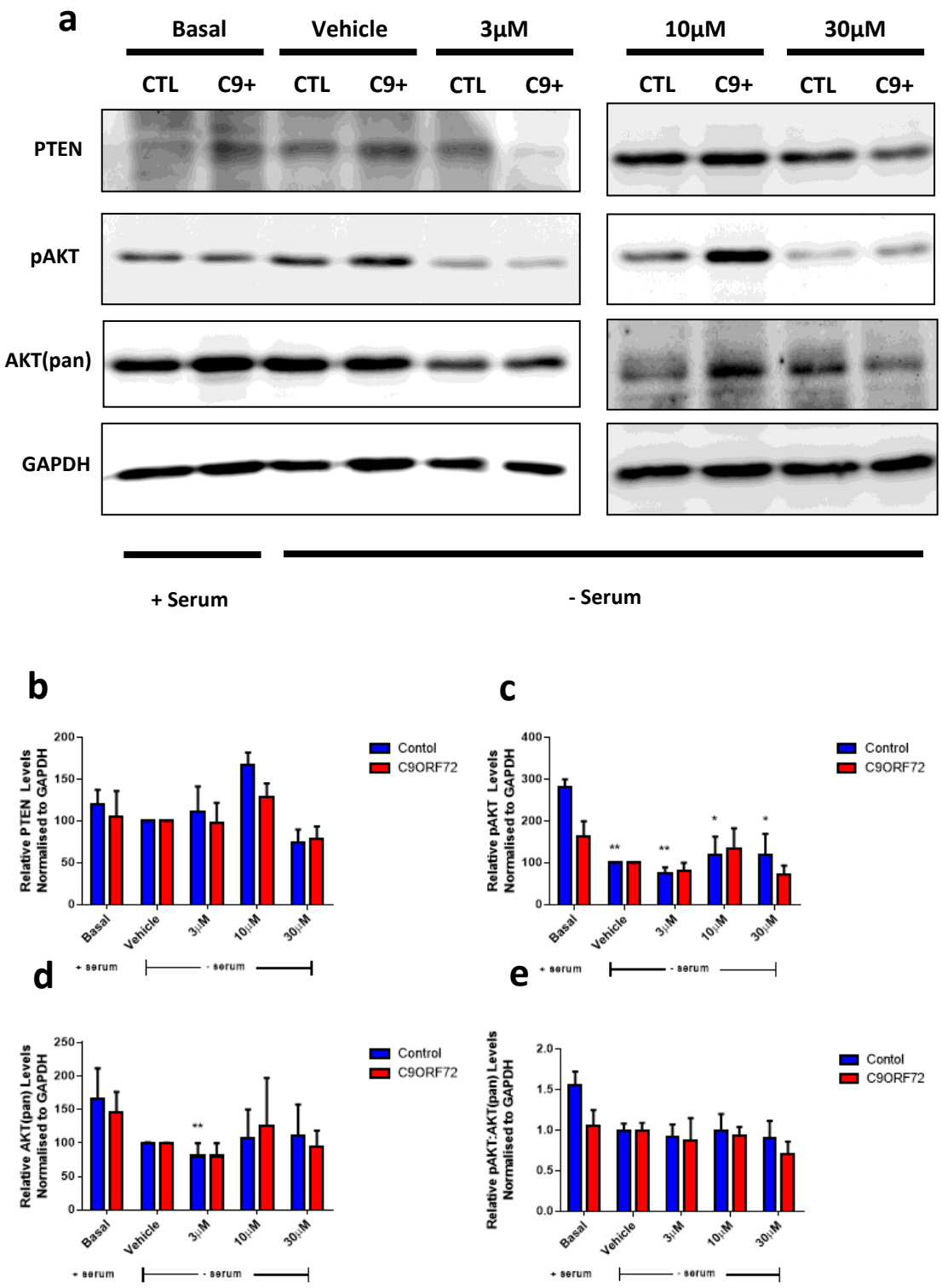

Figure 5.7. Scriptaid treatment to iPS derived cells does not positively impact PI3K Pathway components. a) Western blots reveal: **b)** no significant changes in total PTEN protein expression, **c)** a significant reduction in pAKT levels with serum withdrawal. **d)** No significant changes in total AKT expression, apart from a significant reduction of total AKT protein with 3µM control cells compared to basal controls. **e)** The ratio of pAKT:AKT(pan) reveals no significant change to the total amount of pAKT available. Representative western blot shown. (Data are mean of *n*=3 independent experiments of pooled cells and normalised to GAPDH loading control. Where more than one membrane was required, each membrane contained both a basal and vehicle control for comparison- see chapter 2 section 2.4.3**.** ±SEM *p=<0.05, **p=<0.005, analysed with two-way ANOVA)

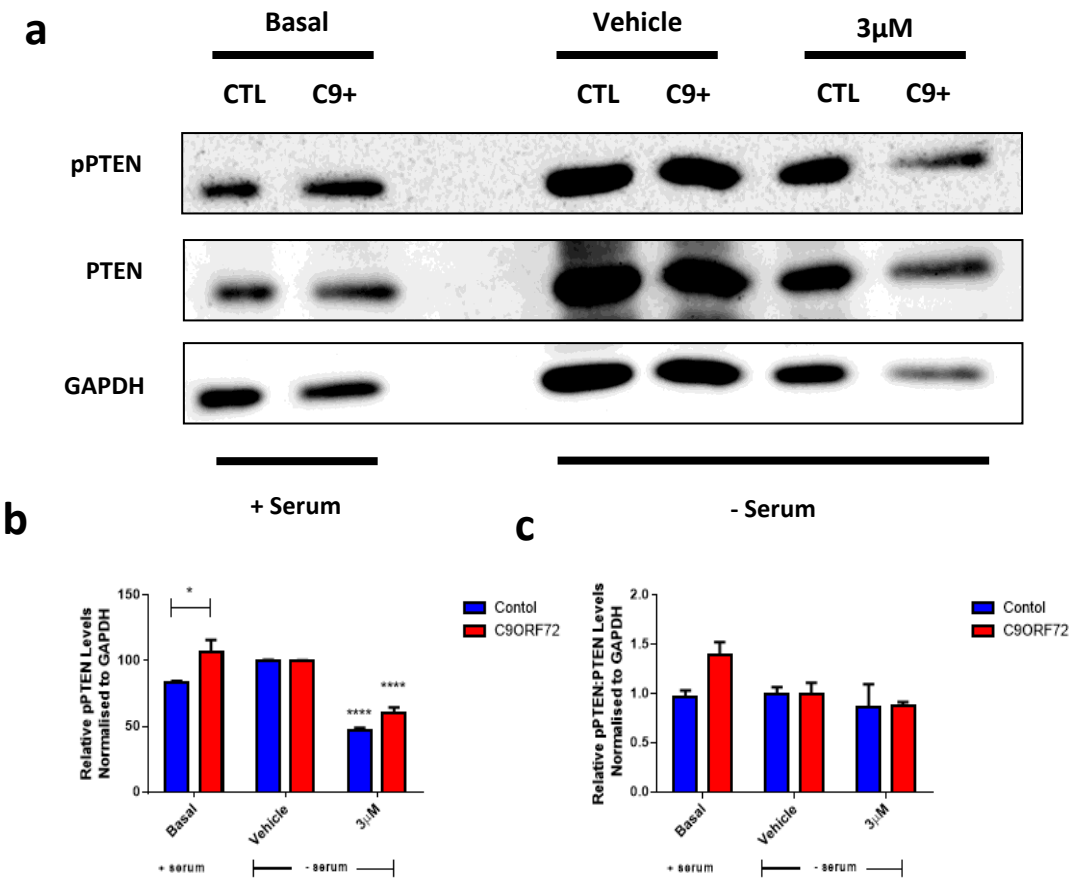

Figure 5.8 Scriptaid has no positive effect on pPTEN but basal pPTEN expression is significantly higher in patient cells. A) Western blots reveal **b)** a significant difference between patient and control pPTEN and a significant downregulation of pPTEN in both patients and control when 3µM scriptaid treatment is applied to iPS-derived cells. **c)** there is no significant change in the total pPTEN available between basal, vehicle or treated conditions. Representative western blot shown. (Data are mean of *n*=3 independent experiments of pooled cells and normalised to GAPDH loading control. ±SEM *p=<0.05, ****p=<0.00005 analysed with two-way ANOVA)

5.4.3 Scriptaid Treatment Does Not Modulate Motor Neuron Cell Number

Given that differentiation is a long process, selecting a paradigm is difficult and there is a multitude of possible variations. After much consideration we went for these paradigms in the first instance, balancing toxicity with predicted active dose and likely dynamics. As the effect of small molecule inhibitors is dynamic and therefore more subtle then a knockdown approach, we considered two paradigms both from the beginning of differentiation as an appropriate start point, one of which was a single dose and the other being multiple weekly doses. For a single application, a dose of 3µM was added to the cells for 24 hours on day 0, or at 2, 4 or 6 weeks into the differentiation protocol, and the cells were allowed to mature to the end of differentiation after which we would be able to identify from motor neuron cell counts of dual ChAT and Tuj1 labelled cell populations, if Scriptaid addition during the differentiation protocol has a positive effect on motor neuron generation at the end. The time points of application were chosen based on key points within our protocol, including the beginning of differentiation on undifferentiated iPS cells, 2 weeks of differentiation when the cells express neuronal marker Tuj1, 4 weeks of differentiation which is the earliest identified expression of mature motor neuronal marker ChAT, and at the end of differentiation. For multiple applications, in a parallel experiment we also applied Scriptaid at the same concentration on iPS cells from the beginning of differentiation (Day 0), and then each week subsequently throughout the differentiation process, to identify if repeated administration would also result in a positive effect on motor neuron cell generation. In the first instance, we were interested in the functional output of MN count after Scriptaid treatment; we then would later investigate the mechanism of action and activity of the drug further.

When cells were treated with Scriptaid for a single application at either Day 0, week 2, week 4 or week 6, motor neuron cell counts revealed no significant increases in motor neuron cell number generated by the end of the differentiation protocol for both patients and controls (figure 5.9 a - d), suggesting Scriptaid does not positively benefit motor neuron generation or increase survival of cells when applied in these conditions. Parallel assays applying Scriptaid for multiple applications at weekly time points

throughout differentiation starting from day 0 and ending at week 6, identified again no significant increases in cell number in either patients or controls (figure 5.9 e).

Notably, a significantly negative effect on motor neuron numbers was found under some conditions. This included a significant decline in motor neurons generated in patient cells treated with Scriptaid at 2 weeks of differentiation compared to control cells treated with Scriptaid at the same timepoint (figure 5.9b). Additionally, a significant decline in motor neuron cell number was found in control cells treated with Scriptaid at 4 weeks of differentiation compared to vehicle control (figure 5.9c). Collectively, these results suggest that Scriptaid had on average little to no measurable positive effect on cells to increase iPS-derived motor neuron cell number.

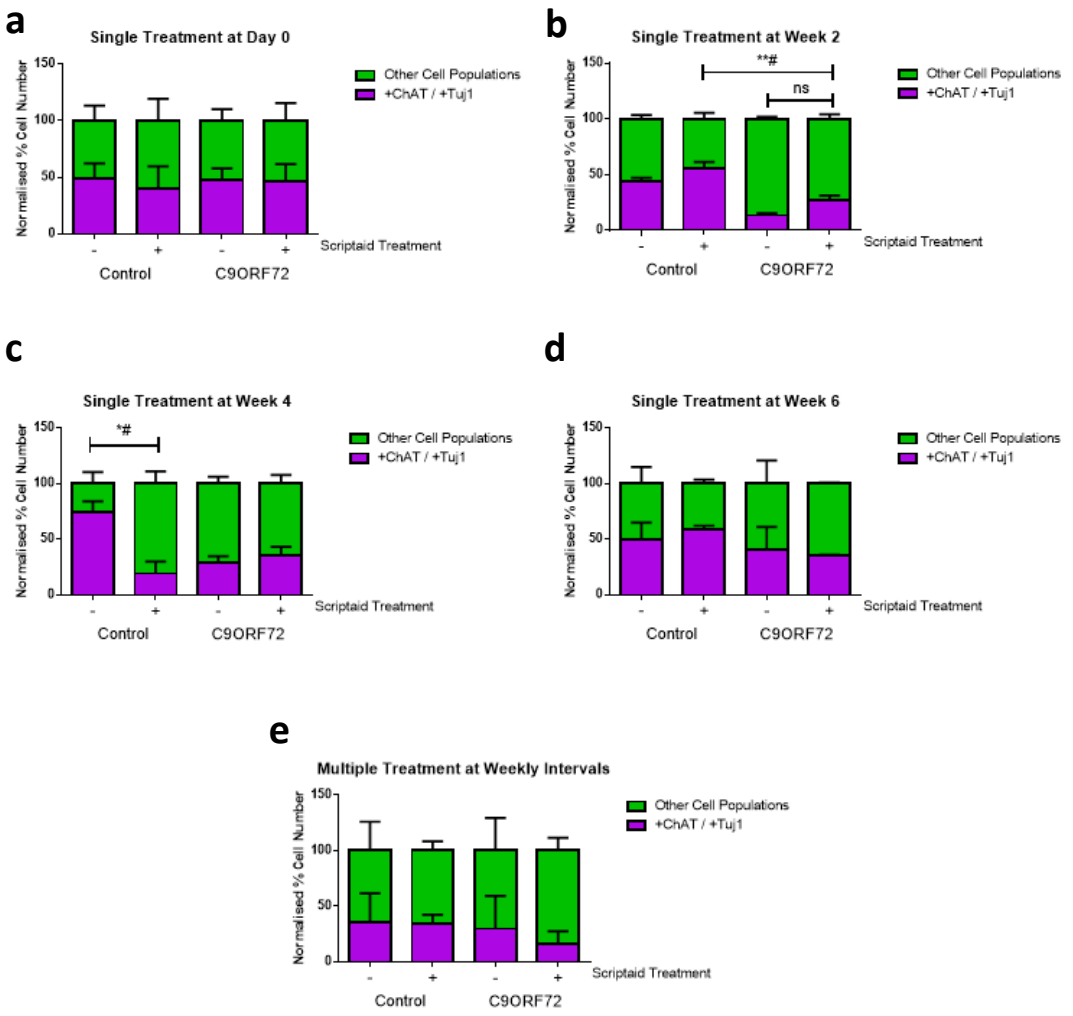

Figure 5.9: Scriptaid treatment during differentiation does not increase motor neuron cell number. iPS cells were treated with 3µM Scriptaid for a single treatment during the differentiation protocol at **a)** Day 0 **b)** 2 weeks **c)** 4 weeks and **d)** 6 weeks of differentiation. IPS cells were also treated with Scriptaid for **e)** multiple applications at weekly intervals from day 0 to 6 weeks of differentiation**.** At the end of the differentiation process cells were counted for the number of dual stained ChAT and Tuj1 positive motor neurons generated. Results found no significant increases in motor neuron number generated with Scriptaid treatment for **a)-d)** either a single treatment or for **e)** for multiple treatments. **b)** A significantly lower number of motor neurons were generated by patient cells treated with Scriptaid compared to control cells treated with Scriptaid when the drug was applied for a single application at 2 weeks of differentiation. **c)** A significantly lower number of motor neurons was generated by control cells treated with Scriptaid compared with vehicle treated control cells when Scriptaid was applied for a single application at 4 weeks of differentiation (Data presented as percentage of total cell counts, mean of *n*=3 independent experiments of pooled cells. ±SEM, Analysed with two-way ANOVA, Bonferroni's correction,-=vehicle control, += Scriptaid 3µM, # between +ChAT/+Tuj1 positive cells (motor neurons))

5.5 DISCUSSION

Promoting the survival of the cells which die in ALS through the manipulation of cell survival pathways could be a valid therapeutic strategy to ameliorate progression of the disease. Indeed, evidence from previous studies in iPS-derived motor neuron models of spinal muscular atrophy, a disease in which the motor neurons are also affected, has found inhibition of apoptotic pathways can reverse cell death phenotypes previously seen in the models (Sareen et al., 2012). Therefore, based on this theory, the aim of our research was to identify if manipulation of PTEN could promote cell survival pathways and thus the survival of cells affected by C9ORF72-related ALS.

In validation of the mechanism to inhibit PTEN for the activation of the PI3K cell survival pathway, we found PTEN knockdown caused a concomitant increase in activated phosphorylated AKT (figure 5.2), a component of the PI3K cell survival cascade which when activated causes increased cell survival through reduced cellular apoptosis. Furthermore, we identified that PTEN knockdown also caused a positive effect on C9ORF72-ALS iPS-derived cells by increasing cell numbers significantly compared to control cells undergoing the same treatment (figure 5.4). We can postulate that this increase in cell number is due to an activation of cell survival pathways. However, these positive effects in patient cell number were only realised from 7 to 9 weeks of differentiation, after which no significant survival benefits were found in patient cells compared to controls (figure 5.4). As the concomitant increase in pAKT was not significant, we may find that with increased PTEN knockdown, through increasing transfection efficiencies from 90% to 95-100%, it may yield significant differences in AKT activation and thus prolong the survival benefits witnessed. However, overall these results agree with existing findings that PTEN inhibition or reduction in neuronal cell models can increase cell survival (Mao et al., 2013, Kirby et al., 2011, Christie et al., 2010, Yang et al., 2014b) and have validated this target for a potential beneficial effect in disease. Interestingly, recent work has found that partial knockdown of PTEN results in a rescue of the toxicity observed in an inducible cell model of C9ORF72- ALS; a knockdown which interestingly did not affect the number of

RNA foci in these cell models (Stopford et al., 2017). This work with not only further supports this mechanism of protection for ALS, but also suggests PTEN manipulation to reduce its activity has a positive effect which is independent of RNA foci hallmarks of C9-ALS, potentially suggesting the foci could be a consequence of disease rather than a cause of cell death.

Taking these results forward, we chose to utilise Scriptaid as a novel therapeutic target for PTEN manipulation due to the positive effects found in cell models of neuronal injury. We were also aware that the use of such drugs could lead to faster translatable results to humans, due to the historical use of similar compounds already in existence (Takai and Narahara, 2010, Yoo and Ko, 2011, Ryu et al., 2005) in comparison to the slow progress of viral vector mediated therapy at the time of investigation. Studies with Scriptaid identified no significant negative effects on cellular viability or cytotoxicity, matching previous reports of low toxicity (Su et al., 2000) (figure 5.5, 5.6). However, when Scriptaid was applied throughout the differentiation process in multiple applications, or at single time points, no positive effect on total motor neuron cell numbers was revealed, implying Scriptaid did not increase motor neuron yield when used during differentiation (figure 5.9). We applied Scriptaid at multiple stages in differentiation to identify when it was best to add the treatment; if added too early we may have inhibited differentiation, however too late and the cells may have already started a cascade towards cell death before any interventions had the opportunity to offer protection. Our results identified no single application which would significantly increase final motor neuron cell number, despite adopting incubation lengths and protocols utilised in the literature for a similar effect (Wang et al., 2015a) and using a concentration reported within the optimal dose for activity (Su et al., 2000, Wang et al., 2015a). When the extent of PTEN manipulation was quantified using western blot analysis, probing for PTEN, pPTEN, AKT and pAKT, no significant positive effects on these components which would suggest an inhibitory response was adopted by the cells was identified (figure 5.7, 5.8). In contrast, we saw a reduction in pPTEN, the inactive form of the protein, and no changes in the amount of pPTEN available (figure 5.8). This suggests in contrast to previous reports, that Scriptaid does not inhibit the activity of PTEN via increasing PTEN phosphorylation; at least in the cell models and conditions tested here. The inability of Scriptaid to upregulate key components in the

PI3K pathway may explain the lack of positive effect on motor neuron cell number after its application; by failing to increase AKT phosphorylation, cell survival pathways are not activated, so motor neurons would be less likely to convey the increased survival mechanisms as a result.

In the work by Wang and colleagues, Scriptaid was found to prevent a decrease in pAKT caused by induced traumatic brain injury, however in our studies no significant reductions in pAKT were identified, meaning unlike their cell models there was no significant patient phenotype in this pathway component for Scriptaid to restore. Additionally, Scriptaid in more recent work was found to have an indirect effect on PTEN, which was thought to offer a neuroprotection through increasing GSK3β mRNA which in turn acts to control the phosphorylation status of PTEN by increasing phosphorylation and therefore inactivation to initiate a disinhibition of the PI3K pathway (Wang et al., 2015a). In our iPS cell models we did witness significantly higher levels of pPTEN in patient cells compared to controls under basal conditions (figure 5.8), therefore it could be possible that in our cell models PTEN phosphorylation had already reached its upper limit, possibly in an endogenous protective activation in disease. Therefore, the addition of Scriptaid could have little to no further effect on a saturated phosphorylation status.

Scriptaid is a HDAC inhibitor with roles acting to control epigenetic gene expression (Su et al., 2000). Cell to cell differences in the expression of genes and protein markers means that these drugs are likely to have different effects across cell types (Wang et al., 2012b). Consequently, one possible explanation for a lack of effect on motor neuron-like cell models could be due to differences between neuronal cell gene expressions. Certainly, when comparing traumatic brain injury, the model the original study was conducted upon, to motor neuron disease, we are likening an acute insult and fast death of neuronal cells in days or even minutes after assault, against a disease which propagates over a patient's lifetime, from chronic accumulation of toxicity culminating in the death of motor neurons. These differences will be reflected in the gene expression profiles of these cells which would have a counteracting effect on how a drug such as Scriptaid would provide its protective properties. In addition, as it is possible to have a disease-causing mutation such as C9ORF72 without developing ALS, this suggests environmental and epigenetic triggers may also be required to initiate

pathogenesis. These epigenetic variations are lost in iPS cell generation, where we have effectively reset a cells epigenetic state. Without this variation between patients and controls we may be losing any disease specific effects on cell survival. It is still possible that Scriptaid's positive therapeutic effect on the survival of cells remains in cells which have retained disease specific epigenetic changes, such as primary neuronal cell models of ALS, or newer models of motor neuron generation such as iMN's from neural progenitor cells which do not lose their epigenetic hallmarks (Meyer et al., 2014).

Although, Scriptaid was unsuccessful in promoting the survival of iPS-derived cell populations, interesting patterns in PI3K pathway components have been revealed in basal iPS-derived cells. Total PTEN levels of both patients and controls are at similar levels in iPS-derived cells (figure 5.7), however in the fibroblast cells the iPS cells originated from, C9ORF72 patient cells showed significantly lower levels of PTEN (Chapter 3 figure 3.5). Whilst this result could be a reflection of the differences between studying a mixed population of cells versus a clone, it also could suggest a modulation of PTEN protein expression in the conversion of fibroblast to iPS-derived cell identity. Fibroblasts are not affected in ALS, whilst motor neurons are, therefore these subtle changes in PTEN expression may reflect some of the differences between a surviving or dying phenotype of the cells. Higher levels of total PTEN in patients could mean increased inhibition through PTEN dephosphorylating PIP3, therefore this would result in less activation of cell survival pathways in iPS cell models of ALS. In contrast, the lower levels of PTEN found in our patient fibroblasts cells compared to controls could reflect a phenotype which confers increased survival to due lower levels of total PTEN to inhibit the pathway, thus increasing cell survival. Contradictory to the iPS-derived cell models studied here, but similar to the results found in our fibroblast models, laser captured micro-dissected motor neurons from ALS patients have been found to express lower levels of total PTEN expression compared to controls (Kirby et al., 2011). However, it is important to note that the cells in the study by Kirby et al. were obtained after the patient's death, and had therefore successfully survived the disease. The reason for their survival could be due to modulation of total PTEN protein in these cells, however as the study did not examine pAKT levels, it is hard to predict if these changes were translated into activation of cell survival pathways for a positive

effect. In our iPS-derived cell models we also examined pAKT expression and found with relative higher levels of PTEN, we see an expected relative lower level of pAKT. However, in comparison with fibroblast cell models, pAKT expression is also significantly reduced in patient cells implying that, although there is a downregulation of this pathway, compensatory mechanisms in the cell may be activated to promote fibroblast cell survival. These discrepancies between patient cell models could also suggest an aberrant signalling cascade in disease, to which motor neurons are potentially selectively vulnerable. Studies have found pAKT expression can remain unaffected in ALS patient tissue despite significant changes in PI3k protein levels and activity, implying aberrant activities of this canonical signalling pathway in ALS (Wagey et al., 1998). As well as this, other survival pathways have also found irregularities in motor neuron disease, with significant caspase-3 and caspase-8 dysregulation and increased motor neuronal cell death in iPS-derived cell models of SMA (Sareen et al., 2012). Their study interestingly found no modification of signalling molecules Bcl2 and Bax which are found downstream of the PI3K cell survival pathway. However, it would be appropriate to understand the behaviours of components upstream of the PI3k pathway such as PTEN, AKT and PI3k for comparison, particularly as factors such as cell models used (SMA vs. ALS), differentiation protocols, and detection methods may all play into cell survival pathway protein expression (Sareen et al., 2012).

Of note, across multiple assays we see patient specific effects. For example, when looking at the stress component of the Scriptaid treatment assays, when cells are exposed to serum withdrawal, both patient models of fibroblasts and iPS-derived cells are less sensitive to serum withdrawal compared to controls (Chapter 3 figure 3.5, figure 5.7). Similarly, for PTEN knockdown, only the patient cell lines are susceptible to increases in cell number. One possible explanation for this could be due to patients conveying aberrant PI3k regulation as a cause or a consequence of disease, becoming least reactive to additional external stressors such as serum withdrawal and exemplifying a possible subtle difference in cell survival cascade regulation in disease. Although under basal conditions we see no difference in the cell viability between patients and controls, subtle changes in the biochemistry and intracellular pathways reflecting a possible early stage of the disease may be present. Many studies have also shown a lack of prominent MN cell death or ALS phenotype in iPS-derived ALS motor

neurons yet still show small biochemical and molecular changes (Kiskinis et al., 2014, Sances et al., 2016). It is possible that these cell models may reflect an early stage of disease which has yet to progress into the full disease phenotype, for example, PTEN dysregulation in the early phases of ALS, showing increased phosphorylation of PTEN possibly in order to promote or maintain survival. Without an obvious apoptotic phenotype in iPS-derived models, future work to age cellular models to try and recapitulate the motor neuron death seen in ALS, subsequently followed by PTEN inhibition might yield a more beneficial result. Additionally, due to technical difficulties in isolating pure populations of iPS-derived motor neurons due to low yields of motor neurons obtained, although PTEN knockdown was successfully achieved in neuronal populations, we were unable to perform cell counts on a pure population of motor neurons. Future experiments adopting newer techniques to obtain yields of up to 95% through the modification of differentiation factors (Du et al., 2015) may increase both motor neuron yield and maturity. This would subsequently make the isolation of motor neurons easier and help us to confirm the benefits of PTEN manipulation on motor neurons independently of other cell populations. Finally, as a further stage to this, experiments to also target PTEN manipulation to the disease affected motor neurons, specifically through the use of viral or Hb9 promotor, would identify a safer, more translatable PTEN manipulation with this methodology, particularly as we observed PTEN knockdown across different cell types in the population.

5.6 Conclusion

Overall, although we were able to validate the targeting of PTEN in the PI3K pathway as a potential target in iPS-derived cell models of C9ORF72 ALS, Scriptaid as a molecule for PTEN inhibition and promotion of this cell survival pathway has failed to produce the desired result. Future work could identify more specific and safer targeting of PTEN, potentially through the use of better molecules or utilising most recent advances in gene therapy allowing targeting of specific cell populations.

CHAPTER 6 : FINAL DISCUSSION

6.1 Lessons Learned From C9ORF72 iPS cell models of ALS

The generation of iPS cells from the somatic cells of humans has revolutionised the study of human disease by providing close replica models of human cells where the use of post-mortem material or primary human cells is either not sufficient or not possible. For neurological diseases, iPS cell technology theoretically provides the opportunity to generate a supply of human neuronal cells for examination and experimental manipulation. In ALS, the degeneration of motor neurons is a primary cause of the disease phenotype, therefore resourcefully, scientists have been utilising the ability to generate "motor-neurons-in-a-dish" to investigate disease causation and attempt to find a therapeutic angle to ameliorate symptoms and progression of a devastating disease. In the above work, our aim was to generate iPS-derived motor neuronal cell models of C9ORF72-related ALS, as a background to investigate PTEN manipulations, including comparing against the originating fibroblasts from which the iPS cells were derived. However, as a relatively novel technique, yet to be universally refined in laboratories across the world, prior to investigating of the effects of PTEN manipulation on cell survival, our characterisation revealed important findings to be noted for the success of future iPS cell differentiations in our hands.

The first observation from our differentiated iPS cells was that we had generated a mixed population of cells, however dual neuronal markers Tuj1 and mature motor neuronal marker ChAT staining revealed a population of motor neuron cells to be 38.3% in controls and 24.9% in patient populations (figure 4.9, 4.10). Although a trend towards lower motor neuron numbers was found in patient samples, no significant difference was found between patient and control motor neuron number, in-line with previous work of a similar investigative nature (figure 4.10) (Devlin et al., 2015, Donnelly et al., 2013a). Whilst these numbers reveal successes in our ability to generate motor neuronal cells through our protocol (Yang et al., 2014b), the cell counts also reveal an opportunity to not only identify the fate of the remaining cells in the population but also highlight that optimisation of motor neuron yield could be undertaken for future differentiations.

With limited international standardisation of iPS cell differentiation protocols, variations in motor neuron yield are common place, with results ranging from 20% to 95% being recently reported (Sances et al., 2016). Differences in the protocol can be found in every stage of the process, and include: variation in the time for total differentiation; time to initiate neural induction, ventralisation, and maturation; factors used for differentiation; concentrations of factors and reagents used; length of incubation period for factors, and point of application in differentiation; time of cell dissociation and plating; cell numbers plated; time assays are performed; as well as differences in vessel and coatings used. Whilst we were able to optimise some of these processes during our differentiations, including cell numbers plated and the timings for the end of our experiments, unfortunately within the time and scope of this project, we were unable to explore further areas such as our factor and reagent choices which may have had a positive effect on final motor neuron yields. Future studies could employ some of the more recently published techniques in this area. For example, a study by Du et al. has successfully used Wnt signalling activation along with varying the concentrations of retinoic acid and purmorphamine throughout differentiation, to achieve highly pure yields of motor neurons of up to 95% over a shorter protocol (Du et al., 2015). Future studies could also identify the constitution of the rest of the population of differentiated iPS cells generated by our protocol, including the number of additional neuronal populations such as interneurons, and the percentage of astrocytes and other neural support cells. If such findings reveal for example a higher proportion of astrocytes, it may aid us in identifying which factors should be modulated to reduce their prevalence, and guide us to where within our protocol modifications could be made. Using an alternative protocol or a similar approach to Du and colleagues could be beneficial in two ways. Firstly, by increasing the total yield of motor neurons it would reduce the need for often yield-limiting further purification processes such as fluorescence activated cell sorting, utilised by some labs to obtain a pure yield of desired cell populations. As cell counts similarly to the above work are often made by marker expression, this alone does not identify the percentage of functional cells, therefore this work would be supported by electrophysiological recordings. However additionally, by generating higher yields of motor neurons, it would also save time in generating multiple batches of differentiated cells; save resource using less factors and using those that were obtained more efficiently; and

finally it would save money, particular as the differentiation process requires the use of expensive reagents in what can soon become an expenditure too large for many labs to run effectively.

Along with increasing the number of motor neurons generated, another method for future differentiations may lie in improving the ability of the models to replicate ALS. In our models we could find no significant difference between patient and control cell number over time or increased cell death in patient cells specifically (figure 4.11). While we cannot rule out from our studies subtle biochemical changes such as caspase-3 dysregulation (Dafinca et al., 2016) which could be relevant to identifying this phenotype in our models, it is important to note that iPS-derived cell models of motor neurons have shown varying levels of patient associated cell survival phenotypes. Whilst some iPS cell models of MND such as SMA have found a degenerative phenotype in patient cells (Ebert et al., 2009), and SOD1 iPS-derived models similarly showing survival differences (Kiskinis et al., 2014), many studies in iPS-derived models of C9ORF72-related ALS have struggled to identify a similar phenotype (Sareen et al., 2012, Devlin et al., 2015, Donnelly et al., 2013a). Interestingly, it is not uncommon for iPS cell models of ALS to present mild or partial phenotypes of disease (Dimos et al., 2008, Mitne-Neto et al., 2011, Wainger et al., 2014). The reported different findings across diseases which ultimately result in the death of the same cell, exemplify how different genetic causes reflect distinct mechanisms of action, and highlight how a "one-size-fits-all" therapeutic may not work in the face of the complexities of motor neuron biochemistry.

As iPS cells represent an embryonic-like state, the relatively short length of time from iPS cell to fully differentiated neuron may not be long enough to imitate life-long cellular stresses which could act as a second trigger for C9ORF72- related ALS pathogenesis. Moreover, iPS cells have effectively had their epigenetic status erased (Mertens et al., 2015), and these features may be the prominent cause to cellular degeneration in specific forms of ALS. Our differentiation and culture period went up to 12 weeks, however studies have found cells as old as 4 months display increased patient associated phenotypes including DNA damage (Lopez-Gonzalez et al., 2016). This suggests that further studies should prolong culture periods to gain an increased

aging phenotype. However, as we show a progressive loss of total cell number over increased culture length (figure 4.11), to do this we would unlikely be able to maintain the volume of cells required to successfully perform such analysis with our current protocol. As iPS derived motor neurons from C9ORF72 patients have been found to display increased oxidative stress and DNA damage (Lopez-Gonzalez et al., 2016), artificial induction of oxidative stress or experimentally induced aging (Miller et al., 2013) on our cell models may improve their ALS phenotype. Alternatively, newer techniques to generate cell models from a direct conversion of human somatic cells may provide a simpler solution. A recent study by Mertens et al. identified that iPS cells derived from human fibroblasts convey an edited transcriptome that is no longer representative of the donor cell, including the loss of key ALS identifiers (Mertens et al., 2015). As many of these gene signatures are developed over a patient's lifetime, consequently this loss of age-associated features in iPS cells could be a reason behind the variable recapitulation of disease found in iPS cell derived models. Future studies to use models which involve a direct conversion of somatic cells to the cell of interest could act as complementary models to iPS-derived motor neurons. Studies have identified that direct conversion techniques developing iastrocytes are able to replicate characteristics of primary ALS tissue well, exerting the same toxic responses to motor neurons as spinal cord-derived astrocytes (Meyer et al., 2014, Haidet-Phillips et al., 2011). Studies comparing motor neurons which have maintained age-related epigenetic patterning against iPS-derived motor neurons, generated from the same originating fibroblast cells, would identify the importance of these signatures for the model to recapitulate C9ORF72- related ALS more effectively.

We have successfully generated motor neurons that positively express mature motor neuronal markers, motor neuronal specific markers and multiple neuronal markers; however future avenues may also lie in improving the electrical maturity of iPS-derived motor neurons generated in our protocol. Electrophysiological recordings revealed an immature phenotype in the motor neurons generated, with cells conveying a lack of repetitive action potential firing on exposure to a depolarising stimulus, wide spikes, low capacitance, and a highly depolarised resting membrane potential (Table 4.1-3, figure 4.12). Whilst some of these features are common in iPS cell models (Gogliotti et al., 2012, Sances et al., 2016) in comparison to other groups improvements can be

made in the electrical excitability (Wainger et al., 2014, Sareen et al., 2013). As differentiation was continued for up to 12 weeks in our studies, steps to improve the maturity of the cells rather than increasing tissue culture lengths, could include changes to the differentiation protocol mentioned above to rapidly generate mature motor neurons, for example at 2-3 weeks rather than 4-6 weeks. Indeed preliminary data from our lab has found that utilising a shorter differentiation protocol and utilising Compound C, an AMP kinase inhibitor, at the start of the protocol for neural induction (Qu et al., 2014), has improved the electrical maturity of the cells (data not shown). Whilst this work will continue, additionally, other methods to improve the electrical maturity of cells could also include using co-cultures with astrocytes which has been shown to improve both the hyperpolarisation of resting membrane potentials and synaptic activity (Johnson et al., 2007). These steps would ensure there is an increased timeframe after motor neuron generation for maturation in culture before total cell numbers decline.

6.2 Molecular Hallmarks of C9ORF72 ALS in iPS-derived Cell Models

Since the discovery of C9ORF72 to be the most common genetic cause of ALS (Renton et al., 2011, DeJesus-Hernandez et al., 2011) researchers have identified several molecular features found to be specifically associated with C9ORF72-related ALS. RNA foci, aggregated material transcribed from both sense and antisense RNA transcripts appearing as punctate species upon RNA FISH are one of those features, and the discovery of them in patient tissue has added to the debate of how the mutated repeat expansion causes disease. Many groups have elucidated that the presence of RNA foci is indicative of a toxic gain of function mechanism being causal or at least contributing towards disease pathogenesis (van Blitterswijk et al., 2012, Harms et al., 2013). In our cells, in addition to corroborating a mechanistic cause of disease, due to their identification in patient tissue alone, we decided to employ them as markers of the hexanucleotide repeat expansion in our cells.

Sense and antisense probes were able to successfully identify foci from both species in our differentiated patient iPS cells, however were absent in our controls (figure 4.13,

4.14). This result is in confirmation with multiple reports of iPS-derived cells with a C9ORF72 background (Almeida et al., 2013, Mizielinska et al., 2013, Lagier-Tourenne et al., 2013, Donnelly et al., 2013a, Cooper-Knock et al., 2015b), and the identification of foci in undifferentiated iPS cells, also confirmed that the expansion remained in patient cells throughout the iPS cell to differentiated cell transition and were not generated during the process. Sense and antisense RNA foci were found in 31.89% and 21.4% of cells respectively and of either species, 1-3 foci per cell was found to be the most frequent number (figure 4.15), corroborative with a number of reports which also find lower foci numbers to be common (Lagier-Tourenne et al., 2013, Sareen et al., 2013, Mizielinska et al., 2013). However, the finding that our foci were predominantly cytoplasmic (figure 4.13, 4.14) whilst dissimilar to some previous reports (Almeida et al., 2013, Mizielinska et al., 2013, Sareen et al., 2013, Lagier-Tourenne et al., 2013), has been noted to be a more common occurrence in iPS cells and differentiated counterparts (Donnelly et al., 2013a, Lagier-Tourenne et al., 2013, Cooper-Knock et al., 2015b). These results show that our models recapitulated aspects of disease pathology including the aberrant molecular biology newly associated with disease (Cooper-Knock et al., 2015b), thus bringing us a step closer to creating a more accurate model of human ALS.

In addition to foci observations, in our cells we were also able to witness GA di-peptide repeat protein aggregates as a second feature of aberrant molecular pathobiology in our cell models (figure 4.16, 4.17) (Mori et al., 2013b, Ash et al., 2013, Almeida et al., 2013). Similarly to foci visualisation, we identified DPR proteins in iPS cells in their differentiated and undifferentiated states, suggesting again the formation of these proteins does not occur during the differentiation period. GA has been reported to be the most common DPR protein in tissue due to its high ability to form aggregates (Zhang et al., 2014). In addition, recent studies have found interesting correlations between age and toxicity, with GA DPR's noted to cause increased toxicity to neuronal cells with increasing age (Flores et al., 2016), and DPR proteins found to be prevalent at higher expression levels in older rather than younger cultures of iPS-derived neurons (Lopez-Gonzalez et al., 2016). Ultrastructural analysis has revealed dynamic physical changes to DPR protein secondary structure, including an increased

propensity for β-pleated sheet formation with age (Flores et al., 2016), which suggests steps to improve the aging phenotype within our models may help to identify other DPR proteins. Our cells also exhibited distinct aggregations of GA DPR proteins, which some studies have proposed as a sign of increased toxicity (Wen et al., 2014). However as we did not identify any cell death phenotype in the studies performed here, it is possible we are witnessing an early stage of neurotoxicty in the cells, a possibility which could fit with the six-step theory of ALS (Al-Chalabi et al., 2014). Alternatively, whilst many studies advocate for their toxic contribution to disease, we cannot rule out the possibility that these aggregates are initiated as a protective mechanism. Future work to optimise the visualisation of the remaining DPR proteins would be of interest, to clarify conflicting reports on their toxicity (Wen et al., 2014, Zhang et al., 2014).

The unusual re-distribution of TDP-43 protein from the nucleus to the cytoplasm in ALS is now a well described hallmark of the disease which has also been shown in iPS cell models. Studies have found that undifferentiated ALS patient iPS cells contained indications of aberrant TDP-43 such as increased soluble full-length TDP-43 and increased detergent resistant C-terminal fragments of TDP-43 (Bilican et al., 2012), implying similar to other hallmarks of disease, the generation of iPS cells from somatic cells does not remove these traits. However, the reports of the relationship between TDP-43 and C9ORF72 has generated mixed results (Lagier-Tourenne and Cleveland, 2009, Mizielinska et al., 2013, Bilican et al., 2012, Almeida et al., 2013, Zhang et al., 2015a), which is also the case for the relationship between TDP-43 and RNA foci (Lagier-Tourenne et al., 2013, Mizielinska et al., 2013, Cooper-Knock et al., 2015b). Therefore examining TDP-43 distribution and foci presence in our iPS derived cell models was of interest. We found that foci and TDP-43 pathology could be identified together in cells, however there were no significant increases in the number of patient cells with re-location of TDP-43 to the cytoplasm (figure 4.18). We did find patient cells expressed a granular diffuse staining pattern compared to controls and patient cells were also identified to contain lower levels of nuclear TDP-43 protein after quantification of staining intensity (figure 4.18). The lack of a strong TDP-43 phenotype may be reflective of the inability of our cell models to fully recapitulate this part of disease pathology, and it is possible, given the length of time to differentiate and the

dramatic reduction of total cell number over extended culture, cells with a heavy pathology are lost in this process potentially akin to pathology material. The contrasting findings in other C9ORF72 studies, coupled with inconsistent iPS cell differentiation techniques between them, exemplifies how the variability in the generation of the cells could be producing a spectrum of ALS phenotypes. These could range from severe with strong phenotypic characteristics of disease, to mild. As our iPS cell models also do not show a distinct cell death phenotype and express an intermediate TDP-43 pathology, it is possible our models represent a milder representation of the disease.

6.3 Cell Specific Variation of PTEN in ALS

Phosphatase and Tensin Homologue Deleted on Chromosome Ten (PTEN), is a key component in the ubiquitous PI3k cell survival pathway. As a tumour suppressor, its roles in preventing the activation of AKT, and thus through a canonical cascade, the inhibition of cell survival and the increase in apoptosis, have created an increased level of interest into how this protein can be targeted for beneficial therapeutic effects. The death of motor neurons in ALS prompted us to investigate what happens when we manipulate PTEN in cell models of ALS, and whether or not this manipulation promotes the survival of these cells in disease.

As a pathway that is present in every cell of the body, each cell will have various degrees of pathway activation. Indeed our studies across two different cell models of ALS has found that patient fibroblast cells under basal conditions exhibit significantly lower levels of total PTEN protein expression compared to their controls (figure 3.5). However, when the same fibroblast cells are converted to iPS cells and differentiated into neuronal and motor neuronal identities, the total levels of PTEN expression are similar between patients and controls, with no significant difference between them (figure 5.5). Whilst we recognise this findings could be an artefact from comparing a mixed population (fibroblasts) with a clone (iPS cells), the differences between patients and controls may reflect variation in control of cell survival; as motor neurons are specifically vulnerable to cell death in ALS, their methods of control in the PI3k pathway may be aberrantly regulated as a cause or a consequence of disease. As

fibroblast cells are unaffected in ALS, they could promote mechanisms which maintain cell survival, including maintaining low levels of total PTEN protein to reduce the inactivation of AKT. Correspondingly, differences in cellular response to PTEN manipulation performed via PTEN knockdown have been found between cells of a mesodermal origin such as fibroblasts, compared to those of a neuronal origin (Duan et al., 2015) . Duan et al. found that mesenchymal stem cells and fibroblasts underwent cellular senescence after PTEN knockdown but exhibited no changes in AKT phosphorylation status. However in neural stem cells, PTEN deficiency resulted in neoplastic transformation and activation of AKT through increased phosphorylation (Duan et al., 2015). Further work expanding the investigations in iPS-derived cell PTEN protein levels, may help further identify if there are indeed intrinsic cellular differences in PI3K cell survival pathway regulation which may be emulated in the variance in total PTEN expression found between patients and controls in our two cell models.

Our results found that experimental reduction of PTEN through knockdown leads to a concomitant increase in pAKT and can result in an increase in cell number of differentiated patient iPS cell populations at 7 to 9 weeks of differentiation (figure 5.2 5.4). As only patient cells were affected, this coupled with a change in total PTEN expression from fibroblast to iPS derived cells, could suggest ALS specific regulation in the cell models which more closely replicate the cells affected in ALS. This difference may be irregular cell survival pathway activation in these cells, which could then lead to increased cell death, and may explain why patient cell numbers are more affected by PTEN knockdown. Further to the above study, neural stem cells deficient in PTEN, whilst able to differentiate into neuronal cell populations, were also found to be more resistant to stress induced cell death (Duan et al., 2015). As our results showed, PTEN deficient cells were more successful in maintaining cell numbers in total iPS cell populations, compared to their counterparts, one conclusion could be that removing the action of PTEN in this pathway could help to improve resistance to cell death in these cells. A caveat to the above work is that our studies examined one parameter of PTEN knockdown; the effect on total cell population numbers rather than specifically in motor neurons. Recent studies have highlighted how differentiated PTEN-deficient neural stem cells confer higher numbers of neuronal class III β-Tubulin (Tuj1) positive neurons, in a protein phosphatase dependent mechanism (Lyu et al., 2015), therefore

further studies to isolate not only neuronal population numbers but also to quantify key neuronal and motor neuronal proteins such as Tuj1, Hb9 and ChAT could reveal interesting neuronal specific effects.

As PTEN in its phosphorylated form indicates inactivation of the protein, we also quantified this in differentiated iPS cell models. Unfortunately, due to an inability to measure pPTEN within its dynamic range in fibroblast cells, we were unable to make a comparison between fibroblast and differentiated iPS cells pPTEN levels from our studies. However results in iPS-derived cells revealed significantly higher phosphorylation of PTEN in patient cells compared to controls under basal conditions (figure 5.9). This finding suggests that in patient cells there is an effort to inactivate PTEN, which could promote increased cell survival pathway activation and thus cell survival in disease. However, this increased phosphorylation is not translated into increased total phosphorylated PTEN available in the cell (figure 5.9), nor does it translate into increased AKT activation (figure 5.8) which could again suggest irregular pathway control in disease, as we would expect to see high pPTEN to cause a positive effect on AKT phosphorylation. A recent study examining the regulation of PTEN phosphorylation in the c-terminal tail has highlighted some interesting results which may explain why firstly we were unable to visualise pPTEN in fibroblast cells. The c-terminal tail of PTEN hosts 4 phosphorylation sites Ser^{380}, Thr^{382}, Thr^{383} and Ser^{385}, which are known to contribute towards the conformation change which closes PTEN to membrane binding and thus inactivating its catalytic activity (Bolduc et al., 2013, Rahdar et al., 2009). However, the order of their phosphorylation and whether or not phosphorylation of all of these sites was required for this reaction has until recently been unidentified. In a controversial new study, Chen and colleagues identified that phosphorylation at a single site cannot dominantly cause this conformational change, however a successive and progressive phosphorylation is required of all 4 or at least 3 of these sites to inactivate the protein (Chen et al., 2016). Whilst this study remains to be validated in other laboratories, it could suggest a more dynamic nature of PTEN phosphorylation than previously thought which could be regulated by multiple partners intracellularly, further adding to the complexity of PTEN regulation in the cell. Of note, this study also identified that p380 phosphorylation was key in the ability of pPTEN to be visualised by their western blotting techniques. Whilst pPTEN (ser380)

antibodies were used in our studies, the phosphorylation of the other sites still remains unknown. Taking this into account, as there are limitations of using antibodies to measure PTEN phosphorylation, future studies to use antibodies sensitive to additional residues for probing individually, in turn, and together, would clarify the phosphorylation status of PTEN, however nevertheless analysis of such findings should be interpreted with care.

6.4 Scriptaid as a PTEN Manipulator

As a novel and alternative method of PTEN inhibition, Wang et al. identified that Scriptaid a HDAC inhibitor, could protect neurons from traumatic brain injury through PI3k pathway manipulation by increasing PTEN inactivation, and thus AKT phosphorylation and cell survival (Wang et al., 2012a, Wang et al., 2015a). As additional studies also reported that HDAC inhibition on cerebellar granule cells offered neuroprotection against glutamate induced excitotoxicity (Leng and Chuang, 2006, Biermann et al., 2010), the similarity in neuronal specific targeting and pathways implicated in ALS pathogenesis prompted us to investigate HDAC inhibition as a method of PTEN manipulation in our cell models of disease. However, when Scriptaid was tested in our first model of ALS, fibroblast cells, it had no significant effect on AKT phosphorylation status (figure 3.5). Whilst this suggests a lack of the ability of Scriptaid to modulate the PI3k pathway as described in the literature, we recognised it could be an indicator that these otherwise healthy cells are not susceptible to any protective effects of the drug, particularly as previous work has been described in neuronal cells. Therefore, as the cells assayed were not akin to the neurons affected in ALS, we postulated the lack of activated cell survival pathways seen with addition of this drug was due to this, and thus proceeded with generating a cell model which more closely replicated the cell damaged in disease.

Nonetheless, when similar studies were performed in iPS –derived cell models of ALS, Scriptaid did not cause a positive change in motor neuron cell number when applied throughout differentiation, and when investigated further, Scriptaid did not illicit an increase in cellular AKT phosphorylation (figure 5.7, 5.8). As mentioned above, the basal levels of pPTEN in our patient iPS cells were significantly higher than controls.

However, when we examined the effect of Scriptaid on this, rather than see an increase in PTEN phosphorylation after treatment we saw a reduction in pPTEN in both patients and controls suggesting that the drug does not act as described in the literature (figure 5.8). Of note, later work by Wang and colleagues has suggested that the neuroprotective effect of Scriptaid via PTEN inactivation is a non-direct mechanism of action. They described how knockdown of GSK3β, an interactor of PTEN, abolished a Scriptaid-mediated phosphorylation of PTEN, and as Scriptaid exposure increased GSK3β mRNA, the authors suggested that regulation by Scriptaid was through non-HDAC cellular targets (Wang et al., 2015a). HDACs have numerous non-histone targets, therefore in light of these more recent findings, further work to examine the changes to other cellular cascade interactors in the PI3K, pathway including GSK3β, could reveal why Scriptaid has failed to illicit the required response in our cells. The response from Scriptaid could be reliant upon a combination of cell-to-cell HDAC expression, activity, and non-HDAC targeting. Each cell type and tissue holds varying levels of HDAC expression and activity which can even be stage-specific (Morrison et al., 2007, Simoes-Pires et al., 2013). Evidence has shown how some HDACs can promote neuronal survival (Chen and Cepko, 2009) whilst others are suggested as viable targets for inhibition in neurodegeneration (Simoes-Pires et al., 2013). Because of this variability, the cell specific effects of HDAC inhibition may have wider implications for their therapeutic use. While Scriptaid has been described as a potential therapeutic for the survival of degenerative and damaged neuronal cells, it has also been proposed as a novel cancer therapeutic. As a HDAC inhibitor, by promoting reduced transcriptional repression it is thought to modulate the role histone deacetylation plays in cancer cell growth, and has been shown to slow down the growth and promote apoptosis of endometrial and ovarian cancer cells specifically, not affecting non-cancerous cells (Takai et al., 2006). In breast cancer cell lines, Scriptaid was found again to inhibit apoptosis, slow growth, and increase oestrogen receptor (α-ER) expression in α-ER absent cell lines, the loss of which is an indicator of accelerated disease progression (Giacinti et al., 2012). Scriptaid also has been shown to increase the sensitivity of cells to radiation-induced cell death, indicating that Scriptaid may be an excellent therapeutic coupled with radiotherapy to target radio-resistant cells by increasing the number of DNA double strand breaks and promoting cell cycle arrest (Kuribayashi et al., 2010). Whilst in neuronal cells, Scriptaid is thought to promote cell survival through

the AKT pathway (Wang et al., 2012a), in glia, HDAC inhibition targeted a different pathway, promoting Jun N-Terminal kinase (JNK) induced apoptosis in glioblastoma multiform and supported the idea that Scriptaid induced apoptosis in cancer is mediated by DNA damage repair responses and cell cycle inhibition (Sharma et al., 2010). With these studies in mind, it may be a property of Scriptaid or HDAC inhibition to treat cells according to the prerequisites of the cells gene and protein expresion. Of note, as studies have identified that PTEN can associate with chromatin to control gene transcriptional repression (Duan et al., 2015) using Scriptaid for a therapeutic effect in cell survival may result in a number of effects on gene expression that may be difficult to predict due to a potential combination of PTEN modulation and HDAC inhibition with the drug. Therefore, the use of HDAC inhibition with dynamic compounds such as Scriptaid, may need cautious monitoring to guarantee not only the success of the therapy, but also to control any potential off-target effects.

6.5 Final Conclusions

The first conclusion to be derived from this body of work is related to the development and use of iPS cell models for the study of ALS. We have successfully generated iPS-derived neuronal and motor neuronal models of ALS which recapitulate many features of disease. However whilst these models act as an excellent human models for neuronal cell investigations, we must recognise caveats in their use, including their ability to fully model C9ORF72-related ALS. We have found, similar to others, an intermediate representation of disease, which although shows molecular pathobiological hallmarks of ALS does not replicate cell death and degeneration to the same extent of other forms of MND or primary animal cell models. Certainly steps to refine our models, for instance by improving the electrical activity and aging phenotype, should be undertaken in future work. Nevertheless even with these improvements, studies are now beginning to unravel how each subtype of ALS from C9ORF72 to SOD1 now represents distinct subtypes in relation to pathobiology and response to treatment (Ferraiuolo et al., 2016); findings which will have significant consequences upon the translational benefits of ALS research.

The above body of work, has identified some key findings related to the study of PTEN in cell models of ALS, which with further investigation could lead towards the reduction of motor neuron cell death and the promotion of cell survival in disease. Comparing against the same genetic background for directly comparable results, we have identified some potential key differences in the quantities of PTEN protein and downstream cascade components between fibroblast cell and iPS derived cell models of ALS. C9ORF72 ALS patient fibroblast cells display significantly lower total PTEN protein compared to their control counterparts, yet once converted to iPS cell and differentiated towards the fate of motor neurons, the cells no longer display this difference, a finding that additional investigations could further validate. As PTEN knockdown was found to cause a concomitant increase in the phosphorylation of AKT, thereby increasing the activation of well described cell survival pathways, it validates the manipulation of this pathway for this purpose in iPS-derived cell models. Additionally, as PTEN knockdown was identified to cause a positive increase in total iPS-derived cell survival between 7 and 9 weeks post differentiation, specifically in patient cells, it demonstrates the unique differences in PTEN regulation between patient and control models can be a targeted towards a beneficial effect. Whilst the effects of Scriptaid as a PTEN manipulator were not realised above, it shows us how direct targeting of the protein is likely to be the most viable method for PTEN manipulation for the complex and dynamic roles and regulation of PTEN and PI3K pathway components. What these findings mean in the context of C9ORF72-ALS patient therapies, including whether or not PTEN manipulation to improve motor neuron cell survival will translate into prolonged life and slower disease progression for the patient, remains to be elucidated. Nevertheless from our studies above, tentative first steps have been made in this direction.

REFERENCES

ABEL, O., POWELL, J. F., ANDERSEN, P. M. & AL-CHALABI, A. 2012. ALSoD: A user-friendly online bioinformatics tool for amyotrophic lateral sclerosis genetics. *Hum Mutat,* 33**,** 1345-51.

AL-CHALABI, A., CALVO, A., CHIO, A., COLVILLE, S., ELLIS, C. M., HARDIMAN, O., HEVERIN, M., HOWARD, R. S., HUISMAN, M. H. B., KEREN, N., LEIGH, P. N., MAZZINI, L., MORA, G., ORRELL, R. W., ROONEY, J., SCOTT, K. M., SCOTTON, W. J., SEELEN, M., SHAW, C. E., SIDLE, K. S., SWINGLER, R., TSUDA, M., VELDINK, J. H., VISSER, A. E., VAN DEN BERG, L. H. & PEARCE, N. 2014. Analysis of amyotrophic lateral sclerosis as a multistep process: a population-based modelling study. *The Lancet. Neurology,* 13**,** 1108-1113.

AL-CHALABI, A. & HARDIMAN, O. 2013. The epidemiology of ALS: a conspiracy of genes, environment and time. *Nat Rev Neurol,* 9**,** 617-628.

AL-SAIF, A., AL-MOHANNA, F. & BOHLEGA, S. 2011. A mutation in sigma-1 receptor causes juvenile amyotrophic lateral sclerosis. *Ann Neurol,* 70**,** 913-9.

ALLEN, S. P., RAJAN, S., DUFFY, L., MORTIBOYS, H., HIGGINBOTTOM, A., GRIERSON, A. J. & SHAW, P. J. 2014. Superoxide dismutase 1 mutation in a cellular model of amyotrophic lateral sclerosis shifts energy generation from oxidative phosphorylation to glycolysis. *Neurobiol Aging,* 35**,** 1499-509.

ALMEIDA, S., GASCON, E., TRAN, H., CHOU, H., GENDRON, T., DEGROOT, S., TAPPER, A., SELLIER, C., CHARLET-BERGUERAND, N., KARYDAS, A., SEELEY, W., BOXER, A., PETRUCELLI, L., MILLER, B. & GAO, F.-B. 2013. Modeling key pathological features of frontotemporal dementia with C9ORF72 repeat expansion in iPSC-derived human neurons. *Acta Neuropathologica***,** 1-15.

AMOROSO, M. W., CROFT, G. F., WILLIAMS, D. J., O'KEEFFE, S., CARRASCO, M. A., DAVIS, A. R., ROYBON, L., OAKLEY, D. H., MANIATIS, T., HENDERSON, C. E. & WICHTERLE, H. 2013. Accelerated high-yield generation of limb-innervating motor neurons from human stem cells. *J Neurosci,* 33**,** 574-86.

ARAI, T., HASEGAWA, M., AKIYAMA, H., IKEDA, K., NONAKA, T., MORI, H., MANN, D., TSUCHIYA, K., YOSHIDA, M., HASHIZUME, Y. & ODA, T. 2006. TDP-43 is a component of ubiquitin-positive tau-negative inclusions in frontotemporal lobar degeneration and amyotrophic lateral sclerosis. *Biochem Biophys Res Commun,* 351**,** 602-11.

ARBER, S., HAN, B., MENDELSOHN, M., SMITH, M., JESSELL, T. M. & SOCKANATHAN, S. 1999. Requirement for the homeobox gene Hb9 in the consolidation of motor neuron identity. *Neuron,* 23**,** 659-74.

ARRINGTON, D. D. & SCHNELLMANN, R. G. 2008. Targeting of the molecular chaperone oxygen-regulated protein 150 (ORP150) to mitochondria and its induction by cellular stress. *American Journal of Physiology - Cell Physiology,* 294**,** C641-C650.

ASH, P. E. A., BIENIEK, K. F., GENDRON, T. F., CAULFIELD, T., LIN, W.-L., DEJESUS-HERNANDEZ, M., VAN BLITTERSWIJK, M. M., JANSEN-WEST, K., PAUL, J. W., RADEMAKERS, R., BOYLAN, K. B., DICKSON, D. W. & PETRUCELLI, L. 2013. Unconventional translation of C9ORF72 GGGGCC expansion generates insoluble polypeptides specific to c9FTD/ALS. *Neuron,* 77**,** 639-646.

ATKINSON, R. A. K., FERNANDEZ-MARTOS, C. M., ATKIN, J. D., VICKERS, J. C. & KING, A. E. 2015. C9ORF72 expression and cellular localization over mouse development. *Acta Neuropathologica Communications,* 3**,** 1-11.

BACKMAN, S. A., STAMBOLIC, V., SUZUKI, A., HAIGHT, J., ELIA, A., PRETORIUS, J., TSAO, M. S., SHANNON, P., BOLON, B., IVY, G. O. & MAK, T. W. 2001. Deletion of Pten in mouse brain causes seizures, ataxia and defects in soma size resembling Lhermitte-Duclos disease. *Nat Genet,* 29**,** 396-403.

BARANYI, A., SZENTE, M. B. & WOODY, C. D. 1993. Electrophysiological characterization of different types of neurons recorded in vivo in the motor cortex of the cat. II. Membrane parameters, action potentials, current-induced voltage responses and electrotonic structures. *J Neurophysiol,* 69**,** 1865-79.

BASSI, C., HO, J., SRIKUMAR, T., DOWLING, R. J. O., GORRINI, C., MILLER, S. J., MAK, T. W., NEEL, B. G., RAUGHT, B. & STAMBOLIC, V. 2013. Nuclear PTEN Controls DNA Repair and Sensitivity to Genotoxic Stress. *Science,* 341**,** 395-399.

BEAUDET, M.-J., YANG, Q., CADAU, S., BLAIS, M., BELLENFANT, S., GROS-LOUIS, F. & BERTHOD, F. 2015. High yield extraction of pure spinal motor neurons, astrocytes and microglia from single embryo and adult mouse spinal cord. *Scientific Reports,* 5**,** 16763.

BECK, J., POULTER, M., HENSMAN, D., ROHRER, JONATHAN D., MAHONEY, C. J., ADAMSON, G., CAMPBELL, T., UPHILL, J., BORG, A., FRATTA, P., ORRELL, RICHARD W., MALASPINA, A., ROWE, J., BROWN, J., HODGES, J., SIDLE, K., POLKE, JAMES M., HOULDEN, H., SCHOTT, JONATHAN M., FOX, NICK C., ROSSOR, MARTIN N., TABRIZI, SARAH J., ISAACS, ADRIAN M., HARDY, J., WARREN, J. D., COLLINGE, J. & MEAD, S. 2013. Large C9orf72 Hexanucleotide Repeat Expansions Are Seen in Multiple Neurodegenerative Syndromes and Are More Frequent Than Expected in the UK Population. *American Journal of Human Genetics,* 92**,** 345-353.

BENATAR, M. 2007. Lost in translation: treatment trials in the SOD1 mouse and in human ALS. *Neurobiol Dis,* 26**,** 1-13.

BENSIMON , G., LACOMBLEZ , L., MEININGER , V. & GROUP, T. A. R. S. 1994. A Controlled Trial of Riluzole in Amyotrophic Lateral Sclerosis. *New England Journal of Medicine,* 330**,** 585-591.

BERRIDGE, M. V., HERST, P. M. & TAN, A. S. 2005. Tetrazolium dyes as tools in cell biology: new insights into their cellular reduction. *Biotechnol Annu Rev,* 11**,** 127-52.

BIERMANN, J., GRIESHABER, P., GOEBEL, U., MARTIN, G., THANOS, S., DI GIOVANNI, S. & LAGREZE, W. A. 2010. Valproic acid-mediated neuroprotection and regeneration in injured retinal ganglion cells. *Invest Ophthalmol Vis Sci,* 51**,** 526-34.

BILICAN, B., SERIO, A., BARMADA, S. J., NISHIMURA, A. L., SULLIVAN, G. J., CARRASCO, M., PHATNANI, H. P., PUDDIFOOT, C. A., STORY, D., FLETCHER, J., PARK, I.-H., FRIEDMAN, B. A., DALEY, G. Q., WYLLIE, D. J. A., HARDINGHAM, G. E., WILMUT, I., FINKBEINER, S., MANIATIS, T., SHAW, C. E. & CHANDRAN, S. 2012. Mutant induced pluripotent stem cell lines recapitulate aspects of TDP-43 proteinopathies and reveal cell-specific vulnerability. *Proceedings of the National Academy of Sciences,* 109**,** 5803-5808.

BILSLAND, L. G., SAHAI, E., KELLY, G., GOLDING, M., GREENSMITH, L. & SCHIAVO, G. 2010. Deficits in axonal transport precede ALS symptoms in vivo. *Proc Natl Acad Sci U S A,* 107**,** 20523-8.

BOERGERMANN, J. H., KOPF, J., YU, P. B. & KNAUS, P. 2010. Dorsomorphin and LDN-193189 inhibit BMP-mediated Smad, p38 and Akt signalling in C2C12 cells. *Int J Biochem Cell Biol,* 42**,** 1802-7.

BOEYNAEMS, S., BOGAERT, E., MICHIELS, E., GIJSELINCK, I., SIEBEN, A., JOVICIC, A., DE BAETS, G., SCHEVENEELS, W., STEYAERT, J., CUIJT, I., VERSTREPEN, K. J., CALLAERTS, P., ROUSSEAU, F., SCHYMKOWITZ, J., CRUTS, M., VAN BROECKHOVEN, C., VAN DAMME, P., GITLER, A. D., ROBBERECHT, W. & VAN DEN BOSCH, L. 2016. Drosophila screen connects nuclear transport genes to DPR pathology in c9ALS/FTD. *Sci Rep,* 6.

BOILLEE, S., YAMANAKA, K., LOBSIGER, C. S., COPELAND, N. G., JENKINS, N. A., KASSIOTIS, G., KOLLIAS, G. & CLEVELAND, D. W. 2006. Onset and progression in inherited ALS determined by motor neurons and microglia. *Science,* 312**,** 1389-92.

BOLDUC, D., RAHDAR, M., TU-SEKINE, B., SIVAKUMAREN, S. C., RABEN, D., AMZEL, L. M., DEVREOTES, P., GABELLI, S. B. & COLE, P. 2013. Phosphorylation-mediated PTEN conformational closure and deactivation revealed with protein semisynthesis. *eLife,* 2**,** e00691.

BONONI, A., BONORA, M., MARCHI, S., MISSIROLI, S., POLETTI, F., GIORGI, C., PANDOLFI, P. P. & PINTON, P. 2013. Identification of PTEN at the ER and MAMs and its regulation of Ca2+ signaling and apoptosis in a protein phosphatase-dependent manner. *Cell Death Differ,* 20**,** 1631-1643.

BORGATTI, P., MARTELLI, A. M., TABELLINI, G., BELLACOSA, A., CAPITANI, S. & NERI, L. M. 2003. Threonine 308 phosphorylated form of akt translocates to the nucleus of PC12 cells under nerve growth factor stimulation and associates with the nuclear matrix protein nucleolin. *Journal of Cellular Physiology,* 196**,** 79-88.

BOSTROM, J., COBBERS, J., WOLTER, M., TABATABAI, G., WEBER, R. G., LICHTER, P., COLLINS, V. P. & REIFENBERGER, G. 1998. Mutation of the PTEN (MMAC1) tumor suppressor gene in a subset of glioblastomas but not in meningiomas with loss of chromosome arm 10q. *Cancer Research,* 58**,** 29-33.

BRUIJN, L. I., BECHER, M. W., LEE, M. K., ANDERSON, K. L., JENKINS, N. A., COPELAND, N. G., SISODIA, S. S., ROTHSTEIN, J. D., BORCHELT, D. R., PRICE, D. L. & CLEVELAND, D. W. 1997. ALS-linked SOD1 mutant G85R mediates damage to astrocytes and promotes rapidly progressive disease with SOD1-containing inclusions. *Neuron,* 18**,** 327-38.

BRUIJN, L. I., HOUSEWEART, M. K., KATO, S., ANDERSON, K. L., ANDERSON, S. D., OHAMA, E., REAUME, A. G., SCOTT, R. W. & CLEVELAND, D. W. 1998. Aggregation and motor neuron toxicity of an ALS-linked SOD1 mutant independent from wild-type SOD1. *Science,* 281**,** 1851-4.

BUNTON-STASYSHYN, R. K. A., SACCON, R. A., FRATTA, P. & FISHER, E. M. C. 2014. SOD1 Function and Its Implications for Amyotrophic Lateral Sclerosis Pathology: New and Renascent Themes. *The Neuroscientist*.

BURGHES, A. H. & BEATTIE, C. E. 2009. Spinal muscular atrophy: why do low levels of survival motor neuron protein make motor neurons sick? *Nat Rev Neurosci,* 10**,** 597-609.
CAI, Q. Y., CHEN, X. S., ZHONG, S. C., LUO, X. & YAO, Z. X. 2009. Differential expression of PTEN in normal adult rat brain and upregulation of PTEN and p-Akt in the ischemic cerebral cortex. *Anat Rec (Hoboken),* 292**,** 498-512.
CARPENTER, D., STONE, D. M., BRUSH, J., RYAN, A., ARMANINI, M., FRANTZ, G., ROSENTHAL, A. & DE SAUVAGE, F. J. 1998. Characterization of two patched receptors for the vertebrate hedgehog protein family. *Proc Natl Acad Sci U S A,* 95**,** 13630-4.
CASHMAN, N. R., DURHAM, H. D., BLUSZTAJN, J. K., ODA, K., TABIRA, T., SHAW, I. T., DAHROUGE, S. & ANTEL, J. P. 1992. Neuroblastoma x spinal cord (NSC) hybrid cell lines resemble developing motor neurons. *Dev Dyn,* 194**,** 209-21.
CHALHOUB, N. & BAKER, S. J. 2009. PTEN and the PI3-Kinase Pathway in Cancer. *Annual Review of Pathology,* 4**,** 127-150.
CHAMBERS, S. M., FASANO, C. A., PAPAPETROU, E. P., TOMISHIMA, M., SADELAIN, M. & STUDER, L. 2009. Highly efficient neural conversion of human ES and iPS cells by dual inhibition of SMAD signaling. *Nature Biotechnology,* 27**,** 275-280.
CHANG, C. J., MULHOLLAND, D. J., VALAMEHR, B., MOSESSIAN, S., SELLERS, W. R. & WU, H. 2008a. PTEN nuclear localization is regulated by oxidative stress and mediates p53-dependent tumor suppression. *Mol Cell Biol,* 28**,** 3281-9.
CHANG, Y., KONG, Q., SHAN, X., TIAN, G., ILIEVA, H., CLEVELAND, D. W., ROTHSTEIN, J. D., BORCHELT, D. R., WONG, P. C. & LIN, C. L. 2008b. Messenger RNA oxidation occurs early in disease pathogenesis and promotes motor neuron degeneration in ALS. *Plos One,* 3**,** e2849.
CHARCOT, J.-M. & JOFFROY, A. 1869. *Deux cas d'atrophie musculaire progressive avec lésions de la substance grise et des faisceaux antérolatéraux de la moelle épinière,* Paris, Masson.
CHEN, B. & CEPKO, C. L. 2009. HDAC4 regulates neuronal survival in normal and diseased retinas. *Science,* 323**,** 256-9.
CHEN, Y., LUO, C., ZHAO, M., LI, Q., HU, R., ZHANG, J. H., LIU, Z. & FENG, H. 2015. Administration of a PTEN inhibitor BPV(pic) attenuates early brain injury via modulating AMPA receptor subunits after subarachnoid hemorrhage in rats. *Neurosci Lett,* 588**,** 131-6.
CHEN, Y. Z., BENNETT, C. L., HUYNH, H. M., BLAIR, I. P., PULS, I., IROBI, J., DIERICK, I., ABEL, A., KENNERSON, M. L., RABIN, B. A., NICHOLSON, G. A., AUER-GRUMBACH, M., WAGNER, K., DE JONGHE, P., GRIFFIN, J. W., FISCHBECK, K. H., TIMMERMAN, V., CORNBLATH, D. R. & CHANCE, P. F. 2004. DNA/RNA helicase gene mutations in a form of juvenile amyotrophic lateral sclerosis (ALS4). *Am J Hum Genet,* 74**,** 1128-35.
CHEN, Z., DEMPSEY, D. R., THOMAS, S. N., HAYWARD, D., BOLDUC, D. M. & COLE, P. A. 2016. Molecular Features of PTEN Regulation by C-Terminal Phosphorylation. *Journal of Biological Chemistry*.
CHIANG, G. G. & ABRAHAM, R. T. 2005. Phosphorylation of mammalian target of rapamycin (mTOR) at Ser-2448 is mediated by p70S6 kinase. *J Biol Chem,* 280**,** 25485-90.
CHIO, A., LOGROSCINO, G., HARDIMAN, O., SWINGLER, R., MITCHELL, D., BEGHI, E. & TRAYNOR, B. G. 2009. Prognostic factors in ALS: A critical review. *Amyotroph Lateral Scler,* 10**,** 310-23.
CHIO, A., LOGROSCINO, G., TRAYNOR, B. J., COLLINS, J., SIMEONE, J. C., GOLDSTEIN, L. A. & WHITE, L. A. 2013. Global epidemiology of amyotrophic lateral sclerosis: a systematic review of the published literature. *Neuroepidemiology,* 41**,** 118-30.
CHOW, C. Y., LANDERS, J. E., BERGREN, S. K., SAPP, P. C., GRANT, A. E., JONES, J. M., EVERETT, L., LENK, G. M., MCKENNA-YASEK, D. M., WEISMAN, L. S., FIGLEWICZ, D., BROWN, R. H. & MEISLER, M. H. 2009. Deleterious variants of FIG4, a phosphoinositide phosphatase, in patients with ALS. *Am J Hum Genet,* 84**,** 85-8.
CHRISTIE, K. J., MARTINEZ, J. A. & ZOCHODNE, D. W. 2012. Disruption of E3 ligase NEDD4 in peripheral neurons interrupts axon outgrowth: Linkage to PTEN. *Mol Cell Neurosci,* 50**,** 179-92.
CHRISTIE, K. J., WEBBER, C. A., MARTINEZ, J. A., SINGH, B. & ZOCHODNE, D. W. 2010. PTEN inhibition to facilitate intrinsic regenerative outgrowth of adult peripheral axons. *J Neurosci,* 30**,** 9306-15.
CIRULLI, E. T., LASSEIGNE, B. N., PETROVSKI, S., SAPP, P. C., DION, P. A., LEBLOND, C. S., COUTHOUIS, J., LU, Y. F., WANG, Q., KRUEGER, B. J., REN, Z., KEEBLER, J., HAN, Y., LEVY, S. E., BOONE, B. E., WIMBISH, J. R., WAITE, L. L., JONES, A. L., CARULLI, J. P., DAY-WILLIAMS, A. G., STAROPOLI, J. F., XIN, W. W., CHESI, A., RAPHAEL, A. R., MCKENNA-YASEK, D., CADY, J., VIANNEY DE JONG, J. M., KENNA, K. P., SMITH, B. N., TOPP, S., MILLER, J., GKAZI, A., AL-CHALABI, A., VAN DEN BERG, L. H., VELDINK, J., SILANI, V., TICOZZI, N., SHAW, C. E., BALOH, R. H., APPEL, S., SIMPSON, E., LAGIER-TOURENNE, C., PULST, S. M., GIBSON, S., TROJANOWSKI, J. Q., ELMAN, L., MCCLUSKEY, L., GROSSMAN, M., SHNEIDER, N. A., CHUNG, W. K., RAVITS, J. M., GLASS, J. D., SIMS, K. B., VAN

DEERLIN, V. M., MANIATIS, T., HAYES, S. D., ORDUREAU, A., SWARUP, S., LANDERS, J., BAAS, F., ALLEN, A. S., BEDLACK, R. S., HARPER, J. W., GITLER, A. D., ROULEAU, G. A., BROWN, R., HARMS, M. B., COOPER, G. M., HARRIS, T., MYERS, R. M. & GOLDSTEIN, D. B. 2015. Exome sequencing in amyotrophic lateral sclerosis identifies risk genes and pathways. *Science,* 347**,** 1436-41.

CLEVELAND, D. W. & ROTHSTEIN, J. D. 2001. From Charcot to Lou Gehrig: deciphering selective motor neuron death in ALS. *Nat Rev Neurosci,* 2**,** 806-19.

COLOMBRITA, C., ZENNARO, E., FALLINI, C., WEBER, M., SOMMACAL, A., BURATTI, E., SILANI, V. & RATTI, A. 2009. TDP-43 is recruited to stress granules in conditions of oxidative insult. *J Neurochem,* 111**,** 1051-61.

COOPER-KNOCK, J., BURY, J. J., HEATH, P. R., WYLES, M., HIGGINBOTTOM, A., GELSTHORPE, C., HIGHLEY, J. R., HAUTBERGUE, G., RATTRAY, M., KIRBY, J. & SHAW, P. J. 2015a. C9ORF72 GGGGCC Expanded Repeats Produce Splicing Dysregulation which Correlates with Disease Severity in Amyotrophic Lateral Sclerosis. *PLoS One,* 10.

COOPER-KNOCK, J., HEWITT, C., HIGHLEY, J. R., BROCKINGTON, A., MILANO, A., MAN, S., MARTINDALE, J., HARTLEY, J., WALSH, T., GELSTHORPE, C., BAXTER, L., FORSTER, G., FOX, M., BURY, J., MOK, K., MCDERMOTT, C. J., TRAYNOR, B. J., KIRBY, J., WHARTON, S. B., INCE, P. G., HARDY, J. & SHAW, P. J. 2012. Clinico-pathological features in amyotrophic lateral sclerosis with expansions in C9ORF72. *Brain,* 135**,** 751-64.

COOPER-KNOCK, J., HIGGINBOTTOM, A., CONNOR-ROBSON, N., BAYATTI, N., BURY, J. J., KIRBY, J., NINKINA, N., BUCHMAN, V. L. & SHAW, P. J. 2013. C9ORF72 transcription in a frontotemporal dementia case with two expanded alleles. *Neurology,* 81**,** 1719-21.

COOPER-KNOCK, J., HIGGINBOTTOM, A., STOPFORD, M. J., HIGHLEY, J. R., INCE, P. G., WHARTON, S. B., PICKERING-BROWN, S., KIRBY, J., HAUTBERGUE, G. M. & SHAW, P. J. 2015b. Antisense RNA foci in the motor neurons of C9ORF72-ALS patients are associated with TDP-43 proteinopathy. *Acta Neuropathologica,* 130**,** 63-75.

COOPER-KNOCK, J., KIRBY, J., HIGHLEY, R. & SHAW, P. J. 2015c. The Spectrum of C9orf72-mediated Neurodegeneration and Amyotrophic Lateral Sclerosis. *Neurotherapeutics,* 12**,** 326-39.

COOPER-KNOCK, J., WALSH, M. J., HIGGINBOTTOM, A., ROBIN HIGHLEY, J., DICKMAN, M. J., EDBAUER, D., INCE, P. G., WHARTON, S. B., WILSON, S. A., KIRBY, J., HAUTBERGUE, G. M. & SHAW, P. J. 2014. Sequestration of multiple RNA recognition motif-containing proteins by C9orf72 repeat expansions. *Brain,* 137**,** 2040-51.

DAFINCA, R., SCABER, J., ABABNEH, N., LALIC, T., WEIR, G., CHRISTIAN, H., VOWLES, J., DOUGLAS, A. G., FLETCHER-JONES, A., BROWNE, C., NAKANISHI, M., TURNER, M. R., WADE-MARTINS, R., COWLEY, S. A. & TALBOT, K. 2016. C9orf72 Hexanucleotide Expansions Are Associated with Altered Endoplasmic Reticulum Calcium Homeostasis and Stress Granule Formation in Induced Pluripotent Stem Cell-Derived Neurons from Patients with Amyotrophic Lateral Sclerosis and Frontotemporal Dementia. *STEM CELLS,* 34**,** 2063-78.

DAMIANO, M., STARKOV, A. A., PETRI, S., KIPIANI, K., KIAEI, M., MATTIAZZI, M., FLINT BEAL, M. & MANFREDI, G. 2006. Neural mitochondrial Ca2+ capacity impairment precedes the onset of motor symptoms in G93A Cu/Zn-superoxide dismutase mutant mice. *J Neurochem,* 96**,** 1349-61.

DANILOV, C. A. & STEWARD, O. 2015. Conditional genetic deletion of PTEN after a spinal cord injury enhances regenerative growth of CST axons and motor function recovery in mice. *Experimental Neurology,* 266**,** 147-160.

DATTA, S. R., BRUNET, A. & GREENBERG, M. E. 1999. Cellular survival: a play in three Akts. *Genes Dev,* 13**,** 2905-27.

DAVIDSON, Y., ROBINSON, A. C., LIU, X., WU, D., TROAKES, C., ROLLINSON, S., MASUDA-SUZUKAKE, M., SUZUKI, G., NONAKA, T., SHI, J., TIAN, J., HAMDALLA, H., EALING, J., RICHARDSON, A., JONES, M., PICKERING-BROWN, S., SNOWDEN, J. S., HASEGAWA, M. & MANN, D. M. A. 2016. Neurodegeneration in frontotemporal lobar degeneration and motor neurone disease associated with expansions in C9orf72 is linked to TDP-43 pathology and not associated with aggregated forms of dipeptide repeat proteins. *Neuropathology and Applied Neurobiology,* 42**,** 242-254.

DAYTON, R. D., WANG, D. B. & KLEIN, R. L. 2012. The advent of AAV9 expands applications for brain and spinal cord gene delivery. *Expert Opinion on Biological Therapy,* 12**,** 757-766.

DE MARCO, G., LOMARTIRE, A., CALVO, A., RISSO, A., DE LUCA, E., MOSTERT, M., MANDRIOLI, J., CAPONNETTO, C., BORGHERO, G., MANERA, U., CANOSA, A., MOGLIA, C., RESTAGNO, G., FINI, N., TARELLA, C., GIORDANA, M. T., RINAUDO, M. T. & CHIÒ, A. 2017. Monocytes of patients

with amyotrophic lateral sclerosis linked to gene mutations display altered TDP-43 subcellular distribution. *Neuropathology and Applied Neurobiology,* 43**,** 133-153.

DE VOS, K. J., CHAPMAN, A. L., TENNANT, M. E., MANSER, C., TUDOR, E. L., LAU, K. F., BROWNLEES, J., ACKERLEY, S., SHAW, P. J., MCLOUGHLIN, D. M., SHAW, C. E., LEIGH, P. N., MILLER, C. C. & GRIERSON, A. J. 2007. Familial amyotrophic lateral sclerosis-linked SOD1 mutants perturb fast axonal transport to reduce axonal mitochondria content. *Hum Mol Genet,* 16**,** 2720-8.

DEJESUS-HERNANDEZ, M., MACKENZIE, I. R., BOEVE, B. F., BOXER, A. L., BAKER, M. & RUTHERFORD, N. J. 2011. Expanded GGGGCC hexanucleotide repeat in noncoding region of C9ORF72 causes chromosome 9p-linked FTD and ALS. *Neuron,* 72.

DENG, H. X., CHEN, W., HONG, S. T., BOYCOTT, K. M., GORRIE, G. H., SIDDIQUE, N., YANG, Y., FECTO, F., SHI, Y., ZHAI, H., JIANG, H., HIRANO, M., RAMPERSAUD, E., JANSEN, G. H., DONKERVOORT, S., BIGIO, E. H., BROOKS, B. R., AJROUD, K., SUFIT, R. L., HAINES, J. L., MUGNAINI, E., PERICAK-VANCE, M. A. & SIDDIQUE, T. 2011. Mutations in UBQLN2 cause dominant X-linked juvenile and adult-onset ALS and ALS/dementia. *Nature,* 477**,** 211-5.

DENG, H. X., HENTATI, A., TAINER, J. A., IQBAL, Z., CAYABYAB, A., HUNG, W. Y., GETZOFF, E. D., HU, P., HERZFELDT, B., ROOS, R. P. & ET AL. 1993. Amyotrophic lateral sclerosis and structural defects in Cu,Zn superoxide dismutase. *Science,* 261**,** 1047-51.

DEVLIN, A.-C., BURR, K., BOROOAH, S., FOSTER, J. D., CLEARY, E. M., GETI, I., VALLIER, L., SHAW, C. E., CHANDRAN, S. & MILES, G. B. 2015. Human iPSC-derived motoneurons harbouring TARDBP or C9ORF72 ALS mutations are dysfunctional despite maintaining viability. *Nat Commun,* 6.

DEWIL, M., LAMBRECHTS, D., SCIOT, R., SHAW, P. J., INCE, P. G., ROBBERECHT, W. & VAN DEN BOSCH, L. 2007. Vascular endothelial growth factor counteracts the loss of phospho-Akt preceding motor neurone degeneration in amyotrophic lateral sclerosis. *Neuropathol Appl Neurobiol,* 33**,** 499-509.

DI GIORGIO, F. P., CARRASCO, M. A., SIAO, M. C., MANIATIS, T. & EGGAN, K. 2007. Non-cell autonomous effect of glia on motor neurons in an embryonic stem cell-based ALS model. *Nat Neurosci,* 10**,** 608-14.

DIAPER, D. C., ADACHI, Y., SUTCLIFFE, B., HUMPHREY, D. M., ELLIOTT, C. J., STEPTO, A., LUDLOW, Z. N., VANDEN BROECK, L., CALLAERTS, P., DERMAUT, B., AL-CHALABI, A., SHAW, C. E., ROBINSON, I. M. & HIRTH, F. 2013. Loss and gain of Drosophila TDP-43 impair synaptic efficacy and motor control leading to age-related neurodegeneration by loss-of-function phenotypes. *Hum Mol Genet,* 22**,** 1539-57.

DIAZ-RUIZ, O., ZAPATA, A., SHAN, L., ZHANG, Y., TOMAC, A. C., MALIK, N., DE LA CRUZ, F. & BÄCKMAN, C. M. 2009. Selective Deletion of PTEN in Dopamine Neurons Leads to Trophic Effects and Adaptation of Striatal Medium Spiny Projecting Neurons. *Plos One,* 4**,** e7027.

DIMOS, J. T., RODOLFA, K. T., NIAKAN, K. K., WEISENTHAL, L. M., MITSUMOTO, H., CHUNG, W., CROFT, G. F., SAPHIER, G., LEIBEL, R., GOLAND, R., WICHTERLE, H., HENDERSON, C. E. & EGGAN, K. 2008. Induced Pluripotent Stem Cells Generated from Patients with ALS Can Be Differentiated into Motor Neurons. *Science,* 321**,** 1218-1221.

DOMANSKYI, A., GEIßLER, C., VINNIKOV, I. A., ALTER, H., SCHOBER, A., VOGT, M. A., GASS, P., PARLATO, R. & SCHÜTZ, G. 2011. Pten ablation in adult dopaminergic neurons is neuroprotective in Parkinson's disease models. *The FASEB Journal,* 25**,** 2898-2910.

DONNELLY, CHRISTOPHER J., ZHANG, P.-W., PHAM, JACQUELINE T., HAEUSLER, AARON R., MISTRY, NIPUN A., VIDENSKY, S., DALEY, ELIZABETH L., POTH, ERIN M., HOOVER, B., FINES, DANIEL M., MARAGAKIS, N., TIENARI, PENTTI J., PETRUCELLI, L., TRAYNOR, BRYAN J., WANG, J., RIGO, F., BENNETT, C. F., BLACKSHAW, S., SATTLER, R. & ROTHSTEIN, JEFFREY D. 2013a. RNA Toxicity from the ALS/FTD C9ORF72 Expansion Is Mitigated by Antisense Intervention. *Neuron,* 80**,** 415-428.

DONNELLY, C. J., ZHANG, P.-W., PHAM, J. T., HEUSLER, A. R., MISTRY, N. A. & VIDENSKY, S. 2013b. RNA Toxicity from the ALS/FTD C9ORF72 Expansion Is Mitigated by Antisense Intervention. *Neuron,* 80.

DU, Z.-W., CHEN, H., LIU, H., LU, J., QIAN, K., HUANG, C.-L., ZHONG, X., FAN, F. & ZHANG, S.-C. 2015. Generation and expansion of highly pure motor neuron progenitors from human pluripotent stem cells. *Nat Commun,* 6.

DUAN, S., YUAN, G., LIU, X., REN, R., LI, J., ZHANG, W., WU, J., XU, X., FU, L., LI, Y., YANG, J., ZHANG, W., BAI, R., YI, F., SUZUKI, K., GAO, H., ESTEBAN, C. R., ZHANG, C., BELMONTE, J. C. I., CHEN, Z., WANG, X., JIANG, T., QU, J., TANG, F. & LIU, G.-H. 2015. PTEN deficiency reprogrammes human neural stem cells towards a glioblastoma stem cell-like phenotype. *Nature Communications,* 6**,** 10068.

DUERR, E. M., ROLLBROCKER, B., HAYASHI, Y., PETERS, N., MEYER-PUTTLITZ, B., LOUIS, D. N., SCHRAMM, J., WIESTLER, O. D., PARSONS, R., ENG, C. & VON DEIMLING, A. 1998. PTEN mutations in gliomas and glioneuronal tumors. *Oncogene,* 16**,** 2259-64.

DUFFY, J. R., PEACH, R. K. & STRAND, E. A. 2007. Progressive apraxia of speech as a sign of motor neuron disease. *Am J Speech Lang Pathol,* 16**,** 198-208.

DURHAM, H. D., DAHROUGE, S. & CASHMAN, N. R. 1993. Evaluation of the spinal cord neuron X neuroblastoma hybrid cell line NSC-34 as a model for neurotoxicity testing. *Neurotoxicology,* 14**,** 387-95.

EBERT, A. D., YU, J., ROSE, F. F., JR., MATTIS, V. B., LORSON, C. L., THOMSON, J. A. & SVENDSEN, C. N. 2009. Induced pluripotent stem cells from a spinal muscular atrophy patient. *Nature,* 457**,** 277-80.

EDDY, J. & MAIZELS, N. 2008. Conserved elements with potential to form polymorphic G-quadruplex structures in the first intron of human genes. *Nucleic Acids Res,* 36**,** 1321-33.

ELDEN, A. C., KIM, H.-J., HART, M. P., CHEN-PLOTKIN, A. S., JOHNSON, B. S., FANG, X., ARMAKOLA, M., GESER, F., GREENE, R., LU, M. M., PADMANABHAN, A., CLAY-FALCONE, D., MCCLUSKEY, L., ELMAN, L., JUHR, D., GRUBER, P. J., RUEB, U., AUBURGER, G., TROJANOWSKI, J. Q., LEE, V. M. Y., VAN DEERLIN, V. M., BONINI, N. M. & GITLER, A. D. 2010. Ataxin-2 intermediate-length polyglutamine expansions are associated with increased risk for ALS. *Nature,* 466**,** 1069-U77.

ERICSON, J., MORTON, S., KAWAKAMI, A., ROELINK, H. & JESSELL, T. M. 1996. Two critical periods of Sonic Hedgehog signaling required for the specification of motor neuron identity. *Cell,* 87**,** 661-73.

FARG, M. A., SUNDARAMOORTHY, V., SULTANA, J. M., YANG, S., ATKINSON, R. A., LEVINA, V., HALLORAN, M. A., GLEESON, P. A., BLAIR, I. P., SOO, K. Y., KING, A. E. & ATKIN, J. D. 2014. C9ORF72, implicated in amytrophic lateral sclerosis and frontotemporal dementia, regulates endosomal trafficking. *Hum Mol Genet,* 23**,** 3579-95.

FECTO, F., YAN, J., VEMULA, S. P., LIU, E., YANG, Y., CHEN, W., ZHENG, J. G., SHI, Y., SIDDIQUE, N., ARRAT, H., DONKERVOORT, S., AJROUD-DRISS, S., SUFIT, R. L., HELLER, S. L., DENG, H. X. & SIDDIQUE, T. 2011. SQSTM1 mutations in familial and sporadic amyotrophic lateral sclerosis. *Arch Neurol,* 68**,** 1440-6.

FERGUSON, R., SERAFEIMIDOU-POULIOU, E. & SUBRAMANIAN, V. 2016. Dynamic expression of the mouse orthologue of the human amyotropic lateral sclerosis associated gene C9orf72 during central nervous system development and neuronal differentiation. *Journal of Anatomy,* 229**,** 871-891.

FERGUSON, T. A. & ELMAN, L. B. 2007. Clinical presentation and diagnosis of amyotrophic lateral sclerosis. *NeuroRehabilitation,* 22**,** 409-16.

FERRAIUOLO, L., HIGGINBOTTOM, A., HEATH, P. R., BARBER, S., GREENALD, D., KIRBY, J. & SHAW, P. J. 2011. Dysregulation of astrocyte-motoneuron cross-talk in mutant superoxide dismutase 1-related amyotrophic lateral sclerosis. *Brain,* 134**,** 2627-41.

FERRAIUOLO, L., MEYER, K., SHERWOOD, T. W., VICK, J., LIKHITE, S., FRAKES, A., MIRANDA, C. J., BRAUN, L., HEATH, P. R., PINEDA, R., BEATTIE, C. E., SHAW, P. J., ASKWITH, C. C., MCTIGUE, D. & KASPAR, B. K. 2016. Oligodendrocytes contribute to motor neuron death in ALS via SOD1-dependent mechanism. *Proc Natl Acad Sci U S A,* 113**,** E6496-E6505.

FERRARI, R., KAPOGIANNIS, D., HUEY, E. D. & MOMENI, P. 2011. FTD and ALS: a tale of two diseases. *Current Alzheimer research,* 8**,** 273-294.

FINNIN, M. S., DONIGIAN, J. R., COHEN, A., RICHON, V. M., RIFKIND, R. A., MARKS, P. A., BRESLOW, R. & PAVLETICH, N. P. 1999. Structures of a histone deacetylase homologue bound to the TSA and SAHA inhibitors. *Nature,* 401**,** 188-93.

FISCHER, L. R., CULVER, D. G., TENNANT, P., DAVIS, A. A., WANG, M., CASTELLANO-SANCHEZ, A., KHAN, J., POLAK, M. A. & GLASS, J. D. 2004. Amyotrophic lateral sclerosis is a distal axonopathy: evidence in mice and man. *Experimental Neurology,* 185**,** 232-240.

FLORES, B. N., DULCHAVSKY, M. E., KRANS, A., SAWAYA, M. R., PAULSON, H. L., TODD, P. K., BARMADA, S. J. & IVANOVA, M. I. 2016. Distinct C9orf72-Associated Dipeptide Repeat Structures Correlate with Neuronal Toxicity. *PLoS One,* 11**,** e0165084.

FOUST, K. D., NURRE, E., MONTGOMERY, C. L., HERNANDEZ, A., CHAN, C. M. & KASPAR, B. K. 2009. Intravascular AAV9 preferentially targets neonatal-neurons and adult-astrocytes in CNS. *Nature biotechnology,* 27**,** 59-65.

FRAKES, A. E., BRAUN, L., FERRAIUOLO, L., GUTTRIDGE, D. C. & KASPAR, B. K. 2017. Additive amelioration of ALS by co-targeting independent pathogenic mechanisms. *Ann Clin Transl Neurol,* 4**,** 76-86.

FRAME, S. & COHEN, P. 2001. GSK3 takes centre stage more than 20 years after its discovery. *Biochem J,* 359**,** 1-16.

FRATTA, P., MIZIELINSKA, S., NICOLL, A. J., ZLOH, M., FISHER, E. M., PARKINSON, G. & ISAACS, A. M. 2012. C9orf72 hexanucleotide repeat associated with amyotrophic lateral sclerosis and frontotemporal dementia forms RNA G-quadruplexes. *Sci Rep,* 2**,** 21.

FREEMAN, D. J., LI, A. G., WEI, G., LI, H. H., KERTESZ, N., LESCHE, R., WHALE, A. D., MARTINEZ-DIAZ, H., ROZENGURT, N., CARDIFF, R. D., LIU, X. & WU, H. 2003. PTEN tumor suppressor regulates p53 protein levels and activity through phosphatase-dependent and -independent mechanisms. *Cancer Cell,* 3**,** 117-30.

FREIBAUM, B. D., LU, Y., LOPEZ-GONZALEZ, R., KIM, N. C., ALMEIDA, S., LEE, K. H., BADDERS, N., VALENTINE, M., MILLER, B. L., WONG, P. C., PETRUCELLI, L., KIM, H. J., GAO, F. B. & TAYLOR, J. P. 2015. GGGGCC repeat expansion in C9orf72 compromises nucleocytoplasmic transport. *Nature,* 525**,** 129-33.

FREISCHMIDT, A., WIELAND, T., RICHTER, B., RUF, W., SCHAEFFER, V., MULLER, K., MARROQUIN, N., NORDIN, F., HUBERS, A., WEYDT, P., PINTO, S., PRESS, R., MILLECAMPS, S., MOLKO, N., BERNARD, E., DESNUELLE, C., SORIANI, M. H., DORST, J., GRAF, E., NORDSTROM, U., FEILER, M. S., PUTZ, S., BOECKERS, T. M., MEYER, T., WINKLER, A. S., WINKELMAN, J., DE CARVALHO, M., THAL, D. R., OTTO, M., BRANNSTROM, T., VOLK, A. E., KURSULA, P., DANZER, K. M., LICHTNER, P., DIKIC, I., MEITINGER, T., LUDOLPH, A. C., STROM, T. M., ANDERSEN, P. M. & WEISHAUPT, J. H. 2015. Haploinsufficiency of TBK1 causes familial ALS and fronto-temporal dementia. *Nat Neurosci,* 18**,** 631-6.

FRITZ, E., IZAURIETA, P., WEISS, A., MIR, F. R., ROJAS, P., GONZALEZ, D., ROJAS, F., BROWN, R. H., JR., MADRID, R. & VAN ZUNDERT, B. 2013. Mutant SOD1-expressing astrocytes release toxic factors that trigger motoneuron death by inducing hyperexcitability. *J Neurophysiol,* 109**,** 2803-14.

FURNARI, F. B., LIN, H., HUANG, H. S. & CAVENEE, W. K. 1997. Growth suppression of glioma cells by PTEN requires a functional phosphatase catalytic domain. *Proc Natl Acad Sci U S A,* 94**,** 12479-84.

GARY, D. S. & MATTSON, M. P. 2002. PTEN Regulates Akt Kinase Activity in Hippocampal Neurons and Increases Their Sensitivity to Glutamate and Apoptosis. *Neuromolecular Medicine,* 2**,** 261-270.

GENDRON, T. F., BIENIEK, K. F., ZHANG, Y. J., JANSEN-WEST, K., ASH, P. E., CAULFIELD, T., DAUGHRITY, L., DUNMORE, J. H., CASTANEDES-CASEY, M., CHEW, J., COSIO, D. M., VAN BLITTERSWIJK, M., LEE, W. C., RADEMAKERS, R., BOYLAN, K. B., DICKSON, D. W. & PETRUCELLI, L. 2013. Antisense transcripts of the expanded C9ORF72 hexanucleotide repeat form nuclear RNA foci and undergo repeat-associated non-ATG translation in c9FTD/ALS. *Acta Neuropathologica,* 126**,** 829-44.

GIACINTI, L., GIACINTI, C., GABELLINI, C., RIZZUTO, E., LOPEZ, M. & GIORDANO, A. 2012. Scriptaid effects on breast cancer cell lines. *J Cell Physiol,* 227**,** 3426-33.

GIJSELINCK, I., VAN LANGENHOVE, T., VAN DER ZEE, J., SLEEGERS, K., PHILTJENS, S., KLEINBERGER, G., JANSSENS, J., BETTENS, K., VAN CAUWENBERGHE, C., PERESON, S., ENGELBORGHS, S., SIEBEN, A., DE JONGHE, P., VANDENBERGHE, R., SANTENS, P., DE BLEECKER, J., MAES, G., BÄUMER, V., DILLEN, L., JORIS, G., CUIJT, I., CORSMIT, E., ELINCK, E., VAN DONGEN, J., VERMEULEN, S., VAN DEN BROECK, M., VAERENBERG, C., MATTHEIJSSENS, M., PEETERS, K., ROBBERECHT, W., CRAS, P., MARTIN, J.-J., DE DEYN, P. P., CRUTS, M. & VAN BROECKHOVEN, C. 2012. A C9orf72 promoter repeat expansion in a Flanders-Belgian cohort with disorders of the frontotemporal lobar degeneration-amyotrophic lateral sclerosis spectrum: a gene identification study. *The Lancet Neurology,* 11**,** 54-65.

GLASL, L., KLOOS, K., GIESERT, F., ROETHIG, A., DI BENEDETTO, B., KUHN, R., ZHANG, J., HAFEN, U., ZERLE, J., HOFMANN, A., DE ANGELIS, M. H., WINKLHOFER, K. F., HOLTER, S. M., VOGT WEISENHORN, D. M. & WURST, W. 2012. Pink1-deficiency in mice impairs gait, olfaction and serotonergic innervation of the olfactory bulb. *Exp Neurol,* 235**,** 214-27.

GOGLIOTTI, R. G., QUINLAN, K. A., BARLOW, C. B., HEIER, C. R., HECKMAN, C. J. & DIDONATO, C. J. 2012. Motor Neuron Rescue in Spinal Muscular Atrophy Mice Demonstrates That Sensory-Motor Defects Are a Consequence, Not a Cause, of Motor Neuron Dysfunction. *The Journal of Neuroscience,* 32**,** 3818-3829.

GOH, C.-P., PUTZ, U., HOWITT, J., LOW, L.-H., GUNNERSEN, J., BYE, N., MORGANTI-KOSSMANN, C. & TAN, S.-S. 2014. Nuclear trafficking of Pten after brain injury leads to neuron survival not death. *Experimental Neurology,* 252**,** 37-46.

GONG, Y. H., PARSADANIAN, A. S., ANDREEVA, A., SNIDER, W. D. & ELLIOTT, J. L. 2000. Restricted expression of G86R Cu/Zn superoxide dismutase in astrocytes results in astrocytosis but does not cause motoneuron degeneration. *J Neurosci,* 20**,** 660-5.

GORDON, P. H., CHENG, B., KATZ, I. B., PINTO, M., HAYS, A. P., MITSUMOTO, H. & ROWLAND, L. P. 2006. The natural history of primary lateral sclerosis. *Neurology,* 66**,** 647-53.

GRAFFMO, K. S., FORSBERG, K., BERGH, J., BIRVE, A., ZETTERSTROM, P., ANDERSEN, P. M., MARKLUND, S. L. & BRANNSTROM, T. 2013. Expression of wild-type human superoxide dismutase-1 in mice causes amyotrophic lateral sclerosis. *Hum Mol Genet,* 22**,** 51-60.

GREENWAY, M. J., ANDERSEN, P. M., RUSS, C., ENNIS, S., CASHMAN, S., DONAGHY, C., PATTERSON, V., SWINGLER, R., KIERAN, D., PREHN, J., MORRISON, K. E., GREEN, A., ACHARYA, K. R., BROWN, R. H., JR. & HARDIMAN, O. 2006. ANG mutations segregate with familial and 'sporadic' amyotrophic lateral sclerosis. *Nat Genet,* 38**,** 411-3.

GRIFFIN, R., MOLONEY, A., KELLIHER, M., JOHNSTON, J., RAVID, R., DOCKERY, P., O'CONNOR, R. & O'NEILL, C. 2005. Activation of Akt/PKB, increased phosphorylation of Akt substrates and loss and altered distribution of Akt and PTEN are features of Alzheimer's disease pathology. *J Neurochem,* 93**,** 105 - 117.

GROSSKREUTZ, J., VAN DEN BOSCH, L. & KELLER, B. U. 2010. Calcium dysregulation in amyotrophic lateral sclerosis. *Cell Calcium,* 47**,** 165-74.

GROSZER, M., ERICKSON, R., SCRIPTURE-ADAMS, D. D., LESCHE, R., TRUMPP, A., ZACK, J. A., KORNBLUM, H. I., LIU, X. & WU, H. 2001. Negative regulation of neural stem/progenitor cell proliferation by the Pten tumor suppressor gene in vivo. *Science,* 294**,** 2186-9.

GURNEY, M. E., PU, H., CHIU, A. Y., DAL CANTO, M. C., POLCHOW, C. Y., ALEXANDER, D. D., CALIENDO, J., HENTATI, A., KWON, Y. W., DENG, H. X. & ET AL. 1994. Motor neuron degeneration in mice that express a human Cu,Zn superoxide dismutase mutation. *Science,* 264**,** 1772-5.

HAEUSLER, A. R., DONNELLY, C. J., PERIZ, G., SIMKO, E. A. J., SHAW, P. G., KIM, M.-S., MARAGAKIS, N. J., TRONCOSO, J. C., PANDEY, A., SATTLER, R., ROTHSTEIN, J. D. & WANG, J. 2014. C9orf72 nucleotide repeat structures initiate molecular cascades of disease. *Nature,* 507**,** 195-200.

HAHNEN, E., HAUKE, J., TRANKLE, C., EYUPOGLU, I. Y., WIRTH, B. & BLUMCKE, I. 2008. Histone deacetylase inhibitors: possible implications for neurodegenerative disorders. *Expert Opin Investig Drugs,* 17**,** 169-84.

HAIDET-PHILLIPS, A. M., HESTER, M. E., MIRANDA, C. J., MEYER, K., BRAUN, L., FRAKES, A., SONG, S., LIKHITE, S., MURTHA, M. J., FOUST, K. D., RAO, M., EAGLE, A., KAMMESHEIDT, A., CHRISTENSEN, A., MENDELL, J. R., BURGHES, A. H. & KASPAR, B. K. 2011. Astrocytes from familial and sporadic ALS patients are toxic to motor neurons. *Nat Biotechnol,* 29**,** 824-8.

HAND, C. K., KHORIS, J., SALACHAS, F., GROS-LOUIS, F., LOPES, A. A. S., MAYEUX-PORTAS, V., BREWER, C. G., BROWN, R. H., MEININGER, V., CAMU, W. & ROULEAU, G. A. 2002. A novel locus for familial amyotrophic lateral sclerosis, on chromosome 18q (vol 70, pg 251, 2001). *American Journal of Human Genetics,* 71**,** 1007-1007.

HAQUE, M. E., THOMAS, K. J., D'SOUZA, C., CALLAGHAN, S., KITADA, T., SLACK, R. S., FRASER, P., COOKSON, M. R., TANDON, A. & PARK, D. S. 2008. Cytoplasmic Pink1 activity protects neurons from dopaminergic neurotoxin MPTP. *Proceedings of the National Academy of Sciences,* 105**,** 1716-1721.

HARMS, M. B., CADY, J., ZAIDMAN, C., COOPER, P., BALI, T., ALLRED, P., CRUCHAGA, C., BAUGHN, M., PESTRONK, A., GOATE, A., RAVITS, J. & BALOH, R. H. 2013. Lack of C9ORF72 coding mutations supports a gain of function for repeat expansions in ALS. *Neurobiology of Aging,* 34**,** 2234.e13-2234.e19.

HARRIS, H. & RUBINSZTEIN, D. C. 2012. Control of autophagy as a therapy for neurodegenerative disease. *Nat Rev Neurol,* 8**,** 108-117.

HARWOOD, C. A., MCDERMOTT, C. J. & SHAW, P. J. 2012. Clinical aspects of motor neurone disease. *Medicine,* 40**,** 540-545.

HAYNES, B. F., SCEARCE, R. M., LOBACH, D. F. & HENSLEY, L. L. 1984. Phenotypic characterization and ontogeny of mesodermal-derived and endocrine epithelial components of the human thymic microenvironment. *J Exp Med,* 159**,** 1149-68.

HOPKINS, B. D., FINE, B., STEINBACH, N., DENDY, M., RAPP, Z., SHAW, J., PAPPAS, K., YU, J. S., HODAKOSKI, C., MENSE, S., KLEIN, J., PEGNO, S., SULIS, M.-L., GOLDSTEIN, H., AMENDOLARA, B., LEI, L., MAURER, M., BRUCE, J., CANOLL, P., HIBSHOOSH, H. & PARSONS, R. 2013. A Secreted PTEN Phosphatase That Enters Cells to Alter Signaling and Survival. *Science,* 341**,** 399-402.

HOWITT, J., LACKOVIC, J., LOW, L. H., NAGUIB, A., MACINTYRE, A., GOH, C. P., CALLAWAY, J. K., HAMMOND, V., THOMAS, T., DIXON, M., PUTZ, U., SILKE, J., BARTLETT, P., YANG, B., KUMAR, S.,

TROTMAN, L. C. & TAN, S. S. 2012. Ndfip1 regulates nuclear Pten import in vivo to promote neuronal survival following cerebral ischemia. *J Cell Biol,* 196**,** 29-36.

HSIA, H. E., KUMAR, R., LUCA, R., TAKEDA, M., COURCHET, J., NAKASHIMA, J., WU, S., GOEBBELS, S., AN, W., EICKHOLT, B. J., POLLEUX, F., ROTIN, D., WU, H., ROSSNER, M. J., BAGNI, C., RHEE, J. S., BROSE, N. & KAWABE, H. 2014. Ubiquitin E3 ligase Nedd4-1 acts as a downstream target of PI3K/PTEN-mTORC1 signaling to promote neurite growth. *Proc Natl Acad Sci U S A,* 111**,** 13205-10.

HUANG, Z., HU, Z., XIE, P. & LIU, Q. 2017. Tyrosine-mutated AAV2-mediated shRNA silencing of PTEN promotes axon regeneration of adult optic nerve. *PLoS One,* 12.

HUPPERT, J. L., BUGAUT, A., KUMARI, S. & BALASUBRAMANIAN, S. 2008. G-quadruplexes: the beginning and end of UTRs. *Nucleic Acids Research,* 36**,** 6260-6268.

HUTTON, M., LENDON, C. L., RIZZU, P., BAKER, M., FROELICH, S., HOULDEN, H., PICKERING-BROWN, S., CHAKRAVERTY, S., ISAACS, A., GROVER, A., HACKETT, J., ADAMSON, J., LINCOLN, S., DICKSON, D., DAVIES, P., PETERSEN, R. C., STEVENS, M., DE GRAAFF, E., WAUTERS, E., VAN BAREN, J., HILLEBRAND, M., JOOSSE, M., KWON, J. M., NOWOTNY, P., CHE, L. K., NORTON, J., MORRIS, J. C., REED, L. A., TROJANOWSKI, J., BASUN, H., LANNFELT, L., NEYSTAT, M., FAHN, S., DARK, F., TANNENBERG, T., DODD, P. R., HAYWARD, N., KWOK, J. B., SCHOFIELD, P. R., ANDREADIS, A., SNOWDEN, J., CRAUFURD, D., NEARY, D., OWEN, F., OOSTRA, B. A., HARDY, J., GOATE, A., VAN SWIETEN, J., MANN, D., LYNCH, T. & HEUTINK, P. 1998. Association of missense and 5'-splice-site mutations in tau with the inherited dementia FTDP-17. *Nature,* 393**,** 702-5.

INCE, P. G., LOWE, J. & SHAW, P. J. 1998. Amyotrophic lateral sclerosis: current issues in classification, pathogenesis and molecular pathology. *Neuropathol Appl Neurobiol,* 24**,** 104-17.

INGRE, C., ROOS, P. M., PIEHL, F., KAMEL, F. & FANG, F. 2015. Risk factors for amyotrophic lateral sclerosis. *Clinical Epidemiology,* 7**,** 181-193.

ISHIGURO, A., KIMURA, N., WATANABE, Y., WATANABE, S. & ISHIHAMA, A. 2016. TDP-43 binds and transports G-quadruplex-containing mRNAs into neurites for local translation. *Genes Cells,* 21**,** 466-81.

ISMAIL, A., NING, K., AL-HAYANI, A., SHARRACK, B. & AZZOUZ, M. 2012. PTEN: A molecular target for neurodegenerative disorders. *Translational Neuroscience,* 3**,** 132-142.

ITO, Y., SAKAGAMI, H. & KONDO, H. 1996. Enhanced gene expression for phosphatidylinositol 3-kinase in the hypoglossal motoneurons following axonal crush. *Brain Res Mol Brain Res,* 37**,** 329-32.

JESSELL, T. M. & SANES, J. R. 2000. Development. The decade of the developing brain. *Curr Opin Neurobiol,* 10**,** 599-611.

JIANG, J., ZHU, Q., GENDRON, T. F., SABERI, S., MCALONIS-DOWNES, M., SEELMAN, A., STAUFFER, J. E., JAFAR-NEJAD, P., DRENNER, K., SCHULTE, D., CHUN, S., SUN, S., LING, S. C., MYERS, B., ENGELHARDT, J., KATZ, M., BAUGHN, M., PLATOSHYN, O., MARSALA, M., WATT, A., HEYSER, C. J., ARD, M. C., DE MUYNCK, L., DAUGHRITY, L. M., SWING, D. A., TESSAROLLO, L., JUNG, C. J., DELPOUX, A., UTZSCHNEIDER, D. T., HEDRICK, S. M., DE JONG, P. J., EDBAUER, D., VAN DAMME, P., PETRUCELLI, L., SHAW, C. E., BENNETT, C. F., DA CRUZ, S., RAVITS, J., RIGO, F., CLEVELAND, D. W. & LAGIER-TOURENNE, C. 2016. Gain of Toxicity from ALS/FTD-Linked Repeat Expansions in C9ORF72 Is Alleviated by Antisense Oligonucleotides Targeting GGGGCC-Containing RNAs. *Neuron,* 90**,** 535-50.

JIN, D., LIU, Y., SUN, F., WANG, X., LIU, X. & HE, Z. 2015. Restoration of skilled locomotion by sprouting corticospinal axons induced by co-deletion of PTEN and SOCS3. *Nature Communications,* 6**,** 8074.

JOHNSON, J. O., MANDRIOLI, J., BENATAR, M., ABRAMZON, Y., VAN DEERLIN, V. M., TROJANOWSKI, J. Q., GIBBS, J. R., BRUNETTI, M., GRONKA, S., WUU, J., DING, J. H., MCCLUSKEY, L., MARTINEZ-LAGE, M., FALCONE, D., HERNANDEZ, D. G., AREPALLI, S., CHONG, S., SCHYMICK, J. C., ROTHSTEIN, J., LANDI, F., WANG, Y. D., CALVO, A., MORA, G., SABATELLI, M., MONSURRO, M. R., BATTISTINI, S., SALVI, F., SPATARO, R., SOLA, P., BORGHERO, G., GALASSI, G., SCHOLZ, S. W., TAYLOR, J. P., RESTAGNO, G., CHIO, A., TRAYNOR, B. J. & CONSORTIUM, I. 2011. Exome Sequencing Reveals VCP Mutations as a Cause of Familial ALS (vol 68, pg 857, 2010). *Neuron,* 69**,** 397-397.

JOHNSON, J. O., PIORO, E. P., BOEHRINGER, A., CHIA, R., FEIT, H., RENTON, A. E., PLINER, H. A., ABRAMZON, Y., MARANGI, G., WINBORN, B. J., GIBBS, J. R., NALLS, M. A., MORGAN, S., SHOAI, M., HARDY, J., PITTMAN, A., ORRELL, R. W., MALASPINA, A., SIDLE, K. C., FRATTA, P., HARMS, M. B., BALOH, R. H., PESTRONK, A., WEIHL, C. C., ROGAEVA, E., ZINMAN, L., DRORY, V. E., BORGHERO, G., MORA, G., CALVO, A., ROTHSTEIN, J. D., DREPPER, C., SENDTNER, M., SINGLETON, A. B., TAYLOR, J. P., COOKSON, M. R., RESTAGNO, G., SABATELLI, M., BOWSER, R.,

CHIO, A. & TRAYNOR, B. J. 2014. Mutations in the Matrin 3 gene cause familial amyotrophic lateral sclerosis. *Nat Neurosci,* 17**,** 664-6.

JOHNSON, M. A., WEICK, J. P., PEARCE, R. A. & ZHANG, S. C. 2007. Functional neural development from human embryonic stem cells: accelerated synaptic activity via astrocyte coculture. *J Neurosci,* 27**,** 3069-77.

JONES, K. R., FARINAS, I., BACKUS, C. & REICHARDT, L. F. 1994. Targeted disruption of the BDNF gene perturbs brain and sensory neuron development but not motor neuron development. *Cell,* 76**,** 989-99.

JONSSON, P. A., ERNHILL, K., ANDERSEN, P. M., BERGEMALM, D., BRANNSTROM, T., GREDAL, O., NILSSON, P. & MARKLUND, S. L. 2004. Minute quantities of misfolded mutant superoxide dismutase-1 cause amyotrophic lateral sclerosis. *Brain,* 127**,** 73-88.

JOVICIC, A., MERTENS, J., BOEYNAEMS, S., BOGAERT, E., CHAI, N., YAMADA, S. B., PAUL, J. W., 3RD, SUN, S., HERDY, J. R., BIERI, G., KRAMER, N. J., GAGE, F. H., VAN DEN BOSCH, L., ROBBERECHT, W. & GITLER, A. D. 2015. Modifiers of C9orf72 dipeptide repeat toxicity connect nucleocytoplasmic transport defects to FTD/ALS. *Nat Neurosci,* 18**,** 1226-9.

KANAI, K., KUWABARA, S., MISAWA, S., TAMURA, N., OGAWARA, K., NAKATA, M., SAWAI, S., HATTORI, T. & BOSTOCK, H. 2006. Altered axonal excitability properties in amyotrophic lateral sclerosis: impaired potassium channel function related to disease stage. *Brain,* 129**,** 953-962.

KARUMBAYARAM, S., NOVITCH, B. G., PATTERSON, M., UMBACH, J. A., RICHTER, L., LINDGREN, A., CONWAY, A., CLARK, A., GOLDMAN, S. A., PLATH, K., WIEDAU-PAZOS, M., KORNBLUM, H. I. & LOWRY, W. E. 2009. Directed differentiation of human induced pluripotent stem cells generates active motor neurons. *Stem cells (Dayton, Ohio),* 27**,** 806-811.

KENNA, K. P., VAN DOORMAAL, P. T. C., DEKKER, A. M., TICOZZI, N., KENNA, B. J., DIEKSTRA, F. P., VAN RHEENEN, W., VAN EIJK, K. R., JONES, A. R., KEAGLE, P., SHATUNOV, A., SPROVIERO, W., SMITH, B. N., VAN ES, M. A., TOPP, S. D., KENNA, A., MILLER, J. W., FALLINI, C., TILOCA, C., MCLAUGHLIN, R. L., VANCE, C., TROAKES, C., COLOMBRITA, C., MORA, G., CALVO, A., VERDE, F., AL-SARRAJ, S., KING, A., CALINI, D., DE BELLEROCHE, J., BAAS, F., VAN DER KOOI, A. J., DE VISSER, M., TEN ASBROEK, A. L. M. A., SAPP, P. C., MCKENNA-YASEK, D., POLAK, M., ASRESS, S., MUNOZ-BLANCO, J. L., STROM, T. M., MEITINGER, T., MORRISON, K. E., CONSORTIUM, S., LAURIA, G., WILLIAMS, K. L., LEIGH, P. N., NICHOLSON, G. A., BLAIR, I. P., LEBLOND, C. S., DION, P. A., ROULEAU, G. A., PALL, H., SHAW, P. J., TURNER, M. R., TALBOT, K., TARONI, F., BOYLAN, K. B., VAN BLITTERSWIJK, M., RADEMAKERS, R., ESTEBAN-PEREZ, J., GARCIA-REDONDO, A., VAN DAMME, P., ROBBERECHT, W., CHIO, A., GELLERA, C., DREPPER, C., SENDTNER, M., RATTI, A., GLASS, J. D., MORA, J. S., BASAK, N. A., HARDIMAN, O., LUDOLPH, A. C., ANDERSEN, P. M., WEISHAUPT, J. H., BROWN JR, R. H., AL-CHALABI, A., SILANI, V., SHAW, C. E., VAN DEN BERG, L. H., VELDINK, J. H. & LANDERS, J. E. 2016. NEK1 variants confer susceptibility to amyotrophic lateral sclerosis. *Nat Genet,* 48**,** 1037-1042.

KERNOCHAN, L. E., RUSSO, M. L., WOODLING, N. S., HUYNH, T. N., AVILA, A. M., FISCHBECK, K. H. & SUMNER, C. J. 2005. The role of histone acetylation in SMN gene expression. *Human Molecular Genetics,* 14**,** 1171-1182.

KIERNAN, M. C., VUCIC, S., CHEAH, B. C., TURNER, M. R., EISEN, A., HARDIMAN, O., BURRELL, J. R. & ZOING, M. C. 2011. Amyotrophic lateral sclerosis. *The Lancet,* 377**,** 942-955.

KIM, D. Y., KIM, W., LEE, K. H., KIM, S. H., LEE, H. R., KIM, H. J., JUNG, Y., CHOI, J. H. & KIM, K. T. 2013. hnRNP Q regulates translation of p53 in normal and stress conditions. *Cell Death Differ,* 20**,** 226-34.

KIRBY, J., NING, K., FERRAIUOLO, L., HEATH, P. R., ISMAIL, A., KUO, S.-W., VALORI, C. F., COX, L., SHARRACK, B., WHARTON, S. B., INCE, P. G., SHAW, P. J. & AZZOUZ, M. 2011. Phosphatase and tensin homologue/protein kinase B pathway linked to motor neuron survival in human superoxide dismutase 1-related amyotrophic lateral sclerosis. *Brain*.

KISKINIS, E., SANDOE, J., WILLIAMS, L. A., BOULTING, G. L., MOCCIA, R., WAINGER, B. J., HAN, S., PENG, T., THAMS, S., MIKKILINENI, S., MELLIN, C., MERKLE, F. T., DAVIS-DUSENBERY, B. N., ZILLER, M., OAKLEY, D., ICHIDA, J., DICOSTANZA, S., ATWATER, N., MAEDER, M. L., GOODWIN, M. J., NEMESH, J., HANDSAKER, R. E., PAULL, D., NOGGLE, S., MCCARROLL, S. A., JOUNG, J. K., WOOLF, C. J., BROWN, R. H. & EGGAN, K. 2014. Pathways Disrupted in Human ALS Motor Neurons Identified Through Genetic Correction of Mutant SOD1. *Cell Stem Cell,* 14**,** 781-795.

KITCHENS, D. L., SNYDER, E. Y. & GOTTLIEB, D. I. 1994. FGF and EGF are mitogens for immortalized neural progenitors. *J Neurobiol,* 25**,** 797-807.

KNAFO, S., SANCHEZ-PUELLES, C., PALOMER, E., DELGADO, I., DRAFFIN, J. E., MINGO, J., WAHLE, T., KALEKA, K., MOU, L., PEREDA-PEREZ, I., KLOSI, E., FABER, E. B., CHAPMAN, H. M., LOZANO-

MONTES, L., ORTEGA-MOLINA, A., ORDONEZ-GUTIERREZ, L., WANDOSELL, F., VINA, J., DOTTI, C. G., HALL, R. A., PULIDO, R., GERGES, N. Z., CHAN, A. M., SPALLER, M. R., SERRANO, M., VENERO, C. & ESTEBAN, J. A. 2016. PTEN recruitment controls synaptic and cognitive function in Alzheimer's models. *Nat Neurosci,* 19**,** 443-53.

KOPPERS, M., BLOKHUIS, A. M., WESTENENG, H.-J., TERPSTRA, M. L., ZUNDEL, C. A. C., VIEIRA DE SÁ, R., SCHELLEVIS, R. D., WAITE, A. J., BLAKE, D. J., VELDINK, J. H., VAN DEN BERG, L. H. & PASTERKAMP, R. J. 2015. C9orf72 ablation in mice does not cause motor neuron degeneration or motor deficits. *Annals of Neurology,* 78**,** 426-438.

KOVANDA, A., ZALAR, M., ŠKET, P., PLAVEC, J. & ROGELJ, B. 2015. Anti-sense DNA d(GGCCCC)n expansions in C9ORF72 form i-motifs and protonated hairpins. *Scientific Reports,* 5**,** 17944.

KOZIKOWSKI, A. P., CHEN, Y., GAYSIN, A., CHEN, B., D'ANNIBALE, M. A., SUTO, C. M. & LANGLEY, B. C. 2007. Functional Differences in Epigenetic ModulatorsSuperiority of Mercaptoacetamide-Based Histone Deacetylase Inhibitors Relative to Hydroxamates in Cortical Neuron Neuroprotection Studies. *Journal of Medicinal Chemistry,* 50**,** 3054-3061.

KURIBAYASHI, T., OHARA, M., SORA, S. & KUBOTA, N. 2010. Scriptaid, a novel histone deacetylase inhibitor, enhances the response of human tumor cells to radiation. *Int J Mol Med,* 25**,** 25-9.

KWAK, Y.-D., MA, T., DIAO, S., ZHANG, X., CHEN, Y., HSU, J., LIPTON, S., MASLIAH, E., XU, H. & LIAO, F.-F. 2010. NO signaling and S-nitrosylation regulate PTEN inhibition in neurodegeneration. *Molecular Neurodegeneration,* 5**,** 49.

KWIATKOWSKI, T. J., JR., BOSCO, D. A., LECLERC, A. L., TAMRAZIAN, E., VANDERBURG, C. R., RUSS, C., DAVIS, A., GILCHRIST, J., KASARSKIS, E. J., MUNSAT, T., VALDMANIS, P., ROULEAU, G. A., HOSLER, B. A., CORTELLI, P., DE JONG, P. J., YOSHINAGA, Y., HAINES, J. L., PERICAK-VANCE, M. A., YAN, J., TICOZZI, N., SIDDIQUE, T., MCKENNA-YASEK, D., SAPP, P. C., HORVITZ, H. R., LANDERS, J. E. & BROWN, R. H., JR. 2009. Mutations in the FUS/TLS Gene on Chromosome 16 Cause Familial Amyotrophic Lateral Sclerosis. *Science,* 323**,** 1205-1208.

KWON, C. H., LUIKART, B. W., POWELL, C. M., ZHOU, J., MATHENY, S. A., ZHANG, W., LI, Y., BAKER, S. J. & PARADA, L. F. 2006. Pten regulates neuronal arborization and social interaction in mice. *Neuron,* 50**,** 377-88.

KWON, I., XIANG, S., KATO, M., WU, L., THEODOROPOULOS, P., WANG, T., KIM, J., YUN, J., XIE, Y. & MCKNIGHT, S. L. 2014. Poly-dipeptides encoded by the C9ORF72 repeats bind nucleoli, impede RNA biogenesis, and kill cells. *Science (New York, N.Y.),* 345**,** 1139-1145.

LACHYANKAR, M. B., SULTANA, N., SCHONHOFF, C. M., MITRA, P., POLUHA, W., LAMBERT, S., QUESENBERRY, P. J., LITOFSKY, N. S., RECHT, L. D., NABI, R., MILLER, S. J., OHTA, S., NEEL, B. G. & ROSS, A. H. 2000. A role for nuclear PTEN in neuronal differentiation. *J Neurosci,* 20**,** 1404-13.

LAGIER-TOURENNE, C., BAUGHN, M., RIGO, F., SUN, S., LIU, P., LI, H.-R., JIANG, J., WATT, A. T., CHUN, S., KATZ, M., QIU, J., SUN, Y., LING, S.-C., ZHU, Q., POLYMENIDOU, M., DRENNER, K., ARTATES, J. W., MCALONIS-DOWNES, M., MARKMILLER, S., HUTT, K. R., PIZZO, D. P., CADY, J., HARMS, M. B., BALOH, R. H., VANDENBERG, S. R., YEO, G. W., FU, X.-D., BENNETT, C. F., CLEVELAND, D. W. & RAVITS, J. 2013. Targeted degradation of sense and antisense C9orf72 RNA foci as therapy for ALS and frontotemporal degeneration. *Proceedings of the National Academy of Sciences,* 110**,** E4530-E4539.

LAGIER-TOURENNE, C. & CLEVELAND, D. W. 2009. Rethinking ALS: the FUS about TDP-43. *Cell,* 136**,** 1001-1004.

LAZAR, D. F. & SALTIEL, A. R. 2006. Lipid phosphatases as drug discovery targets for type 2 diabetes. *Nat Rev Drug Discov,* 5**,** 333-42.

LEE, J. O., YANG, H., GEORGESCU, M. M., DI CRISTOFANO, A., MAEHAMA, T., SHI, Y., DIXON, J. E., PANDOLFI, P. & PAVLETICH, N. P. 1999. Crystal structure of the PTEN tumor suppressor: implications for its phosphoinositide phosphatase activity and membrane association. *Cell,* 99**,** 323-34.

LEE, S. & KIM, H.-J. 2015. Prion-like Mechanism in Amyotrophic Lateral Sclerosis: are Protein Aggregates the Key? *Experimental Neurobiology,* 24**,** 1-7.

LEFEBVRE, S., BURGLEN, L., REBOULLET, S., CLERMONT, O., BURLET, P., VIOLLET, L., BENICHOU, B., CRUAUD, C., MILLASSEAU, P., ZEVIANI, M. & ET AL. 1995. Identification and characterization of a spinal muscular atrophy-determining gene. *Cell,* 80**,** 155-65.

LEHMER, C., OECKL, P., WEISHAUPT, J. H., VOLK, A. E., DIEHL-SCHMID, J., SCHROETER, M. L., LAUER, M., KORNHUBER, J., LEVIN, J., FASSBENDER, K., LANDWEHRMEYER, B., SCHLUDI, M. H., ARZBERGER, T., KREMMER, E., FLATLEY, A., FEEDERLE, R., STEINACKER, P., WEYDT, P., LUDOLPH, A. C., EDBAUER, D. & OTTO, M. 2017. Poly-GP in cerebrospinal fluid links C9orf72-associated

dipeptide repeat expression to the asymptomatic phase of ALS/FTD. *EMBO Mol Med,* 13**,** 201607486.
LENG, Y. & CHUANG, D. M. 2006. Endogenous alpha-synuclein is induced by valproic acid through histone deacetylase inhibition and participates in neuroprotection against glutamate-induced excitotoxicity. *J Neurosci,* 26**,** 7502-12.
LEVINE, T. P., DANIELS, R. D., GATTA, A. T., WONG, L. H. & HAYES, M. J. 2013. The product of C9orf72, a gene strongly implicated in neurodegeneration, is structurally related to DENN Rab-GEFs. *Bioinformatics,* 29**,** 499-503.
LI, D., QU, Y., MAO, M., ZHANG, X., LI, J., FERRIERO, D. & MU, D. 2009. Involvement of the PTEN-AKT-FOXO3a pathway in neuronal apoptosis in developing rat brain after hypoxia-ischemia. *J Cereb Blood Flow Metab,* 29**,** 1903-1913.
LI, L. & HU, G.-K. 2015. Pink1 protects cortical neurons from thapsigargin-induced oxidative stress and neuronal apoptosis. *Bioscience Reports,* 35**,** e00174.
LI, P., WANG, D., LI, H., YU, Z., CHEN, X. & FANG, J. 2014. Identification of nucleolus-localized PTEN and its function in regulating ribosome biogenesis. *Molecular Biology Reports,* 41**,** 6383-6390.
LI, X., ALAFUZOFF, I., SOININEN, H., WINBLAD, B. & PEI, J.-J. 2005. Levels of mTOR and its downstream targets 4E-BP1, eEF2, and eEF2 kinase in relationships with tau in Alzheimer's disease brain. *FEBS Journal,* 272**,** 4211-4220.
LI, Y., BALASUBRAMANIAN, U., COHEN, D., ZHANG, P. W., MOSMILLER, E., SATTLER, R., MARAGAKIS, N. J. & ROTHSTEIN, J. D. 2015. A comprehensive library of familial human amyotrophic lateral sclerosis induced pluripotent stem cells. *PLoS One,* 10.
LIAW, D., MARSH, D. J., LI, J., DAHIA, P. L., WANG, S. I., ZHENG, Z., BOSE, S., CALL, K. M., TSOU, H. C., PEACOCKE, M., ENG, C. & PARSONS, R. 1997. Germline mutations of the PTEN gene in Cowden disease, an inherited breast and thyroid cancer syndrome. *Nat Genet,* 16**,** 64-7.
LIN, L. F., DOHERTY, D. H., LILE, J. D., BEKTESH, S. & COLLINS, F. 1993. GDNF: a glial cell line-derived neurotrophic factor for midbrain dopaminergic neurons. *Science,* 260**,** 1130-2.
LINDSAY, Y., MCCOULL, D., DAVIDSON, L., LESLIE, N. R., FAIRSERVICE, A., GRAY, A., LUCOCQ, J. & DOWNES, C. P. 2006. Localization of agonist-sensitive PtdIns(3,4,5)P3 reveals a nuclear pool that is insensitive to PTEN expression. *J Cell Sci,* 119**,** 5160-8.
LIPPMANN, ETHAN S., WILLIAMS, CLAY E., RUHL, DAVID A., ESTEVEZ-SILVA, MARIA C., CHAPMAN, EDWIN R., COON, JOSHUA J. & ASHTON, RANDOLPH S. 2015. Deterministic HOX Patterning in Human Pluripotent Stem Cell-Derived Neuroectoderm. *Stem Cell Reports,* 4**,** 632-644.
LITTLE, D., VALORI, C. F., MUTSAERS, C. A., BENNETT, E. J., WYLES, M., SHARRACK, B., SHAW, P. J., GILLINGWATER, T. H., AZZOUZ, M. & NING, K. 2015. PTEN Depletion Decreases Disease Severity and Modestly Prolongs Survival in a Mouse Model of Spinal Muscular Atrophy. *Mol Ther,* 23**,** 270-277.
LIU, D., YU, Y. & SCHACHNER, M. 2014. Ptena, but not Ptenb, reduces regeneration after spinal cord injury in adult zebrafish. *Experimental Neurology,* 261**,** 196-205.
LIU, J.-L., SHENG, X., HORTOBAGYI, Z. K., MAO, Z., GALLICK, G. E. & YUNG, W. K. A. 2005. Nuclear PTEN-Mediated Growth Suppression Is Independent of Akt Down-Regulation. *Molecular and Cellular Biology,* 25**,** 6211-6224.
LIU, K., LU, Y., LEE, J. K., SAMARA, R., WILLENBERG, R., SEARS-KRAXBERGER, I., TEDESCHI, A., PARK, K. K., JIN, D., CAI, B., XU, B., CONNOLLY, L., STEWARD, O., ZHENG, B. & HE, Z. 2010. PTEN deletion enhances the regenerative ability of adult corticospinal neurons. *Nat Neurosci,* 13**,** 1075-81.
LIU, W., JAMES, C. D., FREDERICK, L., ALDERETE, B. E. & JENKINS, R. B. 1997. PTEN/MMAC1 mutations and EGFR amplification in glioblastomas. *Cancer Res,* 57**,** 5254-7.
LIU, Y., PATTAMATTA, A., ZU, T., REID, T., BARDHI, O., BORCHELT, D. R., YACHNIS, A. T. & RANUM, L. P. 2016. C9orf72 BAC Mouse Model with Motor Deficits and Neurodegenerative Features of ALS/FTD. *Neuron,* 90**,** 521-34.
LIU, Y. & ZHANG, S. C. 2010. Human stem cells as a model of motoneuron development and diseases. *Ann N Y Acad Sci*.
LOMEN-HOERTH, C., ANDERSON, T. & MILLER, B. 2002. The overlap of amyotrophic lateral sclerosis and frontotemporal dementia. *Neurology,* 59**,** 1077-9.
LOPEZ-GONZALEZ, R., LU, Y., GENDRON, T. F., KARYDAS, A., TRAN, H., YANG, D., PETRUCELLI, L., MILLER, B. L., ALMEIDA, S. & GAO, F. B. 2016. Poly(GR) in C9ORF72-Related ALS/FTD Compromises Mitochondrial Function and Increases Oxidative Stress and DNA Damage in iPSC-Derived Motor Neurons. *Neuron,* 92**,** 383-391.
LUDOLPH, A. C. 2017. Motor neuron disease: Genetic testing in amyotrophic lateral sclerosis. *Nat Rev Neurol,* 13**,** 262-263.

LUTY, A. A., KWOK, J. B., DOBSON-STONE, C., LOY, C. T., COUPLAND, K. G., KARLSTROM, H., SOBOW, T., TCHORZEWSKA, J., MARUSZAK, A., BARCIKOWSKA, M., PANEGYRES, P. K., ZEKANOWSKI, C., BROOKS, W. S., WILLIAMS, K. L., BLAIR, I. P., MATHER, K. A., SACHDEV, P. S., HALLIDAY, G. M. & SCHOFIELD, P. R. 2010. Sigma nonopioid intracellular receptor 1 mutations cause frontotemporal lobar degeneration-motor neuron disease. *Ann Neurol,* 68**,** 639-49.

LYU, J., YU, X., HE, L., CHENG, T., ZHOU, J., CHENG, C., CHEN, Z., CHENG, G., QIU, Z. & ZHOU, W. 2015. The protein phosphatase activity of PTEN is essential for regulating neural stem cell differentiation. *Molecular Brain,* 8**,** 26.

MACKENZIE, I. R. A., BIGIO, E. H., INCE, P. G., GESER, F., NEUMANN, M., CAIRNS, N. J., KWONG, L. K., FORMAN, M. S., RAVITS, J., STEWART, H., EISEN, A., MCCLUSKY, L., KRETZSCHMAR, H. A., MONORANU, C. M., HIGHLEY, J. R., KIRBY, J., SIDDIQUE, T., SHAW, P. J., LEE, V. M. Y. & TROJANOWSKI, J. Q. 2007. Pathological TDP-43 distinguishes sporadic amyotrophic lateral sclerosis from amyotrophic lateral sclerosis with SOD1 mutations. *Ann Neurol,* 61**,** 427-434.

MAEHAMA, T. & DIXON, J. E. 1998. The tumor suppressor, PTEN/MMAC1, dephosphorylates the lipid second messenger, phosphatidylinositol 3,4,5-trisphosphate. *J Biol Chem,* 273**,** 13375-8.

MAIER, O., BOHM, J., DAHM, M., BRUCK, S., BEYER, C. & JOHANN, S. 2013. Differentiated NSC-34 motoneuron-like cells as experimental model for cholinergic neurodegeneration. *Neurochem Int,* 62**,** 1029-38.

MANJALY, Z. R., SCOTT, K. M., ABHINAV, K., WIJESEKERA, L., GANESALINGAM, J., GOLDSTEIN, L. H., JANSSEN, A., DOUGHERTY, A., WILLEY, E., STANTON, B. R., TURNER, M. R., AMPONG, M. A., SAKEL, M., ORRELL, R. W., HOWARD, R., SHAW, C. E., LEIGH, P. N. & AL-CHALABI, A. 2010. The sex ratio in amyotrophic lateral sclerosis: A population based study. *Amyotroph Lateral Scler,* 11**,** 439-42.

MAO, L., JIA, J., ZHOU, X., XIAO, Y., WANG, Y., MAO, X., ZHEN, X., GUAN, Y., ALKAYED, N. J. & CHENG, J. 2013. Delayed administration of a PTEN inhibitor BPV improves functional recovery after experimental stroke. *Neuroscience,* 231**,** 272-81.

MARINO, S., KRIMPENFORT, P., LEUNG, C., VAN DER KORPUT, H., TRAPMAN, J., CAMENISCH, I., BERNS, A. & BRANDNER, S. 2002. PTEN is essential for cell migration but not for fate determination and tumourigenesis in the cerebellum. *Development,* 129**,** 3513-3522.

MARUYAMA, H., MORINO, H., ITO, H., IZUMI, Y., KATO, H., WATANABE, Y., KINOSHITA, Y., KAMADA, M., NODERA, H., SUZUKI, H., KOMURE, O., MATSUURA, S., KOBATAKE, K., MORIMOTO, N., ABE, K., SUZUKI, N., AOKI, M., KAWATA, A., HIRAI, T., KATO, T., OGASAWARA, K., HIRANO, A., TAKUMI, T., KUSAKA, H., HAGIWARA, K., KAJI, R. & KAWAKAMI, H. 2010. Mutations of optineurin in amyotrophic lateral sclerosis. *Nature,* 465**,** 223-6.

MASSON, G. R., PERISIC, O., BURKE, J. E. & WILLIAMS, R. L. 2016. The intrinsically disordered tails of PTEN and PTEN-L have distinct roles in regulating substrate specificity and membrane activity. *Biochem J,* 473**,** 135-44.

MAURY, Y., COME, J., PISKOROWSKI, R. A., SALAH-MOHELLIBI, N., CHEVALEYRE, V., PESCHANSKI, M., MARTINAT, C. & NEDELEC, S. 2015. Combinatorial analysis of developmental cues efficiently converts human pluripotent stem cells into multiple neuronal subtypes. *Nat Biotech,* 33**,** 89-96.

MAY, S., HORNBURG, D., SCHLUDI, M. H., ARZBERGER, T., RENTZSCH, K., SCHWENK, B. M., GRASSER, F. A., MORI, K., KREMMER, E., BANZHAF-STRATHMANN, J., MANN, M., MEISSNER, F. & EDBAUER, D. 2014. C9orf72 FTLD/ALS-associated Gly-Ala dipeptide repeat proteins cause neuronal toxicity and Unc119 sequestration. *Acta Neuropathologica,* 128**,** 485-503.

MERTENS, J., PAQUOLA, APUÃ C. M., KU, M., HATCH, E., BÖHNKE, L., LADJEVARDI, S., MCGRATH, S., CAMPBELL, B., LEE, H., HERDY, JOSEPH R., GONÇALVES, J. T., TODA, T., KIM, Y., WINKLER, J., YAO, J., HETZER, MARTIN W. & GAGE, FRED H. 2015. Directly Reprogrammed Human Neurons Retain Aging-Associated Transcriptomic Signatures and Reveal Age-Related Nucleocytoplasmic Defects. *Cell Stem Cell,* 17**,** 705-718.

MEYER, K., FERRAIUOLO, L., MIRANDA, C. J., LIKHITE, S., MCELROY, S., RENUSCH, S., DITSWORTH, D., LAGIER-TOURENNE, C., SMITH, R. A., RAVITS, J., BURGHES, A. H., SHAW, P. J., CLEVELAND, D. W., KOLB, S. J. & KASPAR, B. K. 2014. Direct conversion of patient fibroblasts demonstrates non-cell autonomous toxicity of astrocytes to motor neurons in familial and sporadic ALS. *Proc Natl Acad Sci U S A,* 111**,** 829-32.

MILLER, J. D., GANAT, Y. M., KISHINEVSKY, S., BOWMAN, R. L., LIU, B., TU, E. Y., MANDAL, P. K., VERA, E., SHIM, J. W., KRIKS, S., TALDONE, T., FUSAKI, N., TOMISHIMA, M. J., KRAINC, D., MILNER, T. A., ROSSI, D. J. & STUDER, L. 2013. Human iPSC-based modeling of late-onset disease via progerin-induced aging. *Cell Stem Cell,* 13**,** 691-705.

MILLER, S. J., LOU, D. Y., SELDIN, D. C., LANE, W. S. & NEEL, B. G. 2002. Direct identification of PTEN phosphorylation sites. *FEBS Lett,* 528**,** 145-53.

MILLER, T. M., KIM, S. H., YAMANAKA, K., HESTER, M., UMAPATHI, P., ARNSON, H., RIZO, L., MENDELL, J. R., GAGE, F. H., CLEVELAND, D. W. & KASPAR, B. K. 2006. Gene transfer demonstrates that muscle is not a primary target for non-cell-autonomous toxicity in familial amyotrophic lateral sclerosis. *Proc Natl Acad Sci U S A,* 103**,** 19546-51.

MITCHELL, J., PAUL, P., CHEN, H. J., MORRIS, A., PAYLING, M., FALCHI, M., HABGOOD, J., PANOUTSOU, S., WINKLER, S., TISATO, V., HAJITOU, A., SMITH, B., VANCE, C., SHAW, C., MAZARAKIS, N. D. & DE BELLEROCHE, J. 2010. Familial amyotrophic lateral sclerosis is associated with a mutation in D-amino acid oxidase. *Proc Natl Acad Sci U S A,* 107**,** 7556-61.

MITNE-NETO, M., MACHADO-COSTA, M., MARCHETTO, M. C. N., BENGTSON, M. H., JOAZEIRO, C. A., TSUDA, H., BELLEN, H. J., SILVA, H. C. A., OLIVEIRA, A. S. B., LAZAR, M., MUOTRI, A. R. & ZATZ, M. 2011. Downregulation of VAPB expression in motor neurons derived from induced pluripotent stem cells of ALS8 patients. *Human Molecular Genetics,* 20**,** 3642-3652.

MIZIELINSKA, S., LASHLEY, T., NORONA, F. E., CLAYTON, E. L., RIDLER, C. E., FRATTA, P. & ISAACS, A. M. 2013. C9orf72 frontotemporal lobar degeneration is characterised by frequent neuronal sense and antisense RNA foci. *Acta Neuropathologica,* 126**,** 845-57.

MORI, K., ARZBERGER, T., GRASSER, F. A., GIJSELINCK, I., MAY, S., RENTZSCH, K., WENG, S. M., SCHLUDI, M. H., VAN DER ZEE, J., CRUTS, M., VAN BROECKHOVEN, C., KREMMER, E., KRETZSCHMAR, H. A., HAASS, C. & EDBAUER, D. 2013a. Bidirectional transcripts of the expanded C9orf72 hexanucleotide repeat are translated into aggregating dipeptide repeat proteins. *Acta Neuropathologica,* 126**,** 881-93.

MORI, K., WENG, S.-M., ARZBERGER, T., MAY, S., RENTZSCH, K., KREMMER, E., SCHMID, B., KRETZSCHMAR, H. A., CRUTS, M., VAN BROECKHOVEN, C., HAASS, C. & EDBAUER, D. 2013b. The C9orf72 GGGGCC Repeat Is Translated into Aggregating Dipeptide-Repeat Proteins in FTLD/ALS. *Science,* 339**,** 1335-1338.

MORRISON, B. E., MAJDZADEH, N. & D'MELLO, S. R. 2007. Histone deacetylases: focus on the nervous system. *Cell Mol Life Sci,* 64**,** 2258-69.

MYERS, M. P., STOLAROV, J. P., ENG, C., LI, J., WANG, S. I., WIGLER, M. H., PARSONS, R. & TONKS, N. K. 1997. P-TEN, the tumor suppressor from human chromosome 10q23, is a dual-specificity phosphatase. *Proceedings of the National Academy of Sciences,* 94**,** 9052-9057.

NAMIKAWA, K., HONMA, M., ABE, K., TAKEDA, M., MANSUR, K., OBATA, T., MIWA, A., OKADO, H. & KIYAMA, H. 2000. Akt/protein kinase B prevents injury-induced motoneuron death and accelerates axonal regeneration. *J Neurosci,* 20**,** 2875-86.

NASSIF, M., HOPPE, J., SANTIN, K., FROZZA, R., ZAMIN, L. L., SIMÃO, F., HORN, A. P. & SALBEGO, C. 2007. β-Amyloid peptide toxicity in organotypic hippocampal slice culture involves Akt/PKB, GSK-3β, and PTEN. *Neurochemistry International,* 50**,** 229-235.

NEUMANN, M., SAMPATHU, D. M., KWONG, L. K., TRUAX, A. C., MICSENYI, M. C., CHOU, T. T., BRUCE, J., SCHUCK, T., GROSSMAN, M., CLARK, C. M., MCCLUSKEY, L. F., MILLER, B. L., MASLIAH, E., MACKENZIE, I. R., FELDMAN, H., FEIDEN, W., KRETZSCHMAR, H. A., TROJANOWSKI, J. Q. & LEE, V. M. 2006. Ubiquitinated TDP-43 in frontotemporal lobar degeneration and amyotrophic lateral sclerosis. *Science,* 314**,** 130-3.

NIEUWKOOP, P. D. & NIGTEVECHT, G. V. 1954. Neural activation and transformation in explants of competent ectoderm under the influence of fragments of anterior notochord in urodeles *Journal of Embryology and Experimental Morphology,* 2**,** 175-193.

NING, K., DREPPER, C., VALORI, C. F., AHSAN, M., WYLES, M., HIGGINBOTTOM, A., HERRMANN, T., SHAW, P., AZZOUZ, M. & SENDTNER, M. 2010. PTEN depletion rescues axonal growth defect and improves survival in SMN-deficient motor neurons. *Hum Mol Genet,* 19**,** 3159-68.

NING, K., PEI, L., LIAO, M., LIU, B., ZHANG, Y., JIANG, W., MIELKE, J. G., LI, L., CHEN, Y., EL-HAYEK, Y. H., FEHLINGS, M. G., ZHANG, X., LIU, F., EUBANKS, J. & WAN, Q. 2004. Dual neuroprotective signaling mediated by downregulating two distinct phosphatase activities of PTEN. *J Neurosci,* 24**,** 4052-60.

NISHIMURA, A. L., MITNE-NETO, M., SILVA, H. C., RICHIERI-COSTA, A., MIDDLETON, S., CASCIO, D., KOK, F., OLIVEIRA, J. R., GILLINGWATER, T., WEBB, J., SKEHEL, P. & ZATZ, M. 2004. A mutation in the vesicle-trafficking protein VAPB causes late-onset spinal muscular atrophy and amyotrophic lateral sclerosis. *Am J Hum Genet,* 75**,** 822-31.

NORO, R., GEMMA, A., MIYANAGA, A., KOSAIHIRA, S., MINEGISHI, Y., NARA, M., KOKUBO, Y., SEIKE, M., KATAOKA, K., MATSUDA, K., OKANO, T., YOSHIMURA, A. & KUDOH, S. 2007. PTEN inactivation

in lung cancer cells and the effect of its recovery on treatment with epidermal growth factor receptor tyrosine kinase inhibitors. *Int J Oncol,* 31**,** 1157-63.

NUMAJIRI, N., TAKASAWA, K., NISHIYA, T., TANAKA, H., OHNO, K., HAYAKAWA, W., ASADA, M., MATSUDA, H., AZUMI, K., KAMATA, H., NAKAMURA, T., HARA, H., MINAMI, M., LIPTON, S. A. & UEHARA, T. 2011. On-off system for PI3-kinase-Akt signaling through S-nitrosylation of phosphatase with sequence homology to tensin (PTEN). *Proc Natl Acad Sci U S A,* 108**,** 10349-54.

O'CONNOR, M. D., KARDEL, M. D., IOSFINA, I., YOUSSEF, D., LU, M., LI, M. M., VERCAUTEREN, S., NAGY, A. & EAVES, C. J. 2008. Alkaline Phosphatase-Positive Colony Formation Is a Sensitive, Specific, and Quantitative Indicator of Undifferentiated Human Embryonic Stem Cells. *Stem Cells,* 26**,** 1109-1116.

O'ROURKE, J. G., BOGDANIK, L., MUHAMMAD, A. K., GENDRON, T. F., KIM, K. J., AUSTIN, A., CADY, J., LIU, E. Y., ZARROW, J., GRANT, S., HO, R., BELL, S., CARMONA, S., SIMPKINSON, M., LALL, D., WU, K., DAUGHRITY, L., DICKSON, D. W., HARMS, M. B., PETRUCELLI, L., LEE, E. B., LUTZ, C. M. & BALOH, R. H. 2015. C9orf72 BAC Transgenic Mice Display Typical Pathologic Features of ALS/FTD. *Neuron,* 88**,** 892-901.

O'ROURKE, J. G., BOGDANIK, L., YANEZ, A., LALL, D., WOLF, A. J., MUHAMMAD, A. K., HO, R., CARMONA, S., VIT, J. P., ZARROW, J., KIM, K. J., BELL, S., HARMS, M. B., MILLER, T. M., DANGLER, C. A., UNDERHILL, D. M., GOODRIDGE, H. S., LUTZ, C. M. & BALOH, R. H. 2016. C9orf72 is required for proper macrophage and microglial function in mice. *Science,* 351**,** 1324-9.

OMORI, N., JIN, G., LI, F., ZHANG, W. R., WANG, S. J., HAMAKAWA, Y., NAGANO, I., MANABE, Y., SHOJI, M. & ABE, K. 2002. Enhanced phosphorylation of PTEN in rat brain after transient middle cerebral artery occlusion. *Brain Res,* 954**,** 317-22.

ORLACCHIO, A., BABALINI, C., BORRECA, A., PATRONO, C., MASSA, R., BASARAN, S., MUNHOZ, R. P., ROGAEVA, E. A., ST GEORGE-HYSLOP, P. H., BERNARDI, G. & KAWARAI, T. 2010. SPATACSIN mutations cause autosomal recessive juvenile amyotrophic lateral sclerosis. *Brain,* 133**,** 591-8.

ORR, HARRY T. 2011. FTD and ALS: Genetic Ties that Bind. *Neuron,* 72**,** 189-190.

OU, S. H., WU, F., HARRICH, D., GARCIA-MARTINEZ, L. F. & GAYNOR, R. B. 1995. Cloning and characterization of a novel cellular protein, TDP-43, that binds to human immunodeficiency virus type 1 TAR DNA sequence motifs. *J Virol,* 69**,** 3584-96.

PARK, K. K., LIU, K., HU, Y., SMITH, P. D., WANG, C., CAI, B., XU, B., CONNOLLY, L., KRAMVIS, I., SAHIN, M. & HE, Z. 2008. Promoting axon regeneration in the adult CNS by modulation of the PTEN/mTOR pathway. *Science,* 322**,** 963-6.

PARKINSON, N., INCE, P. G., SMITH, M. O., HIGHLEY, R., SKIBINSKI, G., ANDERSEN, P. M., MORRISON, K. E., PALL, H. S., HARDIMAN, O., COLLINGE, J., SHAW, P. J., FISHER, E. M., STUDY, M. R. C. P. I. A. & CONSORTIUM, F. R. 2006. ALS phenotypes with mutations in CHMP2B (charged multivesicular body protein 2B). *Neurology,* 67**,** 1074-7.

PEARSON, C. E. 2011. Repeat Associated Non-ATG Translation Initiation: One DNA, Two Transcripts, Seven Reading Frames, Potentially Nine Toxic Entities! *PLoS Genet,* 7**,** e1002018.

PETERS, O. M., CABRERA, G. T., TRAN, H., GENDRON, T. F., MCKEON, J. E., METTERVILLE, J., WEISS, A., WIGHTMAN, N., SALAMEH, J., KIM, J., SUN, H., BOYLAN, K. B., DICKSON, D., KENNEDY, Z., LIN, Z., ZHANG, Y. J., DAUGHRITY, L., JUNG, C., GAO, F. B., SAPP, P. C., HORVITZ, H. R., BOSCO, D. A., BROWN, S. P., DE JONG, P., PETRUCELLI, L., MUELLER, C. & BROWN, R. H., JR. 2015. Human C9ORF72 Hexanucleotide Expansion Reproduces RNA Foci and Dipeptide Repeat Proteins but Not Neurodegeneration in BAC Transgenic Mice. *Neuron,* 88**,** 902-9.

PETIT, A., KAWARAI, T., PAITEL, E., SANJO, N., MAJ, M., SCHEID, M., CHEN, F., GU, Y., HASEGAWA, H., SALEHI-RAD, S., WANG, L., ROGAEVA, E., FRASER, P., ROBINSON, B., ST GEORGE-HYSLOP, P. & TANDON, A. 2005. Wild-type PINK1 Prevents Basal and Induced Neuronal Apoptosis, a Protective Effect Abrogated by Parkinson Disease-related Mutations. *Journal of Biological Chemistry,* 280**,** 34025-34032.

PHILIPPIDOU, P. & DASEN, J. S. 2013. Hox genes: choreographers in neural development, architects of circuit organization. *Neuron,* 80**,** 12-34.

POLYMENIDOU, M., LAGIER-TOURENNE, C., HUTT, K. R., HUELGA, S. C., MORAN, J., LIANG, T. Y., LING, S. C., SUN, E., WANCEWICZ, E., MAZUR, C., KORDASIEWICZ, H., SEDAGHAT, Y., DONOHUE, J. P., SHIUE, L., BENNETT, C. F., YEO, G. W. & CLEVELAND, D. W. 2011. Long pre-mRNA depletion and RNA missplicing contribute to neuronal vulnerability from loss of TDP-43. *Nat Neurosci,* 14**,** 459-68.

PUN, S., SANTOS, A. F., SAXENA, S., XU, L. & CARONI, P. 2006. Selective vulnerability and pruning of phasic motoneuron axons in motoneuron disease alleviated by CNTF. *Nat Neurosci,* 9**,** 408-19.

PUTZ, U., MAH, S., GOH, C. P., LOW, L. H., HOWITT, J. & TAN, S. S. 2015. PTEN secretion in exosomes. *Methods,* 78**,** 157-63.

QU, Q., LI, D., LOUIS, K. R., LI, X., YANG, H., SUN, Q., CRANDALL, S. R., TSANG, S., ZHOU, J., COX, C. L., CHENG, J. & WANG, F. 2014. High-efficiency motor neuron differentiation from human pluripotent stem cells and the function of Islet-1. *Nat Commun,* 5.

RAHDAR, M., INOUE, T., MEYER, T., ZHANG, J., VAZQUEZ, F. & DEVREOTES, P. N. 2009. A phosphorylation-dependent intramolecular interaction regulates the membrane association and activity of the tumor suppressor PTEN. *Proceedings of the National Academy of Sciences,* 106**,** 480-485.

RENTON, A. E., MAJOUNIE, E., WAITE, A., SIMON-SANCHEZ, J., ROLLINSON, S., GIBBS, J. R., SCHYMICK, J. C., LAAKSOVIRTA, H., VAN SWIETEN, J. C., MYLLYKANGAS, L., KALIMO, H., PAETAU, A., ABRAMZON, Y., REMES, A. M., KAGANOVICH, A., SCHOLZ, S. W., DUCKWORTH, J., DING, J., HARMER, D. W., HERNANDEZ, D. G., JOHNSON, J. O., MOK, K., RYTEN, M., TRABZUNI, D., GUERREIRO, R. J., ORRELL, R. W., NEAL, J., MURRAY, A., PEARSON, J., JANSEN, I. E., SONDERVAN, D., SEELAAR, H., BLAKE, D., YOUNG, K., HALLIWELL, N., CALLISTER, J. B., TOULSON, G., RICHARDSON, A., GERHARD, A., SNOWDEN, J., MANN, D., NEARY, D., NALLS, M. A., PEURALINNA, T., JANSSON, L., ISOVIITA, V. M., KAIVORINNE, A. L., HOLTTA-VUORI, M., IKONEN, E., SULKAVA, R., BENATAR, M., WUU, J., CHIO, A., RESTAGNO, G., BORGHERO, G., SABATELLI, M., CONSORTIUM, I., HECKERMAN, D., ROGAEVA, E., ZINMAN, L., ROTHSTEIN, J. D., SENDTNER, M., DREPPER, C., EICHLER, E. E., ALKAN, C., ABDULLAEV, Z., PACK, S. D., DUTRA, A., PAK, E., HARDY, J., SINGLETON, A., WILLIAMS, N. M., HEUTINK, P., PICKERING-BROWN, S., MORRIS, H. R., TIENARI, P. J. & TRAYNOR, B. J. 2011. A hexanucleotide repeat expansion in C9ORF72 is the cause of chromosome 9p21-linked ALS-FTD. *Neuron,* 72**,** 257-68.

RICKLE, A., BOGDANOVIC, N., VOLKMANN, I., ZHOU, X., PEI, J.-J., WINBLAD, B. & COWBURN, R. F. 2006. PTEN levels in Alzheimer's disease medial temporal cortex. *Neurochemistry International,* 48**,** 114-123.

RIES, V., HENCHCLIFFE, C., KAREVA, T., RZHETSKAYA, M., BLAND, R., DURING, M. J., KHOLODILOV, N. & BURKE, R. E. 2006. Oncoprotein Akt/PKB induces trophic effects in murine models of Parkinson's disease. *Proceedings of the National Academy of Sciences of the United States of America,* 103**,** 18757-18762.

RISS TL, M. R., NILES AL, ET AL. 2013 Cell Viability Assays. *In:* IN: SITTAMPALAM GS, C. N., NELSON H, ET AL., EDITORS. (ed.) *Assay Guidance Manual [Internet].* Bethesda (MD): Eli Lilly & Company and the National Center for Advancing Translational Sciences;.

RIVIECCIO, M. A., BROCHIER, C., WILLIS, D. E., WALKER, B. A., D'ANNIBALE, M. A., MCLAUGHLIN, K., SIDDIQ, A., KOZIKOWSKI, A. P., JAFFREY, S. R., TWISS, J. L., RATAN, R. R. & LANGLEY, B. 2009. HDAC6 is a target for protection and regeneration following injury in the nervous system. *Proceedings of the National Academy of Sciences,* 106**,** 19599-19604.

ROJAS, F., CORTES, N., ABARZUA, S., DYRDA, A. & VAN ZUNDERT, B. 2014. Astrocytes expressing mutant SOD1 and TDP43 trigger motoneuron death that is mediated via sodium channels and nitroxidative stress. *Front Cell Neurosci,* 8.

ROJAS, F., GONZALEZ, D., CORTES, N., AMPUERO, E., HERNANDEZ, D. E., FRITZ, E., ABARZUA, S., MARTINEZ, A., ELORZA, A. A., ALVAREZ, A., COURT, F. & VAN ZUNDERT, B. 2015. Reactive oxygen species trigger motoneuron death in non-cell-autonomous models of ALS through activation of c-Abl signaling. *Front Cell Neurosci,* 9.

ROSEN, D. R., SIDDIQUE, T., PATTERSON, D., FIGLEWICZ, D. A., SAPP, P., HENTATI, A., DONALDSON, D., GOTO, J., O'REGAN, J. P., DENG, H. X. & ET AL. 1993. Mutations in Cu/Zn superoxide dismutase gene are associated with familial amyotrophic lateral sclerosis. *Nature,* 362**,** 59-62.

ROSS, A. H. & GERICKE, A. 2009. Phosphorylation keeps PTEN phosphatase closed for business. *Proceedings of the National Academy of Sciences,* 106**,** 1297-1298.

ROUAUX, C., JOKIC, N., MBEBI, C., BOUTILLIER, S., LOEFFLER, J. P. & BOUTILLIER, A. L. 2003. Critical loss of CBP/p300 histone acetylase activity by caspase-6 during neurodegeneration. *The EMBO Journal,* 22**,** 6537-6549.

ROUAUX, C., PANTELEEVA, I., RENÉ, F., GONZALEZ DE AGUILAR, J.-L., ECHANIZ-LAGUNA, A., DUPUIS, L., MENGER, Y., BOUTILLIER, A.-L. & LOEFFLER, J.-P. 2007. Sodium Valproate Exerts Neuroprotective Effects In Vivo through CREB-Binding Protein-Dependent Mechanisms But Does Not Improve Survival in an Amyotrophic Lateral Sclerosis Mouse Model. *The Journal of Neuroscience,* 27**,** 5535-5545.

RUTHERFORD, N. J., HECKMAN, M. G., DEJESUS-HERNANDEZ, M., BAKER, M. C., SOTO-ORTOLAZA, A. I., RAYAPROLU, S., STEWART, H., FINGER, E., VOLKENING, K., SEELEY, W. W., HATANPAA, K. J.,

LOMEN-HOERTH, C., KERTESZ, A., BIGIO, E. H., LIPPA, C., KNOPMAN, D. S., KRETZSCHMAR, H. A., NEUMANN, M., CASELLI, R. J., WHITE, C. L., 3RD, MACKENZIE, I. R., PETERSEN, R. C., STRONG, M. J., MILLER, B. L., BOEVE, B. F., UITTI, R. J., BOYLAN, K. B., WSZOLEK, Z. K., GRAFF-RADFORD, N. R., DICKSON, D. W., ROSS, O. A. & RADEMAKERS, R. 2012. Length of normal alleles of C9ORF72 GGGGCC repeat do not influence disease phenotype. *Neurobiol Aging,* 33**,** 26.

RYU, H., SMITH, K., CAMELO, S. I., CARRERAS, I., LEE, J., IGLESIAS, A. H., DANGOND, F., CORMIER, K. A., CUDKOWICZ, M. E., BROWN, R. H., JR. & FERRANTE, R. J. 2005. Sodium phenylbutyrate prolongs survival and regulates expression of anti-apoptotic genes in transgenic amyotrophic lateral sclerosis mice. *J Neurochem,* 93**,** 1087-98.

SABATELLI, M., CONFORTI, F. L., ZOLLINO, M., MORA, G., MONSURRÒ, M. R., VOLANTI, P., MARINOU, K., SALVI, F., CORBO, M., GIANNINI, F., BATTISTINI, S., PENCO, S., LUNETTA, C., QUATTRONE, A., GAMBARDELLA, A., LOGROSCINO, G., SIMONE, I., BARTOLOMEI, I., PISANO, F., TEDESCHI, G., CONTE, A., SPATARO, R., LA BELLA, V., CAPONNETTO, C., MANCARDI, G., MANDICH, P., SOLA, P., MANDRIOLI, J., RENTON, A. E., MAJOUNIE, E., ABRAMZON, Y., MARROSU, F., MARROSU, M. G., MURRU, M. R., SOTGIU, M. A., PUGLIATTI, M., RODOLICO, C., MOGLIA, C., CALVO, A., OSSOLA, I., BRUNETTI, M., TRAYNOR, B. J., BORGHERO, G., RESTAGNO, G. & CHIÒ, A. 2012. C9ORF72 hexanucleotide repeat expansions in the Italian sporadic ALS population. *Neurobiology of aging,* 33**,** 1848.e15-1848.e20.

SABATELLI, M., ZOLLINO, M., CONTE, A., DEL GRANDE, A., MARANGI, G., LUCCHINI, M., MIRABELLA, M., ROMANO, A., PIACENTINI, R., BISOGNI, G., LATTANTE, S., LUIGETTI, M., ROSSINI, P. M. & MONCADA, A. 2015. Primary fibroblasts cultures reveal TDP-43 abnormalities in amyotrophic lateral sclerosis patients with and without SOD1 mutations. *Neurobiology of Aging,* 36**,** 2005.e5-2005.e13.

SACCON, R. A., BUNTON-STASYSHYN, R. K., FISHER, E. M. & FRATTA, P. 2013. Is SOD1 loss of function involved in amyotrophic lateral sclerosis? *Brain,* 136**,** 2342-58.

SAEED, M., YANG, Y., DENG, H. X., HUNG, W. Y., SIDDIQUE, N., DELLEFAVE, L., GELLERA, C., ANDERSEN, P. M. & SIDDIQUE, T. 2009. Age and founder effect of SOD1 A4V mutation causing ALS. *Neurology,* 72**,** 1634-1639.

SAID AHMED, M., HUNG, W. Y., ZU, J. S., HOCKBERGER, P. & SIDDIQUE, T. 2000. Increased reactive oxygen species in familial amyotrophic lateral sclerosis with mutations in SOD1. *J Neurol Sci,* 176**,** 88-94.

SANCES, S., BRUIJN, L. I., CHANDRAN, S., EGGAN, K., HO, R., KLIM, J. R., LIVESEY, M. R., LOWRY, E., MACKLIS, J. D., RUSHTON, D., SADEGH, C., SAREEN, D., WICHTERLE, H., ZHANG, S.-C. & SVENDSEN, C. N. 2016. Modeling ALS with motor neurons derived from human induced pluripotent stem cells. *Nat Neurosci,* 16**,** 542-553.

SANCHO-PELLUZ, J., ALAVI, M. V., SAHABOGLU, A., KUSTERMANN, S., FARINELLI, P., AZADI, S., VAN VEEN, T., ROMERO, F. J., PAQUET-DURAND, F. & EKSTROM, P. 2010. Excessive HDAC activation is critical for neurodegeneration in the rd1 mouse. *Cell Death Dis,* 1**,** 4.

SANO, T., LIN, H., CHEN, X., LANGFORD, L. A., KOUL, D., BONDY, M. L., HESS, K. R., MYERS, J. N., HONG, Y. K., YUNG, W. K. & STECK, P. A. 1999. Differential expression of MMAC/PTEN in glioblastoma multiforme: relationship to localization and prognosis. *Cancer Res,* 59**,** 1820-4.

SAPP, P. C., HOSLER, B. A., MCKENNA-YASEK, D., CHIN, W., GANN, A., GENISE, H., GORENSTEIN, J., HUANG, M., SAILER, W., SCHEFFLER, M., VALESKY, M., HAINES, J. L., PERICAK-VANCE, M., SIDDIQUE, T., HORVITZ, H. R. & BROWN, R. H., JR. 2003. Identification of two novel loci for dominantly inherited familial amyotrophic lateral sclerosis. *Am J Hum Genet,* 73**,** 397-403.

SAREEN, D., EBERT, A. D., HEINS, B. M., MCGIVERN, J. V., ORNELAS, L. & SVENDSEN, C. N. 2012. Inhibition of Apoptosis Blocks Human Motor Neuron Cell Death in a Stem Cell Model of Spinal Muscular Atrophy. *PLoS One,* 7**,** e39113.

SAREEN, D., O'ROURKE, J. G., MEERA, P., MUHAMMAD, A. K. M. G., GRANT, S., SIMPKINSON, M., BELL, S., CARMONA, S., ORNELAS, L., SAHABIAN, A., GENDRON, T., PETRUCELLI, L., BAUGHN, M., RAVITS, J., HARMS, M. B., RIGO, F., BENNETT, C. F., OTIS, T. S., SVENDSEN, C. N. & BALOH, R. H. 2013. Targeting RNA Foci in iPSC-Derived Motor Neurons from ALS Patients with a C9ORF72 Repeat Expansion. *Science Translational Medicine,* 5**,** 208ra149-208ra149.

SCEKIC-ZAHIROVIC, J., OUSSINI, H. E., MERSMANN, S., DRENNER, K., WAGNER, M., SUN, Y., ALLMEROTH, K., DIETERLÉ, S., SINNIGER, J., DIRRIG-GROSCH, S., RENÉ, F., DORMANN, D., HAASS, C., LUDOLPH, A. C., LAGIER-TOURENNE, C., STORKEBAUM, E. & DUPUIS, L. 2017. Motor neuron intrinsic and extrinsic mechanisms contribute to the pathogenesis of FUS-associated amyotrophic lateral sclerosis. *Acta Neuropathologica***,** 1-20.

SCHEIBE, R. J. & WAGNER, J. A. 1992. Retinoic acid regulates both expression of the nerve growth factor receptor and sensitivity to nerve growth factor. *J Biol Chem,* 267**,** 17611-6.

SCHLUDI, M. H., BECKER, L., GARRETT, L., GENDRON, T. F., ZHOU, Q., SCHREIBER, F., POPPER, B., DIMOU, L., STROM, T. M., WINKELMANN, J., VON THADEN, A., RENTZSCH, K., MAY, S., MICHAELSEN, M., SCHWENK, B. M., TAN, J., SCHOSER, B., DIETERICH, M., PETRUCELLI, L., HÖLTER, S. M., WURST, W., FUCHS, H., GAILUS-DURNER, V., DE ANGELIS, M. H., KLOPSTOCK, T., ARZBERGER, T. & EDBAUER, D. 2017. Spinal poly-GA inclusions in a C9orf72 mouse model trigger motor deficits and inflammation without neuron loss. *Acta Neuropathologica***,** 1-14.

SCHMID, A. C., BYRNE, R. D., VILAR, R. & WOSCHOLSKI, R. 2004. Bisperoxovanadium compounds are potent PTEN inhibitors. *FEBS Lett,* 566**,** 35-8.

SCHWENK, B. M., HARTMANN, H., SERDAROGLU, A., SCHLUDI, M. H., HORNBURG, D., MEISSNER, F., OROZCO, D., COLOMBO, A., TAHIROVIC, S., MICHAELSEN, M., SCHREIBER, F., HAUPT, S., PEITZ, M., BRUSTLE, O., KUPPER, C., KLOPSTOCK, T., OTTO, M., LUDOLPH, A. C., ARZBERGER, T., KUHN, P. H. & EDBAUER, D. 2016. TDP-43 loss of function inhibits endosomal trafficking and alters trophic signaling in neurons. *Embo J,* 35**,** 2350-2370.

SELLIER, C., CAMPANARI, M. L., JULIE CORBIER, C., GAUCHEROT, A., KOLB-CHEYNEL, I., OULAD-ABDELGHANI, M., RUFFENACH, F., PAGE, A., CIURA, S., KABASHI, E. & CHARLET-BERGUERAND, N. 2016. Loss of C9ORF72 impairs autophagy and synergizes with polyQ Ataxin-2 to induce motor neuron dysfunction and cell death. *Embo J,* 21.

SEPHTON, C. F., CENIK, C., KUCUKURAL, A., DAMMER, E. B., CENIK, B., HAN, Y., DEWEY, C. M., ROTH, F. P., HERZ, J., PENG, J., MOORE, M. J. & YU, G. 2011. Identification of neuronal RNA targets of TDP-43-containing ribonucleoprotein complexes. *J Biol Chem,* 286**,** 1204-15.

SHARMA, V., KOUL, N., JOSEPH, C., DIXIT, D., GHOSH, S. & SEN, E. 2010. HDAC inhibitor, scriptaid, induces glioma cell apoptosis through JNK activation and inhibits telomerase activity. *J Cell Mol Med,* 14**,** 2151-61.

SHAW, P. J., INCE, P. G., FALKOUS, G. & MANTLE, D. 1995. Oxidative damage to protein in sporadic motor neuron disease spinal cord. *Ann Neurol,* 38**,** 691-5.

SHI, G. D., OUYANG, Y. P., SHI, J. G., LIU, Y., YUAN, W. & JIA, L. S. 2011a. PTEN deletion prevents ischemic brain injury by activating the mTOR signaling pathway. *Biochem Biophys Res Commun,* 404**,** 941-5.

SHI, P., SCOTT, M. A., GHOSH, B., WAN, D., WISSNER-GROSS, Z., MAZITSCHEK, R., HAGGARTY, S. J. & YANIK, M. F. 2011b. Synapse microarray identification of small molecules that enhance synaptogenesis. *Nat Commun,* 2**,** 510.

SHOESMITH, C. L., FINDLATER, K., ROWE, A. & STRONG, M. J. 2007. Prognosis of amyotrophic lateral sclerosis with respiratory onset. *Journal of Neurology, Neurosurgery, and Psychiatry,* 78**,** 629-631.

SIMM, A., BERTSCH, G., FRANK, H., ZIMMERMANN, U. & HOPPE, J. 1997. Cell death of AKR-2B fibroblasts after serum removal: a process between apoptosis and necrosis. *Journal of Cell Science,* 110**,** 819-828.

SIMOES-PIRES, C., ZWICK, V., NURISSO, A., SCHENKER, E., CARRUPT, P.-A. & CUENDET, M. 2013. HDAC6 as a target for neurodegenerative diseases: what makes it different from the other HDACs? *Molecular Neurodegeneration,* 8**,** 7.

SIMON, N. G., HUYNH, W., VUCIC, S., TALBOT, K. & KIERNAN, M. C. 2015. Motor neuron disease: current management and future prospects. *Intern Med J,* 45**,** 1005-13.

SINGH, B., SINGH, V., KRISHNAN, A., KOSHY, K., MARTINEZ, J. A., CHENG, C., ALMQUIST, C. & ZOCHODNE, D. W. 2014. Regeneration of diabetic axons is enhanced by selective knockdown of the PTEN gene. *Brain,* 137**,** 1051-67.

SINHA, S. & CHEN, J. K. 2006. Purmorphamine activates the Hedgehog pathway by targeting Smoothened. *Nat Chem Biol,* 2**,** 29-30.

SMITH, B. N., NEWHOUSE, S., SHATUNOV, A., VANCE, C., TOPP, S., JOHNSON, L., MILLER, J., LEE, Y., TROAKES, C., SCOTT, K. M., JONES, A., GRAY, I., WRIGHT, J., HORTOBAGYI, T., AL-SARRAJ, S., ROGELJ, B., POWELL, J., LUPTON, M., LOVESTONE, S., SAPP, P. C., WEBER, M., NESTOR, P. J., SCHELHAAS, H. J., ASBROEK, A. A., SILANI, V., GELLERA, C., TARONI, F., TICOZZI, N., VAN DEN BERG, L., VELDINK, J., VAN DAMME, P., ROBBERECHT, W., SHAW, P. J., KIRBY, J., PALL, H., MORRISON, K. E., MORRIS, A., DE BELLEROCHE, J., VIANNEY DE JONG, J. M., BAAS, F., ANDERSEN, P. M., LANDERS, J., BROWN, R. H., JR., WEALE, M. E., AL-CHALABI, A. & SHAW, C. E. 2013. The C9ORF72 expansion mutation is a common cause of ALS+/-FTD in Europe and has a single founder. *Eur J Hum Genet,* 21**,** 102-8.

SMITH, B. N., TICOZZI, N., FALLINI, C., GKAZI, A. S., TOPP, S., KENNA, K. P., SCOTTER, E. L., KOST, J., KEAGLE, P., MILLER, J. W., CALINI, D., VANCE, C., DANIELSON, E. W., TROAKES, C., TILOCA, C., AL-SARRAJ, S., LEWIS, E. A., KING, A., COLOMBRITA, C., PENSATO, V., CASTELLOTTI, B., DE BELLEROCHE, J., BAAS, F., TEN ASBROEK, A. L., SAPP, P. C., MCKENNA-YASEK, D., MCLAUGHLIN, R. L., POLAK, M., ASRESS, S., ESTEBAN-PEREZ, J., MUNOZ-BLANCO, J. L., SIMPSON, M., VAN RHEENEN, W., DIEKSTRA, F. P., LAURIA, G., DUGA, S., CORTI, S., CEREDA, C., CORRADO, L., SORARU, G., MORRISON, K. E., WILLIAMS, K. L., NICHOLSON, G. A., BLAIR, I. P., DION, P. A., LEBLOND, C. S., ROULEAU, G. A., HARDIMAN, O., VELDINK, J. H., VAN DEN BERG, L. H., AL-CHALABI, A., PALL, H., SHAW, P. J., TURNER, M. R., TALBOT, K., TARONI, F., GARCIA-REDONDO, A., WU, Z., GLASS, J. D., GELLERA, C., RATTI, A., BROWN, R. H., JR., SILANI, V., SHAW, C. E. & LANDERS, J. E. 2014. Exome-wide rare variant analysis identifies TUBA4A mutations associated with familial ALS. *Neuron,* 84**,** 324-31.

SOCKANATHAN, S. & JESSELL, T. M. 1998. Motor Neuron–Derived Retinoid Signaling Specifies the Subtype Identity of Spinal Motor Neurons. *Cell,* 94**,** 503-514.

SOTELO, N. S., SCHEPENS, J. T., VALIENTE, M., HENDRIKS, W. J. & PULIDO, R. 2015. PTEN-PDZ domain interactions: binding of PTEN to PDZ domains of PTPN13. *Methods,* 78**,** 147-56.

SPINELLI, L., LINDSAY, Y. E. & LESLIE, N. R. 2015. PTEN inhibitors: an evaluation of current compounds. *Adv Biol Regul,* 57**,** 102-11.

SREEDHARAN, J., BLAIR, I. P., TRIPATHI, V. B., HU, X., VANCE, C., ROGELJ, B., ACKERLEY, S., DURNALL, J. C., WILLIAMS, K. L., BURATTI, E., BARALLE, F., DE BELLEROCHE, J., MITCHELL, J. D., LEIGH, P. N., AL-CHALABI, A., MILLER, C. C., NICHOLSON, G. & SHAW, C. E. 2008. TDP-43 Mutations in Familial and Sporadic Amyotrophic Lateral Sclerosis. *Science,* 319**,** 1668-1672.

STACHOWIAK, E. K., FANG, X., MYERS, J., DUNHAM, S. & STACHOWIAK, M. K. 2003. cAMP-induced differentiation of human neuronal progenitor cells is mediated by nuclear fibroblast growth factor receptor-1 (FGFR1). *J Neurochem,* 84**,** 1296-312.

STAMBOLIC, V., MACPHERSON, D., SAS, D., LIN, Y., SNOW, B., JANG, Y., BENCHIMOL, S. & MAK, T. W. 2001. Regulation of PTEN Transcription by p53. *Molecular Cell,* 8**,** 317-325.

STAMBOLIC, V., TSAO, M. S., MACPHERSON, D., SUZUKI, A., CHAPMAN, W. R. & MAK, T. W. 2000. High incidence of breast and endometrial neoplasia resembling human Cowden syndrome in pten(+/-) mice. *Cancer Research,* 60**,** 3605-3611.

STECK, P. A., PERSHOUSE, M. A., JASSER, S. A., YUNG, W. K., LIN, H., LIGON, A. H., LANGFORD, L. A., BAUMGARD, M. L., HATTIER, T., DAVIS, T., FRYE, C., HU, R., SWEDLUND, B., TENG, D. H. & TAVTIGIAN, S. V. 1997. Identification of a candidate tumour suppressor gene, MMAC1, at chromosome 10q23.3 that is mutated in multiple advanced cancers. *Nat Genet,* 15**,** 356-62.

STERN, C. D. 2001. Initial patterning of the central nervous system: How many organizers? *Nat Rev Neurosci,* 2**,** 92-98.

STEWART, M. 2014. Ran in Nucleocytoplasmic Transport. *In:* WITTINGHOFER, A. (ed.) *Ras Superfamily Small G Proteins: Biology and Mechanisms 2: Transport.* Cham: Springer International Publishing.

STOPFORD, M. J., HIGGINBOTTOM, A., HAUTBERGUE, G. M., COOPER-KNOCK, J., MULCAHY, P. J., DE VOS, K. J., RENTON, A. E., PLINER, H., CALVO, A., CHIO, A., TRAYNOR, B. J., AZZOUZ, M., HEATH, P. R., KIRBY, J. & SHAW, P. J. 2017. C9ORF72 hexanucleotide repeat exerts toxicity in a stable, inducible motor neuronal cell model, which is rescued by partial depletion of Pten. *Hum Mol Genet,* 26**,** 1133-1145.

SU, G. H., SOHN, T. A., RYU, B. & KERN, S. E. 2000. A Novel Histone Deacetylase Inhibitor Identified by High-Throughput Transcriptional Screening of a Compound Library. *Cancer Research,* 60**,** 3137-3142.

SUBRAMANIAN, M., RAGE, F., TABET, R., FLATTER, E., MANDEL, J. L. & MOINE, H. 2011. G-quadruplex RNA structure as a signal for neurite mRNA targeting. *EMBO Rep,* 12**,** 697-704.

SUDRIA-LOPEZ, E., KOPPERS, M., DE WIT, M., VAN DER MEER, C., WESTENENG, H. J., ZUNDEL, C. A., YOUSSEF, S. A., HARKEMA, L., DE BRUIN, A., VELDINK, J. H., VAN DEN BERG, L. H. & PASTERKAMP, R. J. 2016. *Full ablation of C9orf72 in mice causes immune system-related pathology and neoplastic events but no motor neuron defects*, Acta Neuropathol. 2016 Jul;132(1):145-7. doi: 10.1007/s00401-016-1581-x. Epub 2016 May 20.

SUMNER, C. J., HUYNH, T. N., MARKOWITZ, J. A., PERHAC, J. S., HILL, B., COOVERT, D. D., SCHUSSLER, K., CHEN, X., JARECKI, J., BURGHES, A. H. M., TAYLOR, J. P. & FISCHBECK, K. H. 2003. Valproic acid increases SMN levels in spinal muscular atrophy patient cells. *Annals of Neurology,* 54**,** 647-654.

SUZUKI, A., DE LA POMPA, J. L., STAMBOLIC, V., ELIA, A. J., SASAKI, T., DEL BARCO BARRANTES, I., HO, A., WAKEHAM, A., ITIE, A., KHOO, W., FUKUMOTO, M. & MAK, T. W. 1998. High cancer

susceptibility and embryonic lethality associated with mutation of the PTEN tumor suppressor gene in mice. *Curr Biol,* 8**,** 1169-78.

SUZUKI, N., MAROOF, A. M., MERKLE, F. T., KOSZKA, K., INTOH, A. & ARMSTRONG, I. 2013. The mouse C9ORF72 ortholog is enriched in neurons known to degenerate in ALS and FTD. *Nat Neurosci,* 16.

TAKAHASHI, K., TANABE, K., OHNUKI, M., NARITA, M., ICHISAKA, T., TOMODA, K. & YAMANAKA, S. 2007. Induction of Pluripotent Stem Cells from Adult Human Fibroblasts by Defined Factors. *Cell,* 131**,** 861-872.

TAKAHASHI, K. & YAMANAKA, S. 2006. Induction of Pluripotent Stem Cells from Mouse Embryonic and Adult Fibroblast Cultures by Defined Factors. *Cell,* 126**,** 663-676.

TAKAHASHI, T., LORD, B., SCHULZE, P. C., FRYER, R. M., SARANG, S. S., GULLANS, S. R. & LEE, R. T. 2003. Ascorbic acid enhances differentiation of embryonic stem cells into cardiac myocytes. *Circulation,* 107**,** 1912-6.

TAKAHASHI, Y., FUKUDA, Y., YOSHIMURA, J., TOYODA, A., KURPPA, K., MORITOYO, H., BELZIL, VERONIQUE V., DION, PATRICK A., HIGASA, K., DOI, K., ISHIURA, H., MITSUI, J., DATE, H., AHSAN, B., MATSUKAWA, T., ICHIKAWA, Y., MORITOYO, T., IKOMA, M., HASHIMOTO, T., KIMURA, F., MURAYAMA, S., ONODERA, O., NISHIZAWA, M., YOSHIDA, M., ATSUTA, N., SOBUE, G., JACALS, FIFITA, JENNIFER A., WILLIAMS, KELLY L., BLAIR, IAN P., NICHOLSON, GARTH A., GONZALEZ-PEREZ, P., BROWN, ROBERT H., NOMOTO, M., ELENIUS, K., ROULEAU, GUY A., FUJIYAMA, A., MORISHITA, S., GOTO, J. & TSUJI, S. 2013. ERBB4 Mutations that Disrupt the Neuregulin-ErbB4 Pathway Cause Amyotrophic Lateral Sclerosis Type 19. *American Journal of Human Genetics,* 93**,** 900-905.

TAKAI, N. & NARAHARA, H. 2010. Preclinical Studies of Chemotherapy Using Histone Deacetylase Inhibitors in Endometrial Cancer. *Obstetrics and Gynecology International,* 2010**,** 8.

TAKAI, N., UEDA, T., NISHIDA, M., NASU, K. & NARAHARA, H. 2006. A novel histone deacetylase inhibitor, Scriptaid, induces growth inhibition, cell cycle arrest and apoptosis in human endometrial cancer and ovarian cancer cells. *Int J Mol Med,* 17**,** 323-9.

TANEJA, K. L., MCCURRACH, M., SCHALLING, M., HOUSMAN, D. & SINGER, R. H. 1995. Foci of trinucleotide repeat transcripts in nuclei of myotonic dystrophy cells and tissues. *The Journal of Cell Biology,* 128**,** 995-1002.

TANG, Y. & ENG, C. 2006. PTEN autoregulates its expression by stabilization of p53 in a phosphatase-independent manner. *Cancer Res,* 66**,** 736-42.

THALER, J. P., KOO, S. J., KANIA, A., LETTIERI, K., ANDREWS, S., COX, C., JESSELL, T. M. & PFAFF, S. L. 2004. A Postmitotic Role for Isl-Class LIM Homeodomain Proteins in the Assignment of Visceral Spinal Motor Neuron Identity. *Neuron,* 41**,** 337-350.

TODD, P. K. & PAULSON, H. L. 2010. RNA Mediated Neurodegeneration in Repeat Expansion Disorders. *Annals of Neurology,* 67**,** 291-300.

TORRES, J. & PULIDO, R. 2001. The Tumor Suppressor PTEN Is Phosphorylated by the Protein Kinase CK2 at Its C Terminus: IMPLICATIONS FOR PTEN STABILITY TO PROTEASOME-MEDIATED DEGRADATION. *Journal of Biological Chemistry,* 276**,** 993-998.

TRAMUTOLA, A., TRIPLETT, J. C., DI DOMENICO, F., NIEDOWICZ, D. M., MURPHY, M. P., COCCIA, R., PERLUIGI, M. & BUTTERFIELD, D. A. 2015. Alteration of mTOR signaling occurs early in the progression of Alzheimer disease (AD): analysis of brain from subjects with pre-clinical AD, amnestic mild cognitive impairment and late-stage AD. *J Neurochem,* 133**,** 739-49.

TROTMAN, L. C., WANG, X., ALIMONTI, A., CHEN, Z., TERUYA-FELDSTEIN, J., YANG, H., PAVLETICH, N. P., CARVER, B. S., CORDON-CARDO, C., ERDJUMENT-BROMAGE, H., TEMPST, P., CHI, S. G., KIM, H. J., MISTELI, T., JIANG, X. & PANDOLFI, P. P. 2007. Ubiquitination regulates PTEN nuclear import and tumor suppression. *Cell,* 128**,** 141-56.

VAJDA, A., MCLAUGHLIN, R. L., HEVERIN, M., THORPE, O., ABRAHAMS, S., AL-CHALABI, A. & HARDIMAN, O. 2017. Genetic testing in ALS: A survey of current practices. *Neurology,* 88**,** 991-999.

VALENTE, E. M., ABOU-SLEIMAN, P. M., CAPUTO, V., MUQIT, M. M., HARVEY, K., GISPERT, S., ALI, Z., DEL TURCO, D., BENTIVOGLIO, A. R., HEALY, D. G., ALBANESE, A., NUSSBAUM, R., GONZALEZ-MALDONADO, R., DELLER, T., SALVI, S., CORTELLI, P., GILKS, W. P., LATCHMAN, D. S., HARVEY, R. J., DALLAPICCOLA, B., AUBURGER, G. & WOOD, N. W. 2004. Hereditary early-onset Parkinson's disease caused by mutations in PINK1. *Science,* 304**,** 1158-60.

VALORI, C. F., NING, K., WYLES, M., MEAD, R. J., GRIERSON, A. J., SHAW, P. J. & AZZOUZ, M. 2010. Systemic delivery of scAAV9 expressing SMN prolongs survival in a model of spinal muscular atrophy. *Science translational medicine,* 2**,** 35ra42.

VAN BLITTERSWIJK, M., DEJESUS-HERNANDEZ, M. & RADEMAKERS, R. 2012. How do C9ORF72 repeat expansions cause amyotrophic lateral sclerosis and frontotemporal dementia: can we learn from other noncoding repeat expansion disorders? *Current Opinion in Neurology,* 25**,** 689-700 10.1097/WCO.0b013e32835a3efb.

VAN DER ZEE, J., GIJSELINCK, I., DILLEN, L., VAN LANGENHOVE, T., THEUNS, J., ENGELBORGHS, S., PHILTJENS, S., VANDENBULCKE, M., SLEEGERS, K., SIEBEN, A., BÄUMER, V., MAES, G., CORSMIT, E., BORRONI, B., PADOVANI, A., ARCHETTI, S., PERNECZKY, R., DIEHL-SCHMID, J., DE MENDONÇA, A., MILTENBERGER-MILTENYI, G., PEREIRA, S., PIMENTEL, J., NACMIAS, B., BAGNOLI, S., SORBI, S., GRAFF, C., CHIANG, H.-H., WESTERLUND, M., SANCHEZ-VALLE, R., LLADO, A., GELPI, E., SANTANA, I., ALMEIDA, M. R., SANTIAGO, B., FRISONI, G., ZANETTI, O., BONVICINI, C., SYNOFZIK, M., MAETZLER, W., VOM HAGEN, J. M., SCHÖLS, L., HENEKA, M. T., JESSEN, F., MATEJ, R., PAROBKOVA, E., KOVACS, G. G., STRÖBEL, T., SARAFOV, S., TOURNEV, I., JORDANOVA, A., DANEK, A., ARZBERGER, T., FABRIZI, G. M., TESTI, S., SALMON, E., SANTENS, P., MARTIN, J.-J., CRAS, P., VANDENBERGHE, R., DE DEYN, P. P., CRUTS, M., VAN BROECKHOVEN, C., VAN DER ZEE, J., GIJSELINCK, I., DILLEN, L., VAN LANGENHOVE, T., THEUNS, J., PHILTJENS, S., SLEEGERS, K., BÄUMER, V., MAES, G., CORSMIT, E., CRUTS, M., VAN BROECKHOVEN, C., VAN DER ZEE, J., GIJSELINCK, I., DILLEN, L., VAN LANGENHOVE, T., PHILTJENS, S., THEUNS, J., SLEEGERS, K., BÄUMER, V., MAES, G., CRUTS, M., VAN BROECKHOVEN, C., ENGELBORGHS, S., DE DEYN, P. P., CRAS, P., ENGELBORGHS, S., DE DEYN, P. P., VANDENBULCKE, M., VANDENBULCKE, M., BORRONI, B., PADOVANI, A., ARCHETTI, S., PERNECZKY, R., DIEHL-SCHMID, J., SYNOFZIK, M., MAETZLER, W., MÜLLER VOM HAGEN, J., et al. 2013. A Pan-European Study of the C9orf72 Repeat Associated with FTLD: Geographic Prevalence, Genomic Instability, and Intermediate Repeats. *Human Mutation,* 34**,** 363-373.

VAN ZUNDERT, B., IZAURIETA, P., FRITZ, E. & ALVAREZ, F. J. 2012. Early pathogenesis in the adult-onset neurodegenerative disease amyotrophic lateral sclerosis. *Journal of Cellular Biochemistry,* 113**,** 3301-3312.

VANCE, C., ROGELJ, B., HORTOBAGYI, T., DE VOS, K. J., NISHIMURA, A. L., SREEDHARAN, J., HU, X., SMITH, B., RUDDY, D., WRIGHT, P., GANESALINGAM, J., WILLIAMS, K. L., TRIPATHI, V., AL-SARAJ, S., AL-CHALABI, A., LEIGH, P. N., BLAIR, I. P., NICHOLSON, G., DE BELLEROCHE, J., GALLO, J. M., MILLER, C. C. & SHAW, C. E. 2009. Mutations in FUS, an RNA processing protein, cause familial amyotrophic lateral sclerosis type 6. *Science,* 323**,** 1208-11.

VERGARA, C. & RAMIREZ, B. 2004. CNTF, a pleiotropic cytokine: emphasis on its myotrophic role. *Brain Res Brain Res Rev,* 47**,** 161-73.

WAGEY, R., PELECH, S. L., DURONIO, V. & KRIEGER, C. 1998. Phosphatidylinositol 3-kinase: increased activity and protein level in amyotrophic lateral sclerosis. *J Neurochem,* 71**,** 716-22.

WAINGER, B. J., KISKINIS, E., MELLIN, C., WISKOW, O., HAN, S. S., SANDOE, J., PEREZ, N. P., WILLIAMS, L. A., LEE, S., BOULTING, G., BERRY, J. D., BROWN, R. H., JR., CUDKOWICZ, M. E., BEAN, B. P., EGGAN, K. & WOOLF, C. J. 2014. Intrinsic membrane hyperexcitability of amyotrophic lateral sclerosis patient-derived motor neurons. *Cell Rep,* 7**,** 1-11.

WALKER, C. L., WALKER, M. J., LIU, N. K., RISBERG, E. C., GAO, X., CHEN, J. & XU, X. M. 2012. Systemic bisperoxovanadium activates Akt/mTOR, reduces autophagy, and enhances recovery following cervical spinal cord injury. *Plos One,* 7**,** e30012.

WALKER, C. L., WANG, X., BULLIS, C., LIU, N.-K., LU, Q., FRY, C., DENG, L. & XU, X.-M. 2015. Biphasic bisperoxovanadium administration and Schwann cell transplantation for repair after cervical contusive spinal cord injury. *Experimental Neurology,* 264**,** 163-172.

WALKER, C. L. & XU, X.-M. 2014. PTEN inhibitor bisperoxovanadium protects oligodendrocytes and myelin and prevents neuronal atrophy in adult rats following cervical hemicontusive spinal cord injury. *Neuroscience Letters,* 573**,** 64-68.

WANG, G., JIANG, X., PU, H., ZHANG, W., AN, C., HU, X., LIOU, A. K. F., LEAK, R. K., GAO, Y. & CHEN, J. 2012a. Scriptaid, a Novel Histone Deacetylase Inhibitor, Protects Against Traumatic Brain Injury via Modulation of PTEN and AKT Pathway. *Neurotherapeutics***,** 1-19.

WANG, G., PU, H., JIANG, X., ZHANG, W., HU, X., LIOU, A., GAO, Y. & CHEN, J. 2012b. Scriptaid, a new histone decetylase inhibitor protects against tramatic brain injury via modulation of PTEN and the AKT pathway. *Society for Neuroscience Abstract Viewer and Itinerary Planner,* 42.

WANG, G., SHI, Y., JIANG, X., LEAK, R. K., HU, X., WU, Y., PU, H., LI, W. W., TANG, B., WANG, Y., GAO, Y., ZHENG, P., BENNETT, M. V. & CHEN, J. 2015a. HDAC inhibition prevents white matter injury by modulating microglia/macrophage polarization through the GSK3beta/PTEN/Akt axis. *Proc Natl Acad Sci U S A,* 112**,** 2853-8.

WANG, X., TROTMAN, L. C., KOPPIE, T., ALIMONTI, A., CHEN, Z., GAO, Z., WANG, J., ERDJUMENT-BROMAGE, H., TEMPST, P., CORDON-CARDO, C., PANDOLFI, P. P. & JIANG, X. 2007. NEDD4-1 is a proto-oncogenic ubiquitin ligase for PTEN. *Cell,* 128**,** 129-39.

WANG, Y. L., LI, F. & CHEN, X. 2015b. Pten Inhibitor-bpV Ameliorates Early Postnatal Propofol Exposure-Induced Memory Deficit and Impairment of Hippocampal LTP. *Neurochem Res,* 40**,** 1593-9.

WATANABE, K., UENO, M., KAMIYA, D., NISHIYAMA, A., MATSUMURA, M., WATAYA, T., TAKAHASHI, J. B., NISHIKAWA, S., NISHIKAWA, S., MUGURUMA, K. & SASAI, Y. 2007. A ROCK inhibitor permits survival of dissociated human embryonic stem cells. *Nat Biotechnol,* 25**,** 681-6.

WEBSTER, C. P., SMITH, E. F., BAUER, C. S., MOLLER, A., HAUTBERGUE, G. M., FERRAIUOLO, L., MYSZCZYNSKA, M. A., HIGGINBOTTOM, A., WALSH, M. J., WHITWORTH, A. J., KASPAR, B. K., MEYER, K., SHAW, P. J., GRIERSON, A. J. & DE VOS, K. J. 2016. The C9orf72 protein interacts with Rab1a and the ULK1 complex to regulate initiation of autophagy. *EMBO J,* 22.

WEN, X., TAN, W., WESTERGARD, T., KRISHNAMURTHY, K., MARKANDAIAH, S. S., SHI, Y., LIN, S., SHNEIDER, N. A., MONAGHAN, J., PANDEY, U. B., PASINELLI, P., ICHIDA, J. K. & TROTTI, D. 2014. Antisense proline-arginine RAN dipeptides linked to C9ORF72-ALS/FTD form toxic nuclear aggregates that initiate in vitro and in vivo neuronal death. *Neuron,* 84**,** 1213-25.

WIEDAU-PAZOS, M., GOTO, J. J., RABIZADEH, S., GRALLA, E. B., ROE, J. A., LEE, M. K., VALENTINE, J. S. & BREDESEN, D. E. 1996. Altered Reactivity of Superoxide Dismutase in Familial Amyotrophic Lateral Sclerosis. *Science,* 271**,** 515-518.

WILLIAMS, T. L., DAY, N. C., INCE, P. G., KAMBOJ, R. K. & SHAW, P. J. 1997. Calcium-permeable alpha-amino-3-hydroxy-5-methyl-4-isoxazole propionic acid receptors: a molecular determinant of selective vulnerability in amyotrophic lateral sclerosis. *Ann Neurol,* 42**,** 200-7.

WILLIAMSON, T. L. & CLEVELAND, D. W. 1999. Slowing of axonal transport is a very early event in the toxicity of ALS-linked SOD1 mutants to motor neurons. *Nat Neurosci,* 2**,** 50-56.

WILSON, J. M., HARTLEY, R., MAXWELL, D. J., TODD, A. J., LIEBERAM, I., KALTSCHMIDT, J. A., YOSHIDA, Y., JESSELL, T. M. & BROWNSTONE, R. M. 2005. Conditional rhythmicity of ventral spinal interneurons defined by expression of the Hb9 homeodomain protein. *J Neurosci,* 25**,** 5710-9.

WONG, P. C., PARDO, C. A., BORCHELT, D. R., LEE, M. K., COPELAND, N. G., JENKINS, N. A., SISODIA, S. S., CLEVELAND, D. W. & PRICE, D. L. 1995. An adverse property of a familial ALS-linked SOD1 mutation causes motor neuron disease characterized by vacuolar degeneration of mitochondria. *Neuron,* 14**,** 1105-16.

WOOD-ALLUM, C. & SHAW, P. J. 2010. Motor neurone disease: a practical update on diagnosis and management. *Clin Med,* 10**,** 252-8.

WU, C. H., FALLINI, C., TICOZZI, N., KEAGLE, P. J., SAPP, P. C., PIOTROWSKA, K., LOWE, P., KOPPERS, M., MCKENNA-YASEK, D., BARON, D. M., KOST, J. E., GONZALEZ-PEREZ, P., FOX, A. D., ADAMS, J., TARONI, F., TILOCA, C., LECLERC, A. L., CHAFE, S. C., MANGROO, D., MOORE, M. J., ZITZEWITZ, J. A., XU, Z. S., VAN DEN BERG, L. H., GLASS, J. D., SICILIANO, G., CIRULLI, E. T., GOLDSTEIN, D. B., SALACHAS, F., MEININGER, V., ROSSOLL, W., RATTI, A., GELLERA, C., BOSCO, D. A., BASSELL, G. J., SILANI, V., DRORY, V. E., BROWN, R. H., JR. & LANDERS, J. E. 2012. Mutations in the profilin 1 gene cause familial amyotrophic lateral sclerosis. *Nature,* 488**,** 499-503.

WYATT, L. A., FILBIN, M. T. & KEIRSTEAD, H. S. 2014. PTEN inhibition enhances neurite outgrowth in human embryonic stem cell–derived neuronal progenitor cells. *Journal of Comparative Neurology,* 522**,** 2741-2755.

XIAO, A., YIN, C., YANG, C., DI CRISTOFANO, A., PANDOLFI, P. P. & VAN DYKE, T. 2005. Somatic induction of Pten loss in a preclinical astrocytoma model reveals major roles in disease progression and avenues for target discovery and validation. *Cancer Res,* 65**,** 5172-80.

XIAO, S., MACNAIR, L., MCGOLDRICK, P., MCKEEVER, P. M., MCLEAN, J. R., ZHANG, M., KEITH, J., ZINMAN, L., ROGAEVA, E. & ROBERTSON, J. 2015. Isoform-specific antibodies reveal distinct subcellular localizations of C9orf72 in amyotrophic lateral sclerosis. *Ann Neurol,* 78**,** 568-83.

XU, Y., LIU, C., CHEN, S., YE, Y., GUO, M., REN, Q., LIU, L., ZHANG, H., XU, C., ZHOU, Q., HUANG, S. & CHEN, L. 2014. Activation of AMPK and inactivation of Akt result in suppression of mTOR-mediated S6K1 and 4E-BP1 pathways leading to neuronal cell death in in vitro models of Parkinson's disease. *Cellular signalling,* 26**,** 1680-1689.

YAMANAKA, K., CHUN, S. J., BOILLEE, S., FUJIMORI-TONOU, N., YAMASHITA, H., GUTMANN, D. H., TAKAHASHI, R., MISAWA, H. & CLEVELAND, D. W. 2008. Astrocytes as determinants of disease progression in inherited amyotrophic lateral sclerosis. *Nature Neuroscience,* 11**,** 251-253.

YANG, D. J., WANG, X. L., ISMAIL, A., ASHMAN, C. J., VALORI, C. F., WANG, G., GAO, S., HIGGINBOTTOM, A., INCE, P. G., AZZOUZ, M., XU, J., SHAW, P. J. & NING, K. 2014a. PTEN regulates AMPA receptor-mediated cell viability in iPS-derived motor neurons. *Cell Death Dis,* 27**,** 55.

YANG, D. J., WANG, X. L., ISMAIL, A., ASHMAN, C. J., VALORI, C. F., WANG, G., GAO, S., HIGGINBOTTOM, A., INCE, P. G., AZZOUZ, M., XU, J., SHAW, P. J. & NING, K. 2014b. PTEN regulates AMPA receptor-mediated cell viability in iPS-derived motor neurons. *Cell Death Dis,* 5**,** e1096.

YANG, J. M., SCHIAPPARELLI, P., NGUYEN, H. N., IGARASHI, A., ZHANG, Q., ABBADI, S., AMZEL, L. M., SESAKI, H., QUIÑONES-HINOJOSA, A. & IIJIMA, M. 2017. Characterization of PTEN mutations in brain cancer reveals that pten mono-ubiquitination promotes protein stability and nuclear localization. *Oncogene*.

YANG, Y., HENTATI, A., DENG, H. X., DABBAGH, O., SASAKI, T., HIRANO, M., HUNG, W. Y., OUAHCHI, K., YAN, J., AZIM, A. C., COLE, N., GASCON, G., YAGMOUR, A., BEN-HAMIDA, M., PERICAK-VANCE, M., HENTATI, F. & SIDDIQUE, T. 2001. The gene encoding alsin, a protein with three guanine-nucleotide exchange factor domains, is mutated in a form of recessive amyotrophic lateral sclerosis. *Nat Genet,* 29**,** 160-5.

YOO, Y. E. & KO, C. P. 2011. Treatment with trichostatin A initiated after disease onset delays disease progression and increases survival in a mouse model of amyotrophic lateral sclerosis. *Exp Neurol,* 231**,** 147-59.

YOON, E. J., PARK, H. J., KIM, G. Y., CHO, H. M., CHOI, J. H., PARK, H. Y., JANG, J. Y., RHIM, H. S. & KANG, S. M. 2009. Intracellular amyloid beta interacts with SOD1 and impairs the enzymatic activity of SOD1: implications for the pathogenesis of amyotrophic lateral sclerosis. *Exp Mol Med,* 41**,** 611-7.

YU, J., VODYANIK, M. A., SMUGA-OTTO, K., ANTOSIEWICZ-BOURGET, J., FRANE, J. L., TIAN, S., NIE, J., JONSDOTTIR, G. A., RUOTTI, V., STEWART, R., SLUKVIN, II & THOMSON, J. A. 2007. Induced pluripotent stem cell lines derived from human somatic cells. *Science,* 318**,** 1917-20.

ZHANG, D., IYER, L. M., HE, F. & ARAVIND, L. 2012a. Discovery of Novel DENN Proteins: Implications for the Evolution of Eukaryotic Intracellular Membrane Structures and Human Disease. *Front Genet,* 3.

ZHANG, K., DONNELLY, C. J., HAEUSLER, A. R., GRIMA, J. C., MACHAMER, J. B., STEINWALD, P., DALEY, E. L., MILLER, S. J., CUNNINGHAM, K. M., VIDENSKY, S., GUPTA, S., THOMAS, M. A., HONG, I., CHIU, S.-L., HUGANIR, R. L., OSTROW, L. W., MATUNIS, M. J., WANG, J., SATTLER, R., LLOYD, T. E. & ROTHSTEIN, J. D. 2015a. The C9ORF72 repeat expansion disrupts nucleocytoplasmic transport. *Nature,* 525**,** 56-61.

ZHANG, L., ZHANG, S., YAO, J., LOWERY, F. J., ZHANG, Q., HUANG, W.-C., LI, P., LI, M., WANG, X., ZHANG, C., WANG, H., ELLIS, K., CHEERATHODI, M., MCCARTY, J. H., PALMIERI, D., SAUNUS, J., LAKHANI, S., HUANG, S., SAHIN, A. A., ALDAPE, K. D., STEEG, P. S. & YU, D. 2015b. Microenvironment-induced PTEN loss by exosomal microRNA primes brain metastasis outgrowth. *Nature,* 527**,** 100-104.

ZHANG, S., TAGHIBIGLOU, C., GIRLING, K., DONG, Z., LIN, S. Z., LEE, W., SHYU, W. C. & WANG, Y. T. 2013. Critical role of increased PTEN nuclear translocation in excitotoxic and ischemic neuronal injuries. *J Neurosci,* 33**,** 7997-8008.

ZHANG, Y., GRANHOLM, A. C., HUH, K., SHAN, L., DIAZ-RUIZ, O., MALIK, N., OLSON, L., HOFFER, B. J., LUPICA, C. R., HOFFMAN, A. F. & BACKMAN, C. M. 2012b. PTEN deletion enhances survival, neurite outgrowth and function of dopamine neuron grafts to MitoPark mice. *Brain,* 135**,** 2736-49.

ZHANG, Y. J., JANSEN-WEST, K., XU, Y. F., GENDRON, T. F., BIENIEK, K. F., LIN, W. L., SASAGURI, H., CAULFIELD, T., HUBBARD, J., DAUGHRITY, L., CHEW, J., BELZIL, V. V., PRUDENCIO, M., STANKOWSKI, J. N., CASTANEDES-CASEY, M., WHITELAW, E., ASH, P. E., DETURE, M., RADEMAKERS, R., BOYLAN, K. B., DICKSON, D. W. & PETRUCELLI, L. 2014. Aggregation-prone c9FTD/ALS poly(GA) RAN-translated proteins cause neurotoxicity by inducing ER stress. *Acta Neuropathologica,* 128**,** 505-24.

ZHAO, J., CHEN, Y., XU, Y. & PI, G. 2016. Effects of PTEN inhibition on the regulation of Tau phosphorylation in rat cortical neuronal injury after oxygen and glucose deprivation. *Brain Inj,* 31**,** 1-10.

ZHAO, J., QU, Y., WU, J., CAO, M., FERRIERO, D. M., ZHANG, L. & MU, D. 2013. PTEN inhibition prevents rat cortical neuron injury after hypoxia-ischemia. *Neuroscience,* 238**,** 242-51.

ZHU, Y., HOELL, P., AHLEMEYER, B. & KRIEGLSTEIN, J. 2006. PTEN: a crucial mediator of mitochondria-dependent apoptosis. *Apoptosis,* 11**,** 197-207.

ZHU, Y., HOELL, P., AHLEMEYER, B., SURE, U., BERTALANFFY, H. & KRIEGLSTEIN, J. 2007. Implication of PTEN in production of reactive oxygen species and neuronal death in in vitro models of stroke and Parkinson's disease. *Neurochem Int,* 50**,** 507-16.

ZU, T., GIBBENS, B., DOTY, N. S., GOMES-PEREIRA, M., HUGUET, A., STONE, M. D., MARGOLIS, J., PETERSON, M., MARKOWSKI, T. W., INGRAM, M. A. C., NAN, Z., FORSTER, C., LOW, W. C., SCHOSER, B., SOMIA, N. V., CLARK, H. B., SCHMECHEL, S., BITTERMAN, P. B., GOURDON, G., SWANSON, M. S., MOSELEY, M. & RANUM, L. P. W. 2011. Non-ATG–initiated translation directed by microsatellite expansions. *Proceedings of the National Academy of Sciences,* 108**,** 260-265.